EXPLORATION OF INTERACTIONS OF SOME VITAMINS PREVAILING IN LIQUID SYSTEMS BY PHYSICOCHEMICAL CONTRIVANCES

A Thesis submitted to the

UNIVERSITY OF NORTH BENGAL

For the Award of

Doctor of Philosophy (Ph. D.)

in

CHEMISTRY

By

PALASH CHAKRABORTI, **M.Sc. in Chemistry**

Research Guide

DR. MAHENDRA NATH ROY

Professor of Physical Chemistry

DEPARTMENT OF STUDIES IN CHEMISTRY

UNIVERSITY OF NORTH BENGAL

DECEMBER, 2014

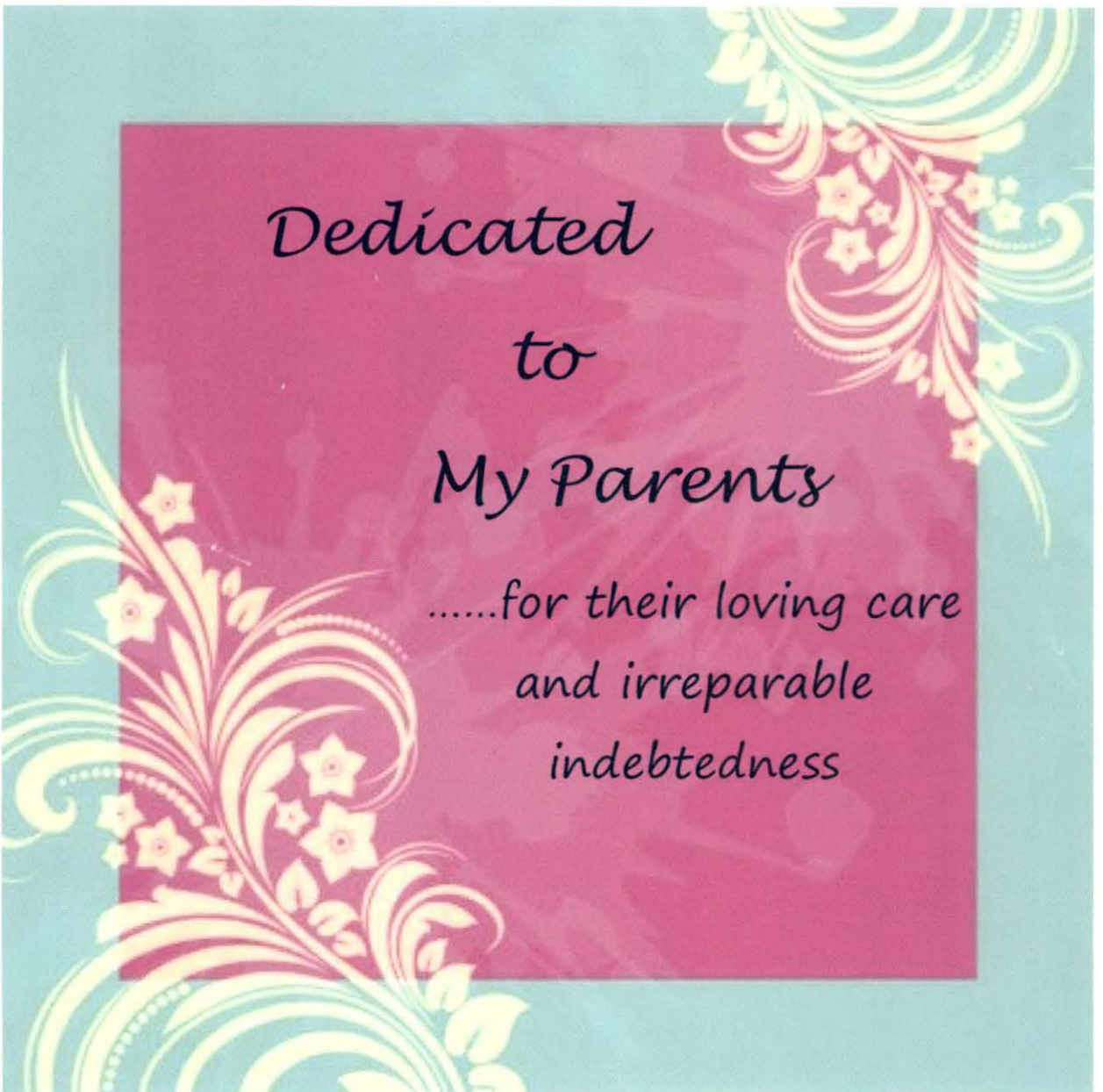
Dedicated
to
My Parents
.....for their loving care
and irreparable
indebtedness

DECLARATION

I declare that the thesis entitled "**EXPLORATION OF INTERACTIONS OF SOME VITAMINS PREVAILING IN LIQUID SYSTEMS BY PHYSICOCHEMICAL CONTRIVANCES**" has been prepared by me under the guidance of **Dr. Mahendra Nath Roy**, Professor of Chemistry, University of North Bengal. No part of this thesis has formed the basis for the award of any degree or fellowship previously.

Palash Chakraborti

PALASH CHAKRABORTI,

Department of Chemistry,

University of North Bengal,

Darjeeling: 734013,

West Bengal, India

Date: 15.12.2014

UNIVERSITY OF NORTH BENGAL

Dr. M. N. Roy,

M. Sc., Ph. D., DSA
Professor of Physical Chemistry
DEPARTMENT OF CHEMISTRY
E-mail: *mahendraroy2002@yahoo.co.in*

उत्तर बङ्ग
विश्वविद्यालय

Phone : 0353 2776381
Fax: 91 353 2699001
Mobile: 09434496154
Darjeeling-734 013,
West Bengal, INDIA.

CERTIFICATE

I certify that **Palash Chakraborti** has prepared the thesis entitled **"EXPLORATION OF INTERACTIONS OF SOME VITAMINS PREVAILING IN LIQUID SYSTEMS BY PHYSICOCHEMICAL CONTRIVANCES"**, for the award of Ph.D. Degree of the University of North Bengal, under my guidance. He has carried out the work at the Department of Chemistry, University of North Bengal.

Mahendra Nath Roy

DR. MAHENDRA NATH ROY,
Professor of Chemistry,
Department of Chemistry,
University of North Bengal,
Darjeeling: 734013,
West Bengal, India

Prof. M. N. Roy, M. Sc., Ph. D.
Programme Coordinator, SAP, DRS-III
DEPARTMENT OF CHEMISTRY
University of North Bengal
Darjeeling - 734013, (W.B) India

DATE: 15-12-2014

PHYSICO-CHEMICAL PARAMETERS AND THEIR SIGNIFICANCE:

Apparent molar volume (ϕ_V^0) from experimental density values is estimated, the sign and magnitude of apparent molar volume (ϕ_V^0) also provides information about the nature and magnitude of solute-solvent interaction while the experimental slope (S_v^*) provides information about solute-solute interactions. Viscosity Deviation($\Delta\eta$), viscosity B -coefficients are estimated from experimental viscosity values. From experimental speed of sound values, Deviation in Isentropic Compressibility (ΔK_S), limiting apparent molal isentropic compressibility ($\phi°_K$) and the experimental slope S_k^* were estimated. These parameters along with many other parameters estimated from Refractometric, conductometric measurements helps to establish the results obtained from density and viscosity measurements.

WORK SUMMARY

CHAPTER I

This chapter contains the objective and applications of the research work.

CHAPTER II

This chapter contains the general introduction of the thesis and forms the background of the present work. A brief review of notable works in the field of solute-solvent interaction has been given.

CHAPTER III

This chapter contains the experimental section which mainly involves the structure, source, purification and application of the solutes and solvents used in the research work and the details of the instruments used for the study.

CHAPTER IV

In this chapter molecular interaction prevailing in α-amino acids (glycine, L-alanine, L-valine) and aqueous solution of Folic acid (FA) have been reported by physico-chemical properties as density (ρ), viscosity (η), refractive index (n_D) and

ultrasonic speed (u) at 298.15 K. The extent of interaction (solute-solvent interaction) is expressed in terms of the limiting apparent molar volume (ϕ_V°), viscosity B-coefficient, molar refraction (R_M) and limiting apparent molar adiabatic compressibility (ϕ_K°). The trends in transfer volumes, $\Delta\phi_V^\circ$, have been interpreted in terms of solute-cosolute interactions on the basis of a cosphere overlap model. The role of the cosolute (FA), and the contribution of solute-solute and solute-solvent interactions to the solution complexes, has also been analyzed through the derived properties.

CHAPTER V

This chapter contains precise electrical conductance measurements are reported for some ethanoates, viz. ammonium, lithium, sodium and potassium in pure tetrahydrofuran (THF) and dimethyl sulphoxide (DMSO) and their binary mixtures at 298.15 K. The conductance data have been analyzed by the Fuoss conductance-concentration equation in terms of the limiting molar conductance (Λ_0), the thermodynamic association constant (K_A) and the association diameter (R). The limiting ionic conductances have been estimated from the appropriate division of the limiting molar conductivity value of the "reference electrolyte" Bu_4NBPh_4. Furthermore, the conductance data for pure THF have been analyzed by the Fuoss–Kraus theory of triple ions and the values of the ion-pair and triple-ion formation constants (K_P and K_T) were made and the results have been discussed in terms of molecular scale model.

CHAPTER VI

The apparent molar volume (ϕ_V), viscosity B-coefficient and molal refraction (R) of some carbohydrates (D-Glucose, D-Sucrose, and D-Maltose monohydrate) have been determined in 0.01, 0.03, 0.05 mol·dm^{-3} aqueous ascorbic acid solutions at 298.15 K from the experimental density (ρ), viscosity (η) and refractive index (n_D) values respectively. The limiting apparent molar volumes (ϕ_V^0), experimental slopes (S_V^*) have been derived from the Masson equation and they have been interpreted in terms of solute-solvent and solute-solute interactions respectively.

The viscosity data have been analysed using the Jones-Dole equation and the derived parameters viscosity-A and B coefficient obtained have also been interpreted in terms of solute-solute and solute-solvent interactions respectively in the solutions. Molal refractions (R) have been calculated using the Lorentz-Lorenz equation and discussed.

CHAPTER VII

In this chapter apparent molar volumes (V_ϕ), viscosity B-coefficients for Nicotinamide (NA) in (0.03, 0.05, 0.07 and 0.10) mol·dm^{-3} aqueous Citric Acid monohydrate (CA) solutions have been determined from solution density and viscosity measurements at (298.15, 308.15 and 318.15) K as function of concentration of NA. In the investigated temperature range, the relation: $V_\phi^0 = a_0 + a_1 + a_2 T^2$, have been used to describe the temperature dependence of standard partial molar volume V_ϕ^0. This results have, in conjunction with the results obtained in pure water, been used to calculate the standard volumes of transfer ΔV_ϕ^0 and viscosity B-coefficients of transfer for NA from water to aqueous CA solutions for rationalizing various interactions in the ternary solutions. The structure making or breaking ability of NA has been discussed in terms of the sign of $\left[\frac{\partial^2 V_\phi^0}{\partial T^2}\right]_p$ and dB/dT. An increase in the transfer volume of NA with increasing CA concentration has been explained by Friedman-Krishnan co-sphere model. The activation parameters of viscous flow for the ternary solutions studied have also been calculated and explained by the application of transition state theory.

CHAPTER VIII

Here, apparent molar volume (ϕ_V), viscosity B-coefficient, molal refraction (R) and adiabatic compressibility (ϕ_K) of Nicotinic Acid, Ascorbic Acid, and Folic Acid have been determined in 0.01, 0.03, 0.05 mol·dm^{-3} aqueous Cysteine solutions at 298.15 K from density (ρ), viscosity (η), refractive index (n_D) and speed of sound (u) respectively. The limiting apparent molar volumes (ϕ_V^0) and

experimental slopes (S_V^*), derived from the Masson equation, have been interpreted in terms of solute-solvent and solute-solute interactions respectively. The viscosity data were analyzed using the Jones-Dole equation and the derived parameters *A* and *B* have also been interpreted in terms of solute-solute and solute-solvent interactions respectively in the solutions. Using the Lorentz-Lorenz equation, molal refractions (R) have been calculated. At infinite dilution, limiting apparent molar adiabatic compressibilities (ϕ_K^0) of these vitamins were evaluated and discussed.

CHAPTER IX

In this chapter molecular interaction in terms of apparent molar volume (ϕ_V), viscosity *B*-coefficient, apparent molar adiabatic compressibility (ϕ_K) and molal refraction (R) of Glycine, L-Alanine, L-Valine have been structured in 0.01, 0.03, 0.05 mass fraction of aqueous nicotinic acid solutions at 298.15 K. Using the density data to Masson equation, the limiting apparent molar volumes (ϕ_V^0) and experimental slopes (S_V^*) have been obtained at the infinite dilution by extrapolated to zero concentration, which interpreted the solute-solvent and solute-solute interactions, respectively. Similarly, using the Jones-Dole equation the viscosity data were analyzed to determine the viscosity *A* and *B*- coefficient, which have also been interpreted the solute-solute and solute-solvent interaction respectively in the solutions. Molar refractions (R) also signify the solute-solvent interaction; have been calculated from refractive indices by the Lorentz-Lorenz equation. From the ultrasonic speeds, the limiting apparent molar adiabatic compressibilities (ϕ_K^0) of the amino acids at infinite dilution have been evaluated and discussed for the same.

CHAPTER X

This chapter contains the concluding remarks of the works about this thesis.

PREFACE

The work entitled **"EXPLORATION OF INTERACTIONS OF SOME VITAMINS PREVAILING IN LIQUID SYSTEMS BY PHYSICOCHEMICAL CONTRIVANCES"** in the Thesis was initiated in 2009 under the supervision of Dr. M. N. Roy, Prof. of Chemistry in the Department of Chemistry, University of North Bengal. The work is an attempt to explore mainly molecular interaction of some water soluble Vitamins by studying their thermodynamic and acoustic properties.

During the course of my research work through participation in several meets and seminars in this University and across the country, I was highly inspired by listening and interacting with distinguished scientists and experts.

In this research work, I have tried to find out various type of interactions of some water soluble Vitamins with some biologically active solutes so that my findings may help in the manufacturing of different pharmaceutical products.

I must take the responsibility of any unintentional oversights and errors, which might have crept in spite of precautions. In keeping with general practice of reporting scientific observation, due acknowledgement has been made whenever the work described was based on the finding of other investigators.

I hope that the knowledge that I have earned during my research work can be effectively put into action in the future.

ACKNOWLEDGEMENT

At the onset, I am extremely delighted to express my most sincere and wholehearted gratitude to my respected teacher and Research Guide, Dr. Mahendra Nath Roy, Professor, Department of Chemistry, University of North Bengal, Darjeeling. Throughout my research period, I have received unvarying guidance, valuable suggestions, inspiration and constructive criticism from him. I am deeply indebted to him for his keen concern, strong motivation, constant encouragement and sympathetic consideration. Without his loving care, meticulous guidance and priceless supervision, the formulation of my work associated with my thesis in its present form could not have been possible.

I express my deep sense of gratitude to all the respected teachers, Department of Chemistry, University of North Bengal for their helpful assistance and persistent inspiration during the course of my research work. I am thankful to the non-teaching staff of my Department for their kind cooperation and help.

The encouragement, inspiration and whole-hearted cooperation that I received from my parents, other family members and friends are most gracefully acknowledged.

In the long run, I would like to acknowledge my thanks to my beloved wife, Dr. Nayana Bhattacharjya for her sincere help, ceaseless inspiration and wholehearted unconditional enthusiastic cooperation to complete my work. I also would like to mention the name of my loving daughter, Piyal for her curiosity in my research work.

My special thanks go to Dr. Riju Chanda, Dr. Arijit Bhattacharjee, Dr. Rajani Dewan, Mr. Deepak Ekka, Miss Ishani Banik, Miss Tanuasree Ray, Mr. Milan Chandra Roy, Mr. Biswajit Datta, Mr. Saptarshi Basak, of my research laboratory for their valuable assistance and cooperation during my research work and all my well wishers.

I am constantly aware of what a huge debt I owe to the sources of the information required for my research work: the numerous books, articles, monographs, computer website, etc. I put on record some measure of my thanks to those whose references I have cited in this thesis.

I must thank my colleagues of Siliguri Boys' High School, where I am working as an Assistant Teacher in Chemistry, for their support and encouragement in course of my work.

Finally, I am grateful to the Departmental Special Assistance Scheme under the University Grants Commission, New Delhi (No· F 540 / 27 / DRS / 2007, SAP-1) and the 'ONE TIME GRANT' Ref No. F.4-10/2010(BSR) awarded to my Supervisor, Prof. M. N. Roy, under Basic Scientific Research (BSR), UGC, New Delhi for financial and instrumental aid in connection with my research works.

Palash Chakraborti,
Research Scholar,
Department of Chemistry,
University of North Bengal,
Darjeeling–734013, WB, INDIA.

TABLE OF CONTENTS

Topic	Page No.
Declaration	(iii)
Certificate	(iv)
Abstract	(v)-(ix)
Preface	(x)
Acknowledgement	(xi)-(xii)
List of Tables	1-5
List of Figures	7-8
List of Appendices	9
Appendix A: List of Research Publications	10
Appendix B: List of Seminars/Symposiums/Conferences Attended	11
CHAPTER I	13-16
Necessity of the Research Work	
1.1. Objective, Scope and Application of the Research Work	
1.2. Choice of Solvents and Solutes Used	
1.3. Methods of Investigation	
CHAPTER II	17-75
General Introduction	
2.1. Solution Chemistry	
2.2. Interactions in Solution Phase	
2.3. Density	
2.4. Viscosity	
2.5. Ultrasonic Speed	
2.6. Conductance	
2.7. Refractive Index	
CHAPTER III	77-99
Experimental Section	
3.1. Name, Structure, Physical properties, Purification and Applications of the Solutes and Solvents used in the Research work	
3.2. Experimental Methods	

CHAPTER IV 101-124

EXPLORATION OF INTERACTIONS BETWEEN BIOACTIVE SOLUTES AND VITAMIN B9 IN AQUEOUS MEDIUM BY PHYSICOCHEMICAL CONTRIVANCES

4.1. Introduction

4.2. Experimental Section

4.3. Results and Discussion

4.4. Conclusion

Tables & Figures

** Published in Molecular physics,* **2014, 112, 2215-2226**

CHAPTER V 125-148

CONDUCTIVITY IS A CONTRIVANCE TO EXPLORE ION-PAIR AND TRIPLE ION STRUCTURE OF ETHANOATES IN TETRAHYDROFURAN, DIMETHYL SULPHOXIDE AND THEIR BINARIES

5.1. Introduction

5.2. Experimental Section

5.3. Results and Discussion

5.4. Conclusion

Tables & Figures

Published in Fluid Phase Equilibria,* **2012, 322, 159– 166

CHAPTER VI 149-160

EXPLORATION OF MOLECULAR INTERACTIONS OF CARBOHYDRATES IN AQUEOUS VITAMIN-C ENVIRONMENTS WITH MANIFESTATION OF SOLVATION CONSEQUENCES

6.1. Introduction

6.2. Experimental Section

6.3. Results and Discussion

6.4. Conclusion

Tables & Figures

Published in JTRC,* **2013, 20(1), 46-56

CHAPTER-VII 161-181

INVESTIGATION ON MOLECULAR INTERACTIONS OF NICOTINAMIDE IN AQUEOUS CITRIC ACID SOLUTIONS WITH

REFERENCE TO MANIFESTATION OF PARTIAL MOLAR VOLUME AND VISCOSITY *B*-COEFFICIENT MEASUREMENTS

7.1. Introduction

7.2. Experimental Section

7.3. Results and Discussion

7.4. Conclusion

Tables & Figures

***Published in Thermochimica Acta*, 2010, 507, 135-141**

CHAPTER-VIII: 183-196

EXPLORATION OF DIVERSE INTERACTIONS OF SOME VITAMINS IN AQUEOUS MIXTURES OF CYSTEINE

8.1. Introduction

8.2. Experimental Section

8.3. Results and Discussion

8.4. Conclusion

Tables & Figures

***Published in J. Mexican Chemical Society.* 2014, 58(2),106–112**

CHAPTER-IX 197-213

EXPLORATION OF MOLECULAR INTERACTIONS OF SOME STANDARD AMINO ACIDS IN H_2O + VITAMIN-B_3 MIXTURES

9.1. Introduction

9.2. Experimental Section

9.3. Results and Discussion

9.4. Conclusion

Tables & Figures

Communicated

CHAPTER-X 215-217

Concluding Remarks

BIBLIOGRAPHY 219-240

INDEX 241-242

LIST OF TABLES

CHAPTERS	TABLES	PAGE NO.
Chapter IV	**Table 1.** Values of density (ρ), viscosity (η), refractive index (n_D) and ultrasonic speed (u) in different mass fraction (w_1) of aqueous Folic Acid at 298.15K	115
	Table 2 Experimental values of density (ρ), viscosity (η), refractive index (n_D) and ultrasonic speed (u) of amino acids in different mass fraction (w_1) of aqueous Folic Acid (FA) at 298.15K	115
	Table 3. Molarity (m), apparent molar volume (ϕ_v), $(\eta_r-1)/\sqrt{m}$, molar refraction (R_m) and apparent molar adiabatic compressibility (ϕ_K) of amino acids in different mass fraction of aqueous FA (w_1) at 298.15K	117
	Table 4. Limiting apparent molar volumes (ϕ_V^0), experimental slopes (S_V^*), viscosity A, B-coefficients, limiting partial molar adiabatic compressibilities (ϕ_K^0), and experimental slopes (S_K^*) of amino acids in different mass fraction of aqueous FA (w_1) at 298.15K	120
	Table 5. Contributions of zwitter ionic group (NH_3^+, COO^-), CH_2 group, and the other alkyl chains to the limiting apparent molar volume, ϕ_V^0, for amino acids in different mass fraction of aqueous FA (w_1) at 298.15K	121
	Table 6. Values of $\Delta\phi_V^0$, ϕ_V^0(elect), ϕ_K^0(elect), and hydration number (n_H) for amino acids in different mass fraction of aqueous FA (w_1) at 298.15 K	121
	Table 7. Contributions of zwitter ionic group (NH_3^+,	122

	COO^-), CH_2 group, and the other alkyl chains to the *B*-coefficient in different mass fraction of aqueous FA (w_1) at 298.15 K	
	Table 8. Values of A_1, and A_2 coefficient for the amino acids in different mass fraction of aqueous FA at 298.15 K	122
Chapter V	**Table 1.** Physical properties of pure THF, DMSO and different binary mixtures of (THF + DMSO) at 298.15 K.	136
	Table 2 Molar conductivities and corresponding molarities of electrolytes in different binary mixtures of THF + DMSO at 298.15 K.	137
	Table 3. Derived conductance and thermodynamic parameters for different electrolytes in different binary mixtures of THF + DMSO at 298.15 K.	141
	Table 4. Limiting ionic conductance, ionic Walden product, Stoke's radii (r_s) and crystallographic radii (r_c) in different binary mixtures of THF + DMSO at 298.15 K	143
	Table 5 Calculated limiting molar conductance of ion pair and triple ions, slope and intercepts and ion pair and triple ion formation constant for different electrolytes in pure THF at 298.15 K.	144
	Table 6. Maximum concentration, the ion pair fraction (α), triple ion fraction (α_T), ion pair concentration (C_P) and triple ion concentration (C_T) for different electrolytes in pure THF at 298.15 K.	144
Chapter VI	**Table 1** The values of Density (ρ), Viscosity (η) and Refractive index (n_D), in different mass fraction of Ascorbic acid in water at 298.15K	154
	Table 2. . Experimental values of Densities (ρ), Viscosities (η) and Refractive Index (n_D) of D-Glucose, D-	154

	Sucrose and D-Maltose Monohydrate in different mass fraction of Ascorbic acid in water at 298.15K	
	Table 3. Molality, apparent molar volume (ϕ_V), $(\eta/\eta_0-1)/m^{1/2}$ and molar refraction (R),of D-Glucose, D-Sucrose and D-Maltose Monohydrate in different mass fraction of Ascorbic acid in water at 298.15K	**156**
	Table 4. Limiting apparent molar volumes (ϕ_V^0), experimental slopes (S_V^*) and A, B coefficients of D-Glucose, D-Sucrose and D-Maltose Monohydrate in different mass fraction of Ascorbic acid in water at 298.15	**158**
Chapter VII	**Table 1.** Density ρ, and viscosity η, of different aqueous CA solution at different temperatures	**171**
	Table 2. Molarity c, density ρ, viscosity η, apparent molar volumes V_ϕ^0, and $(\eta_r - 1)/c^{1/2}$ for NA in different aqueous CA solutions at different temperatures.	**171**
	Table 3. Limiting Partial molar volume V_ϕ^0, and adjustable parameters A_v and B_v for NA in different aqueous CA acid solutions with standard deviations σ at different temperatures.	**175**
	Table 4. Partial molar volume of NA and (CA + Water) mixtures at different temperatures.	**176**
	Table 5. Values of various coefficients of Eq. 4 for NA in different aqueous CA solutions.	**176**
	Table 6. Partial molar expansibility ϕ_E° for NA in different aqueous CA solutions at different temperatures	**177**
	Table 7. Values of A and B coefficients with standard errors for NA in different aqueous CA solutions at different temperatures.	**177**

	Table 8. Partial molar volumes V_ϕ^0, Partial molar volumes of transfer, ΔV_ϕ^0, viscosity *B*-coefficients, and Viscosity *B*-coefficients of transfer, ΔB, from water to different aqueous CA solutions for NA at three different temperatures.	178
	Table 9. Values of $\overline{V}_1^0$, $\Delta\mu_1^{0*}$, $\overline{V}_2^0 - \overline{V}_1^0$, $\Delta\mu_2^{0*}$, $T\Delta S_2^{0*}$, and ΔH_2^{0*} for NA in different aqueous CA solutions at different temperatures	178
Chapter VIII	**Table 1.** The values of Density (ρ), Viscosity (η), Refractive index (n_D), and Speed of sound (u) in different mass fraction of Cysteine at 298.15K	189
	Table 2. Experimental values of Densities (ρ), Viscosities (η), Refractive Index (n_D) and Ultrasonic Speed (u) of Nicotinic Acid, Ascorbic Acid and Folic Acid in different mass fraction of Cysteine at 298.15K	190
	Table 3. Molality, apparent molar volume (ϕ_V), $(\eta/\eta_0-1)/m^{1/2}$, molar refraction (R), adiabatic compressibility (β) and apparent molal adiabatic compressibility (ϕ_K) of Nicotinic Acid, Ascorbic Acid and Folic Acid in Cysteine at 298.15 K	191
	Table 4. Limiting apparent molar volumes (ϕ_V^0), experimental slopes (S_V^*), *A*, *B* coefficients, limiting partial adiabatic compressibility (ϕ_K^0), and experimental slope (S_K^*) of Nicotinic Acid, Ascorbic Acid, and Folic Acid in aqueous Cysteine at 298.15 K	194
	Table 1. The values of density (ρ), viscosity (η), refractive index (n_D), and speed of sound (u) in different mass	204

Chapter IX	fractions (m_1) of aqueous nicotinic acid (NA) solutions at 298.15K.	
	Table 2. Values of concentration, density (ρ), apparent molar volume, limiting apparent molar volume and experimental slope (obtained from eq. 3) of glycine, L-alanine and L-valine in different mass fractions (m_1) of aqueous nicotinic acid solutions at 298.15K.	**205**
	Table 3. Values of concentration, viscosity (η), $(\eta/\eta_0-1)/m^{1/2}$, Viscosity *A*, *B* coefficients of L -glycine, L-alanine, and L-valine in different mass fractions (m_1) of aqueous nicotinic acid solutions at 298.15K.	**207**
	Table 4. Values of concentration, refractive indices (n_D) and molar refraction (R) of of Glycine, L-alanine and L-valine in different mass fractions (m_1) of aqueous nicotinic acid solutions at 298.15K	**209**
	Table 5. Values of concentration, ultrasonic speed (u), adiabatic compressibility (β), apparent molar adiabatic compressibility (ϕ_K), limiting apparent molar adiabatic compressibility (ϕ_K^0), and experimental slope (S_K^*) (obtained from eq. 8) of Glycine, L-alanine, and L-valine in different mass fractions (m_1) of aqueous nicotinic acid solutions at 298.15K	**210**

LIST OF FIGURES

CHAPTERS	FIGURES	PAGE NO.
Chapter IV	**Figure 1.** Plot of limiting apparent molar volume (ϕ_V^o) for glycine (♦), alanine (▲), valine (●), and limiting molar isentropic compressibility (ϕ_K^o) for glycine (◊), alanine (Δ), valine (○), against mass fraction of aq. FA (w_1) respectively	123
	Figure 2. Plot of Viscosity *B*-coefficient for glycine (♦), alanine (▲) and valine (●) Vs mass fraction of aq. FA (w_1)	123
Chapter V	**Figure 1:** Plots of Walden product ($\Lambda^o\eta$) of CH_3COONH_4 (x), CH_3COOK (▯), CH_3COONa (■) and CH_3COOLi (▲) in different THF + DMSO binary mixtures containing 0, 25, 50, and 75 mass % of THF at 298.15 K.	145
	Figure 2: Plots of Ionic Walden product ($\lambda^o_{\pm}\eta$) of NH_4^+(x), K^+ (♦), Na^+(■) and Li^+(▲) in different THF + DMSO binary mixtures containing 0, 25, 50, and 75 mass % of THF at 298.15 K.	145
	Figure 3: Plots of Gibbs energy of ion-pair formation (ΔG^o) of CH_3COONH_4 (x), CH_3COOK (♦), CH_3COONa (■) and CH_3COOLi (▲) in different THF + DMSO binary mixtures containing 0, 25, 50, and 75 mass % of THF at 298.15 K.	146
Chapter VI	**Figure 1:** The plots of limiting apparent molar volumes (ϕ_V^0) for D-Glucose (—♦—), D-Sucrose (—■—), D-Maltose Monohydrate (—▲—) in different mass fractions (w_1) of ascorbic acid in aqueous mixture at 298.15K	159
	Figure 2: The plots of viscosity *B*-coefficient for D-Glucose (—♦—), D-Sucrose (—■—), D-Maltose Monohydrate (—▲—) in different mass fractions (w_1) of ascorbic acid in aqueous mixture at 298.15K.	159
Chapter VII	**Figure 1:** Plots of partial molar volume (ΔV_ϕ^0) and viscosity *B*-coefficients (ΔB) against molarity for the transfer from water to different aqueous CA solutions for NA at T = 298.15 K. Dotted lines for ΔV_ϕ^0 and solid lines for ΔB.	180

	Figure 2: Plots of partial molar volume (ΔV_ϕ^0) and viscosity *B*-coefficients (ΔB) against molarity for the transfer from water to different aqueous CA solutions for NA at T = 308.15 K. Dotted lines for ΔV_ϕ^0 and solid lines for ΔB.	180
	Figure 3: Plots of partial molar volume (ΔV_ϕ^0) and viscosity *B*-coefficients (ΔB) against molarity for the transfer from water to different aqueous CA solutions for NA at T = 318.15 K. Dotted lines for ΔV_ϕ^0 and solid lines for ΔB.	181
Chapter VIII	**Figure 1:** The plots of limiting apparent molar volumes (ϕ_V^0) for Nicotinic Acid (—♦—), Ascorbic Acid (—■—), Folic Acid (—▲—) in different mass fractions (w_1) of Cysteine in aqueous mixture at 298.15K	195
	Figure 2: The plots of viscosity *B*-coefficient for Nicotinic Acid (—♦—),Ascorbic Acid (—■—), Folic Acid (—▲—) in different mass fractions (w_1) of Cysteine in aqueous mixture at 298.15K	195
	Figure 3: The plots of limiting partial adiabatic compressibility (ϕ_K^0) for Nicotinic Acid (—♦—), Ascorbic Acid (—■—), Folic Acid (—▲—) in different mass fractions (w_1) of Cysteine in aqueous mixture at 298.15K	196
Chapter IX	**Figure 1.** Plot of $\phi_V^\circ \cdot 10^6/m^3 \cdot mol^{-1}$ of Glycine (—♦—), L-Alanine (—■—) and L- Valine (—▲—) in different mass fractions (m_1) of aqueous nicotinic acid solutions at 298.15K.	212
	Figure 2. Plot of B /$kg^{1/2}$ $mol^{-1/2}$ of Glycine (—♦—), L-Alanine (—■—) and L- Valine (—▲—) in different mass fractions (m_1)of aqueous nicotinic acid solutions at 298.15K.	212
	Figure 3. Plot of ϕ_K x 10^{10} (m^3 mol^{-1} Pa^{-1}) of Glycine (—♦—), L-Alanine (—■—) and L- Valine (—▲—) in different mass fractions (m_1) of aqueous nicotinic acid solutions at 298.15K	213

LIST OF APPENDICES

APPENDIX A:

LIST OF RESEARCH PUBLICATION(S)

APPENDIX B:

LIST OF SEMINARS/SYMPOSIUMS/CONVENTIONS ATTENDED

APPENDIX A

LIST OF RESEARCH PUBLICATION(S)

1. Exploration of Interactions Between Bioactive Solutes and Vitamin B9 in Aqueous Medium by Physicochemical Contrivances.

   ***Molecular Physics,* 2014, 112, 2215-2226**

2. Conductivity is a Contrivance to Explore ion-pair and triple-ion structure of Ethanoates in Tetrahydrofuran, Dimethyl sulphoxide and their binaries.

   ***Fluid Phase Equilibria,* 2012, 322, 159- 166**

3. Exploration of Molecular Interactions of Carbohydrates in Aqueous Vitamin-C Environments with Manifestation of Solvation Consequences.

   ***JTRC,* 2013, 20(1), 46-56**

4. Investigation on Molecular Interactions of Nicotinamide in Aqueous Citric Acid Solutions with Reference to Manifestation of Partial Molar Volume and Viscosity *B*-Coefficient Measurements.
   ***Thermochimica Acta,* 2010, 507,135-141**

5. Exploration of Diverse Interactions of Some Vitamins in Aqueous Mixtures of Cysteine.
   ***J. Mexican Chemical Society.* 2014, 58(*2*), 106–112**

6. Exploration of Molecular Interactions of Some Standard Amino Acids in H_2O+Vitamin-B_3 Mixtures.
   Communicated and under review in the *Journal of Indian Chemical Society.*

APPENDIX-B

LIST OF SEMINARS/ SYMPOSIUMS/ CONFERENCES ATTENDED

1. Presented a poster in 12th CRSI National Symposium in Chemistry held at **Indian Institute of Chemical Technology, Hyderabad** and National Institute of Pharmaceutical Education and Research (NIPER) Hyderabad during February 4-7, 2010.

2. Presented a poster in Chemical Research Society of India, Eastern Zonal Meeting 2011 and Celebration of the International year of Chemistry 2011, July 22-24, 2011 organized by **Department of Chemistry, University of North Bengal, Darjeeling.**

3. Participated in the Science Academies' Lecture Workshop on Recent Trends in Chemistry, November 11-12, 2011, organized by the **Department of Chemistry, University of North Bengal, Darjeeling.**

4. Participated in the Science Academies' Lecture Workshop on Recent Trends in Chemistry, November 22-23, 2012, organized by the **Department of Chemistry, University of North Bengal, Darjeeling**

5. Presented a poster in 15th CRSI National Symposium in Chemistry held at Banaras Hindu University, Varanasi during February 1-3, 2013, organized by **Department of Chemistry, Faculty of Science, Banaras Hindu University, Varanasi.**

6. Participated and presented a poster in Workshop on **"Diversities and Frontiers in Chemistry"** held at the **Department of Chemistry, University of North Bengal,** on August, 7-8th, 2013, Sponsored by West Bengal State Council of Higher Education [SUN], West Bengal.

CHEPTER-I

NECESSITY OF THE RESEARCH WORK

1.1. OBJECTIVE, SCOPE AND APPLICATION OF THE RESEARCH WORK

When a small amount of substance, called solute (solid, liquid or gas), dissolves to a certain limit in a liquid or solid substance (pure, or a mixture itself) called the solvent, then this mixture between dissimilar components is known as 'solution'. In general, solutions are more complex than assemblies of weakly interacting molecules. An investigation shows that in solution a large assembly of molecules held together by non-covalent interactions.

Vitamins are vital nutrients [1] that an organism requires in limited amounts. They are essential precursors for various coenzymes. These coenzymes are therefore required in almost all metabolic pathways. Other bio-active solutes such as amino acids, carbohydrates also serve as adjusting factors in human body due to their physiological activity. Various methods have been developed to enhance the level of bioactive components in food materials, including thermal, alkali, acid and chemical treatments.

The physical and chemical properties, of a solution (liquid) are a result of the strength of their intermolecular forces and the forces between molecules arises from the same source, differing charges on adjacent molecules that lead to electrostatic attractions and governed by coulombs law. Partial charges acquired by molecules results in dipole-dipole forces, dipole-induced dipole forces, hydrogen bonding, etc and are collectively termed as intermolecular forces. Intermolecular forces in a solution control their thermodynamic properties and the understanding of the solvation thermodynamics is essential to the characterization and interpretation of any process carried out in liquid phase. These thermodynamic properties are quantities which are either an attribute of an entire system or are functions of position which is continuous and does not vary rapidly over

microscopic distances, except in cases where there are abrupt changes at boundaries between phases of the system.

Studies on the thermodynamic along with the transport properties of a solution would give a clear idea about the nature of the forces existing within the constituents of a solution. Hence, the main objective of the present research work is to investigate and to understand the interactions prevailing in solutions by studying their thermodynamic and transport properties.

The study of molecular interaction in fluids by thermodynamic methods has attracted attention, as thermodynamic parameters are convenient for interpreting intermolecular interaction patterns in non-electrolytic solvent mixtures involving both hydrogen bonding and non-hydrogen bonding solvents. The different sequence of solubility, difference in solvating power and possibilities of chemical or electrochemical reactions unfamiliar in aqueous chemistry have open vistas for chemists and interest in the organic solvents transcends the traditional boundaries of inorganic, physical, organic, analytical and electrochemistry [2].

The thermodynamic and transport properties are of great importance in characterizing the properties and structural aspects of solutions. The sign and magnitude of partial molar volume (ϕ_V^0), a thermodynamic quantity, provides information about the nature and magnitude of solute-solvent interaction while the experimental slope (S_v^*) provides information about solute-solute interactions [3]. Valuable information about the nature and strength of forces operating in solutions can be obtained from viscosity data. Properties derived from experimental density, viscosity and speeds of sound data and subsequent interpretation of the nature and strength of intermolecular interaction help in testing and development of various theories of solution. Recently the use of computer simulation of molecular dynamics has led to significant improvement towards a successful molecular theory of transport properties in fluids and a proper understanding of molecular motions and interaction patterns in non-electrolytic solvent mixtures involving both hydrogen bonding and non-hydrogen bonding solvents has been established [4,5].

The refractive index is an important physical property of liquids and liquid mixtures, which affects the solution of different problems in chemical engineering in order to develop industrial processes. Knowledge of refractive index of

multicomponent mixtures provides information regarding the interactions in these mixtures [6-8] which is essential for many physicochemical calculations, including the correlation of refractive index with density [9-11].

The study of physico-chemical behaviours like dissociation or association from acoustic measurements and from the calculation of isentropic compressibility has gained much importance. The acoustic measurements can also be used for the test of various solvent theories and statistical models and are quite sensitive to changes in ionic concentrations as well as useful in elucidating the solute-solvent interactions. The importance and use of the chemistry of electrolytes in non-aqueous and mixed solvents are well-recognised. However, the studies on properties of aqueous solutions have provided sufficient information on the thermodynamic properties of different electrolytes and non-electrolytes, the effects of variation in structure, mobility along with a host of other properties [12]. The solute-solute and solute–solvent interactions have been subject of wide interest and have been explicitly presented in Faraday Trans. of the Chemical Society [13].

Drug transport across biological cells and membranes is dependent on physicochemical properties of drugs. But direct study of the physico-chemical properties in physiological media such as blood, intracellular fluids is difficult to accomplish. One of the well-organized approaches is the study of molecular interactions in fluids by thermodynamic methods as thermodynamic parameters are convenient for interpreting intermolecular interactions in solution phase. Also the study of thermodynamic properties of drug in a suitable medium can be correlated to its therapeutic effects [14,15].

1.2. CHOICE OF SOLUTES AND SOLVENTS USED

Important chemicals have been used in this research work are Ascorbic acid(vitamin C), Nicotinic acid/Nicotinamide(vitamin B3), Folic acid(vitamin B9), Glycine, L-Alanine, L-Valine, Cysteine(amino acids), D-Glucose, D-Sucrose, D-Maltose monohydrate, Citric acid monohydrate, Lithium acetate, Sodium acetate, Potassium acetate, Ammonium acetate, Tetrahydrofuran(THF), Dimethylsulphoxide(DMSO), Water, having wide use in pharmaceutical industries.

1.3. METHODS OF INVESTIGATION

It is of interest to employ different experimental techniques to get a better insight into the phenomena of solvation and different interactions prevailing in solution. We have, therefore, employed some important methods, namely, densitometry, viscometry, conductometry, ultrasonic interferometry and refractometry to probe the problem of solvation phenomena. The study of various interactions and equilibrium of solute and solvent in different concentration regions are of immense importance to the technologist and theoretician as most of the chemical processes occurs in these systems.

Thermodynamic properties, like partial molar volumes obtained from density measurements, are generally convenient parameters for interpreting solute-solvent and solute-solute interactions in solution. The compressibility, a second derivative to Gibbs energy, is also a sensitive indicator of molecular interactions and can provide useful information in such cases where partial molar volume data alone cannot provide an unequivocal interpretation of these interactions.

Viscosity *B*-coefficients provides satisfactory interpretation of solute-solvent interactions such as the effects of solvation, structure-breaking or structure-making, polarization, etc. is quite useful in different studies related to ionic and molecular interactions.

CHAPTER II

GENERAL INTRODUCTION

2.1 SOLUTION CHEMISTRY:

Solution Chemistry is an important branch of physical chemistry which studies the change in properties that arise when solute dissolves in solvent . The mixing of different solute or solvent with another solvent/solvent mixtures gives rise to solutions that generally do not behave ideally. This deviation from ideality is expressed in terms of many thermodynamic parameters. These thermodynamic properties of solution corresponds to the difference between the actual property and the property if the system behaves ideally and thus are useful in the study of molecular interactions and arrangements. Knowledge of the thermodynamic properties is essential for the proper design of industrial processes. Measurements of the bulk properties, such as viscosities and densities of liquids, measurement of refractive indices, sound velocity- provides insight into the molecular arrangement in liquids and help one to understand the thermodynamic properties of liquid mixtures.

Vitamins are organic compounds which are needed in small quantities to sustain life. We get vitamins from food, because the human body either does not produce enough of them, or not at all. Vitamin is a vital nutrient that an organism requires in limited amounts. They are essential precursors for various coenzymes. These coenzymes are therefore required in almost all metabolic pathways [1].

SOME WATER SOLUBLE VITAMINS:

Vitamin C is required for the synthesis of collagen, the intercellular "cement" which gives the structure of muscles, vascular tissues, bones, and tendon. Importantly Ascorbic acid (vitamin C) is also able to regenerate other antioxidants as vitamin E. Vitamin C with Zn is also important for the healing of wounds. It is also needed for the metabolism of bile acids which may have implications for blood

cholesterol levels and gallstones. Ascorbic acid and its sodium, potassium, and calcium salts are commonly used as antioxidants food additives. Vitamin C plays an important role for the synthesis of several important peptide hormones neurotransmitters and creatinine. It also enhances the eye's ability and delay the progression of advanced age related muscular degeneration.

Vitamin B3 is a water-soluble vitamin, an essential micronutrient and a reactive moiety of the coenzyme nicotinamide adenine dinucleotide (NAD).[2] It is sometimes referred to as nothing more than vitamin PP (Pellagra Preventive) [3,4], since its deficiency in human diet causes pellagra. It is an essential part of the coenzyme – nicotinamide adenine dinucleotide phosphate (NADP), its reduced form NADPH, NAD and its reduced form NADH. It also serves to maintain normal function of the digestive systems and cholesterol levels in human body [1].The combination of nicotinic acid and nicotinamide is clinically referred as niacin [3-5], since nicotinic acid is converted in the body into the amide very fast and for nutritional purposes both of them have equal biological activities. NA is an interesting molecule because of its two nitrogen atoms – one in the heterocyclic ring and the other as the amide group.

Folic acid (also known as folate, vitamin M, vitamin B9, vitamin B_c (or folacin), pteroyl-L-glutamic acid, pteroyl-L-glutamate, and pteroylmonoglutamic acid) is water-soluble vitamin. Folic acid (FA) is composed of three components: an aromatic pteridine ring system (Pteridine), a *p*-amino benzoic acid (PABA) portion and the amino acid glutamic acid (Glu).. It is an essential vitamin that is yellow-orange in color, is reported to be present in photosensitive organs, various mammalian metabolic pathways, and possibly involved in photosynthesis [6]. Folic acid is itself not biologically active, but its biological importance is due to tetrahydrofolate and other derivatives after its conversion to dihydrofolic acid in the liver [7]. Humans cannot synthesize folate de novo; therefore, folate has to be supplied through the diet to meet their daily requirements. The human body needs folate to synthesize DNA, repair DNA, and methylate DNA as well as to act as a cofactor in certain biological reactions [8]. It is especially important in aiding rapid cell division and growth, such as in infancy and pregnancy, and reproduction of cells, particularly red blood cells. Children and adults both require folic acid to produce healthy red blood cells and prevent anemia [9]. Folate is also necessary for the

production and maintenance of new cells, for DNA synthesis and RNA synthesis, and for preventing changes to DNA, and, thus, for preventing cancer [10].

Bio-active solutes such as amino acids[11], carbohydrates also serve as adjusting factors in human body due to their physiological activity. Various methods have been developed to enhance the level of bioactive components in food materials, including thermal, alkali, acid and chemical treatments.

2.2 INTERACTIONS IN SOLUTION PHASE

There are three types of interactions in the solution process:

a. **Solvent - solvent interactions**: energy required to break weak bonds between solvent molecules.

b. **Solute - solute interactions**: energy required to break intermolecular bonds between the solute molecules.

c. **Solute - solvent interactions**: ΔH is negative since bonds are formed between them.

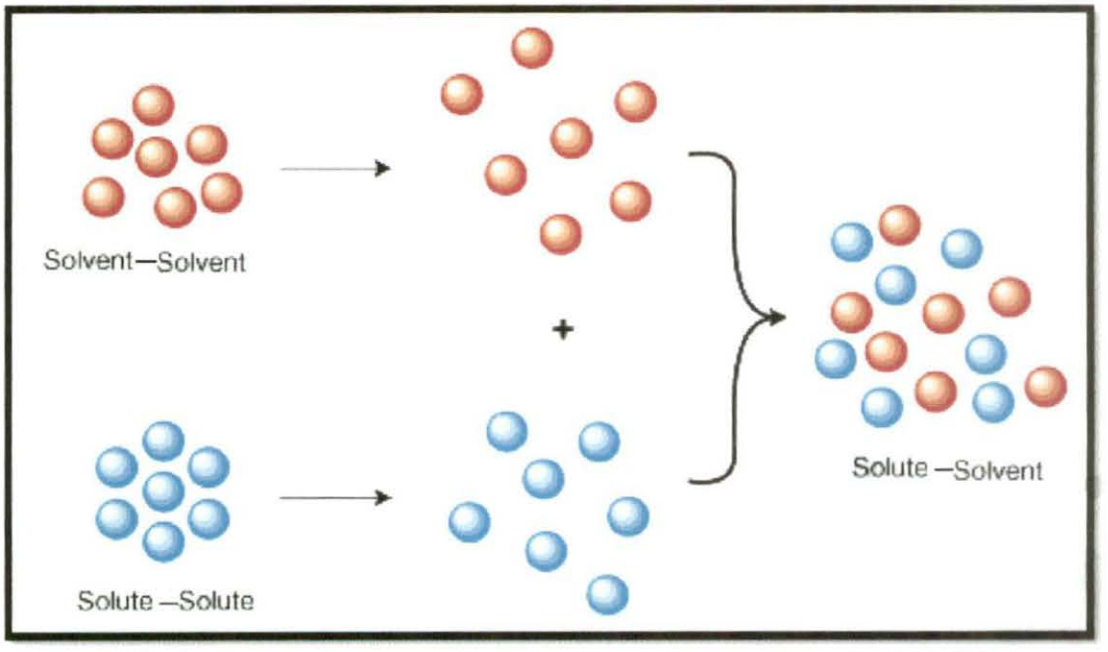

For liquid systems, the macroscopic properties are usually quite well known, whereas the microscopic structure is often much less studied. The liquid phase is characterized by local order and long-range disorder, and to study processes in liquids, it is therefore valuable to use methods that probe the local surrounding of

the constituent particles. The same is also true for solvation processes, a local probe is important to obtain insight into the occuring physical and chemical processes.

2.3 VARIOUS FORCES OF ATTRACTION

Intermolecular forces are forces of attraction or repulsion which act between surrounding particles (atoms, molecules or ions). In a molecule the forces binding atoms are due to chemical bonding. The energy required to break a bond is called the bond-energy. For example the average bond-energy for O-H bonds in water is 463kJ/mol. The forces holding molecules together are generally called intermolecular forces. The energy required to break molecules apart is much smaller than a typical bond-energy, but intermolecular forces play important roles in determining the properties of a substances. Intermolecular forces are particularly important in terms how molecules interact and form biological organisms or even life. This link gives an excellent introduction to the interactions between molecules.

In general, intermolecular forces can be divided into several categories. The prominent types are:

Dipole-dipole forces: Substances, whose molecules have dipole moment have higher melting point or boiling point than those of similar molecular mass, having no dipole moment.

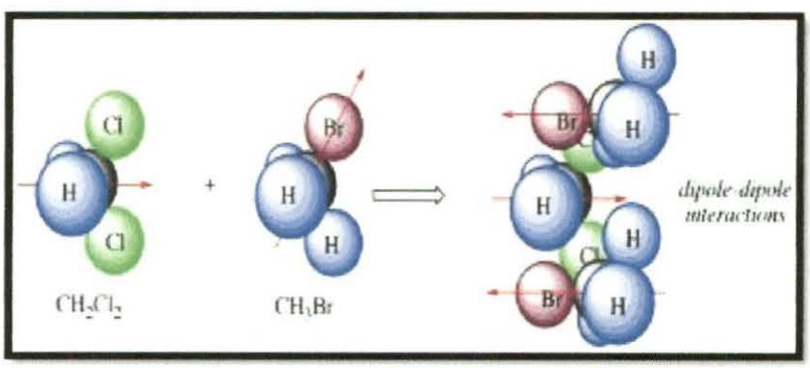

London dispersion forces or van der Waal's force: These forces always operate in any substance. The force arisen from induced dipole and the interaction is weaker than the dipole-dipole interaction. In general, the heavier the molecule, the stronger the van der Waal's force of interaction. For example, the boiling points of

inert gases increase as their atomic masses increases due to stronger Landon dispersion interactions.

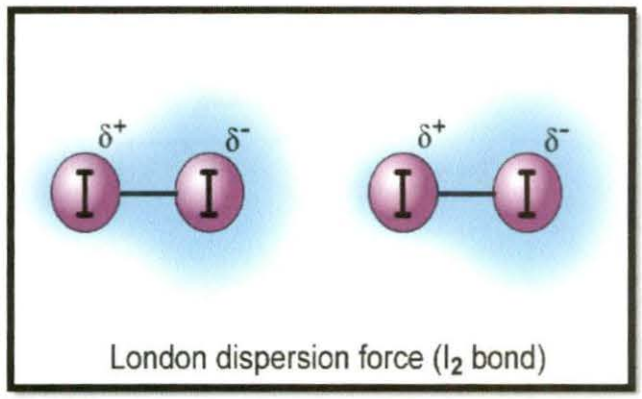

Hydrogen bond: Hydrogen bond is the attractive interactive force of a hydrogen atom with an electronegative atom, such as nitrogen, oxygen or fluorine. The hydrogen must be covalently bonded to another electronegative atom to create the bond. These bonds can occur between molecules (*intermolecularly*), or within different parts of a single molecule (*intramolecularly*). The hydrogen bond (5 to 30 kJ/mole) is stronger than a van der Waals interaction, but weaker than covalent or ionic bonds. This type of bond occurs in both inorganic molecules such as water and organic molecules such as DNA. Certain substances such as H_2O, HF, NH_3 form hydrogen bonds, and the formation of which affects properties (m.p, b.p, solubility) of substance.

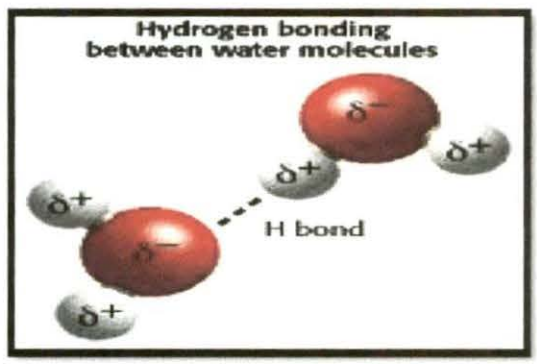

Other compounds containing OH and NH_2 groups also form hydrogen bonds. Molecules of many organic compounds such as acids, alcohols, amines, and amino acids contain these groups, and thus hydrogen bonding plays an important role in biological science.

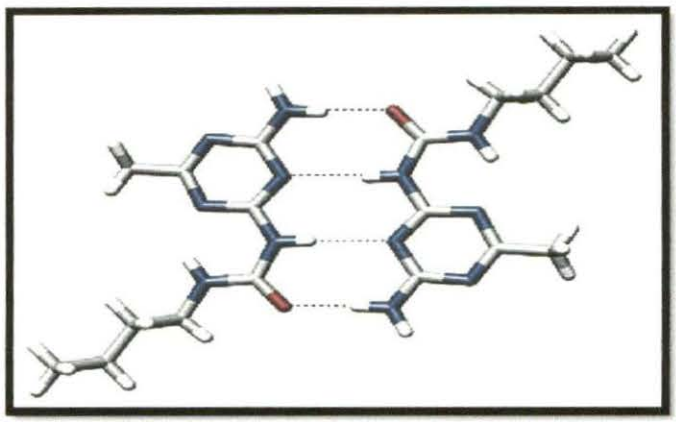

Intermolecular hydrogen bonding in a self-assembled dimer complex

Covalent bonding: Covalent is really intramolecular force rather than intermolecular force. It is mentioned here, because some solids are formed due to covalent bonding. For example, in diamond, silicon, quartz etc., the all atoms in the entire crystal are linked together by covalent bonding. These solids are hard, brittle, and have high melting points. Covalent bonding holds atoms tighter than ionic attraction.

Strong ionic attraction: It has relations to properties of solids. The more ionic compound has the higher lattice energy. The following result can be explained by way of ionic attraction: LiF, 1036; LiI, 737; KF, 821; MgF_2, 2957 kJ/mol.

Metallic bonding: Forces between atom in metallic solids belong to another category. Valence electrons in metals are rampant. They are not restricted to certain atoms or bonds. Rather they run freely in the entire solid, providing good conductivity for heat and electric energy. These behaviours of electrons give special properties such as ductility and mechanical strength to metals.

All types can be present simultaneously for many substances. Usually, intermolecular forces are discussed together with "The States of Matter". Intermolecular forces also play important roles in solutions. A summary of the interactions is illustrated in the following diagram:

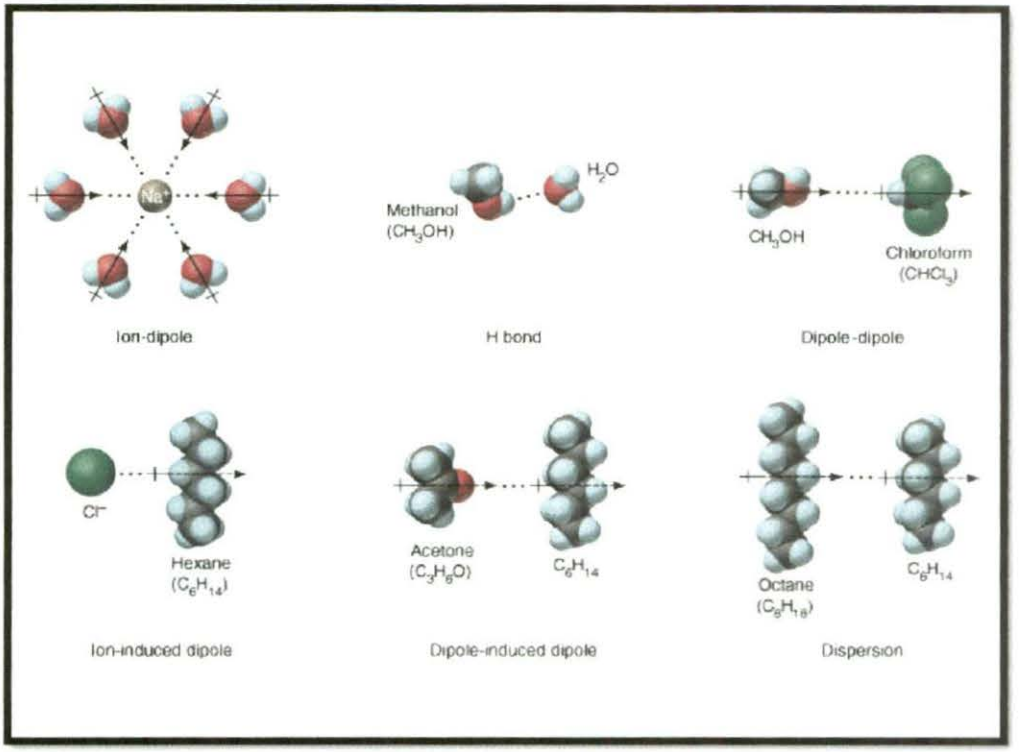

The majority of reactions occurring in solutions are of chemical or biological in nature. It was presumed earlier that the solvent only provides an inert medium for chemical reactions. The significance of solute-solvent interactions was realized after intensive studies in aqueous, non-aqueous and mixed solvents [12,13]. Intermolecular forces are also important in determining the solubility of a substance. "Like" intermolecular forces for solute and solvent will make the solute soluble in the solvent. In this regard ΔH_{soln} is sometimes negative and sometimes positive.

2.4 INVESTIGATION ON DIFFERENT KIND OF INTERACTIONS

One of the causes for the intricacies in solution chemistry is that the structure of the solvent molecule is not known with certainty. The introduction of a solute also modifies the solvent structure to an uncertain magnitude whereas the solute molecule is also modified and the interplay of forces like solute-solute, solute-solvent and solvent-solvent interactions become predominant though the isolated picture of any of the forces is still not known completely to the solution chemist.

The determination of thermodynamic, acoustic, transport and optical properties of different solutes in various solvents would thus provide an important

step in this direction. Naturally, in the development of theories, much attention has been devoted to solute-solvent interactions which are the controlling forces in infinitely dilute solutions where solute-solute interactions are absent.

The problems of solute-solvent interactions which are closely akin to salvation of solute can be studied from different angles using almost all the available physico-chemical techniques.

The solute-solvent interactions can also be studied from the thermodynamic point of view where the changes of free energy, enthalpy and entropy, etc. associated with a particular reaction can be qualitatively and quantitatively evaluated using various physico-chemical techniques from which conclusions regarding the factors associated with the solute-solvent interactions can be worked out.

Similarly, interactions in solution can be studied using solvational approaches involving the studies of different properties such as, density, viscosity, ultrasonic speed, refractive index and conductance of solutes/electrolytes and various derived factors associated with solvation.

We shall particularly reside upon the different aspects of these thermodynamic, transports, acoustic and optical properties as the present research work is familiarly related to the studies of solute-solute, solute-solvent and solvent-solvent interactions.

2.4.1 SOLUTE-SOLVENT INTERACTION

Solvation is a phenomenon of primary interest in many contexts of chemistry because solvated molecules/ions are omnipresent on Earth. Hydrated molecules/ions occur in aqueous solution in many chemical and biological systems [14]. Solvated molecules/ions appear in high concentrations in living organisms, where their presence or absence can fundamentally alter the functions of life. Solutes solvated in organic solvents or mixtures of water and organic solvents are also very common [15]. The exchange of solvent molecules around solutes in solutions is fundamental to the understanding of the reactivity of solutes in solution [16]. Solvated ions also play a key role in electrochemical applications, where for instance the conductivity of electrolytes depends on ion-solvent interactions [17].

The majority of reactions occurring in solutions are chemical or biological in nature. It was presumed earlier that the solvent only provides an inert medium for chemical reactions. The significance of ion-solvent interactions was realized after extensive studies in aqueous, non-aqueous and mixed solvents [18-27]. Most chemical processes of individual and biological importance occur in solution. The role of solvent is so great that million fold rate changes take place in some reactions simply by changing the reaction medium. Our bodies contain 65 to 70 % water, which acts as a lubricant, as an aid to digestion and more specifically as a stabilizing factor to the double helix conformations of DNA. With the exceptions of heterogeneous catalytic reactions most reactions in technical importance occur in solutions. In addition, molecules not only have to travel through a solvent to their reaction partner before reacting, but also need to present a sufficiently unsolvated rate for collision. The solvent governs the movement and energy of the reacting species to such an extent that a reaction suffers a several-million fold change in rate when the solvent is changed. As water is the most abundant solvent in nature and its major importance to chemistry, biology, agriculture, geology, etc., water has been extensively used in kinetic and equilibrium studies. But still our knowledge of molecular interactions in water is extremely limited.

Moreover, the uniqueness of water as a solvent has been questioned [28,29] and it has been realized that the studies of other solvent media like non aqueous and mixed solvents would be of great help in understanding different molecular interactions and a host of complicated phenomena. The organic solvents have been classified on the basis of dielectric constants, organic group types, acid base properties or association through hydrogen bonding [27] donor-acceptor properties [30,31] hard and soft acid-base principles [32] etc. As a result, the different solvents show a wide divergence of properties ultimately influencing their thermodynamic, transport and acoustic properties in presence of electrolytes and non electrolytes in these solvents. The determination of thermodynamic, transport and acoustic properties of different electrolytes or non electrolytes in various solvents would thus provide important information in this direction. Henceforth, in the development of theories of electrolytic solutions, much attention has been devoted to the controlling forces-'ion-solvent interactions' in infinitely dilute solutions wherein ion-ion interactions are almost absent. By separating these functions into

ionic contributions, it is possible to determine the contributions due to cations and anions in the solute-solvent interactions. Thus ion-solvent interactions play a key role to understand the physico-chemical properties of solutions. One of the causes for the intricacies in solution chemistry is the uncertainty about the structure of the solvent molecules in solution. The introduction of a solute modifies the solvent structure to an uncertain magnitude, the solvent molecule and the interplay of forces like solute-solute, solute-solvent also modify the solute molecule and solvent-solvent interactions become predominant, though the isolated picture of any of the forces is still not known completely to the solution chemist. Ion-solvent interactions can be studied by spectrometry [33,34]. The spectral solvent shifts or the chemical shifts are able determine the qualitative and quantitative nature of ion-solvent interactions. But even qualitative or quantitative apportioning of the solute-solvent interactions into the various possible factors is still an mounting task. It is thus apparent that the real understanding of the solute-solvent interaction is a tricky task. The aspect embraces a wide range of topics but we concentrated only on the measurement of transport properties like viscosity, conductance etc. and such thermodynamic properties as apparent and partial molar volumes and apparent molal adiabatic compressibility.

2.4.2 SOLVENT-SOLVENT INTERACTION

As the mixed and non-aqueous solvents are increasingly used in chromatography, solvent extraction, in the elucidation of reaction mechanism, in preparing high density batteries, etc. a number of molecular theories, based on either the radial distribution function or the choice of suitable physical model, have been developed for mixed solvents. Theories of perturbation type have been extended from their successful applicability in pure solvents to mixed solvents. L. Jones and Devonshire [35] were first to evaluate the thermodynamic functions for a single fluid in terms of interchange energy parameters. They used "Free volume" or "Cell model". Prigogine and Garikian [36] extended the above approach to solvent mixtures. Random mixing of solvents was their main assumption provided the molecules have similar sizes. Prigogine and Bellemans [37] developed a two fluid version of the cell model. They found that while excess molar volume (V^E) was negative for mixtures with molecules of almost same size, it was large positive for

mixtures with molecules having small difference in their molecular sizes. Treszczanowicz *et al.* [38] suggested that V^E is the result of several contributions from several opposing effects. These may be divided arbitrarily into three types, viz., physical, chemical and structural.

Physical contributions contribute a positive term to V^E. The chemical or specific intermolecular interactions result in a volume decrease and contribute negative values to V^E. The structural contributions are mostly negative and arise from several effects, especially from interstitial accommodation and changes in the free volume. The actual volume change would therefore depend on the relative strength of these effects. However, it is generally assumed that when V^E is negative, viscosity deviation ($\Delta\eta$) may be positive and vise-versa. This assumption is not a concrete one, as evident from some studies [39,40]. It is observed in many systems that there is no simple correlation between the strength of interaction and the observed properties. Rastogi *et al.*[41] therefore suggested that the observed excess property is a combination of an interaction and non-interaction part. The non-interaction part in the form of size effect can be comparable to the interaction part and may be sufficient to reverse the trend set by the latter. Based on the principle of corresponding states as suggested by Pitzer [42], L. Huggins [43] introduced a new approach in his theory of conformal solutions. Using a simple perturbation approach, he showed that the properties of mixtures could be obtained from the knowledge of intermolecular forces and thermodynamic properties of the pure components.

Recently, Rowlinson *et al.* [44-46] reformulated the average rules for Vander Waal's mixtures and their calculated values were in much better agreement with the experimental values even when one fluid theory was applied. The more recent independent effort is the perturbation theory of Baker and Henderson [47]. A more successful approach is due to Flory who made the use of certain features of cell theory [48-50] and developed a statistical theory for predicting the excess properties of binary mixtures by using the equation of state and the properties of pure components along with some adjustable parameters. This theory is applicable to mixtures containing components with molecules of different shapes and sizes. Patterson and Dilamas [51] combined both Prigogine and Flory theories to a unified one for rationalizing various contributions of free volume, internal pressure, etc. to

the excess thermodynamic properties. Recently, Heintz [52-54] and coworkers suggested a theoretical model based on a statistical mechanical derivation and accounts for self-association and cross association in hydrogen bonded solvent mixtures is termed as Extended Real Associated Solution model (ERAS). It combines the effect of association with non-associative intermolecular interaction occurring in solvent mixtures based on equation of state developed originally by Flory *et al.* [40-42]. Subsequently the ERAS model has been successfully applied by many workers [55-57] to describe the excess thermodynamic properties of alkanol-amine mixtures. Recently, a new symmetrical reformation on the Extended Real Association (ERAS) model has been described in the literature[58]. The symmetrical-ERAS (S-ERAS) model makes it possible to describe excess molar enthalpies and excess molar volumes of binary mixtures containing very similar compounds described by extremely small mixing functions. The symmetrical Extended Real Associated Solution Model (S-ERAS) is, in fact, a simple continuation of the ERAS model. It was developed in order to widen its applicability to the thermodynamic properties of systems that could not be satisfactorily described. by the equations of the ERAS model [58,59]. Gepert *et al.* [60] applied this model for studying some binary systems containing alcohols.

2.4.3 SOLUTE-SOLUTE INTERACTION

Solute-solute interaction in dilute solutions is now theoretically well understood, but solute-solvent interactions or solvation still remains a complex process. The degree of this interactions affects the properties of solution and depends on the nature of solute under investigation. While proton transfer reactions are particularly sensitive to the nature of the solvent, it has become cleared that the solvents significantly modify the majority of the solutes. Conversely, the nature of the strongly structured solvents, such as water, is substantially modified by the presence of solutes. Complete understanding of the phenomena of solution chemistry will become a reality only when solute-solute, solute-solvent and solvent-solvent interactions are elucidated and thus the present dissertation is intimately related to the studies of solute-solute, solute-solvent and solvent-solvent interactions in some solvent media.

2.5. DENSITY

The physicochemical properties of liquid mixtures have attracted much attention from both theoretical and engineering applications points of view. Many engineering applications require quantitative data on the density of liquid mixtures. They also provide information about the nature and molecular interactions between liquid mixture components.

The volumetric information includes 'Density' as a function of weight, volume and mole fraction and excess volumes of mixing. One of the well-recognized approaches to the study of molecular interactions in fluids is the use of thermodynamic methods. Thermodynamic properties are generally convenient parameters for interpreting solute-solvent and solute-solute interactions in the solution phase. Fundamental properties such as enthalpy, entropy and Gibbs energy represent the macroscopic state of the system as an average of numerous microscopic states at a given temperature and pressure. An interpretation of these macroscopic properties in terms of molecular phenomena is generally difficult. Sometimes higher derivatives of these properties can be interpreted more effectively in terms of molecular interactions. The volumetric information may be of immense importance in this regard. Various concepts regarding molecular processes in solutions like electrostriction [61], hydrophobic hydration [62], micellization [63] and co-sphere overlap during solute-solvent interactions [64] have been derived and interpreted from the partial molar volume data of many compounds.

2.5.1. APPARENT AND PARTIAL MOLAR VOLUMES

Density data can be used for the calculation of molar volume of a pure substance. However, the volume contributed to a solvent by the addition of one mole of solute is difficult to determine. This is so because, upon entry into the solvent, the solutes change the volume of the solution due to a break up of the solvent structure. The effective volume of an ion in solution, the partial molar volume, can be determined from a directly obtainable quantity- apparent molar volume (ϕ_V). The apparent molar volumes, (ϕ_V), of the solutes can be calculated by using the following relation [65].

$$\phi_V = \frac{M}{\rho_0} - \frac{1000(\rho - \rho_0)}{c\rho_0} \quad (1)$$

where M is the molar mass of the solute, c is the molarity of the solution; ρ_0 and ρ are the densities of the solvent and the solution respectively. The partial molar volumes, ϕ_{2v} can be obtained from the equation [66]:

$$\phi_{2V} = \phi_V + \frac{(1000 - c\phi_V)}{2000 + c^{3/2}\left(\partial\phi_V / \partial\sqrt{c}\right)} c^{1/2}\left(\partial\phi_V / \partial\sqrt{c}\right) \quad (2)$$

The extrapolation of the apparent molar volume to infinite dilution and the expression of the concentration dependence of the apparent molar volume have been made by four major equations over a period of years – the Masson equation [67], the Redlich-Meyer equation [68], the Owen-Brinkley equation [69], and the Pitzer equation [31]. Masson found that the apparent molar volume of solute, ϕ_V, vary with the square root of the molar concentration by the linear equation:

$$\phi_V = \phi_V^0 + S_V^* \sqrt{c} \quad (3)$$

where, ϕ_V^0 is the apparent molar volume (equal to the partial molar volume) at infinite dilution and S_V^* the experimental slope. The majority of ϕ_V data in water [70] and nearly all ϕ_V data in non-aqueous [71--75] solvents have been extrapolated to infinite dilution through the use of equation (3).

The temperature dependence of ϕ_V^0 or various investigated solutes in various solvents can be expressed by the general equation as follows:

$$\phi_V^0 = a_0 + a_1 T + a_2 T^2 \quad (4)$$

where a_0, a_1, a_2 are the coefficients of a particular solute and T is the temperature in Kelvin.

The limiting apparent molar expansibilities (ϕ_E^0) can be obtained by the following equation:

$$\phi_E^0 = \left(\delta\phi_V^0 / \delta T\right)_P = a_1 + 2a_2 T \quad (5)$$

The limiting apparent molar expansibilities (ϕ_E^0) change in magnitude with the change of temperature. During the past few years it has been emphasized by a

number of workers that S_V^* is not the sole criterion for determining the structure-making or breaking tendency of any solute. Helper [76] developed a technique of examining the sign of $\left(\delta\phi_E^0/\delta T\right)_p$ for the solute in terms of long-range structure-making and breaking capacity of the electrolytes in the mixed solvent systems. The general thermodynamic expression used is as follows:

$$\left(\delta\phi_E^0/\delta T\right)_p = \left(\delta^2\phi_V^0/\delta T^2\right)_p = 2a_2 \tag{6}$$

If the sign of $\left(\delta\phi_E^0/\delta T\right)_p$ is positive or small negative the electrolyte is a structure maker and when the sign of $\left(\delta\phi_E^0/\delta T\right)_p$ is negative, it is a structure breaker. Redlich and Meyer [68] have shown that an equation (3) cannot be any more than a limiting law where for a given solvent and temperature, the slope S_v^* should depend only upon the valence type. They suggested the equation:

$$\phi_v = \phi_v^0 + S_v\sqrt{c} + b_v c \tag{7}$$

$$\text{where} \qquad S_v = Kw^{3/2} \tag{8}$$

S_V is the theoretical slope, based on molar concentration, including the valence factor where

$$w = 0.5\sum_i^j Y_i Z_i^2 \tag{9}$$

$$\text{and } K = N^2e^2\left(\frac{8\pi}{1000\epsilon^3 RT}\right)^{1/2}\left[\left(\frac{\partial \ln \epsilon}{\partial p}\right)_T - \frac{\beta}{3}\right] \tag{10}$$

In equation (10), K is the compressibility of the solvent and the other terms have their usual significance.

The Redlich-Meyer's extrapolation equation [68] adequately represents the concentration dependence of many 1:1 and 2:1 electrolytes in dilute solutions; however, studies [60-71] on some 2:1, 3:1 and 4:1 electrolytes show deviations from this equation. Thus, for polyvalent electrolytes, the more complete Owen-Brinkley equation [69] can be used to aid in the extrapolation to infinite dilution and to adequately represent the concentration dependency of ϕ_V. The Owen-Brinkley equation [69] which includes the ion-size parameter, a (cm), is given by:

$$\phi_V = \phi_V^0 + S_V\tau(\kappa a)\sqrt{c} + 0.5w_V\theta(\kappa a)c + 0.5K_V c \qquad (11)$$

where the symbols have their usual significance. However, this equation is not widely used for non-aqueous solutions.

Recently, the Pitzer formalism has been used by Pogue and Atkinson [77] to fit the apparent molal volume data. The Pitzer equation for the apparent molar volume of a single salt $M\,\gamma_M\,M\,\gamma_X$ is :

$$\phi_V = \phi_V^0 + V|Z_M Z_X|A_V|2bIn\left(I + bI^{\frac{1}{2}}\right) + 2\gamma_M\gamma_X RT\left[mB_{MX}^2 + m^2(\gamma_M\gamma_X)^{\frac{1}{2}}C_{MX}^V\right] \qquad (12)$$

where the symbols have their usual significance.

2.5.2 LIMITING PARTIAL MOLAR VOLUMES

The individual partial molar volumes provide information relevant to the general question of the structure near the solute, i.e., its solvation. The calculation of the limiting partial molar volumes in organic solvents is, however, a difficult one. At present, however, most of the existing limiting partial molar volumes in organic solvents were obtained by the application of methods originally developed for aqueous solutions to non aqueous electrolyte solutions. In the last few years, the method suggested by Conway *et al.* [78] has been used more frequently. These authors used the method to determine the limiting partial molar volumes of the anion for a series of homologous tetra alkyl ammonium chlorides, bromides and iodides in aqueous solution. They plotted the limiting partial molar volume $\phi^0_{v\,R_4NX}$, for a series of these salts with a halide ion in common as a function of the formula weight of the cation, M_{R4N+} and obtained straight-lines for each series. Therefore, they suggested the following equation:

$$\phi^0_{v\,R_4NX} = bM_{R_4N^+} + \phi^0_{v\,X^-} \qquad (13)$$

The extrapolation to zero cationic formula weight gave the limiting partial molar volumes of the halide ions $\phi^0_{V\,X^-}$ .Uosaki *et al.*[79] used this method for the separation of some literature values and of their own $\phi^0_{V\,R_4NX}$ values into ionic contributions in organic electrolyte solutions. Krumgalz [80] applied the same method to a large number of partial molar volume data for non-aqueous electrolyte solutions in a wide temperature range.

2.5.3 EXCESS MOLAR VOLUMES

The excess molar volumes, V^E are calculated from the molar masses M_i and the densities of pure liquids and the mixtures according to the following equation [81,82]

$$V^E = \sum_{i=1}^{n} x_i M_i \left(\frac{1}{\rho} - \frac{1}{\rho_i}\right) \quad (14)$$

where ρ_i and ρ are the density of the i^{th} component and density of the solution mixture respectively. V^E is the resultant of contributions from several opposing effects. These may be divided arbitrarily into three types, namely, chemical, physical and structural. Physical contributions, which are nonspecific interactions between the real species present in the mixture, contribute a positive term to V^E. The chemical or specific intermolecular interactions result in a volume decrease, thereby contributing negative V^E values. The structural contributions are mostly negative and arise from several effects, especially from interstitial accommodation and changes of free volume [16]. These phenomena are the results of difference in energies of interaction between molecules being in solutions and packing effects. Disruption of the ordered structure of pure component during formation of the mixture leads to a positive effect observed on excess volume while an order formation in the mixture leads to negative contribution.

2.6. VISCOSITY

As fundamental and important properties of liquids, viscosity and volume could also provide a lot of information on the structures and molecular interactions of liquid mixtures. Viscosity and volume are different types of properties of one liquid, and there is a certain relationship between them. So by measuring and studying them together, relatively more realistic and comprehensive information could be expected to be gained. The relationship between them could also be studied. The viscometric information includes 'Viscosity' as a function of composition on the basis of weight, volume and mole fraction; comparison of experimental viscosities with those calculated with several equations and excess Gibbs free energy of viscous flow. Viscosity, one of the most important transport properties is used for the determination of ion-solvent interactions and studied extensively [83,84]. Viscosity is not a thermodynamic quantity, but viscosity of an

electrolytic solution along with the thermodynamic property, $\phi_{v,2}^{0}$, i.e., the partial molar volume, gives a lot of information and insight regarding ion-solvent interactions and the nature of structures in the electrolytic solutions.

2.6.1 VISCOSITY OF PURE LIQUIDS AND LIQUID MIXTURES

Since the molecular motion in liquids is controlled by the influence of the neighbouring molecules, the transport of momentum in liquids takes place, in sharp contrast with gases at ordinary pressures, not by the actual movement of molecules but by the intense influence of intermolecular force fields. It is this aspect of the mechanism of momentum transfer which forms the basis of the procedures for predicting the variations in the viscosity of liquids and liquid mixtures.

2.6.2 EARLY THEORETICAL CONSIDERATIONS ON LIQUID VISCOSITY

The theoretical development of liquid viscosity in early stages has been reviewed Andrade [85] and Frenkel [86]. By considering the forces of collision to be the only important factor and assuming that at the melting point, the frequency of vibration is equal to that in the solid state and that one-third of the molecules are vibrating along each of the three directions normal to one another. Andrade [85] developed equations which checked well against data on mono atomic metals at the melting point. Frenkel [86] considered the molecules of a liquid to be spheres moving with an average velocity with respect to the surrounding medium and using Stokes' law and Einstein's relation for self diffusion-coefficient, arrived at a complicated expression for liquid viscosity with only limited applicability. Furth [87] assumed the momentum transfer to take place by the irregular Brownian movement of the holes [88] which were linked to clusters in a gas and thus, in analogy with the gas theory of viscosity and with assumption of the equipartition law of energy, showed that for liquids:

$$\eta = 0.915\frac{RT}{V}\left(\frac{m}{\sigma}\right)e^{\frac{A}{RT}} \qquad (15)$$

where η, V and m are viscosity, volume and mass, respectively, T is the temperature, R is the universal gas constant, σ is the surface tension and A is the work function at the melting point. He compared his theory with experiment as well as with the theories of Andrade [85] and Ewell and Eyring [89] Auluck, De and Kothari [90]

further modified the theory and successfully explained the variations of the viscosity with pressure. A critical review of these simple theories and their abilities to explain momentum transport in liquids is given by Eisenschitz [91].

2.6.3 THE CELL LATTICE THEORY AND LIQUID VISCOSITY

A model related to in the literature by various names such as cell, lattice, cage, free volume or one particle model was introduced by Lennard- Jones and Devonshire [92,93] and further expanded by Pople [94]. Eisenschitz employing this model developed a theory of viscosity by considering the motion of the representative molecules to be Brownian and their distribution according to the Smoluchowski equation. Even with certain assumptions, the final expression showed shortcomings most of which were later overcome in a subsequent publication [95].

2.6.4 STATISTICAL MECHANICAL APPROACH TO LIQUID VISCOSITY

The distribution functions for the liquid molecules were obtained on the basis of statistical mechanical theory mainly by the efforts of Kirkwood [96,97] Mayer and Montroll [98], Mayer [99], Born and Green [100] and the considerations on the basis of the general kinetic theory led Born and Green [100,101] to develop a viscosity equation which provided explanation for several empirical equations [84, 85, 87] proposed for liquid viscosity. In this connection the theoretical contributions of Kirkwood and coworkers [88, 102-108] Zwanzig *et al.*, [109] Rice and coworkers [110-113] Longuet- Higgins and Valleau [114] and Davis and Coworkers [115, 116] are worth mentioning.

2.6.5 PRINCIPLE OF CORRESPONDING STATES AND LIQUID VISCOSITY

The principle of the corresponding states has been applied to liquids in the same way as to gases [117] the basic assumption being that the intermolecular potential between two molecules is a universal function of the reduced intermolecular separation. This assumption is a good approximation for spherically symmetric mono atomic non-polar molecules. For complicated molecules, the principle becomes increasingly crude. In general, more parameters are introduced in the corresponding state correlations on somewhat empirical grounds in the hope

that such modification in some way compensates the shortcomings of the above stated assumption. In this connection the studies by Rogers and Brickwedde [118], Boon and Thomaes [119-120] Boon, Legros and Thomaes [121], and Hollman and Hijmans [122] are worth mentioning.

2.6.6 THE REACTION RATE THEORY FOR VISCOUS FLOW

Considering viscous flow as a chemical reaction in which a molecule moving in a plane occasionally acquires the activation energy necessary to sleep over the potential barrier to the next equilibrium position in the same plane. Eyring [123] showed that the viscosity of the liquid is given by:

$$\eta = \frac{\lambda_i h F_n}{\kappa \lambda^2 \lambda_2 \lambda_3 F_a^*} \exp \frac{\Delta E_{act}}{kT} \qquad (16)$$

where λ is the average distance between the equilibrium positions in the direction of motion, λ_1 is the perpendicular distance between two neighbouring layers of molecules in relative motion, λ_2 is the distance between neighbouring molecules in the same direction and λ_3 is the distance from molecule to molecule in the plane normal to the direction of motion. The transmission coefficient (κ) is the measure of the chance that a molecule having once crossed the potential barrier will react and not recross in the reverse direction, F_n is the partition function of the normal molecules, F_a^* that of the activated molecule with a degree of freedom corresponding to flow, ΔE_{act} is the energy of activation for the flow process, h is Planck's constant and k is Boltzmann constant. Ewell and Eyring argued that for a molecule to flow into a hole, it is not necessary that the latter be of the same size as the molecule. Consequently they assume that ΔE_{act} is a function of ΔE_{vap} for viscous flow because ΔE_{vap} is the energy required to make a hole in the liquid of the size of a molecule. Utilizing the idea and certain other relations [84, 120] finally gets

$$\eta = \frac{N_A h (2\pi m k T)^{\frac{1}{2}}}{Vh} \frac{bRTV^{\frac{1}{3}}}{N_A^{\frac{1}{3}} \Delta E_{Vap}} \exp \frac{\Delta E_{Vap}}{nRT} \qquad (17)$$

where n and b are constants. It was found that the theory could reproduce the trend in temperature dependence of η but the computed values are greater than the

observed values by a factor of 2 or 3 for most liquids. Kincaid, Eyring and Stearn [124] have summarized all the working relations.

2.6.7 THE SIGNIFICANT STRUCTURE THEORY AND LIQUID VISCOSITY

Eyring and coworkers [125-128] improved the "holes in solid" model theory [124-129] to picture the liquid state by identifying three significant structures. In brief, a molecule has solid like properties for the short time it vibrates about an equilibrium position and then it assumes instantly the gas like behaviour on jumping into the neighbouring vacancy. The above idea of significant structures leads to the following relation for the viscosity of liquid [130, 131].

$$\eta = \frac{V_s}{V}\eta_S + \frac{V - V_s}{V}\eta_g \tag{18}$$

where V_S is the molar volume of the solid at the melting point and V is the molar volume of the liquid at the temperature of interest while η_S and η_g are the viscosity contributions from the solid-like and gas-like degrees of freedom, respectively. The expressions for η_S and η_g are given by Carlson, Eyring and Ree. Eyring and Ree [132] have discussed in detail the evaluation of η_S from the reaction rate theory of Eyring [123] assuming that a solid molecule can jump into all neighbouring empty sites. The expression for η_S takes the following form [133]

$$\eta = \frac{N_A h}{Z_K}\frac{V}{V_S}\frac{6}{2^{\frac{1}{2}}}\frac{1}{V - V_S}\frac{1}{1 - e^{\frac{\theta}{T}}}\exp\frac{aE_S V_S}{(V - V_S)RT} \tag{19}$$

where N_A is Avogadro's number, Z is the number of nearest neighbours, θ is the Einstein characteristic temperature, E_S is the energy of sublimation and a' is the proportionality constant. On the other hand, the term η_g is obtained from the kinetic theory of gases [133] by the relation:

$$\eta_g = \frac{2}{3d^2}\left(\frac{mkT}{\pi^3}\right)^{\frac{1}{2}} \tag{20}$$

where d is the molecular diameter and m is the molecular mass.

2.6.8 VISCOSITY OF ELECTROLYTIC SOLUTIONS

The viscosity relationships of electrolytic solutions are highly complicated. Because ion-ion and ion-solvent interactions are occurring in the solution and

separation of the related forces is a difficult task. But, from careful analysis, vivid and valid conclusions can be drawn regarding the structure and the nature of the solvation of the particular system. As viscosity is a measure of the friction between adjacent, relatively moving parallel planes of the liquid, anything that increases or decreases the interaction between the planes will raise or lower the friction and thus, increase or decrease the viscosity. If large spheres are placed in the liquid, the planes will be keyed together in increasing the viscosity. Similarly, increase in the average degree of hydrogen bonding between the planes will increase the friction between the planes, thereby viscosity. An ion with a large rigid co-sphere for a structure-promoting ion will behave as a rigid sphere placed in the liquid and increase the inter-planar friction. Similarly, an ion increasing the degree of hydrogen bonding or the degree of correlation among the adjacent solvent molecules will increase the viscosity. Conversely, ions destroying correlation would decrease the viscosity. In 1905, Grüneisen [134] performed the first systematic measurement of viscosities of a number of electrolytic solutions over a wide range of concentrations. He noted non-linearity and negative curvature in the viscosity concentration curves irrespective of low or high concentrations. In 1929, Jones and Dole [135] suggested an empirical equation quantitatively correlating the relative viscosities of the electrolytes with molar concentrations (c):

$$\frac{\eta}{\eta_o} = \eta_r = 1 + A\sqrt{c} + Bc \qquad (21)$$

The above equation can be rearranged as:

$$\frac{\eta_r - 1}{\sqrt{c}} = A + B\sqrt{c} \qquad (22)$$

where A and B are constants specific to ion-ion and ion-solvent interactions. The equation is applicable equally to aqueous and non aqueous solvent systems where there is no ionic association and has been used extensively. The term $A\sqrt{c}$, originally ascribed to Grüneisen effect, arose from the long-range coulombic forces between the ions. The significance of the term had since then been realized due to the development Debye-Hückel theory [136] of inter-ionic attractions in 1923. The A - coefficient depends on the ion-ion interactions and can be calculated from interionic attraction theory [137-139] and is given by the Falkenhagen Vernon [139] equation:

$$A_{Theo} = \frac{0.2577\Lambda_o}{\eta_o(\varepsilon T)^{0.5}\lambda_+^o\lambda_-^o}\left[1 - 0.6863\left(\frac{\lambda_+^o\lambda_-^o}{\Lambda_o}\right)^2\right] \quad (23)$$

where the symbols have their usual significance. In very accurate work on aqueous solutions [140], A -coefficient has been obtained by fitting η_r to equation (22) and compared with the values calculated from equation (23), the agreement was normally excellent. The accuracy achieved with partially aqueous solutions was however poorer [141]. *A*-coefficient suggesting that should be calculated from conductivity measurements. Crudden *et al.* [142] suggested that if association of the ions occurs to form an ion pair, the viscosity should be analysed by the equation:

$$\frac{\eta_r - 1 - A\sqrt{\alpha c}}{\alpha c} = B_i + B_P\left(\frac{1-\alpha}{\alpha}\right) \quad (24)$$

where A, B_i and B_P are characteristic constants and a is the degree of dissociation of ion pair. Thus, a plot of (η_r-1-A$\sqrt{\alpha c}/\alpha c$) against $(1-\alpha)/\alpha$, when extrapolated to $(1-\alpha)/\alpha = 0$ gave the intercept B_i. However, for the most of the electrolytic solutions both aqueous and nonaqueous, the equation (22) is valid up to 0.1 (M) [143, 144] within experimental errors. At higher concentrations the extended Jones-Dole equation (25), involving an additional coefficient *D*, originally used by Kaminsky, [145] has been used by several workers [147, 148] and is given below:

$$\frac{\eta}{\eta_o} = \eta_r = 1 + A\sqrt{c} + Bc + Dc^2 \quad (25)$$

The coefficient *D* cannot be evaluated properly and the significance of the constant is also not always meaningful and therefore, equation (22) is used by the most of the workers.

The plots of $(\eta/\eta_o - 1)/\sqrt{c}$ against $\sqrt{c}$ for the electrolytes should give the value of *A* - coefficient. But sometimes, the values come out to be negative or considerably scatter and also deviation from linearity occur [148,149]. Thus, instead of determining *A* - coefficient from the plots or by the least square method, the *A* - coefficient are generally calculated using Falkenhagen-Vernon equation (23). *A* - coefficient should be zero for non-electrolytes. According to Jones and Dole, the *A* - coefficient probably represents the stiffening effect on the solution of the electric forces between the ions, which tend to maintain a space-lattice structure [135]. The *B* - coefficient may be either positive or negative and it is actually the ion-solvent

interaction parameter. It is conditioned by the ions and the solvent and cannot be calculated a priori. The B – coefficients are obtained as slopes of the straight lines using the least square method and intercepts equal to the A values.

The factors influencing B - coefficients are [150, 151]:

(1) The effect of ionic solvation and the action of the field of the ion in producing long-range order in solvent molecules, increase η or B - value.

(2) The destruction of the three dimensional structure of solvent molecules (i.e., structure breaking effect or depolymeriation effect) decreases η values.

(3) High molal volume and low dielectric constant, which yield high B-values for similar solvents.

(4) Reduced B-values are obtained when the primary solution of ions is sterically hindered in high molal volume solvents or if either ion of a binary electrolyte cannot be specifically solvated.

2.6.9 VISCOSITIES AT HIGHER CONCENTRATION

It had been found that the viscosity at high concentrations (1M to saturation) can be represented by the empirical formula suggested by Andrade:

$$\eta = A\exp^{\frac{b}{T}} \tag{26}$$

The several alternative formulations have been proposed for representing the results of viscosity measurements in the high concentration range [152-157] and the equation suggested by Angell [158-159] based on an extension of the free volume theory of transport phenomena in liquids and fused salts to ionic solutions is particularly noteworthy. The equation is:

$$\frac{1}{\eta} = A\exp\left[-\frac{K_1}{N_o - N}\right] \tag{27}$$

where N represents the concentration of the salt in eqv. litre^{-1}, A and K_1 are constants supposed to be independent of the salt composition and N_o is the hypothetical concentration at which the system becomes glass. The equation was recast by Majumder *et al.* [160-162] introducing the limiting condition, that is $N \rightarrow 0$, $\eta \rightarrow \eta_o$; which is the viscosity of the pure solvent.

Thus, we have:

$$ln\frac{\eta}{\eta_o} = ln\eta_{Rel} = \frac{K_1 N}{N_o(N_o - N)} \tag{28}$$

Equation (28) predicts a straight line passing through the origin for the plot of $ln\eta_{Rel}$ vs. $N/(N_o\text{-}N)$ if a suitable choice for N_o is made. Majumder *et al.* tested the equation (28) by using literature data as well as their own experimental data. The best choice for N_o and K_1 was selected by a trial and error methods. The set of K_1 and N_o producing minimum deviations between η_{Rel}^{Exp} and η_{Rel}^{Theo} was accepted.

In dilute solutions, $N << N_o$ and we have:

$$\eta_{Rel} = exp\left(\frac{K_1 N}{N_o^2}\right) \cong 1 + \frac{K_1 N}{N_o^2} \tag{29}$$

Equation (29) is nothing but the Jones-Dole equation with the ion-solvent interaction term represented as $B = K_1/N_o^2$. The arrangement between B-values determined in this way and using Jones-Dole equation has been found to be good for several electrolytes.

Further, the equation (28) can be written in the form:

$$\frac{N}{ln\eta_{Rel}} = \frac{N_o^2}{K_1} - \left(\frac{N_o}{K_1}\right)N \tag{30}$$

It closely resembles the Vand's equation [152] for fluidity (reciprocal for viscosity):

$$\frac{2.5c}{2.3log\eta_{Rel}} = \frac{1}{V_h} - Qc \tag{31}$$

where c is the molar concentration of the solute and V_h is the effective rigid molar volume of the salt and Q is the interaction constant.

2.6.10 DIVISION OF *B* -COEFFICIENT INTO IONIC VALUES

The viscosity B -coefficients have been determined by a large number of workers in aqueous, mixed and non-aqueous solvents [163-193]. However, the B -coefficients as determined experimentally using the Jones-Dole equation, does not give any impression regarding ion-solvent interactions unless there is some way to identify the separate contribution of cations and anions to the total solute-solvent interaction. The division of B - values into ionic components is quite arbitrary and

based on some assumptions, the validity of which may be questioned. The following methods have been used for the division of B - values in the ionic components:

(1) Cox and Wolfenden [194] carried out the division on the assumption that B_{ion} values of Li^+ and IO_3^- in $LiIO_3$ are proportional to the ionic volumes which are proportional to the third power of the ionic mobilities. The method of Gurney [195] and also of Kaminsky [150] is based on:

$$B_{K^+} = B_{Cl^-} \text{ (in water)} \tag{32}$$

The argument in favour of this assignment is based on the fact that the B - coefficients for KCl is very small and that the motilities' of K^+ and Cl^- are very similar over the temperature range 288.15 – 318.15 K. The assignment is supported from other thermodynamic properties. Nightingle [196], however preferred RbCl or CsCl to KCl from mobility considerations.

(2) The method suggested by Desnoyers and Perron is based on the assumption that the Et_4N^+ ion in water is probably closest to be neither structure breaker not a structure maker. Thus, they suggest that it is possible to apply with a high degree of accuracy of the Einstein's equation [197],

$$B = 0.0025\overline{V_o} \tag{33}$$

and by having an accurate value of the partial molar volume of the ion, V_o , it is possible to calculate the value of 0.359 for $B_{Et_4N^+}$ in water at 298.15 K. Recently, Sacco *et al.* proposed the "reference electrolytic" method for the division of B -values. Thus, for tetraphenyl phosphonium tetraphenyl borate in water, we have:

$$B_{BPh_4^-} = B_{PPh_4^+} = B_{BPh_4PPh_4} / 2 \tag{34}$$

$B_{BPh_4PPh_4}$ (scarcely soluble in water) has been obtained by the following method:

$$B_{BPh_4PPh_4} = B_{NaBPh_4} + B_{PPh_4Br} - B_{NaBr} \tag{35}$$

The values obtained are in good agreement with those obtained by other methods. The criteria adopted for the separation of B - coefficients in nonaqueous solvents differ from those generally used in water. However, the methods are based on the equality of equivalent conductances of counter ions at infinite dilutions.

(a) Criss and Mastroianni assumed $B_{K^+} = B_{Cl^-}$ in ethanol based on equal mobilities of ions [198]. They also adopted $B^{25}_{Me_4N^+} = 0.25$ as the initial value for acetonitrile solutions.

(b) For acetonitrile solutions, Tuan and Fuoss [199] proposed the equality, as they thought that these ions have similar mobilities. However, according to Springer *et* al. [197], $\lambda^o_{25}(Bu_4N^+) = 61.4$ and $\lambda^o_{25}(Ph_4B^-) = 58.3$ in acetonitrile.

$$B_{Bu_4N^+} = B_{Ph_4B^-} \tag{36}$$

(c) Gopal and Rastogi [164] resolved the B -coefficient in N-methyl propionamide solutions assuming that $B_{Et_4N^+} = B_{I^-}$ at all temperatures.

(d) In dimethyl sulphoxide, the division of B -coefficients were carried out by Yao and Beunion assuming:

$$B_{[(i-pe)_3 Bu_4N^+]} = B_{Ph_4B^-} = \frac{1}{2} B_{[(i-pe)_3 BuNPh_4B]} \tag{37}$$

at all temperatures.

Wide use of this method has been made by other authors for dimethyl sulphoxide, sulpholane, hexamethyl phosphotriamide and ethylene carbonate [200] solutions. The methods, however, have been strongly criticized by Krumgalz [201]. According to him, any method of resolution based on the equality of equivalent conductances for certain ions suffers from the drawback that it is impossible to select any two ions for which $\lambda^+_o = \lambda^-_o$ in all solvents at all temperatures. Thus, though $\lambda^+_K = \lambda^-_{Cl}$ at 298.15 K in methanol, but is not so in ethanol or in any other solvents. In addition, if the mobilities of some ions are even equal at infinite dilution, but it is not necessarily true at moderate concentrations for which the B - coefficient values are calculated. Further, according to him, equality of dimensions of $(i-pe)_3BuN^+$ or $(i-Am)_3BuN^+$ and Ph_4B^- does not necessarily imply the equality of B - coefficients of these ions and they are likely to be solvent and ion-structure dependent. Krumgalz [202, 203] has recently proposed a method for the resolution of B -coefficients. The method is based on the fact that the large tetraalkylammonium cations are not solvated [203, 204] in organic solvents (in the normal sense involving significant electrostatic interaction). Thus, the ionic B -

values for large tetraalkylammonium ions, R_4N^+ (where R > Bu) in organic solvents are proportional to their ionic dimensions. So, we have:

$$B_{R_4NX} = a + br^3 R_4N^+ \tag{38}$$

$a = B_{X^-} B$ and b is a constant dependent on temperature and solvent nature.

The extrapolation of the plot of B_{R_4NX} (R > Pr or Bu) against r^3 toR_4N to zero cation dimension gives directly B_{X^-} in the proper solvent and thus B - ion values can be calculated.

The B -ion values can also be calculated from the equations:

$$B_{R_4N^+} - B_{R_4'N^+} = B_{R_4NX} - B_{R_4'NX} \tag{39}$$

$$\frac{B_{R_4N^+}}{B_{R_4'N^+}} = \frac{r^3_{R_4N^+}}{r^3_{R_4'N^+}} \tag{40}$$

The radii of the tetraalkylammonium ions have been calculated from the conductometric data [205]. Gill and Sharma [184] used Bu_4NBPh_4 as a reference electrolyte. The method of resolution is based on the assumption, like Krumgalz, that Bu_4N^+ and Ph_4B^- ions with large R - groups are not solvated in non-aqueous solvents and their dimensions in such solvents are constant. The ionic radii of Bu_4N^+ (5.00Å) and Ph_4B (5.35 Å) were, in fact, found to remain constant in different non-aqueous and mixed non-aqueous solvents by Gill and co-workers. They proposed the equations:

$$\frac{B_{Ph_4B^-}}{B_{Bu_4N^+}} = \frac{r^3_{Ph_4B^-}}{r^3_{Bu_4N^+}} = \left(\frac{5.35}{5.00}\right)^3 \tag{41}$$

$$B_{Bu_4NBPh_4} = B_{Bu_4N^+} B_{Ph_4B^-} \tag{42}$$

The method requires only the B -values of Bu_4NBPh_4 and is equally applicable to mixed non-aqueous solvents. The B-ion values obtained by this method agree well with those reported by Sacco *et al.* in different organic solvents using the assumption as given below:

$$B_{[(i-Am)_3 Bu_4N^+]} = B_{Ph_4B^-} = \frac{1}{2} B_{[Bu_4NPh_4B]} \tag{43}$$

Recently, Lawrence and Sacco [187] used tetrabutylammonium tetrabutylborate

(Bu_4NBBu_4) as reference electrolyte because the cation and anion in each case are symmetrical in shape and have almost equal Van der Waal's volume. Thus, we have:

$$\frac{B_{Bu_4N^+}}{B_{Bu_4B^-}} = \frac{V_{W(Bu_4N^+)}}{V_{W(Bu_4B^-)}} \tag{44}$$

$$B_{Bu_4N^+} = \frac{B_{Bu_4NBPh_4}}{\left[1 + \frac{V_{W(Bu_4B^-)}}{V_{W(Bu_4N^+)}}\right]} \tag{45}$$

A similar division can be made for Ph_4PBPh_4 system.

Recently, Lawrence *et al.* made the viscosity measurements of tetraalkyl (from propyl to heptyl) ammonium bromides in DMSO and HMPT.

The *B*-coefficients $B_{R_4NBr} = B_{Br^-} + a[f_x R_4N^+]$ were plotted as functions of the Vander Waal's volumes. The B_{Br^-} values thus obtained were compared with the accurately determined B_{Br^-} value using Bu_4NBBu_4 and Ph_4PBPh_4 as reference salts. They concluded that the 'reference salt' method is the best available method for division into ionic contributions.

Jenkins and Pritcheit [206] suggested a least square analytical technique to examine additivity relationship for combined ion thermodynamics data, to effect apportioning into single-ion components for alkali metal halide salts by employing Fajan's competition principle [207] and 'volcano plots' of Morris [208]. The principle was extended to derive absolute single ion *B* coefficients for alkali metals and halides in water. They also observed that $B_{Cs^+} = B_{I^-}$ suggested by Krumgalz [203] to be more reliable than $B_{K^+} = B_{Cl^-}$ in aqueous solutions. However, we require more data to test the validity of this method.

It is apparent that almost all these methods are based on certain approximations and anomalous results may arise unless proper mathematical theory is developed to calculate *B* -values.

2.6.11 TEMPERATURE DEPENDENCE OF B - ION VALUES

Regularity in the behaviour of $B_\pm$ and $dB_\pm/dT$ has been observed both in aqueous and non-aqueous solvents and useful generalizations have been made by

Kaminsky. He observed that (i) within a group of the periodic table the B-ion values decrease as the crystal ionic radii increase, (ii) within a group of periodic system, the temperature co-efficientof B_{Ion} values increase as the ionic radius. The results can be summarized as follows:

(i) A and $dA/dT > 0$ (46)

(ii) $B_{Ion} < 0$ and $dB_{Ion}/dT > 0$ (47)

characteristic of the structure breaking ions.

(iii) $B_{Ion} > 0$ and $dB_{Ion}/dT < 0$ (48)

characteristic of the structure making ions.

An ion when surrounded by a solvent sheath, the properties of the solvent in the solvational layer may be different from those present in the bulk structure. This is well reflected in the 'Co-sphere' model of Gurney [209], A, B, C Zones of Frank and Wen [210] and hydrated radius of Nightingle [196].

Stokes and Mills gave an analysis of the viscosity data incorporating the basic ideas presented before. The viscosity of a dilute electrolyte solution has been equated to the viscosity of the solvent (η_o) plus the viscosity changes resulting from the competition between various effects occurring in the ionic neighborhood. Thus, the Jones-Dole equation:

$$\eta = \eta_o + \eta^* + \eta^E + \eta^A + \eta^D = \eta_o + \eta(A\sqrt{c} + Bc) \quad (49)$$

where η^*, the positive increment in viscosity is caused by coulombic interaction. Thus,

$$\eta^E + \eta^A + \eta^D = \eta_o Bc) \quad (50)$$

B-coefficient can thus be interpreted in terms of the competitive viscosity effects.

Following Stokes, Mills and Krumgalz [201] we can write:

$$B_{Ion} = B_{Ion}^{Einst} + B_{Ion}^{Orient} + B_{Ion}^{Str} + B_{Ion}^{Reinf} \quad (51)$$

whereas according to Lawrence and Sacco:

$$B_{Ion} = B_W + B_{Solv} + B_{Shape} + B_{Ord} + B_{Discord} \quad (52)$$

B_{Ion}^{Einst} is the positive increment arising from the obstruction to the viscous flow of the solvent caused by the shape and size of the ions (the term corresponds to η^E or

B_{Shape}). B_{Ion}^{Orient} is the positive increment arising from the alignment or structure making action of the electric field of the ion on the dipoles of the solvent molecules (the term corresponds to η^A or B_{Ord}). B_{Ion}^{Str} is the negative increment related to the destruction of the solvent structure in the region of the ionic co-sphere arising from the opposing tendencies of the ion to orientate the molecules round itself centrosymetrically and solvent to keep its own structure (this corresponds to η^D or B_{Disord}). B_{Ion}^{Reinf} is the positive increment conditioned by the effect of 'reinforcement of the water structure' by large tetraalkylammonium ions due to hydrophobic hydration. The phenomenon is inherent in the intrinsic water structure and absent in organic solvents. B_W and B_{Solv} account for viscosity increases and attributed to the Vander Waals volume and the volume of the solvation of ions. Thus, small and highly charged cations like Li^+ and Mg^{2+} form a firmly attached primary solvation sheath around these ions (B_{Ion}^{Orient} or η^E positive). At ordinary temperature, alignment of the solvent molecules around the inner layer also cause increase in B_{Ion}^{Orient} (η^A), B_{Ion}^{Orient} (η^D) is small for these ions. Thus, B_{Ion} will be large and positive as $B_{Ion}^{Einst} + B_{Ion}^{Orient} > B_{Ion}^{Str}$ However, B_{Ion}^{Einst} and B_{Ion}^{Orient} would be small for ions of greatest crystal radii (within a group) like Cs^+ or I^- due to small surface charge densities resulting in weak orienting and structure forming effect. B_{Ion}^{Str} would be large due to structural disorder in the immediate neighbourhood of the ion due to competition between the ionic field and the bulk structure. Thus, $B_{Ion}^{Einst} + B_{Ion}^{Orient} < B_{Ion}^{Str}$ and B_{Ion} is negative. Ions of intermediate size (e.g., K^+ and Cl^-) have a close balance of viscous forces in their vicinity, *i.e.*, $B_{Ion}^{Einst} + B_{Ion}^{Orient} = B_{Ion}^{Str}$ so that B is close to zero.

Large molecular ions like tetraalkylammonium ions have large B_{Ion}^{Einst} because of large size but B_{Ion}^{Orient} and B_{Ion}^{Str} would be small, *i.e.*, $B_{Ion}^{Einst} + B_{Ion}^{Orient} >> B_{Ion}^{Str}$ would be positive and large. The value would be further reinforced in water arising from B_{Ion}^{Reinf} due to hydrophobic hydrations.

The increase in temperature will have no effect on B_{Ion}^{Einst}. But the orientation of solvent molecules in the secondary layer will be decreased due to increase in

thermal motion leading to decrease in B_{Ion}^{Str}. B_{Ion}^{Orient} will decrease slowly with temperature as there will be less competition between the ionic field and reduced solvent structure. The positive or negative temperature co-efficient will thus depend on the change of the relative magnitudes of B_{Ion}^{Orient} and B_{Ion}^{Str}.

In case of structure-making ions, the ions are firmly surrounded by a primary solvation sheath and the secondary solvation zone will be considerably ordered leading to an increase in B_{Ion} and concomitant decrease in entropy of solvation and the mobility of ions. Structure breaking ions, on the other hand, are not solvated to a great extent and the secondary solvation zone will be disordered leading to a decrease in B_{Ion} values and increases in entropy of solvation and the mobility of ions. Moreover, the temperature induced change in viscosity of ions (or entropy of solvation or mobility of ions) would be more pronounced in case of smaller ions than in case of the larger ions. So, there is a correlation between the viscosity, entropy of solvation and temperature dependent mobility of ions. Thus, the ionic *B* - coefficient and the entropy of solvation of ions have rightly been used as probes of ion-solvent interactions and as a direct indication of structure making and structure breaking character of ions. The linear plot of ionic *B*-coefficients against the ratios of mobility viscosity products at two temperatures (a more sensitive variable than ionic mobility) by Gurney [195] clearly demonstrates a close relation between ionic *B*-coefficients and ionic mobilities. Gurney also demonstrated a clear correlation between the molar entropy of solution values with *B* -coefficient of salts. The ionic *B* - values show a linear relationship with the partial molar ionic entropies or partial molar entropies of hydration ($\overline{S}_h^o$) as:

$$\overline{S}_h^o = \overline{S}_{aq}^o - \overline{S}_g^o \qquad (53)$$

Where, $\overline{S}_{aq}^o = \overline{S}_{ref}^o + \Delta S^o$, $\overline{S}_g^o$ is the calculated sum of the translational and rotational entropies of the gaseous ions. Gurney obtained a single linear plot between ionic entropies and ionic *B*-coefficients for all mono atomic ions by equating the entropy of the hydrogen ion ($S_{H^+}^o$) to –5.5 cal. mol^{-1} deg^{-1}. Asmus [211] used the entropy of hydration to correlate ionic *B* values and Nightingale [196] showed that a single linear relationship could be obtained with it for both monoatomic and polyatomic

ions. The correlation was utilized by Abraham *et al.* [212]to assign single ion B - coefficients so that a plot of ΔS_e^o [213, 214] the electrostatic entropy of solvation or $\Delta S_{I,II}^o$ the entropic contributions of the first and second solvation layers of ions against B points (taken from the works of Nightingale) for both cations and anions lie on the same curve. There are excellent linear correlations between ΔS_e^o and ΔS_I^o and the single ion B - coefficients. Both entropy criteria (ΔS_e^o and $\Delta S_{I,II}^o$) and B - ion values indicate that in water the ions Li^+, Na^+, Ag^+ and F^- are not structure makers, and the ions Rb^+, Cs^+, Cl^-, Br^-, I^- and $ClO_4^-$are structure breakers and K^+ is a border line case.

2.6.12 THERMODYNAMICS OF VISCOUS FLOW

Assuming viscous flow as a rate process, the viscosity (η) can be represented from Eyring's [215] approaches as:

$$\eta = Ae^{\frac{E_{vis}}{RT}} = \left(\frac{hN_A}{V}\right)e^{\frac{\Delta G^*}{RT}} = \left(\frac{hN_A}{V}\right)e^{\left(\frac{\Delta H^*}{RT} - \frac{\Delta S}{R}\right)} \tag{54}$$

where E_{vis} = the experimental entropy of activation determined from a plot of $\ln\eta$ against 1/T . ΔG^*, ΔH^* and ΔS^* are the free energy, enthalpy and entropy of activation, respectively

Nightingale and Benck [216] dealt in the problem in a different way and calculated the thermodynamics of viscous flow of salts in aqueous solution with the help of the Jones-Dole equation (neglecting the A c term).

Thus, we have:

$$R\left[\frac{d\ln\eta}{d\left(\frac{1}{T}\right)}\right] = r\left[\frac{d\ln\eta_o}{d\left(\frac{1}{T}\right)}\right] + \frac{R}{1+Bc}\frac{d(1+Bc)}{d\left(\frac{1}{T}\right)} \tag{55}$$

$$\Delta E_{\eta(Soln)}^{\neq} = \Delta E_{\eta(Solv)}^{\neq} + \Delta E_V^{\neq} \tag{56}$$

$\Delta E_V^{\neq}$ can be interpreted as the increase or decrease of the activation energies for viscous flow of the pure solvents due to the presence of ions, i.e., the effective influence of the ions upon the viscous flow of the solvent molecules. Feakins *et al.* [217] have suggested an alternative formulation based on the transition state

treatment of the relative viscosity of electrolytic solution. They suggested the following expression:

$$B = \frac{(\phi^0_{V,2} - \phi^0_{V,1})}{1000} + \phi^0_{V,2} \frac{(\Delta\mu_2^{0\neq} - \Delta\mu_1^{0\neq})}{1000RT} \tag{57}$$

where $\phi^0_{v,1}$ and $\phi^0_{v,2}$ are the partial molar volumes of the solvent and solute respectively and $\Delta\mu_2^{o\neq}$ is the contribution per mole of solute to the free energy of activation for viscous flow of solution. $\Delta\mu_1^{o\neq}$ is the free energy of activation for viscous flow per mole of the solvent which is given by:

$$\Delta\mu_1^{0\neq} = \Delta G_1^{0\neq} = RT \ln(\eta_0 \phi^0_{v,1} / hN_A) \tag{58}$$

Further, if B is known at various temperatures, we can calculate the entropy and enthalpy of activation of viscous flow respectively from the following equations as given below:

$$\frac{d(\Delta\mu_2^{o\neq})}{dT} = -\Delta S_2^{o\neq} \tag{59}$$

$$\Delta H_2^{o\neq} = \Delta\mu_2^{o\neq} + T\Delta S_2^{o\neq} \tag{60}$$

2.6.13 EFFECTS OF SHAPE AND SIZE

Stokes and Mills have dealt in the aspect of shape and size extensively. The ions in solution can be regarded to be rigid spheres suspended in continuum. The hydrodynamic treatment presented by Einstein [197] leads to the equation:

$$\frac{\eta}{\eta_0} = 1 + 2.5\phi \tag{61}$$

where ϕ is the volume fraction occupied by the particles. Modifications of the equation have been proposed by (i) Sinha [218] on the basis of departures from spherical shape and (ii) Vand on the basis of dependence of the flow patterns around the neighboring particles at higher concentrations. However, considering the different aspects of the problem, spherical shapes have been assumed for electrolytes having hydrated ions of large effective size (particularly polyvalent monatomic cations). Thus, we have from equation (61):

$$2.5\phi = A\sqrt{c} + Bc \tag{62}$$

Since $A\sqrt{c}$ term can be neglected in comparison with Bc and $\phi = c\phi_{v,1}^0$ where $\phi_{v,1}^0$ is the partial molar volume of the ion, we get:

$$2.5\phi_{v,1}^0 = B \tag{63}$$

In the ideal case, the B-coefficient is a linear function of partial molar volume of the solute, $\phi_{v,1}^0$ with slope to 2.5. Thus, $B_\pm$ can be equated to:

$$B_\pm = 2.5\phi_\pm^0 = \frac{2.5\times 4}{3}\frac{\left(\pi R_\pm^3 N\right)}{1000} \tag{64}$$

assuming that the ions behave like rigid spheres with a effective radii, $R_\pm$ moving in a continuum. $R_\pm$, calculated using the equation (64) should be close to crystallographic radii or corrected Stoke's radii if the ions are scarcely solvated and behave as spherical entities. But, in general, $R_\pm$ values of the ions are higher than the crystallographic radii indicating appreciable solvation.

The number n_b of solvent molecules bound to the ion in the primary solvation shell can be easily calculated by comparing the Jones-Dole equation with the Einstein's equation:

$$B_\pm = \frac{2.5}{1000\left(\phi_i + n_b\phi_s\right)} \tag{65}$$

where ϕ_i is the molar volume of the base ion and ϕ_s, the molar volume of the solvent. The equation (65) has been used by a number of workers to study the nature of solvation and solvation number.

2.6.14 VISCOSITY OF NON-ELECTROLYTIC SOLUTIONS

The equations of Vand [219], Thomas [220] and Moulik proposed mainly to account for the viscosity of the concentrated solutions of bigger spherical particles have been also found to correlate the mixture viscosities of the usual nonelectrolytes [221-223]. These equations are:

Vand equation:
$$\ln\eta_r = \frac{\alpha}{1-Q} = \frac{2.5V_h c}{1-QV_h c} \tag{66}$$

Thomas equation:
$$\eta_r = 1 + 2.5V_h + 10.05cV_h^2 c \tag{67}$$

Moulik equation:
$$\eta^2 = I + Mc^2 \tag{68}$$

where η_r is the relative viscosity, a is constant depending on axial ratios of the particles, Q is the interaction constant, V_h is the molar volume of the solute including rigidly held solvent molecules due to hydration, c is the molar concentration of the solutes; I and M are constants. The viscosity equation proposed by Eyring and coworkers for pure liquids on the basis of pure significant liquid structures theory, can be extended to predict the viscosity of mixed liquids also. The final expression for the liquid mixtures takes the following form:

$$\eta_m = \frac{6N_A h}{\sqrt{2}r_m(V_m - V_{Sm})}\left[\sum_i^n\left\{1-\exp\left(\frac{-\theta_i}{T}\right)\right\}^{-x_i}\right]\exp\left[\frac{a_m E_{Sm} V_{Sm}}{RT(V_m - V_{Sm})}\right] + \frac{V_m - V_{Sm}}{V_m}\left[\sum_i^n \frac{2}{3d_i^2}\left(\frac{m_i kT}{\pi^3}\right)^{\frac{1}{2}} x_i\right] \tag{69}$$

where n is 2 for binary and 3 for ternary liquid mixtures. The mixture parameters, r_m, E_{Sm}, V_m, V_{Sm} and a_m were calculated from the corresponding pure component parameters by using the following relations:

$$r_m = \sum_i^n x_i^2 r_i + \sum_{i\neq j} 2x_i x_j x_{ij} \tag{70}$$

$$E_{Sm} = \sum_i^n x_i^2 E_{Si} + \sum_{i\neq j} 2x_i x_j E_{Sij} \tag{71}$$

$$V_m = \sum_i^n x_i V_i \qquad V_{Sm} = \sum_i^n x_i V_{Si} \qquad a_m = \sum_i^n x_i a_i \tag{72}$$

$$r_{ij} = (r_i r_j)^{\frac{1}{2}} \quad \text{and} \quad E_{Sij} = (E_{Si} E_{Sj})^{\frac{1}{2}} \tag{73}$$

$$\theta = \frac{h}{\kappa 2\pi}\left(\frac{b}{m}\right)^{\frac{1}{2}} \tag{74}$$

$$b = 2Z\varepsilon\left[22.106\left(\frac{N_A\sigma^2}{V_s}\right)^4 - 10.559\left(\frac{N_A\sigma^3}{V_s}\right)^2\right]\frac{1}{\sqrt{2}\sigma^2}\left(\frac{N_A\sigma^3}{V_s}\right)^{\frac{2}{3}} \tag{75}$$

here σ and ε are Lennard-Jones potential parameters and the other symbols have their usual significance.

For interpolation and limited extrapolation purposes, the viscosities of ternary mixture can be correlated to a high degree of accuracy in terms of binary contribution by the following equations [224-230].

$$\eta_m = \sum_i^3 x_i\eta_i + x_1x_2[A_{12} + B_{12}(x_1 - x_2) + C_{12}(x_1 - x_2)^2] + x_2x_3[A_{23} + B_{23}(x_2 - x_3) + C_{23}(x_2 - x_3)^2] + x_3x_1[A_{31} + B_{31}(x_3 - x_1) + C_{31}(x_3 - x_1)^2] \quad (76a)$$

The correlation of ternary is modified to the following form:

$$\eta_m = \sum_i^3 x_i\eta_i + x_1x_2[A_{12} + B_{12}(x_1 - x_2) + C_{12}(x_1 - x_2)^2] + x_2x_3[A_{23} + B_{23}(x_2 - x_3) + C_{23}(x_2 - x_3)^2] + x_3x_1[A_{31} + B_{31}(x_3 - x_1) + C_{31}(x_3 - x_1)^2] + A_{123}(x_1x_2x_3) \quad (76b)$$

However, a better result may be obtained using the following relation:

$$\eta_m = \sum_i^3 x_i\eta_i + x_1x_2[A_{12} + B_{12}(x_1 - x_2) + C_{12}(x_1 - x_2)^2] + x_2x_3[A_{23} + B_{23}(x_2 - x_3) + C_{23}(x_2 - x_3)^2] + x_3x_1[A_{31} + B_{31}(x_3 - x_1) + C_{31}(x_3 - x_1)^2] + x_1x_2x_3[A_{123} + B_{123}x_1^2(x_2 - x_3)^2 + C_{123}x_1^3(x_2 - x_3)^3] \quad (76c)$$

where A_{12}, B_{12}, C_{12}, A_{23}, B_{23}, C_{23}, A_{31}, B_{31} and C_{31}, are constants for binary mixtures; A_{123}, B_{123} and C_{123} are constants for the ternaries; and the other symbols have their usual significance.

2.6.15 VISCOSITY DEVIATION

Viscosity of liquid mixtures can also provide information for the elucidation of the fundamental behaviour of liquid mixtures, aid in the correlation of mixture viscosities with those of pure components, and may provide a basis for the selection of physico-chemical methods of analysis. Quantitatively, as per the absolute reaction rates theory [231], the deviations in viscosities($\Delta\eta$)from the ideal mixture values can be calculated as:

$$\Delta\eta = \eta - \sum_{i=1}^{I}(x_i\eta_i) \quad (77)$$

where η is the dynamic viscosities of the mixture and $x_i\eta_i$ are the mole fraction and viscosity of i^{th} component in the mixture, respectively.

2.6.16 GIBBS EXCESS ENERGY OF ACTIVATION FOR VISCOUS FLOW

Quantitatively, the Gibbs excess energy of activation for viscous flow, ΔG^* can be calculated as [232]:

$$\Delta G^E = RT\left[\ln \eta V - \sum_{i=1}^{i}(x_i \ln \eta_i V_i)\right] \quad (78)$$

where η and V are the viscosity and molar volume of the mixture; η_i and V_i are the viscosity and molar volume of i^{th} pure component, respectively.

2.6.17 VISCOUS SYNERGY AND ANTAGONISM

Rheology is the branch of science that studies [233] material deformation and flow, and is increasingly applied to analyze the viscous behavior of many pharmaceutical products, [234-243] and to establish their stability and even bioavailability, since it has been firmly established that viscosity influences the drug absorption rate in the body [244, 245]. The study of the viscous behavior of pharmaceutical, foodstuffs, cosmetics or industrial products, etc., is essential for conforming that their viscosity is appropriate for the contemplated use of the products.

Viscous synergy is the term used in the application to the interaction between the components of a system that causes the total viscosity of the system to be greater than the sum of the viscosities of each component considered separately. In contraposition to viscous synergy, viscous antagonism is defined as the interaction between the components of a system causing the net viscosity of the latter to be less than the sum of the viscosities of each component considered separately. If the total viscosity of the system is equal to the sum of the viscosities of each component considered separately, the system is said to lack interaction [246, 247].

The method most widely used to analyze the synergic and antagonic behavior of the ternary liquid mixtures used here is that developed by Kaletunc- Gencer and Peleg [248] allowing quantification of the synergic and antagonic interactions taking

place in the mixtures involving variable proportions of the constituent components. The method compares the viscosity of the system, determined experimentally, η_{exp}, with the viscosity expected in the absence of interaction, η_{cal}, as defined by the simple mixing rule as:

$$\eta_{cal} = \sum_{i=1}^{j} w_i \eta_i \tag{79}$$

where w_i and η_i are the fraction by weight and the viscosity of the i^{th} component, measured experimentally and i is an integer.

Accordingly, when $\eta_{exp} > \eta_{cal}$, viscous synergy exists, while, when $\eta_{exp} < \eta_{cal}$, the system is said to exhibit viscous antagonism. The procedure is used when Newtonian fluids are involved, since in non-synergy indices are defined in consequence [249].

In order to secure more comparable viscous synergy results, the so-called synergic interaction index (I_S) as introduced by Howell [250] is taken into account:

$$I_S = \frac{\eta_{exp} - \eta_{mix}}{\eta_{mix}} = \frac{\Delta\eta}{\eta_{mix}} \tag{80}$$

When the values of I_S are negative, it is concerned as antagonic interaction index (I_A).

The method used to analyze volume contraction and expansion is similar to that applied to viscosity, i.e., the density of the mixture is determined experimentally, ρ_{exp}, and a calculation is made for ρ_{cal} based on the expression:

$$\rho_{cal} = \sum_{i=1}^{j} w_i \rho_i \tag{81}$$

where ρ_i is the experimentally measured density of the i^{th} component. Other symbols have their usual significance.

Accordingly, when $\rho_{exp} > \rho_{cal}$, volume contraction occurs, but when $\rho_{exp} < \rho_{cal}$, there is volume expansion in the system.

2.7 ULTRASONIC SPEED

In recent years, there has been considerably progress in the determination of thermodynamic, acoustic and transport properties of working liquids from ultrasonic speeds, density and viscosity measurement. The study of ultrasonic

speeds and isentropic compressibilities of liquids, solutions and liquid mixtures provide useful information about molecular interactions, association and dissociation. Various parameters like molar isentropic and isothermal compressibilities, apparent molal compressibility, isentropic compressibility, deviation in isentropic compressibility from ideality, etc. can very well be evaluated and studied from the measurement of ultrasonic speeds and densities in solutions. Isentropic compressibilities play a vital role in characterization of binary and ternary liquid mixtures particularly in cases where partial molar volume data alone fail to provide an unequivocal interpretation of the interactions.

2.7.1 APPARENT MOLAL ISENTROPIC COMPRESSIBILITY

Although for a long time attention has been paid to the apparent molal isentropic compressibility for electrolytes and other compounds in aqueous solutions,[251-255] measurements in non-aqueous solvents are still scarce. It has been emphasized by many authors that the apparent molal isentropic compressibility data can be used as a useful parameter in elucidating the solute-solvent and solute-solute interactions. The most convenient way to measure the compressibility of a solvent/solution is from the speed of sound in it.

The isentropic compressibility (β) of a solvent/solution can be calculated from the Laplace's equation [256]:

$$\beta = \frac{1}{u^2 \rho} \tag{82}$$

where ρ is the solution density and u is the ultrasonic speed in the solvent/solution. The isentropic compressibility (β) determined by equation (82) is adiabatic, not an isothermal one, because the local compressions occurring when the ultrasound passes through the solvent/solution are too rapid to allow an escape of the heat produced.

The apparent molal isentropic compressibility (ϕ_K) of the solutions was calculated using the relation:

$$\phi_K = M\beta/\rho + 1000(\beta\rho_0 - \beta_0\rho)/m\rho\rho_0 \tag{83}$$

β_o is the isentropic compressibility of the solvent mixture, M is the molar mass of the solute and m is the molality of the solution.

The limiting apparent isentropic compressibility ϕ_K^o may be obtained by extrapolating the plots of ϕ_K versus the square root of the molal concentration of the solutes by the computerized least- square method according to the equation.

$$\phi_K = \phi_K^0 + S_K^* \sqrt{m} \tag{84}$$

The limiting apparent molal isentropic compressibility (ϕ_K^o) and the experimental slope S_K^* can be interpreted in terms of solute-solvent and solute-solute interactions respectively. It is well established that the solutes causing electrostriction leads to the decrease in the compressibility of the solution [257, 258]. This is reflected by the negative values of ϕ_K^o of electrolytic solutions. Hydrophobic solutes often show negative compressibilities due to the ordering induced by them in the water structure. The compressibility of hydrogen-bonded structure, however, varies depending on the nature of the hydrogen bonding involved. However, the poor fit of the solute molecules [259, 260] as well as the possibility of flexible hydrogen bond formation appear to be responsible for causing a more compressible environment and hence positive ϕ_K^o values have been reported in aqueous non-electrolyte [261] and non-aqueous non-electrolyte [262] solutions.

2.7.2 DEVIATION IN ISENTROPIC COMPRESSIBILITY

The deviation in isentropic compressibility (ΔK_S) can be calculated using the following equation [263-265]:

$$\Delta K_S = K_S - \sum_{i=1}^{j} x_i K_{S,i} \tag{85}$$

where $x_i, K_{S,i}$ are the mole fraction and isentropic compressibility of i^{th} component in the mixture, respectively. The observed values of ΔK_S can be qualitatively explained by considering the factors, namely (i) the mutual disruption of associated species present in the pure liquids, (ii) the formation of weak bonds by dipole-induced dipole interaction between unlike molecules, and (iii) geometrical fitting of component molecules into each other structure. The first factor contributes to positive ΔK_S values, whereas the remaining two factors lead to negative ΔK_S values

[266]. The resultant values of ΔK_S for the mixtures are due to the net effect of the combination of (i) to (iii) [267].

Moreover, the excess or deviation properties ($V_m^E, \Delta\eta, \Delta G^E$ and ΔK_S) have been fitted to Redlich-Kister [268] polynomial equation using the method of least squares involving the Marquardt algorithm [269] and the binary coefficients, α_i were determined as follows :

$$Y_{i,j}^E = x_1 x_2 \sum_{i=1}^{j} a_i (x_1 - x_2)^i \qquad (86)$$

where $Y_{i,j}^E$ refers to an excess or deviation property and x_1 and x_2 are the mole fraction of the solvent 1 and solvent 2, respectively. In each case, the optimal number of coefficients was ascertained from an approximation of the variation in the standard deviation (σ). The standard deviation (σ) was calculated using,

$$\sigma = \left[\frac{(Y_{exp}^E - Y_{cal}^E)^2}{n-m} \right]^{\frac{1}{2}} \qquad (87)$$

where n is the number of data points and m is the number of coefficients.

2.8 CONDUCTANCE

One of the most precise and direct technique available to determine the extent of the dissociation constants of electrolytes in aqueous, mixed and non-aqueous solvents is the "conductometric method." Conductance data in conjunction with viscosity measurements, gives much information regarding ion-ion and ion-solvent interaction.

The studies of conductance measurements were pursued vigorously during the last five decades, both theoretically and experimentally and a number of important theoretical equations have been derived. We shall dwell briefly on some of these aspects in relation to the studies in aqueous, non-aqueous, pure and mixed solvents. The successful application of the Debye-Hückel theory of interionic attraction was made by Onsager [270] to derive the Kohlrausch's equation representing the molar conductance of an electrolyte. For solutions of a single symmetrical electrolyte the equation is given by:

$$\Lambda = \Lambda_o - S\sqrt{c} \tag{88}$$

where,
$$S = \alpha\Lambda_o + \beta \tag{89}$$

$$\alpha = \frac{(z^2)k}{3(2+\sqrt{2})\varepsilon_r kT\sqrt{c}} = \frac{82.406\times10^4 z^3}{(\varepsilon_r T)^{\frac{3}{2}}} \tag{90a}$$

$$\beta = \frac{z^2 eFk}{3\pi\eta\sqrt{c}} = \frac{82.487 z^3}{\eta\sqrt{\varepsilon_r T}} \tag{90b}$$

The equation took no account for the short-range interactions and also of shape or size of the ions in solution. The ions were regarded as rigid charged spheres in an electrostatic and hydrodynamic continuum, i.e., the solvent [271]. In the subsequent years, Pitts (1953) [272] and Fuoss and Onsager (1957) [273] independently worked out the solution of the problem of electrolytic conductance accounting for both long-range and short-range interactions. However, the Λ_o values obtained for the conductance at infinite dilution using Fuoss-Onsager theory differed considerably from that obtained using Pitt's theory and the derivation of the Fuoss-Onsager equation was questioned [274,275]. The original Fuoss-Onsager equation was further modified by Fuoss and Hsia [276] who recalculated the relaxation field, retaining the terms which had previously been neglected.

The results of conductance theories can be expressed in a general form:

$$\Lambda = \frac{\Lambda_o - \alpha\Lambda_o\sqrt{c}}{(1+\kappa\alpha)}\left(\frac{1+\kappa\alpha}{\sqrt{2}}\right) - \frac{\beta\sqrt{c}}{(1+\kappa\alpha)} + G(\kappa\alpha) \tag{91}$$

where $G(\kappa\alpha)$ is a complicated function of the variable. The simplified form:

$$\Lambda = \Lambda_o - S\sqrt{c} + Ec\ln c + J_1 c + J_2\sqrt[3]{c} \tag{92}$$

However, it has been found that these equations have certain limitations, in some cases it fails to fit experimental data. Some of these results have been discussed elaborately by Fernandez-Prini [277,278]. Further correction of the equation (92) was made by Fuoss and Accascin. They took into consideration the change in the viscosity of the solutions and assumed the validity of Walden's rule. The new equation becomes:

$$\Lambda = \Lambda_o - S\sqrt{c} + Ec\ln c + J_1 c + J_2\sqrt[3]{c} - F\Lambda c \tag{93}$$

where, $Fc = \frac{4\pi R^3 N_A}{3}$ (94)

In most cases, however, J_2 is made zero but this leads to a systematic deviation of the experimental data from the theoretical equations. It has been observed that Pitt's equation gives better fit to the experimental data in aqueous solutions [279].

2.8.1 IONIC ASSOCIATION

The equation (93) successfully represents the behaviour of completely dissociated electrolytes. The plot of Λ against $\sqrt{c}$ (limiting Onsager equation) is used to assign the dissociation or association of electrolytes. Thus, if $\Lambda_{o\,exp}$ is greater than $\Lambda_{o\,theo}$, i.e., if positive deviation occurs (ascribed to short range hard core repulsive interaction between ions), the electrolyte may be regarded as completely dissociated but if negative deviation ($\Lambda_{o\,exp} < \Lambda_{o\,theo}$) or positive deviation from the Onsager limiting tangent ($\alpha\Lambda_o + \beta$)occurs, the electrolyte may be regarded to be associated. Here the electrostatic interactions are large so as to cause association between cations and anions. The difference in $\Lambda_{o\,exp}$ and $\Lambda_{o\,theo}$ would be considerable with increasing association [280].

Conductance measurements help us to determine the values of the ion-pair association constant, K_A for the process:

$$M^{z+} + A^{z-} = MA \tag{95}$$

$$K_A = \frac{(1-\alpha)}{\alpha^2 c\gamma_{\pm}^2} \tag{96}$$

$$\alpha = 1 - \alpha^2 K_A c\gamma_{\pm}^2 \tag{97}$$

where $\gamma_{\pm}$ is the mean activity coefficient of the free ions at concentration αc

For strongly associated electrolytes, the constant, K_A and Λ_o has been determined using Fuoss-Kraus equation [281] or Shedlovsky's equation [282].

$$\frac{T(z)}{\Lambda} = \frac{1}{\Lambda_o} + \frac{K_A}{\Lambda_o^2} \cdot \frac{c\gamma_{\pm}^2 \Lambda}{T(z)} \tag{98}$$

where $T(z) = F(z)$ (Fuoss-Kraus method) and $1/T(z)=S(z)$ (Shedlovsky's method).

$$F(z) = 1 - z(1 - z(1 - ...)^{\frac{1}{2}})^{\frac{1}{2}} \tag{99a}$$

and

$$\frac{1}{T(z)} = S(z) = 1 + z + \frac{z^2}{2} + \frac{z^3}{8} + \ldots\ldots \qquad (99b)$$

A plot of $T(z)/\Lambda$ against $c\gamma_{\pm}^2\Lambda/T(z)$ should be a straight line having $1/\Lambda_o$ for its intercept and K_A/Λ_o^2 for its slope. Where K_A is large, there will be considerable uncertainty in the determined values of Λ_o and K_A from equation (98).

The Fuoss-Hsia [276] conductance equation for associated electrolytes is given by:

$$\Lambda = \Lambda_o - S\sqrt{\alpha c} + E(\alpha c)\ln(\alpha c) + J_1(\alpha c) - J_2(\alpha c)^{\frac{3}{2}} - K_A\Lambda\gamma_{\pm}^2(\alpha c) \qquad (100)$$

The equation was modified by Justice [283]. The conductance of symmetrical electrolytes in dilute solutions can be represented by the equations:

$$\Lambda = \alpha(\Lambda_o - S\sqrt{\alpha c} + E(\alpha c)\ln(\alpha c) + J_1 R(\alpha c) - J_2 R(\alpha c)^{\frac{3}{2}} \qquad (101)$$

$$\frac{(1-\alpha)}{\alpha^2 c\gamma_{\pm}^2} = K_A \qquad (102)$$

$$\ln\gamma_{\pm} = \frac{-k\sqrt{q}}{(1+kR\sqrt{\alpha c})} \qquad (103)$$

The conductance parameters are obtained from a least square treatment after setting, $R = q = \frac{e^2}{2\varepsilon kT}$ (Bjerrum's critical distance).

According to Justice the method of fixing the J-coefficient by setting, $R = q$ clearly permits a better value of K_A to be obtained. Since the equation (101) is a series expansion truncated at the $c^{3/2}$ term, it would be preferable that the resulting errors be absorbed as must as possible by J_2 rather than by K_A, whose theoretical interest is greater as it contains the information concerning short-range cation-anion interaction. From the experimental values of the association constant K_A, one can use two methods in order to determine the distance of closest approach, a, of two free ions to form an ion-pair. The following equation has been proposed by Fuoss [284]:

$$K_A = \frac{4\pi N_A\alpha^3}{3000}\exp\left(\frac{e^2}{\alpha\varepsilon kT}\right) \qquad (104)$$

In some cases, the magnitude of K_A was too small to permit a calculation of a. The distance parameter was finally determined from the more general equation due to Bjerrum [285].

$$K_A = \frac{4\pi N_A \alpha}{1000} \int_{r=a}^{r=q} r^2 \exp\left(\frac{z^2 e^2}{r\varepsilon kT}\right) dr \qquad (105)$$

The equations neglect specific short-range interactions except for solvation in which the solvated ion can be approximated by a hard sphere model. The method has been successfully utilized by Douheret [286].

2.8.2 ION SIZE PARAMETER AND IONIC ASSOCIATION

For plotting, equation (93) can be rearranged to the 'Λ' function as:

$$\Lambda_1 = \Lambda + S\sqrt{c} - Ec\ln c = \Lambda_o + J_1 c + J_2 \sqrt[3]{c} = \Lambda_o + J_1 c \qquad (106)$$

with J_2 term omitted.

Thus, a plot of Λ_o vs. c gives a straight line with Λ_o as intercept and J_1 as slope and 'a' values can be calculated from J_1 values. The 'a' values obtained by this method for DMSO were much smaller than would be expected from sums of crystallographic radii. One of the reasons attributed to it is that ion-solvent interactions are not included in the continuum theory on which the conductance equations are based. The inclusion of dielectric saturation results in an increase in 'a' values (much in conformity with the crystallographic radii) of alkali metal salts (having ions of high surface charge density) in sulpholane. The viscosity correction leads to a larger value of 'a' [287] but the agreement is still poor. However, little of real physical significance may be attached to the distance of closest approach derived from J_1 [288]. Fuoss [289] in 1975 proposed a new conductance equation. Latter he subsequently put forward another conductance equation in 1978 replacing the old one as suggested by Fuoss and co-workers. He classified the ions of electrolytic solutions in one of the three categories.(i) Ions finding an ion of opposite charge in the first shell of nearest neighbours (contact pairs) with $r_{ij} = a$. The nearest neighbours to a contact pair are the solvent molecules forming a cage around the pairs. (ii) Ions with overlapping Gurney's co-spheres (solvent separated pairs). For them $r_{ij} = a+ns$, where n is generally 1 but may be 2, 3 etc.; 's' is the diameter of sphere corresponding to the average volume (actual plus free) per solvent molecule.

(iii) Ions finding no other unpaired ion in a surrounding sphere of radius *R*, the diameter of the co-sphere (unpaired ions). Thermal motions and interionic forces establish a steady state, represented by the following equilibria:

$$A^+ + B^- \quad = \quad (A^+ \cdots\cdots\cdots B^-) \quad = \quad A^+ + B^- \quad = \quad AB \qquad (107)$$

Solvent separated ion-pair Contact ion-pair Neutral molecule

Contact pairs of ionogens may rearrange to neutral molecules $A^+B^- = AB$, e.g.,H_3O^+ and CH_3COO^-. Let γ be the fraction of solute present as unpaired (r>R) ions. If $c\gamma$ is the concentration of unpaired ion and α is the fraction of paired ions($r \leq R$), then the concentration of unpaired ion and $c(1-\alpha)(1-\gamma)$ and that of contact pair is $\alpha c(1-\gamma)$. The equation constants for eq. 107 are:

$$K_R = \frac{(1-\alpha)(1-\gamma)}{c\gamma^2 f^2} \qquad (108)$$

$$K_S = \frac{\alpha}{1-\alpha} = \exp\left(\frac{-E_S}{kT}\right) = e^{-\varepsilon} \qquad (109)$$

Where K_R describes the formation and separation of solvent separated pairs by diffusion in and out of spheres of diameter *R* around cations and can be calculated by continuum theory; K_S is the constant describing the specific short-range ion-solvent and ion-ion interactions by which contact pairs form and dissociate. E_S is the difference in energy between a pair in the states ($r = R$) and ($r = a$); ε is E_S measured in units of kT.

Now,
$$(1-\alpha) = \frac{1}{1+K_S} \qquad (110)$$

and the conductometric pairing constant is given by:

$$K_A = \frac{(1-\alpha)}{c\gamma^2 f^2} = \frac{K_R}{1-\alpha} = K_R(1+K_S) \qquad (111)$$

The equation determines the concentration, $c\gamma$ of active ions that produce long-range interionic effects. The contact pairs react as dipoles to an external field, *X* and contribute only to changing current. Both contact pairs and solvent separated pairs are left as virtual dipoles by unpaired ions, their interaction with unpaired ions is, therefore, neglected in calculating long-range effects (activity coefficients, relaxation field ΔX and electrophoresis ($\Delta X \Delta \Lambda_e$). The various patterns can be reproduced by theoretical fractions in the form:

$$\Lambda = p\left[\Lambda_o\left(\frac{1+\Delta X}{X}\right)+\Delta\Lambda_e\right] = p\left[\Lambda_o\left(1+R_X\right)+E_L\right] \tag{112}$$

which is a three parameter equation $\Lambda = \Lambda(c, \Lambda_o, R, E_S), \Delta X / X$ (the relaxation field) and $\Delta\Lambda_e$ (the electrophoretic counter current) are long range effects due to electrostatic interionic forces and p is the fraction of Gurney co-sphere.

The parameters K_R (or E_S) is a catch-all for all short range effects:

$$p = 1-\alpha(1-\gamma) \tag{113}$$

In case of ionogens or for ionophores in solvents of low dielectric constant, α is very near to unity ($-E_S/kT$) >> 1 and the equation becomes:

$$\Lambda = \gamma\left[\Lambda_o\left(\frac{1+\Delta X}{X}\right)\right]+\Delta\Lambda_e \tag{114}$$

The equilibrium constant for the effective reaction, $A^+ + B^- + AB$, is then

$$K_A = \frac{(1-\gamma)}{c\gamma^2 f^2} \approx K_R K_S \tag{115}$$

as $K_S >> 1$. The parameters and the variables are related by the set of equations:

$$\gamma = 1-\frac{K_R c\gamma^2 f^2}{(1-\alpha)} \tag{116}$$

$$K_R = \left(\frac{4\pi N_A R^3}{3000}\right)\exp\left(\frac{\beta}{R}\right) \tag{117}$$

$$-\ln f = \frac{\beta\kappa}{2(1+\kappa R)}, \quad \beta = \frac{e^2}{\varepsilon\kappa T} \tag{118}$$

$$\kappa^2 = 8\pi\beta\gamma\eta = \frac{\pi\beta N_A \gamma c}{125} \tag{119}$$

$$-\varepsilon = \ln\left[\frac{\alpha}{1-\alpha}\right] \tag{120}$$

The details of the calculations are presented in the 1978 paper [287]. The shortcomings of the previous equations have been rectified in the present equation that is also more general than the previous equations and can be used for higher concentrations (0.1 N in aqueous solutions).

2.8.3 LIMITING EQUIVALENT CONDUCTANCE

The limiting equivalent conductance of an electrolyte can be easily determined from the theoretical equations and experimental observations. At infinite dilutions, the motion of an ion is limited solely by the interactions with the surroundings solvent molecules as the ions are infinitely apart. Under these conditions, the validity of Kohlrausch's law of independent migration of ions is almost axiomatic. Thus:

$$\Lambda_0 = \lambda_o^+ + \lambda_o^- \tag{121a}$$

At present, limiting equivalent conductance is the only function which can be divided into ionic components using experimentally determined transport number of ions, i.e.,

$$\lambda_o^+ = t_+ \Lambda_0 \text{ and } \lambda_o^- = t_- \Lambda_0 \tag{121b}$$

Thus, from accurate value of λ_0 of ions it is possible to separate the contributions due to cations and anions in the solute-solvent interactions. However, accurate transference number determinations are limited to few solvents only.

In the absence of experimentally measured transference numbers it would be useful to develop indirect methods to obtain the ionic limiting equivalent conductances in solvents for which experimental transference numbers are not yet available. Various attempts were made to develop indirect methods to obtain the limiting ionic equivalent conductance, in ionic solvents for which experimental transference numbers are not yet available.

The method has been summarized by Krumgalz [290] and some important points are mentioned as follows:

(i) Walden equation [291]

$$(\lambda_o^{\pm})^{25}_{\text{water}} \cdot \eta_{o,\text{water}} = (\lambda_o^{\pm})^{25}_{\text{acetone}} \cdot \eta_{o,\text{acetone}} \tag{122}$$

(ii) $(\lambda_{o,\text{pic}} \cdot \eta_o) = 0.267, \quad \lambda_{o,Et_4N^+} \cdot \eta_o = 0.269$ [301,302] (123)

based on $\Lambda_{o,Et_4N_{pic}} = 0.563$

Walden considered the products to be independent of temperature and solvent. However, the $\Lambda_{o,Et_4N_{pic}}$ values used by Walden were found to differ considerably

from the data of subsequent more precise studies and the values of (ii) are considerably different for different solvents.

(iii) $\lambda_o^{25}(Bu_4N^+) = \lambda_o^{25}(Ph_4B^-)$ (124)

The equality holds good in nitrobenzene and in mixture with CCl_4 but not realized in methanol, acetonitrile and nitromethane.

(iv) $\lambda_o^{25}(Bu_4N^+) = \lambda_o^{25}(Bu_4B^-)$ [303] (125)

The method appears to be sound as the negative charge on boron in the Bu_4B^- ion is completely shielded by four inert butyl groups as in the Bu_4N^+ ion while this phenomenon was not observed in case of Ph_4B^-.

(v) The equation suggested by Gill [304] is:

$$\lambda_o^{25}(R_4N^+) = \frac{zF^2}{6\pi N_A \eta_o [r_i - (0.0103\varepsilon_o + r_y)]} \quad (126)$$

where Z and r_i are the charge and crystallographic radius of proper ion, respectively: η_o and ε_o are solvent viscosity and dielectric constant of the medium, respectively; r_y = adjustable parameter taken equal to 0.85 Å and 1.13 Å for dipolar non-associated solvents and for hydrogen bonded and other associated solvents respectively.

However, large discrepancies were observed between the experimental and calculated values [290(a)]. In a paper, [290(b)] Krumgalz examined the Gill's approach more critically using conductance data in many solvents and found the method reliable in three solvents e.g. butan-1-ol, acetonitrile and nitromethane.

(vi) $\lambda_o^{25}\left[(i-Am)_3 BuN^+\right] = \lambda_o^{25}\left(Ph_4B^-\right)$ [305] (127)

It has been found from transference number measurements that the $\lambda_o^{25}\left[(i-Am)_3 BuN^+\right]$ and $\lambda_o^{25}\left(Ph_4B^-\right)$ values differ from one another by 1%.

(vii) $\lambda_o^{25}\left(Ph_4B^-\right) = 1.01\lambda_o^{25}\left[(i-Am)_4 B^-\right]$ [306] (128)

The value is found to be true for various organic solvents.

Krumgalz suggested a method for determining the limiting ion conductance in organic solvents. The method is based on the fact that large tetraalkyl (aryl) onium ions are not solvated in organic solvents due to the extremely weak electrostatic

interactions between solvent molecules and the large ions with low surface charge density and this phenomenon can be utilized as a suitable model for apportioning Λ_o values into ionic components for non-aqueous electrolytic solutions.

Considering the motion of solvated ion in an electrostatic field as a whole, it is possible to calculate the radius of the moving particle by the Stokes equation:

$$r_S = \frac{|z| F^2}{A\pi\eta_o\lambda_o^{\pm}} \tag{129}$$

where A is a coefficient varying from 6 (in the case of perfect sticking) to 4 (in case of perfect slipping). Since the r_S values, the real dimension of the non-solvated tetraalkyl (aryl) onium ions must be constant, we have:

$$\lambda_o^{\pm}\eta_0 = \text{constant} \tag{130}$$

This relation has been verified using $\lambda_o^{\pm}$ values determined with precise transference numbers. The product becomes constant and independent of the chemical nature of the organic solvents for the i-Am_4B^-, Ph_4As^+, Ph_4B^- ions and for tetraalkylammonium cation starting with Et_4N^+. The relationship can be well utilized to determine $\lambda_o^{\pm}$ of ions in other organic solvents from the determined Λ_o values

2.8.4 SOLVATION

Various types of interactions exist between the ions in solutions. These interactions result in the orientation of the solvent molecules towards the ion. The number of solvent molecules that are involved in the solvation of the ion is called solvation number. If the solvent is water, this is called hydration number. Solvation region can be classified as primary and secondary solvation regions. Here we are concerned with the primary solvation region. The primary solvation number is defined as the number of solvent molecules which surrender their own translational freedom and remain with the ion, tightly bound, as it moves around, or the number of solvent molecules which are aligned in the force field of the ion.

If the limiting conductance of the ion i of charge Z_i is known, the effective radius of the solvated ion can be determined from Stokes' law. The volume of the solvation shell is given by the equation.

$$V_S = \left(\frac{4\pi}{3}\right)\left(r_S^3 - r_C^3\right) \tag{131}$$

where r_c is the crystallographic radius of the ion. The solvation number n_s would then be obtained from

$$n_S = \frac{V_S}{V_0} \tag{132}$$

Assuming Stokes' relation to hold well, the ionic solvated volume can be obtained, because of the packing effects [292], from

$$V_S^o = 4.35 r_S^3 \tag{133}$$

where V_S^o is expressed in mol/lit. and r_S in angstroms. However, this method is not applicable to ions of medium size though a number of empirical and theoretical corrections [293-296] have been suggested in order to apply it to most of the ions.

2.8.5 STOKES' LAW AND WALDEN'S RULE

The starting point for most evaluations of ionic conductances is Stokes' law that states that the limiting Walden product (the limiting ionic conductance-solvent viscosity product) for any singly charged, spherical ion is as function only of the ionic radius and thus, under normal conditions, is constant. The limiting conductances λ_i^o of a spherical ion of radius R_i moving in a solvent of dielectric continuum can be written, according to Stokes' hydrodynamics, as

$$\lambda_o^i = \frac{|z_i e| eF}{6\pi\eta_o R_i} = \frac{0.819|z_i|}{\eta_o R_i} \tag{134}$$

where η_o = macroscopic viscosity by the solvent in poise, R_i is in angstroms. If the radius R_i is assumed to be the same in every organic solvent, as would be the case, in case of bulky organic ions, we get:

$$\lambda_o^i \eta_o = \frac{0.819 z_i}{R_i} = constant \tag{135}$$

This is known as the Walden rule [297]. The effective radii obtained using this equation can be used to estimate the solvation numbers. However, Stokes' radii failed to give the effective size of the solvated ions for small ions.

Robinson and Stokes [298], Nightingale [196] and others [299-301] have suggested a method of correcting the radii. The tetraalkylammonium ions were assumed to be not solvated and by plotting the Stokes' radii against the crystal radii

of those large ions, a calibration curve was obtained for each solvent. However, the experimental results indicate that the method is incorrect as the method is based on the wrong assumption of the invariance of Walden's product with temperature. The idea of microscopic viscosity [302] was invoked without much success [303, 304] but it has been found that:

$$\lambda_o^i \eta_0 = \text{constant} \tag{136}$$

where p is usually 0.7 for alkali metal or halide ions and $p = 1$ for the large ions [305, 306]. Gill [307] has pointed out the inapplicability of the Zwanzig theory [308] of dielectric friction for some ions in non-aqueous and mixed solvents and has proposed an empirical modification of Stokes' Law accounting for the dielectric friction effect quantitatively and predicts actual solvated radii of ions in solution. This equation can be written as:

$$r_i = \frac{|z| F^2}{6\pi N_A \eta_o \lambda_o^i} + 0.0103D + r_y \tag{137}$$

where r_i is the actual solvated radius of the ion in solution and r_y is an empirical constant dependent on the nature of the solvent [307, 308].

The dependence of Walden product on the dielectric constant led Fuoss to consider the effect of the electrostatic forces on the hydrodynamics of the system. Considering the excess frictional resistance caused by the dielectric relaxation in the solvent caused by ionic motion, Fuoss proposed the relation:

$$\lambda_o^i = \frac{Fe|z_i|}{6\pi R_\infty}\left(\frac{1+A}{\varepsilon R_\infty^2}\right) \tag{138}$$

or,

$$R_i = R_\infty + \frac{R}{\infty} \tag{139}$$

where R_∞ is the hydrodynamic radius of the ion in a hypothetical medium of dielectric constant where all electrostatic forces vanish and A is an empirical constant.

It is found that the Zwanzig's theory is successful for large organic cations in aprotic media where solvation is likely to be minimum and where viscous friction predominates over that caused by dielectric relaxation. The theory breaks down whenever the dielectric relaxation term becomes large, i.e., for solvents of high P^*

and for ions of small r_i. Like any continuum theory Zwanzig has the inherent weakness of its inability to account for the structural features, [309] e.g.,

(i) It does not allow for any correlation in the orientation of the solvent molecules as the ion passes by and this may be the reason why the equation is not applicable to the hydrogen-bonded solvents [310].

(ii) The theory does not distinguish between positively and negatively charged ions and therefore, cannot explain why certain anions in dipolar aprotic media possess considerably higher molar concentrations than the fastest cations.

The Walden product in case of mixed solvents does not show any constancy but it shows a maximum in case of DMF + water and DMA + water [309-318] mixtures and other aqueous binary mixtures [319-322]. To derive expressions for the variation of the Walden product with the composition of mixed polar solvents, various attempts [323] have been made with different models for ion-solvent interactions but no satisfactory expression has been derived taking into account all types of ion-solvent interactions because

(i) it is difficult to include all types of interactions between ions as well as solvents in a single mathematical expression, and

(ii) it is not possible to account for some specific properties of different kinds of ions and solvent molecules.

Ions moving in a dielectric medium experience a frictional force due to dielectric loss arising from ion-solvent interactions with the hydrodynamic force. Though Zwanzig's expression accounts for a change in Walden product with solvent composition but does not account for the maxima. According to Hemmes [324] the major deviations in the Walden products are due to the variation in the electrochemical equilibrium between ions and solvent molecules of mixed polar solvent composition. In cases where more than one types of solvated complexes are formed, there should be a maximum and/or a minimum in the Walden product. This is supported from experimental observations. Hubbard and Onsager [325] have developed the kinetic theory of ion-solvent interaction within the framework of continuum mechanics where the concept of kinetic polarization deficiency has been introduced. However, quantitative expression is still awaited. Further, improvements [326, 327] naturally must be in terms of (i) sophisticated treatment of dielectric saturation, (ii) specific structural effects involving ion-solvent

interactions. From the discussion, it is apparent that the problem of molecular interactions is intriguing as well as interesting. It is desirable to explore this problem using different experimental techniques. We have, therefore, utilized four important methods, viz., volumetric, viscometric, interferometric and conductometric for the physico-chemical studies in different solvent media.

2.8.6 THERMODYNAMICS OF ION-PAIR FORMATION

The standard Gibbs energy changes (ΔG^o) for the ion- association process can be calculated from the equation

$$\Delta G^o = -RT \ln K_A \tag{140}$$

The values of the standard enthalpy change, ΔH^o and the standard entropy change, ΔS^o, can be evaluated from the temperature dependence of values as follows,

$$\Delta H^o = -T^2 \left[\frac{d(\Delta G^o / T)}{dT} \right]_P \tag{141}$$

$$\Delta S^o = -T^2 \left[\frac{d(\Delta G^o)}{dT} \right]_P \tag{142}$$

The values can be fitted with the help of a polynomial of the type:

$$\Delta G^o = c_0 + c_1(298.15 - T) + c_2(298.15 - T)^2 \tag{143}$$

And the coefficients of the fits can be compiled together with the$\sigma\sigma$ % values of the fits. The standard values at 298.15 K are then:

$$\Delta G^o_{298.15} = c_0 \tag{144}$$

$$\Delta S^o_{298.15} = c_1 \tag{145}$$

$$\Delta H^o_{298.15} = c_o + 298.15 c_1 \tag{146}$$

The main factors which govern the standard entropy of ion-association of electrolytes are: (i) the size and shape of the ions, (ii) charge density on the ions, (iii) electrostriction of the solvent molecules around the ions, and (iv) penetration of the solvent molecules inside the space of the ions, and the influence of these factors are discussed later.

The non-columbic part of the Gibbs energy ΔG^o can also be calculated using the following equation:

$$\Delta G^{o} = N_A W_{\pm} \tag{147}$$

$$K_A = \left(\frac{4\pi N_A}{1000}\right)\int_a^R r^2 \exp\left(\frac{2q}{r} - \frac{W_{\pm}}{kT}\right) dr \tag{148}$$

where the symbols have their usual significance.

The quantity 2q/r is Columbic part of the interionic mean force potential and $W_{\pm}$ is its non-columbic part.

2.8.7 SOLVATION MODELS—SOME RECENT TRENDS

The interactions between particles in chemistry have been based upon empirical laws- principally on Coulomb's law. This is also the basis of the attractive part of the potential energy used in the SchÖdinger equation. Quantum mechanical approach for ion-water interactions was begun by Clementi in 1970. A quantum mechanical approach to salvation can provide information on the energy of the individual ion-water interactions provided it is relevant to solution chemistry, because it concerns potential energy rather than the entropic aspect of salvation. Another problem in quantum approach is the mobility of ions in solution affecting salvation number and coordination number. However, the Clementi calculations concerned stationary models and cannot have much to do with the dynamic salvation numbers. Covalent bond formation enters little into the aqueous calculations; however, with organic solvents the quantum mechanical approaches to bonding may be essential. The trend pointing to the future is thus the molecular dynamics technique. In molecular dynamic approach, a limited number of ions and molecules and Newtonian mechanics of movement of all particles in solution is concerned. The foundation of such a approach is the knowledge of the intermolecular energy of interactions between a pair of particles. Computer simulation approaches may be useful in this regard and the last decade (1990-2000) witnessed some interesting trends in the development of solvation models and computer software. Based on a collection of experimental free energy of solvation data, C.J. Cramer, D.G. Truhlar and co-workers from the University of Minnesota, U.S.A. constructed a series of solvation models (SM1-SM5 series) to predict and calculate the free energy of solvation of a chemical compound [328-332]. These

models are applicable to virtually any substance composed of H, C, N, O, F, P, S, Cl, Br and/or I. The only input data required are, molecular formula, geometry, refractive index, surface tension, Abraham's a (acidity parameter) and b (basicity parameter) values, and, in the latest models, the dielectric constants. The advantage of models like SM5 series is that they can be used to predict the free energy of self-solvation to better than 1 KCl/mole. These are especially useful when other methods are not available. One can also analyze factors like electrostatics, dispersion, hydrogen bonding, etc. using these tools. They are also relatively inexpensive and available in easy to use computer codes.

A. Galindo *et al.* [333,334] have developed Statistical Associating Fluid Theory for Variable Range (SAFT-VR) to model the thermodynamics and phase equilibrium of electrolytic aqueous solutions. The water molecules are modeled as hard spheres with four short-range attractive sites to account for the hydrogen-bond interactions. The electrolyte is modeled as two hard spheres of different diameter to describe the anion and cation. The Debye-Hückel and mean spherical approximations are used to describe the interactions. Good agreement with experimental data is found for a number of aqueous electrolyte solutions. The relative permittivity becomes very close to unity, especially when the mean spherical approximation is used, indicating a good description of the solvent. E. Bosch *et al.* [335] of the University of Barcelona, Spain, have compared several "Preferential Solvation Models".

2.9 REFRACTIVE INDEX

Refractive Index measurement data provides interesting information related to molecular interactions and structure of the solutions, as well as complementary data on practical procedures, such as concentration measurement or estimation of other properties [336].

The ratio of the speed of light in a vacuum to the speed of light in another substance is defined as the index of refraction (n_D) for the substance:

$$\text{Refractive Index } (n_D) \text{ of substance} = \frac{\text{Speed of light in vacuum}}{\text{Speed of light in substance}}$$

Whenever light changes speed as it crosses a boundary from one medium into another, its direction of travel also changes, i.e., it is refracted. The relationship between light's speed in the two mediums (V_A and V_B), the angles of incidence ($sin\theta_A$) and refraction ($sin\theta_B$) and the refractive indexes of the two mediums (n_A and n_B) is shown below:

$$\frac{V_A}{V_B}=\frac{sin\theta_A}{sin\theta_B}=\frac{n_B}{n_A} \tag{149}$$

By measuring the angle of refraction, and knowing the index of refraction of the layer that is in contact with the sample, it is possible to determine the refractive index of the sample quite accurately.

The refractive index of mixing can be correlated by the application of a composition-dependent polynomial equation. Molar refractivity, was obtained from the Lorentz-Lorenz relation by using, n_D experimental data according to the following expression

$$R=[(n_D^2-1)/n_D^2+2](M/\rho) \tag{150}$$

where M is the mean molecular weight of the mixture and ρ is the mixture density. n_D can be expressed as the following:

$$n_D=[(2A+1)/(1-A)]^{0.5} \tag{151}$$

where A is given by:

$$A=[\{\frac{(n_1^2-1)}{(n_1^2+2)}(1/\rho_1)\}-\{\frac{(n_1^2-1)}{(n_1^2+2)}(w_2/\rho_1)\}+\{\frac{(n_2^2-1)}{(n_2^2+2)}(w_2/\rho_2)\}\rho] \tag{152}$$

where n_1 and n_2 are the pure component refractive indices, w_j the weight fraction, ρ the mixture density, and ρ_1 and ρ_2 the pure component densities.

The molar refractivity deviation is calculated by the following expression:

$$\Delta R=R-\phi_1R_1-\phi_2R_2 \tag{153}$$

where ϕ_1 and ϕ_2 are volume fractions and R, R_1, and R_2 the molar refractivity of the mixture and of the pure components, respectively.

The deviations of refractive index were used for the correlation of the binary solvent mixtures:

$$\Delta n_D=n_D-x_1n_{D1}-x_2n_{D2} \tag{154}$$

where Δn_D is the deviation of the refractive index for this binary system and n_D, n_{D1}, and n_{D2} are the refractive index of the binary mixture, refractive index of component-1, and refractive index of component-2, respectively. x is the mole fraction.

The computed deviations of refractive indices of the binary mixtures are fitted using the following Redlich-Kister expression [337].

$$\Delta n_{Dew} = w_e w_w \sum_{P=0}^{S} B_p (w_e w_w)^p \qquad (155)$$

where B_p are the adjustable parameters obtained by a least squares fitting method, w is the mass fraction, and S is the number of terms in the polynomial.

In case of salt-solvent solution the binary systems were fitted to polynomials of the form:

$$n_{Ds,sol} = n_{Dsol} + \sum_{i=1}^{N} A_i m^i \qquad (156)$$

where $n_{Ds,sol}$ is the refractive index of the solute + solvent system and n_{Dsol} is the refractive index of the solvent respectively, m is the molality of the salt in the solution, Ai are the fitting parameters, and N is the number of terms in the polynomial.

There is no general rule that states how to calculate a refractivity deviation function. However, the molar refractivity is isomorphic to a volume for which the ideal behavior may be expressed in terms of mole fraction: in this case smaller deviations occur but data are more scattered because of the higher sensitivity of the expression to rounding errors in the mole fraction. For the sake of completeness, both calculations of refractivity deviation function, molar refractivity deviation was fitted to a Redlich and Kister-type expression and the adjustable parameters and the relevant standard deviation $\acute{o}$ are calculated for the expression in terms of volume fractions and in terms of mole fractions, respectively.

From the discussion, it is apparent that the problem of molecular interactions is stimulating as well as interesting. It is desirable to attack this problem using different experimental techniques. We have, therefore, utilized five important methods, *viz.*, volumetric, viscometric, interferometric, conductometric and refractometric for the physico-chemical studies in different solution systems.

CHAPTER III

EXPERIMENTAL SECTION

3.1 NAME, STRUCTURE, PHYSICAL PROPERTIES, SOURCE, PURIFICATION AND APPLICATIONS OF CHEMICALS USED IN THE RESEARCH WORK

SOLUTES

Folic Acid

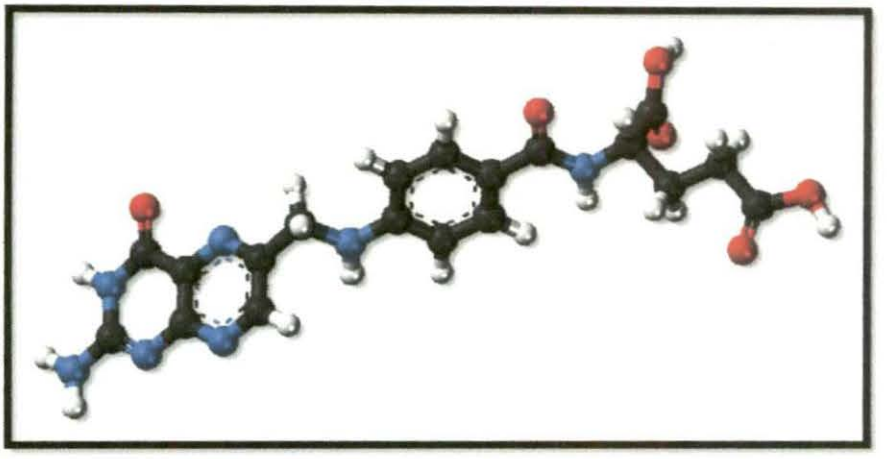

Molecular Formula : $C_{19}H_{19}N_7O_6$, **Molecular Weight**: 441.40 , **Appearance**: yellow-orange solid, **Melting Point**: 523.15K

Source: Sigma-Aldrich, Germany.

Purification: The mass purity as supplied is 0.99. It was dried from moisture at 353K for 24 h, and then cooled and stored in a desiccator prior to use.

Application: Vitamin B9 (folic acid and folate) is essential for numerous bodily functions. Humans cannot synthesize folate de novo; therefore, folate has to be supplied through the diet to meet their daily requirements. The human body needs folate to synthesize DNA, repair DNA, and methylate DNA as well as to act as a cofactor in certain biological reactions. It is especially important in aiding rapid cell division and growth, such as in infancy and pregnancy, and reproduction of cells, particularly red blood cells. Children and adults both require folic acid to produce healthy red blood cells and prevent anemia.[1]

Nicotinic Acid

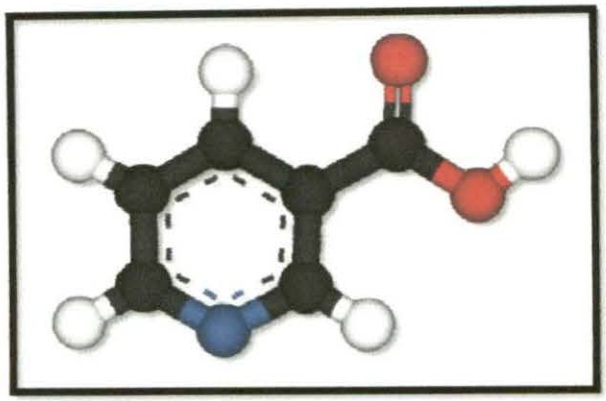

Molecular Formula: $C_6H_5O_2$, **Molecular Weight:** 123.11, **Appearance:** white solid, **Melting Point:** 510.15K

Source: Sigma-Aldrich, Germany.

Purification: It was dried from moisture at 353K for 24 h, and then cooled and stored in a desiccator prior to use.

Application: Nicotinic acid also known as Vitamin B3 is a water-soluble vitamin and an essential in micronutrient [2,3]. It is useful in pharmaceutical industries and food technology as well as in every process of the reaction occurring in protein and peptides chain.

Ascorbic Acid

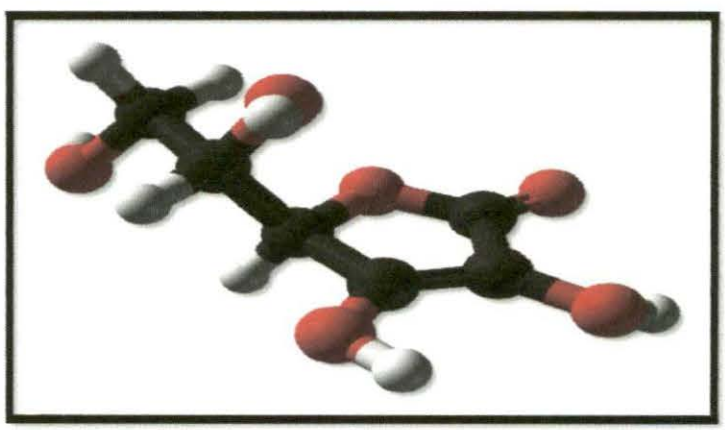

Molecular Formula: $C_6H_8O_6$, **Molecular Weight:** 176.12, **Appearance:** white solid, **Melting Point:** 463.15K

Source: Sigma-Aldrich, Germany.

Purification: Used as purchased as the purity assay of the solute was ≥98%.

Application: It is very important constituent of our physiological system. Vitamin C is required for the synthesis of collagen, the intercellular "cement" which gives the structure of muscles, vascular tissues, bones, and tendon.. It also enhances the eye's ability and delay the progression of advanced age related muscular degeneration [4]. It is helpful in formulation of many pharmaceutical products.

Glycine

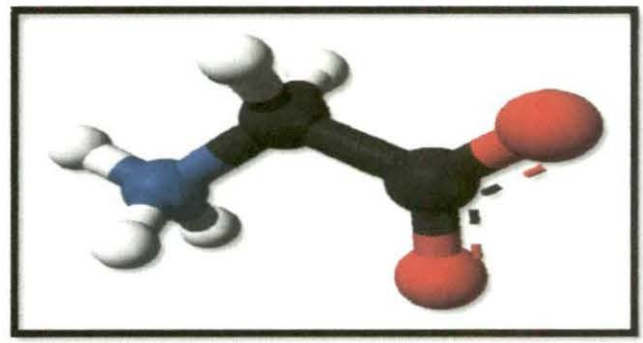

Molecular Formula: $C_2H_5NO_2$, **Molecular Weight**: 75.07, **Appearance**: white solid, **Melting Point**: 506.15K, **Source**: Sigma Aldrich, Germany

Purification: Used as parched without further purification. The purity is 99.99%.

Application: It has some pharmaceutical application. For humans, glycine is solid as a sweetener/taste enhancer. Certain food supplements and protein drinks containing glycine, for drug formulations it used to improve gastric absorption. Many miscellaneous products use glycine or its derivatives to make daily usable commodities.

L- Alanine

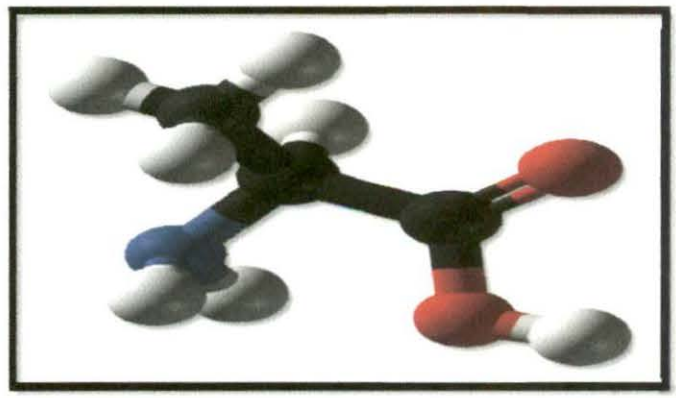

Molecular Formula: $C_3H_9NO_2$, **Molecular Weight**: 89.09, **Appearance**: white solid, **Melting Point**: 531.15K

Source: Sigma Aldrich, Germany

Purification: Used as parched without further purification. The purity is 99.99%.

Application: Alanine plays a key role in glucose–alanine cycle between tissues and liver. Sometimes it is used in case of radiotherapy. It has some medicinal use also.

L-Valine

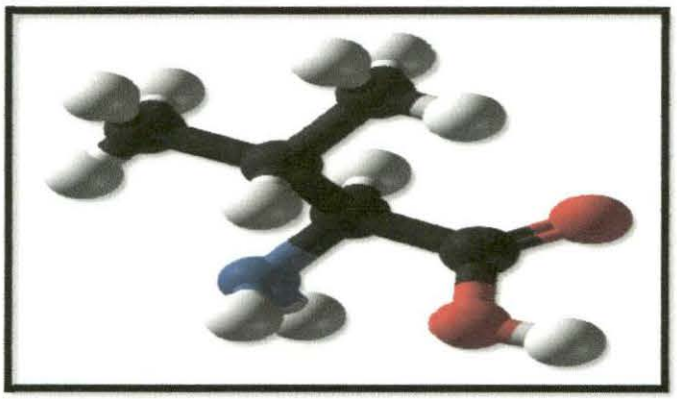

Molecular Formula: $C_5H_{11}NO_2$, **Molecular Weight**: 117.15, **Appearance**: white solid, **Melting Point**: 506.15K, **Source**: Sigma Aldrich, Germany

Purification: Used as parched without further purification. The purity is 99.99%.

Application: It is used for some pharmaceutical applications, industrial applications, food supplements and protein drinks, give out as a buffering agent in antacids, analgesics, antiperspirants, cosmetics, toiletries, production of rubber sponge products, fertilizers, metal complexants etc. Valine is an essential amino acid; hence it must be ingested, usually as a component of proteins.

Cysteine

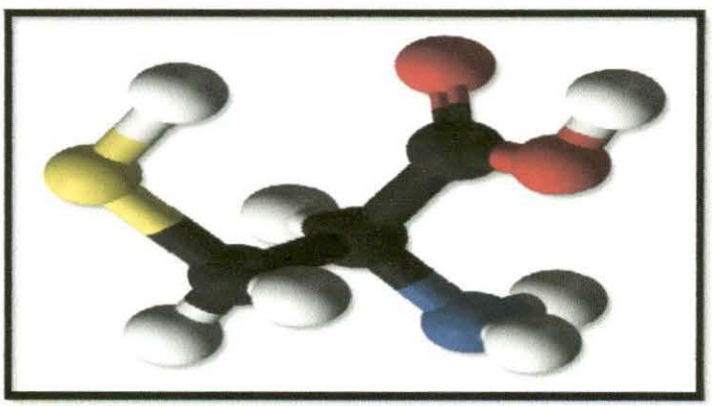

Molecular Formula: $C_3H_7NO_2S$, **Molecular Weight**: 121.16,

Appearance: white solid, **Melting Point**: 513.15K

Source: Sigma Aldrich, Germany

Purification: Used as parched without further purification. The purity is 99.99%

Application: Cysteine is a semi-essential amino acid, which means that it can be bio-synthesized in human body under normal physiological conditions if a sufficient quantity of methionine is available. Although classified as a non-essential amino acid, in rare cases, cysteine may be essential for infants, the elderly, and individuals with certain metabolic disease.

D-Glucose

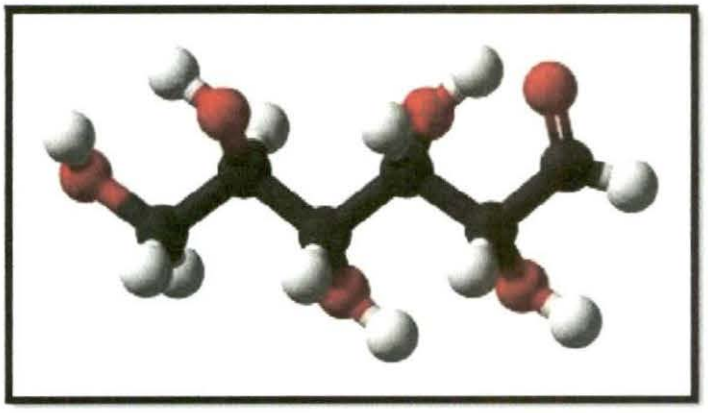

Molecular Formula: $C_6H_{12}O_6$, **Molecular Weight**: 180.16, **Appearance**: white solid, **Melting Point**: 419.15K

Source: Sigma-Aldrich, Germany.

Purification: Used as purchased as the purity assay of the solute was ≥98%.

Application: It is used as an energy source in most organisms, from bacteria to humans. Living cells use it as a secondary source of energy and a metabolic intermediate. Glucose is one of the main products of photosynthesis and fuels for cellular respiration. It is used in energy drinks and having some important pharmaceutical use.

D-Sucrose

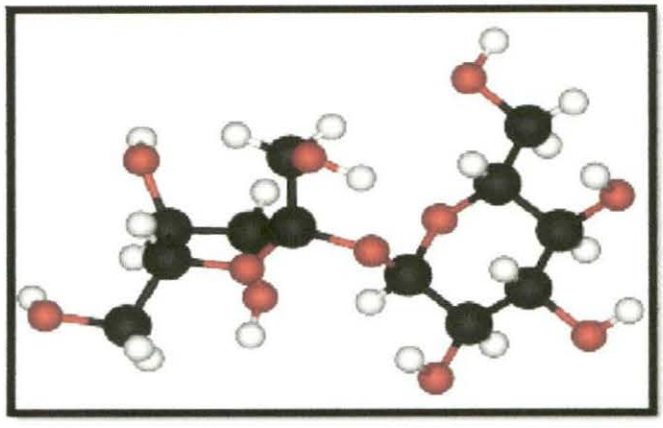

Molecular Formula: $C_{12}H_{22}O_{11}$, **Molecular Weight**: 342.30, **Appearance**: white solid, **Melting Point**: 459.15K

Source: Sigma-Aldrich, Germany.

Purification: Used as purchased as the purity assay of the solute was ≥98%.

Application: Commonly known as table sugar, cane sugar, beet sugar or, usually, just sugar. Widely used as sweetener in different food products. Acts as source of energy in human body system. Industrially used to prepare Ethyl alcohol and having some important pharmaceutical use as well.

D-Maltose monohydrate

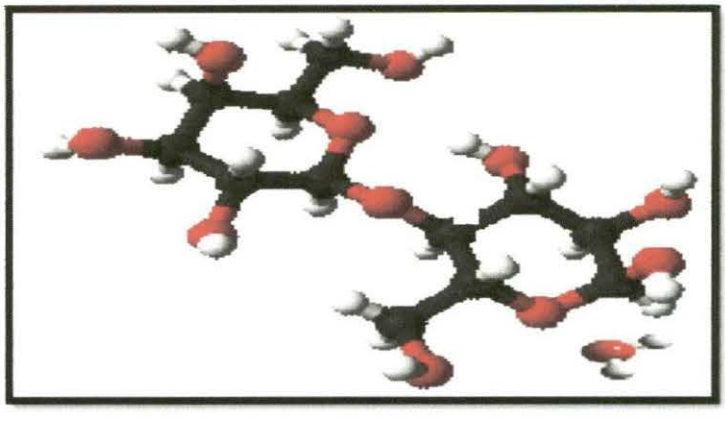

Molecular Formula: $C_{12}H_{22}O_{11}$, **Molecular Weight**: 342.30, **Appearance**: white solid, **Melting Point**: 375.15K

Source: Sigma-Aldrich, Germany.

Purification: Used as purchased as the purity assay of the solute was ≥98%.

Application: It is used to rectify congenital disorder which is most prominent in infancy by human body itself. In humans, maltose is broken down by the enzyme maltase so that there are two glucose molecules from which the glucose metabolism obtains energy. It has specific pharmaceutical and industrial use.

Citric Acid

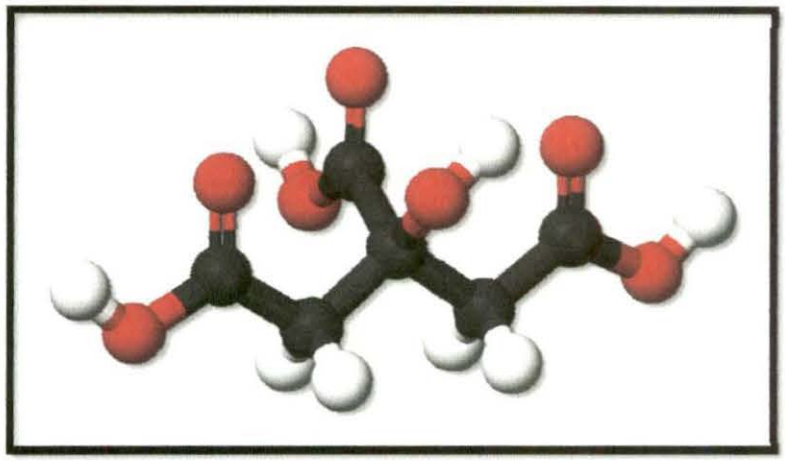

Molecular Formula: $C_6H_8O_7$, **Molecular Weight**: 192.12, **Appearance**: white solid, **Melting Point**: 523.15K

Source: Purchased from Hi Media.

Purification: Its mass purity as supplied is 0.99. The reagent was always placed in the desiccator over P_2O_5 to keep them in dry atmosphere.

Application: The dominant use of citric acid is as a flavouring and preservative in food and beverages, especially soft drinks. It can be used to soften water, which makes it useful in soaps and laundry detergents. Citric acid is widely used as a pH adjusting agent in creams and gels of all kinds. Citric acid is an alpha hydroxy acid and used as an active ingredient in chemical peels. As it occurs in metabolism of almost all living beings, its interactions in an aqueous solution is of great value to the biological scientists. In the pharmaceutical industry, citric acid is used as a stabilizer in various formulations, as a drug component and as an anticoagulant in blood for transfusions and also used as an acidifier in many pharmaceuticals.

Nicotinamide

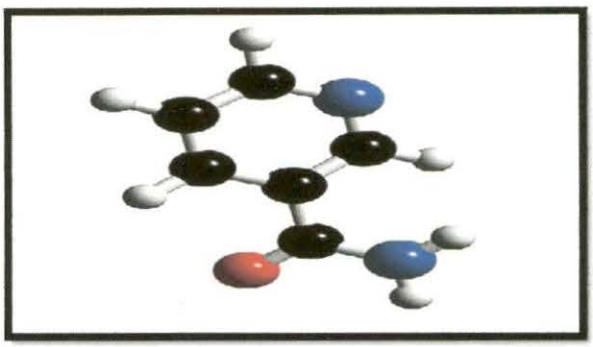

Molecular formula:$C_6H_6N_2O$, **Molecular weight**: 122.12, **Appearance**: white solid, **Melting Point**:401K

Source: Sigma-Aldrich, Germany.

Purification: It was dried from moisture and then cooled and stored in a desiccator prior to use.

Application: Studies show that nicotinamide has anxiolytic (anti-anxiety) properties. A safety study of niacinamide for the treatment of Alzheimer's disease is currently underway. Its anti-inflammatory actions that may be of benefit to patients with inflammatory skin conditions.

Lithium acetate

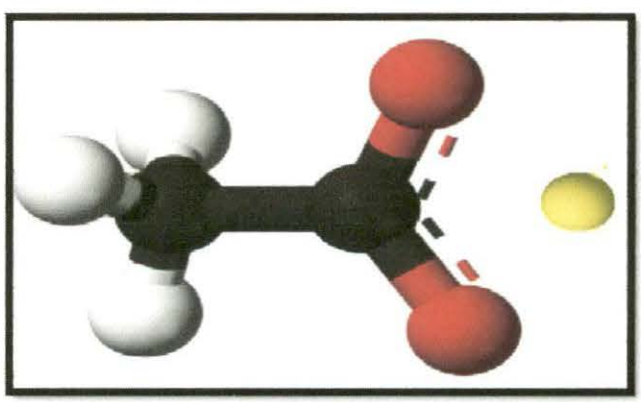

Molecular Formula: $C_3H_3LiO_2$, **Molecular Weight**: 65.99, **Appearance**: white solid, **Melting Point**: 559.15K

Source: Purchased from Merck, India

Purification: Purified by re-crystallization twice from conductivity water. It was dried in vacuum and stored over P_2O_5 under vacuum before use.

Application: Used in the laboratory as buffer for gel electrophoresis of DNA and RNA. This salt has some specific medicinal use.

Sodium acetate

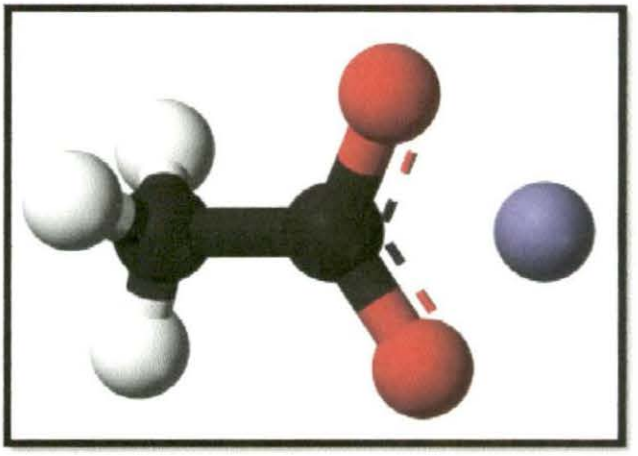

Molecular Formula: $C_3H_3NaO_2$, **Molecular Weight**: 82.03, **Appearance**: white solid, **Melting Point**: 597.15K

Source: Purchased from Merck, India

Purification: Used as parched without further purification.

Application: Sodium acetate may be added to food as a seasoning, helps to impede vulcanization of chloroprene in synthetic rubber production. It is used in the textile industry to neutralize sulphuric acid waste.

Potassium acetate

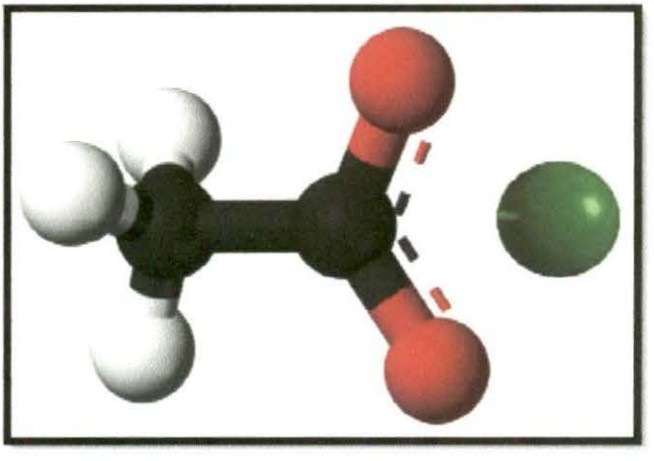

Molecular Formula: $C_3H_3KO_2$, **Molecular Weight**: 98.15, **Appearance**: white solid, **Melting Point**: 565.15K

Source: Purchased from Merck, India

Purification: Used as parched without further purification.

Application: In medicine, potassium acetate is used as part of replacement protocols in the treatment of diabetic ketoacidosis because of its ability to break down into bicarbonate and help neutralize the acidotic state. It is used as a food additive as a preservative and acidity regulator.

Ammonium acetate

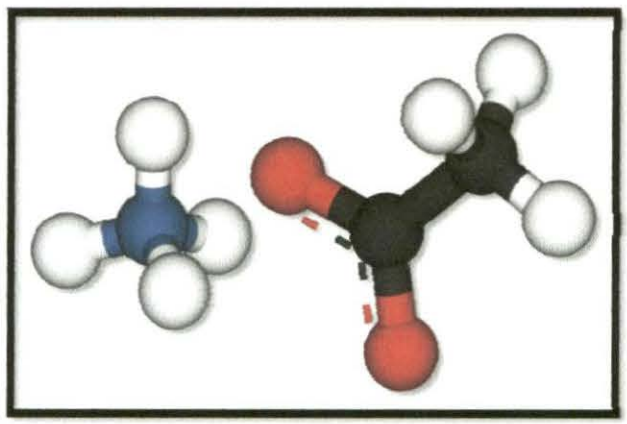

Molecular Formula: $C_3H_7NO_2$, **Molecular Weight**: 77.08, **Appearance**: white solid, **Melting Point**: 387.15K

Source: Purchased from Merck, India

Purification: Purified by re-crystallization twice from conductivity water. It was dried in vacuum and stored over P_2O_5 under vacuum before use.

Application: It is a relatively unusual example of a salt that melts at low temperatures. It is often used as an aqueous buffer for ESI mass spectrometry of proteins and other molecules. It is also used as a food additive as an acidity regulator.

Tetrabutylammonium acetate

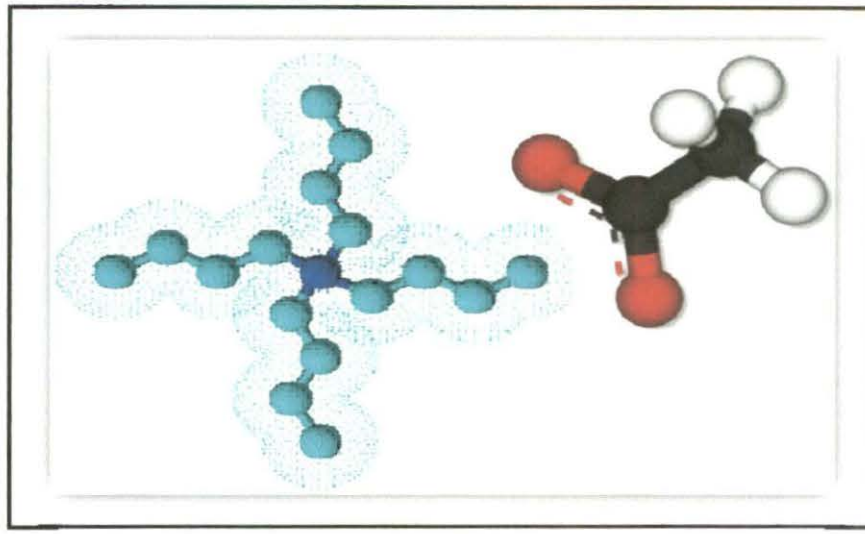

Molecular Formula: $C_{16}H_{36}N.C_2H_3O_2$, **Molecular Weight** : 301.51, **Appearance**: white solid, **Melting Point**: 371.15K

Source: Purchased from Merck, India

Purification: Salt was purified by re-crystallization and the crystallized salt was dried in vacuum for 48 hrs before use.

Application: Used as supporting electrolyte. In organic chemistry it is used as precipitating agent.

Sodiumtetraphenylborate

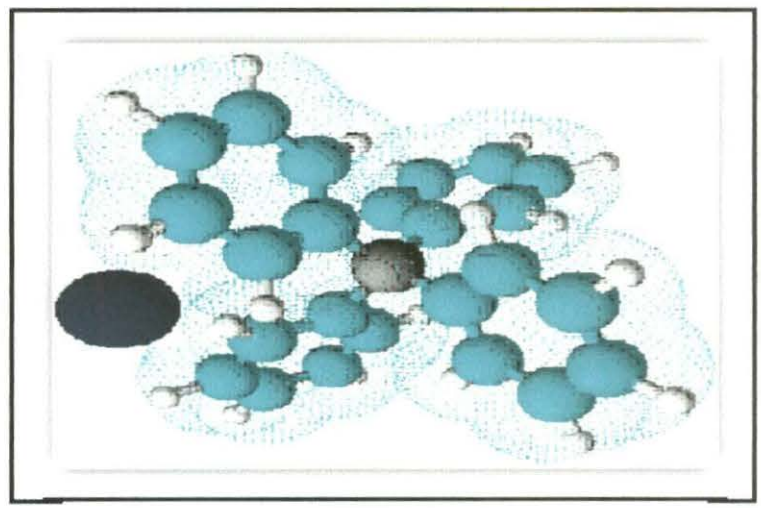

Molecular Formula: $C_{24}H_{20}BNa$, **Molecular Weight**: 342.22 , **Appearance**: white solid, **Melting Point**: 573.15K

Source: Purchased from Merck, India

Purification: Salt was purified by recrystallization and the crystallized salt was dried in vacuum for 72 hrs before use.

Application: It is used to prepare other tetraphenylborate salts, which are often highly soluble in organic solvents. The compound is used in inorganic and organometallic chemistry as a precipitating agent. It is used as supporting electrolyte.

SOLVENTS

Water

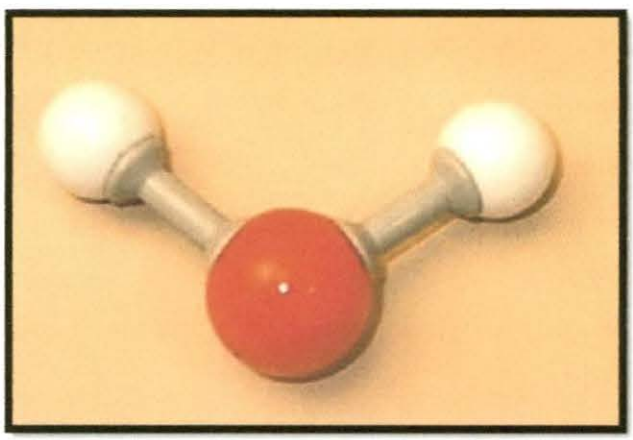

Molecular Formula: H_2O, **Molecular Weight**: 18.02 , **Appearance**: colourless liquid, **Density**: 0.99713 g·cm^3, **Dielectric constant**: 78.35 at 298.15K

Source: Collected by fractional distillation in Laboratory.

Purification: Deionised water was distilled in an all glass distilling set along with alkaline KMnO4 solution to remove organic matter. Precautions were taken to prevent contamination.

Application: Life on earth totally depends on water. It is a superb solvent, generally taken as the universal solvent, due to the marked polarity of the water molecule and its tendency to form hydrogen bonds with other molecules. It is widely used in chemical reactions as a solvent. About 70 to 90 percent of all organic matter is water. The chemical reactions in all plants and animals that support life takes place in a water medium.

Tetrahydrofuran

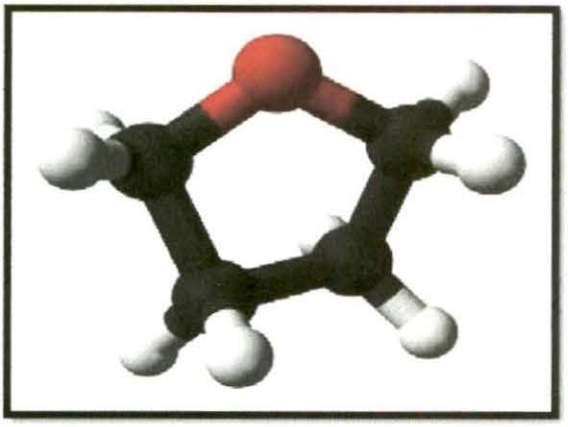

Molecular Formula: C_4H_8O, **Molecular Weight**: 72.11 , **Appearance**: colourless liquid, **Density**: 0.88074 g·cm^3, **Dielectric constant**: 7.58 at 298.15 K

Source: Purchased from Merck, India

Purification: It was kept several days over potassium hydroxide (KOH), refluxed for 24 h and distilled over lithium aluminium hydride (LiAlH4). [5]

Application: THF is often used in polymer science as dissolve polymers prior to determining their molecular mass. The main application of THF is as an industrial solvent for PVC and in varnishes.

Dimethyl sulfoxide

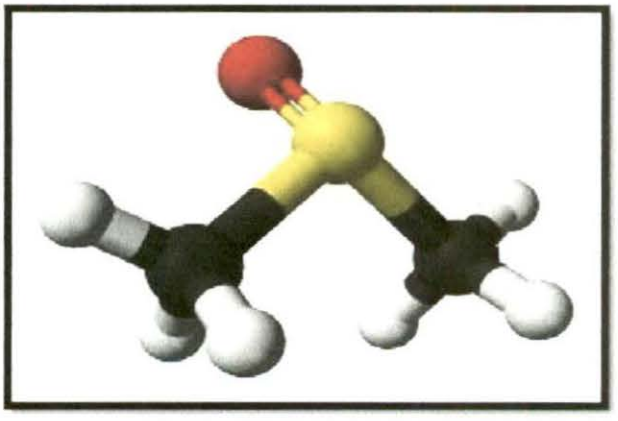

Molecular Formula: $(CH_3)_2SO$, **Molecular Weight**: 78.13 , **Appearance**: Colourless liquid, **Density**: 1.09602 g·cm^3, **Dielectric constant**: 46.7 at 298.15K

Source: Purchased from Thomas Baker, India

Purification: It was purified by passing through Linde 4Å molecular sieves.

Application: Because of its ability to dissolve many kinds of compounds, DMSO plays a role in sample management and high-throughput screening operations in drug design. DMSO increases the rate of absorption of some compounds through organic tissues,
including skin, it can be used as a drug delivery system. It is also extensively used as an extractant in biochemistry and cell biology.

3.2 EXPERIMENTAL METHODS

3.2.1 PREPARATION OF SOLUTIONS

A sock solution for each solute was prepared by mass, and the working solutions were obtained by mass dilution. The uncertainty of molarity of different salt solutions was evaluated to be ± 0.0003 $mol \cdot dm^{-3}$.

3.2.2 MASS MEASUREMENT

Mass measurements were done using digital electronic analytical balance (Mettler Toledo, AG 285, Switzerland).

3.2.3 DENSITY MEASUREMENT

The density was earlier measured by Ostwald- Sprengel type Pycometer having a bulb volume of $25cm^3$ and an internal diameter of the capillary of about

1mm. The pycometer was calibrated at 298.15K with doubly distilled water and THF. The total uncertainity in the density value was ±0.0001gcm^{-3}

The density was measured later with the help of Anton Paar density-meter (DMA 4500M) with a precision of 0.0005 g·cm^{-3}.

It can measure mass to a very high precision and accuracy. The weighing pan of a high precision (0.0001g) is inside a transparent enclosure with doors so that dust does not collect and so any air currents in the room do not affect the balance's operation.

In the digital density meter, the mechanic oscillation of the U-tube is e.g. electromagnetically transformed into an alternating voltage of the same frequency. The period τ can be measured with high resolution and stands in simple relation to the density ρ of the sample in the oscillator[6]:

$$\rho = A \cdot \tau^2 - B \quad (1)$$

A and B are the respective instrument constants of each oscillator. Their values are determined by calibrating with two substances of the precisely known densities ρ_1 and ρ_2. Modern instruments calculate and store the constants A and B after the two calibration measurements, which are mostly performed with air and water. They employ suitable measures to compensate various influences on the measuring result, e.g. the influence of the sample's viscosity and the non-linearity caused by the measuring instrument's finite mass. The instrument was calibrated by double-distilled water and dry air.

3.2.4 VISCOSITY MEASUREMENT

Solvent viscosities were measured using a suspended Ubbelohde-type viscometer,

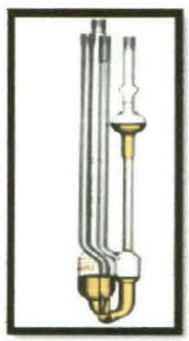

The kinematic viscosity (γ) and the absolute viscosity (η) are given by the following equations.

$$\gamma = k\,t - l/t \quad (2)$$

$$\eta = \gamma \cdot \rho \quad (3)$$

where, t is the time of flow, ρ is the density and k and l are the characteristic constants of the particular viscometer. The precision of the viscosity measurement was ± 0.003 %. In all cases, the experiments were performed in at least three replicates and the results were averaged.

Relative viscosities (η_r) were obtained using the equation:

$$\eta_r = \eta/\eta_0 = \rho\, t\,/\rho_0 t_0 \quad (4)$$

where η, η_0, ρ, ρ_0 and t, t_0 are the absolute viscosities, densities and flow times for the solution and solvent respectively.

The viscosity measurements were also done with the help of Brookfield DV-III Ultra Programmable Rheometer fitted to a Brookfield Digital Bath TC-500.

3.2.5 TEMPERATURE CONTROLLER

All the measurements were carried out in thermostatic water bath (Science India, Kolkata) maintained with an accuracy of ± 0.01 K of the desired temperature.

Laboratory water bath is a system in which a vessel containing the material to be heated is placed into or over the one containing water and to quickly heat it. These laboratory equipments are available in different volumes and construction with both digital and analogue controls and greater temperature uniformity, durability, heat retention and recovery. The chambers of water bath lab products are manufactured using rugged, leak proof and highly resistant stainless steel and other lab supplies.

3.2.6 ULTRASONIC SPEED MEASUREMENT

The ultrasonic speed was measured with an accuracy of 0.2% using single-crystal variable-path ultrasonic interferometer (Model M-81 Mittal Enterprises, New Delhi) operating at 4MHz which was calibrated with water, methanol and benzene at required temperature.

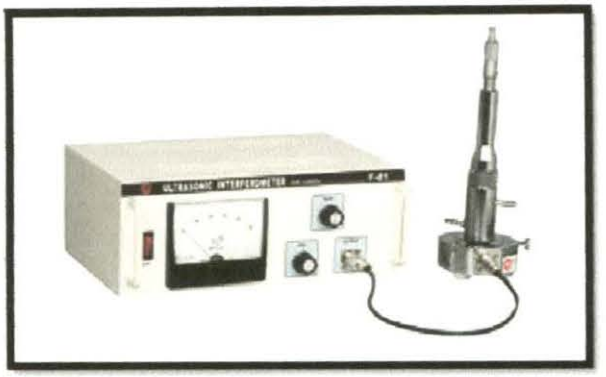

The principle used in the measurement of the ultrasonic speed (u) is based on the accurate determination of the wavelength (λ) in the medium. Ultrasonic waves of known frequency (f) are produced by a quartz crystal fixed at the bottom of the cell. These waves are reflected by a movable metallic plate kept parallel to the quartz crystal. If the separation between these two plates is exactly a whole multiple of the sound wavelength, standing waves are formed in the medium. This acoustic resonance gives rise to an electrical reaction on the generator driving the quartz crystal and the anode current of the generator becomes a maximum.

If the distance is now increased or decreased and the variation is exactly one half of wave length (λ /2) or integral multiples of it, anode current becomes maximum. From the knowledge of the wave length (λ), the speed (u) can be obtained by the relation.

$$\text{Ultrasonic speed } (u) = \text{Wave Length } (\lambda) \times \text{Frequency } (f) \qquad (5)$$

The ultrasonic interferometer consists of the following two parts, (i) the high frequency generator, and (ii) the measuring cell. The measuring cell is

connected to the output terminal of the high frequency generator through a shielded cable. The cell is filled with the experimental liquid before switching on the generator. The ultrasonic waves move normal from the quartz crystal till they are reflected back from the movable plate and the standing waves are formed in the liquid in between the reflector plate and the quartz crystal. The micrometer is slowly moved till the anode current on the meter on the high frequency generator shows a maximum. A number of maxima readings of anode current are passed and their number (n) is counted. The total distance (d) thus moved by the micrometer gives the value of the wavelength (λ) with the following relation.

$$d = n \times \lambda/2 \tag{6}$$

Further, the velocity is determined from which the isentropic compressibility (K_S) is calculated by the following formula:

$$K_S = 1 / (u^2 . \rho) \tag{7}$$

where ρ is the density of the experimental liquid.

Figure. 1 shows the Multifrequency Ultrasonic Interferometer i.e. (a) Cross-section of the measuring cell, (b) Position of reflector vs. crystal current (Note : The extra peaks in between minima and maxima occurs due to a number of reasons, but these do not effect the value of $\lambda/2$) and (c) Electronic circuit diagram of the instrument)

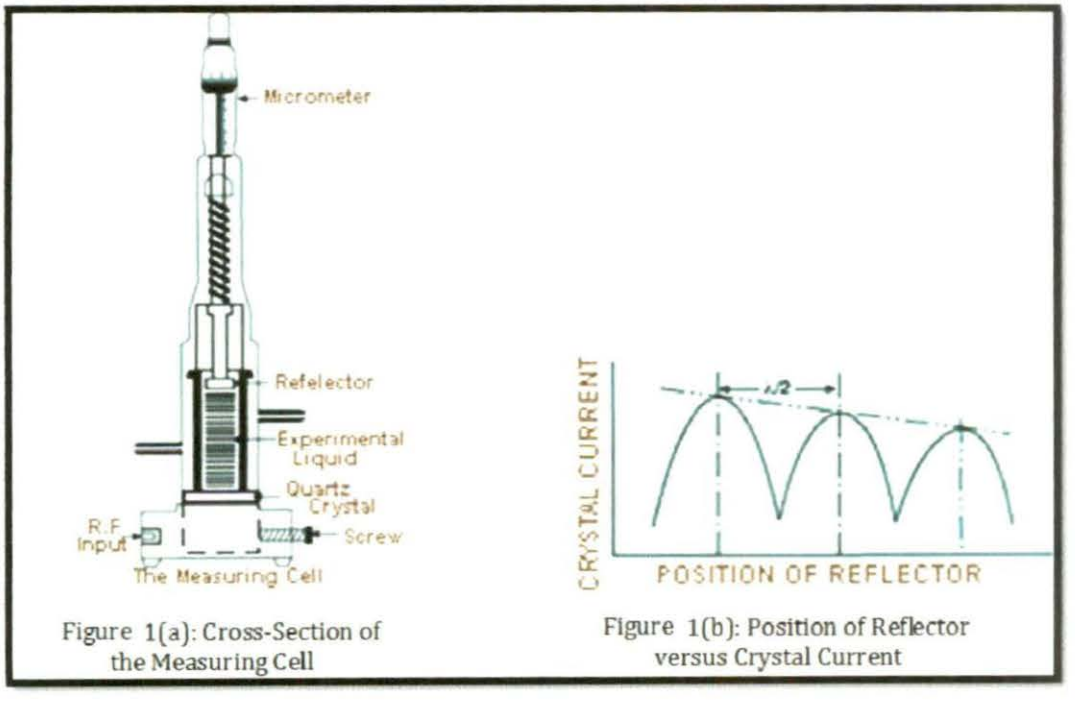

Figure 1(a): Cross-Section of the Measuring Cell

Figure 1(b): Position of Reflector versus Crystal Current

Figure **1: The Multifrequency Ultrasonic Interferometer**

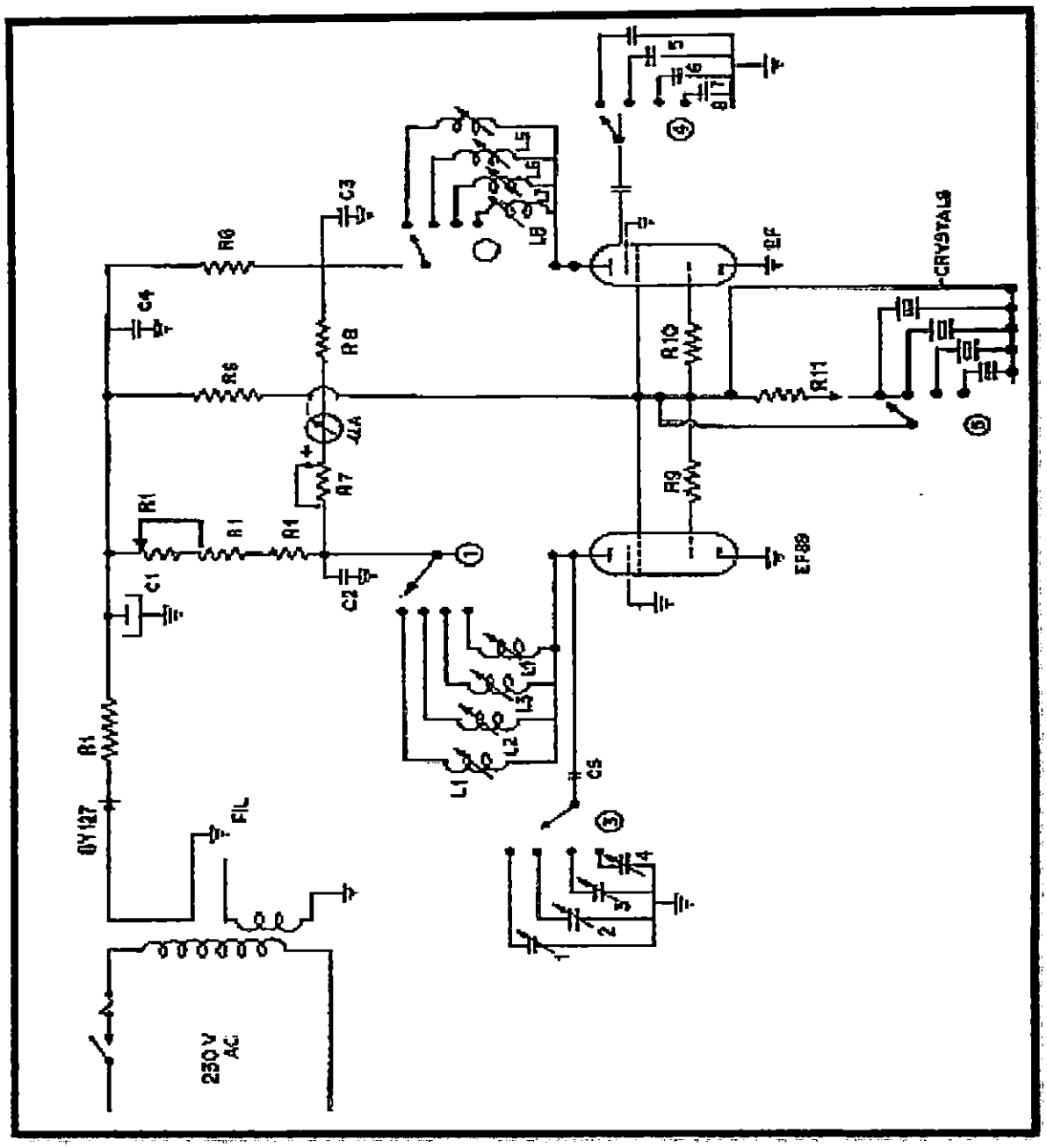

Figure 2: Electronic Circuit Diagram of the Instrument

3.2.7 REFRACTIVE INDEX MEASUREMENT

Refractive index was measured with the help of Digital Refractometer (Mettler Toledo 30GS).

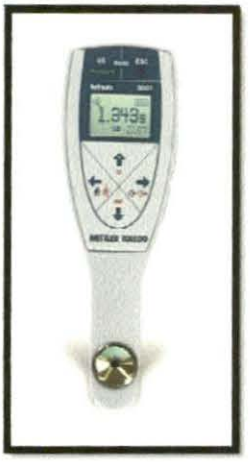

Calibration was performed by measuring the refractive indices of double-distilled water, toluene, cyclohexane, and carbon tetrachloride at defined temperature. The accuracy of the instrument is +/- 0.0005. 2-3 drops of the sample was put onto the measurement cell and the reading was taken. The refractive index of a sample depends on temperature. During measurement, refractometer determines the temperature and then corrects the refractive index to a temperature as desired by the user.

3.2.8 CONDUCTIVITY MEASUREMENT

Conductivity measurement was done using Systronics Conductivity TDS meter-308. It can provide both automatic and manual temperature compensation.

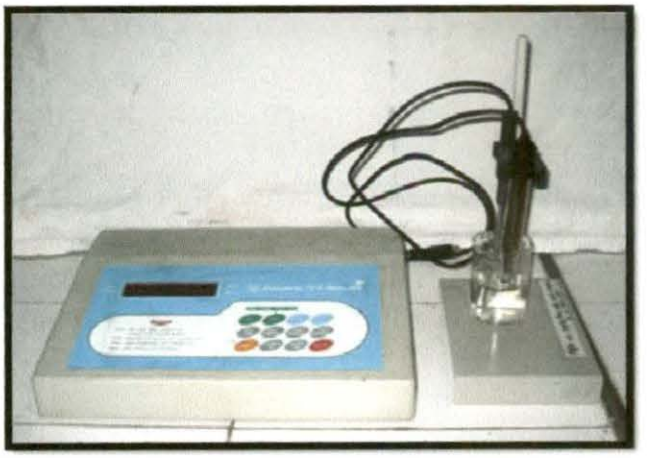

The conductance measurements were carried out on this conductivity bridge using a dip-type immersion conductivity cell of cell constant 1.11cm^{-1}. The entire conductance data were reported at 1 KHz and was found to be ±0.3 % precise. The instrument was standardized using 0.1(M) KCl solution. The cell was calibrated by the method of Lind and co-workers [7]. The conductivity cell was sealed to the side of a 500 cm^3 conical flask closed by a ground glass fitted with a side arm through which dry and pure nitrogen gas was passed to prevent admission of air into the cell when solvent or solution was added. The measurements were made in a thermostatic water bath maintained at the required temperature with an accuracy of ± 0.01 K by means of mercury in glass thermoregulator [8].

Solutions were prepared by weight precise to ± 0.02 %. The weights were taken on a Mettler electronic analytical balance (AG 285, Switzerland). The molarity being converted to molality as required. Several independent solutions were prepared and runs were performed to ensure the reproducibility of the results. Due correction was made for the specific conductance of the solvents at desired temperatures. The following figure shows the Block diagram of the Systronics Conductivity-TDS meter 308.

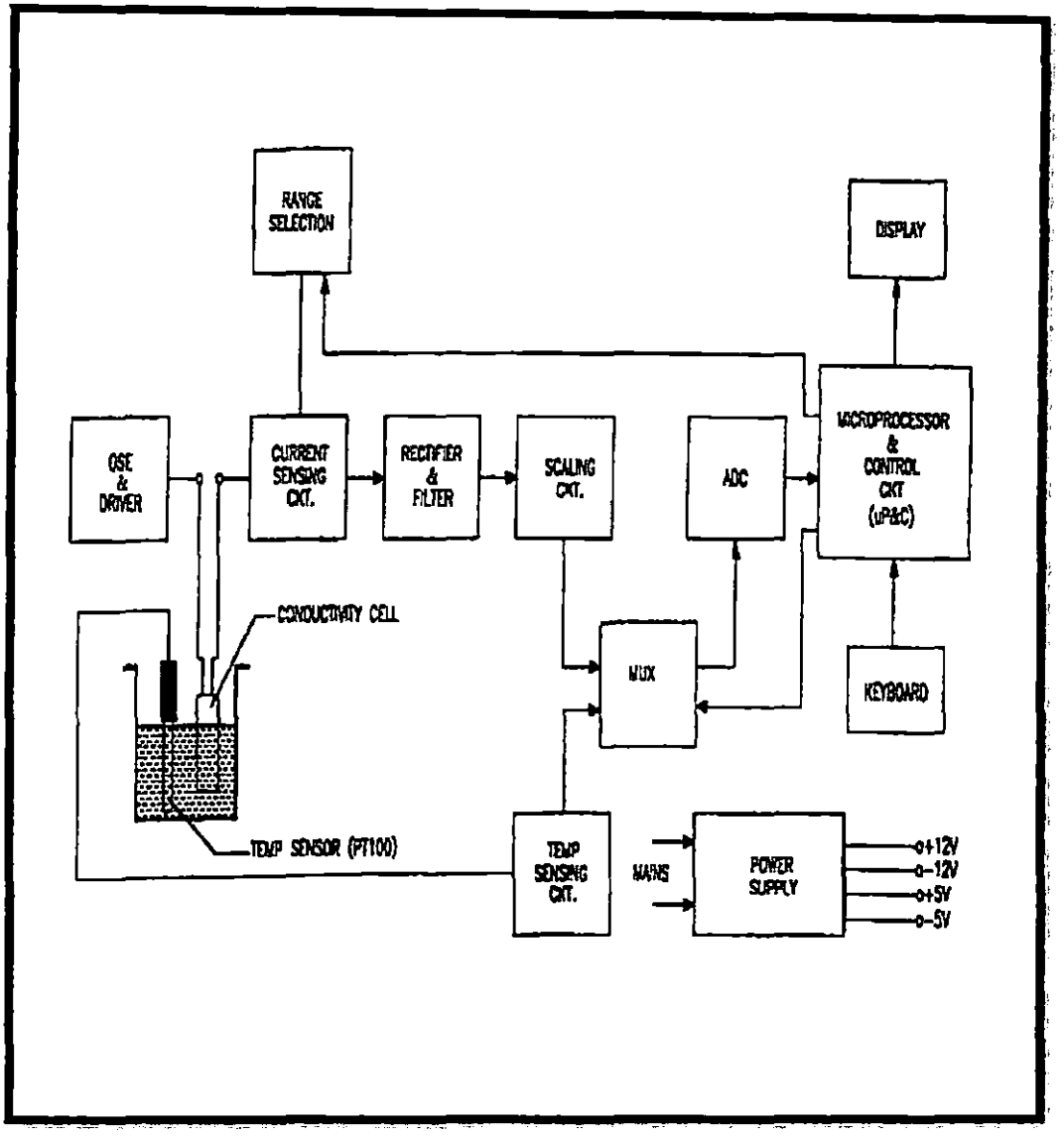

Block Diagram of the Instrument

CHAPTER IV

EXPLORATION OF INTERACTIONS BETWEEN BIOACTIVE SOLUTES AND VITAMIN B9 IN AQUEOUS MEDIUM BY PHYSICOCHEMICAL CONTRIVANCES

4.1 Introduction:

Folic acid (also known as folate, vitamin M, vitamin B9, vitamin B_c (or folacin), pteroyl-L-glutamic acid, pteroyl-L-glutamate, and pteroylmonoglutamic acid) are the water-soluble vitamin B9. Folic acid (FA) is composed of three components: an aromatic pteridine ring system (Pteridine), a *p*-amino benzoic acid (PABA) portion and the amino acid glutamic acid (Glu). The molecular structure of FA is shown in Scheme 1. It is an essential vitamin that is yellow-orange in color, is reported to be present in photosensitive organs, various mammalian metabolic pathways, and possibly involved in photosynthesis [1]. The electrochemical behavior of folic acid has been well studied [2]. Folic acid is itself not biologically active, but its biological importance is due to tetrahydrofolate and other derivatives after its conversion to dihydrofolic acid in the liver [3].

Vitamin B9 (folic acid and folate) is essential for numerous bodily functions. Humans cannot synthesize folate de novo; therefore, folate has to be supplied through the diet to meet their daily requirements. The human body needs folate to synthesize DNA, repair DNA, and methylate DNA as well as to act as a cofactor in certain biological reactions [4]. It is especially important in aiding rapid cell division and growth, such as in infancy and pregnancy, and reproduction of cells, particularly red blood cells. Children and adults both require folic acid to produce healthy red blood cells and prevent anemia [5].

The best natural sources of folic acid are: Leafy vegetables such as spinach, asparagus, turnip greens, lettuce, peas, whole grains, nuts; Legumes such as dried or fresh beans, peas and lentils egg yolk; liver, kidneys, yeast, sunflower seeds, certain fruits (orange juice, canned pineapple juice, cantaloupe, honeydew melon, grapefruit juice, banana, raspberry, grapefruit and strawberry). Folate is also necessary for the

production and maintenance of new cells, for DNA synthesis and RNA synthesis, and for preventing changes to DNA, and, thus, for preventing cancer [6].

The stabilization of native conformations of biological macromolecules is commonly related to several non-covalent interactions including hydrogen bonding, electrostatic and hydrophobic interactions [7]. These interactions are affected by the surrounding solutes and solvent molecules; for this reason, the physico-chemical behaviors of proteins are strongly influenced by the presence of solutes. However, due to the complex conformational and configurational three-dimensional structures of proteins, direct investigations of the solute-solvent effect on these biological macromolecules are very challenging. Amino acids are basic component of proteins and are considered to be one of the important model compounds of protein molecules, which participate in all the physiological processes of living cells are quite helpful in understanding the water–protein-folic acid interactions in solutions. Especially viscometric and volumetric properties (such as viscosity B-coefficients and standard partial molar volumes) and salts solutions can provide valuable clues for comprehending the protein unfolding [8,9] and the hydrophobic interactions of non-polar side chains [10]. In the present study, we have attempted to ascertain the nature of solute–solvent/cosolute interactions of α-amino acids (glycine, L-alanine, and L-valine) in w_1= 0.0001, 0.0003, 0.0005 mass fraction of aqueous folic acid (FA) binary mixtures at 298.15K, as literature survey reveals that very rare work has been carried out in the studied ternary systems.

4.2 Experimental Section:

4.2.1 Source and purity of samples

The studied salts (glycine, L-alanine, L-valine) and cosolute folic acid (FA), puriss grade was procured from Sigma-Aldrich, Germany and was used as purchased. The mass fraction purity of salts were ≥ 0.99. The salts were dried from moisture at 353K for 24 h, and then they were cooled and store in a desiccator prior to use.

4.2.2 Apparatus and Procedure

Aqueous binary solution of folic acid (FA) was prepared by mass (Mettler Toledo AG-285 with uncertainty ±0.0003g), which are used as solvent. Stock

solutions of the salts (amino acids) were also prepared by mass and the working solutions were obtained by mass dilution. The conversion of molality into molarity was accomplished using experimental density values. All solutions were prepared afresh before use. The uncertainty in molarity of the solutions is evaluated to ±0.0001 mol kg^{-3}.

The densities of the solutions (ρ) were measured by means of vibrating-u-tube Anton Paar digital density meter (DMA 4500M) with a precision of ±0.00005g cm^{-3} maintained at ±0.01K of the desired temperature. It was calibrated by triply-distilled water and passing dry air.

The viscosities were measured using a Brookfield DV-III Ultra Programmable Rheometer with fitted spindle size-42. The viscosities were obtained using the following equation

$$\eta = (100 / \text{RPM}) \times \text{TK} \times \text{torque} \times \text{SMC} \quad (1)$$

where RPM, TK (0.09373) and SMC (0.327) are the speed, viscometer torque constant and spindle multiplier constant, respectively. The instrument was calibrated against the standard viscosity samples supplied with the instrument, water and aqueous $CaCl_2$ solutions [11]. Temperature of the solution was maintained to within ± 0.01°C using Brookfield Digital TC-500 temperature thermostat bath. The viscosities were measured with an accuracy of ± 0.1 %. Each measurement reported herein is an average of triplicate reading with a precision of 0.3 %.

Refractive index was measured with the help of a Digital Refractometer Mettler Toledo. The light source was LED, λ=589.3nm. The refractometer was calibrated twice using distilled water and calibration was checked after every few measurements. The uncertainty of refractive index measurement was ±0.0002 units.

The ultrasonic speed (u) was measured by multi frequency ultrasonic interferometer (Model M-81) from Mitral Enterprises, India. The interferometer working at 5 MHz is based on the same principle as was used by Freyer et al. [12] and Kiyoharo et al. [13]. The obtained speeds were corrected for diffraction errors as given by Subrahmayan et al. [14]. The uncertainty in the speed is ±0.2 m s^{-1}. The temperature was controlled within ±0.01 K using a Lauda thermostat during the measurement.

4.3 Result and Discussion:

4.3.1 Apparent molar volume

The salts are freely soluble in all proportions of the solvent mixtures. The physical properties of binary mixtures in different mass fractions (w_1=0.0001, 0.0003, 0.0005) of aqueous FA solutions at 298.15K are reported in Table 1. The measured experimental values of densities, viscosities, refractive indices, ultrasonic speeds of simple three amino acids in different mass fractions of aqueous FA mixture at 298.15K as a function of concentration (molarity) are listed in Table 2. Volumetric properties, such as,ϕ_V,ϕ_V^0, are regarded as sensitive tools for the understanding of interactions in solutions. The apparent molar volume can be considered to be the sum of the geometric volume of the solute molecule and changes in the solvent volume due to its interaction with the solute. For this purpose, the apparent molar volumesϕ_V was determined form the solutions densities using the following equation and the values are given in Table 3.

$$\phi_V = M/\rho \; - 1000(\rho - \rho_o)/m\rho\rho_o \qquad (2)$$

where M is the molar mass of the salt, m is the molarity of the solution, ρ and ρ_0 are the density of the solution and aq. FA mixture respectively.

Table 3 show that the value of ϕ_V are large and positive for all the systems, suggesting strong solute-solvent interactions. The apparent molar volumes ϕ_V were found to decrease with increasing molarity (m) of amino acid in aqueous FA for all the amino acids under study. It is also found that the value increases linearly with increase in size of the alkyl chain of the amino acid and with increase in the mass fraction (w_1) of FA in solution. It indicates that the solute–solvent (cosolute) interactions increase with increasing concentration (w_1) of FA, size of the alkyl side chain of amino acids. The limiting apparent molar volumes ϕ_V^0 were obtained by a least-square treatment to the plots of ϕ_V versus $\sqrt{m}$ using the Masson equation [15].

$$\phi_V = \phi_V^0 + S_V^* \cdot \sqrt{m} \qquad (3)$$

where ϕ_V^0 ($= \bar{V}_2^0$) is the apparent molar volume at infinite dilution and S_V^* is the experimental slope. The ϕ_V^0values has been determined by fitting the dilute data (m

< 0.1 mol·kg^{-1}) to eq 3. The values of ϕ_V^0 and S_V^* are reported in Table 4. The plots of ϕ_V against $\sqrt{m}$ were found to be linear with negative slopes. At infinite dilution, each monomer of solute is surrounded only by the solvent molecules, and being infinite distant with other ones. It follows, therefore, that ϕ_V^0 is unaffected by solute-solute interaction and it is a measure only of the solute-solvent interaction [16,17]. The ϕ_V^0 data are often embeded with important information of solute hydrophobic, hydration properties and solute–solvent interactions [18,19] occured in aqueous FA solution.

A perusal of Table 4 and Fig 1 shows that the values of ϕ_V^0 are large and positive for all the amino acids at the investigated temperature, suggesting the presence of strong solute–solvent interaction [20]. Furthermore, the values of ϕ_V^0 increase with increasing number of carbon atoms (or size of alkyl group) from Gly to Val. A similar increase in ϕ_V^0 with increasing number of carbon atoms for amino acids in aqueous glycerol, at 298.15 K, was also reported by Banipal et al [21]. The behaviour of ϕ_V^0 for the present systems can be explained employing the co-sphere model, proposed by Friedman and Krishnan [22], according to which the effect of overlap of hydration co spheres is destructive. Mishra et al. [23] using this model observed that an overlap of co spheres of two ionic species causes an increase in volume, whereas an overlap of hydrophobic–hydrophobic groups and ion–hydrophobic groups results in a net decrease in volume. Since, the observed positive ϕ_V^0 values (Table 4), is due to the effect of ion–hydrophilic interactions (between zwitterionic centres of the amino acids and the –OH, -NH_2, -NH, -COO^- or ketonic =O groups of FA) which predominate over ion–hydrophobic interactions (between zwitterionic centres and non-polar parts of FA) and hydrophobic–hydrophobic interactions (between non-polar parts of the amino acids and FA) and increase in the following order

glycine < L-alanine < L-valine

at investigated temperature. The increase ϕ_V^0 may be attributed to the release of some solvation molecules from the loose solvation layers of the solutes in solution.

The values of ϕ_V^0 and S_V^* for the amino acids in pure water is adopted from the literature [24,25]. The parameter S_V^* is the volumetric viral coefficient, and it characterizes the pair wise interaction of solute species in solution [26,27]. S_V^* is found to be negative under investigations, which suggest that the pair wise (solute-solute) interaction is restricted by the interaction of the charged functional group one molecule to side chain of the other amino acid molecules. From Table 4, a quantitative comparison between ϕ_V^0 and S_V^* values show that, the magnitude of ϕ_V^0 values is higher than S_V^*, suggesting that the solute-solvent (co solute) interaction dominate over the cosolute-cosolute interactions in all studied solution.

4.3.2 Contributions of the zwitterionic end group, CH_2 groups and other alkyl chains of the amino acids to ϕ_V^0

The ϕ_V^0 value for the homologous series varies linearly with the number of carbon atoms in the alkyl chain (R) of the amino acids. Similar correlations have been reported earlier by a number of Workers [24,25] and this linear variation can be represented as follows:

$$\phi_V^0 = \phi_V^0(NH_3^+, COO^-) + n_c\phi_V^0(CH_2) \quad (4)$$

where n_c is the number of carbon atoms in the alkyl chain of the amino acid, $\phi_V^0(NH_3^+, COO^-)$ and $\phi_V^0(CH_2)$ are the zwitterionic end group and methylene group contribution to ϕ_V^0 respectively. The values of $\phi_V^0(NH_3^+, COO^-)$ and $\phi_V^0(CH_2)$, calculated by a least-square regression analysis and was listed in Table 5, where those values in pure water are also provided from the literature. It is well described in the literature [28] that $\phi_V^0(CH_2)$ obtained by this scheme characterizes the mean contribution of the ϕ_V^0 (CH) and ϕ_V^0 (CH_3) values of the amino acids

$$\phi_V^0(CH) = 0.5\phi_V^0(CH_2) \quad (5)$$

$$\phi_V^0(CH_3) = 1.5\phi_V^0(CH_2) \quad (6)$$

and are listed in Table 5. The table show that the contribution of (NH_3^+, COO^-) to ϕ_V^0 is larger than that of the CH_2- group and increases with the increase in the mass

fraction (w_1) of the co solute FA, which indicates that the interactions between the co solute and charged end groups (NH_3^+, COO^-) of amino acids are much greater than those between the co solute and CH_2- group. Similar results were also reported [29] for some α-amino acids in aqueous sodium caprylate solutions.

4.3.3 Standard Transfer Volume

The standard transfer volume for the homologus series of amino acid, $\Delta\phi_V^0$, from pure water to aqueous FA solutions is defined by

$$\Delta\phi_V^0(\text{amino acid}) = \phi_V^0(\text{amino acis} + \text{aqueous FA}) - \phi_V^0(\text{water}) \quad (7)$$

The results are illustrated in Table 6. The value of $\Delta\phi_V^0$ is, by definition, free from solute-solute interactions and therefore provided information regarding solute-solvent interactions [20]. This agreement among the amino acids can be explained by the co-sphere model, as developed by Friedman and Krishnan [22], according to which the effect of overlap of the hydration co-spheres is constrctive. The overlap of hydration co-spheres of two ionic species results in an increase in volume, but that of hydration co-spheres of hydrophobic-hydrophobic groups and ion-hydrophobic groups results in a net volume decrease. Since amino acids exist predominantly as zwitterions in pure water and there is an overall decrease in volume of water due to electrostriction, the observed increasing positive volumes of transfer, indicate that in the ternary solutions (amino acid +aq. FA), indicates that the amino acids have the ion-hydrophilic and hydrophilic-hydrophilic group interactions predominate over the ion-hydrophobic and hydrophobic-hydrophobic groups interactions, and the contribution increases with increasing the molarity of FA in solutions. The observed trend can also be explained on the basis of the following equation [30, 31].

$$\phi_v^0 = \phi_{vw} + \phi_v - \phi_s \quad (8)$$

where ϕ_{vw} is the van der Waals volume; ϕ_v is the volume associated with voids or empty space; and ϕ_s is the shrinkage volume due to electrostriction. Assuming the ϕ_{vw} and ϕ_v have the same magnitudes in water and in aqueous FA solutions for the same class of solutes [32], the observed positive $\Delta\phi_V^0$ values ascribed to the decrease in the volume of shrinkage. Banipal and co-workers [21] also reported a

decrease in the $\Delta\phi_V^0$ value with increasing size of the non-polar side chain of amino acids in aqueous glycerol. The introduction of a CH_3- group in L-alanine provides an additional tendency for hydrophobic-hydrophilic and hydrophobic-hydrophobic group interactions, and as a result, greater electrostriction of water is produced leading to smaller changes of $\Delta\phi_V^0$. Similarly, when the H-atom of glycine is replaced by the (CH_3CH_2CH-) group in L-valine, the additional propensity for hydrophobic-hydrophilic group interactions increases further and thus leads to change in $\Delta\phi_V^0$ values. This is in good agreement with the conclusion drawn by Li et al. [33] in a study of Glycine, L-Alanine and L-Serine in glycerol-water mixture at 298.15 K.

The contribution of the other alkyl chain groups of the amino acids have been calculated from the difference between the limiting apparent molar volumes (ϕ_V^0) values of each amino acid and that of glycine using the following scheme

$$\Delta\phi_V^0(\mathrm{R}) = \phi_V^0(\text{amino acid}) - \phi_V^0(\text{glycine}) \quad (9)$$

where $\Delta\phi_V^0(\mathrm{R})$ defines the side chain transfer contribution to ϕ_V^0 of the respective amino acid relative to the H-atom of glycine. In this scheme, it is assumed that the volume contribution of the H-atom in glycine is negligible. The results are listed in Table 5. The table shows that the $\Delta\phi_V^0(\mathrm{R})$ values for L-alanine (CH_3CH-) and L-valine (CH_3CH_2CH-) is positive, which suggests the contribution of alkyl chain is greater than relative to the H-atom of glycine in solute-solvent interaction in solution.

4.3.4 Hydration Number estimated from apparent molar volume

The number of water molecules (n_H) hydrated to the amino acids can be estimated from the value of measured standard partial molar volume. The values of ϕ_V^0 of the studied amino acids can be expressed as [24]

$$\phi_V^0(\text{amino acid}) = \phi_V^0(\text{int}) + \phi_V^0(\text{elect}) \quad (10)$$

where $\phi_V^0(\text{int})$ is the intrinsic partial molar volumes of the amino acids and $\phi_V^0(\text{elect})$ is the electrostriction partial molar volume as a result of hydration of the amino acids. The $\phi_V^0(\text{int})$ consists of two terms: the van der Waals volume and the volume

due to packing effects. The values of ϕ_V^0(int) for the amino acids were calculated from their crystal molar volume by [24] using the following relationship,

$$\phi_V^0(\text{int}) = (0.7 / 0.634)\ \phi_V^0(\text{cryst}) \qquad (11)$$

where, 0.7 is the packing density in an organic crystal and 0.634 is the packing density of randomly packed spheres. The molar volume of crystals ϕ_V^0(cryst) was calculated using the crystal densities of the amino acids represented by Berlin and Pallansch (1968) [34,35] at 298.15 K. The ϕ_V^0(elect) values can be calculated [36] from the intrinsic partial molar volumes of the amino acids ϕ_V^0(int), and experimentally determined ϕ_V^0 values. Thus number of water molecules hydrated to the amino acids due to electrostriction causes decrease in volume can be related to the hydration numbers [24] is estimated using the following relation

$$n_H = \frac{\phi_V^0(\text{elect})}{(V_e^0 - V_b^0)} \qquad (12)$$

where V_e^0 is the molar volume of the electrostricted water and V_b^0 is the molar volume of bulk water. This model implies that for every water molecules taken from the bulk phase to the surroundings of amino acid, the volume is decreased by $(V_e^0 - V_b^0)$. The value of $(V_e^0 - V_b^0)$ is calculated [24] to be -3.0 or -3.3 $cm^3\ mol^{-1}$ at 298.15K respectively. The obtained n_H values are listed in Table 6, where n_H varies with the solvent composition, showing a tendency to decrease with an increase in the mass fraction (w_1) of FA, for all the amino acids under investigation. The observed decreasing tendency of n_H supports the view [37] that the FA has a dehydration effect on these amino acids in aqueous FA solutions.

The positive sign of the transfer volumes can be ascribed mainly to the fact that the hydration number n_H of the amino acids is reduced by the addition of FA; i.e., the electrostriction effect which brings about the shrinking in the volume of the solvent caused by the electric field of the dipolar solutes is reduced in the mixture as compared with that in pure water.

The schematic representation of solute-solvent interaction, for the studied amino acids in aqueous folic acids binary mixtures, in view of various derived parameters is depicted in Scheme 2.

4.3.5 Viscosity

The experimental viscosity data for the studied systems are listed in Table 2. The relative viscosity (η_r) has been analyzed using the Jones-Dole equation [38]

$$(\eta/\eta_o - 1)/\sqrt{m} = (\eta_r - 1)/\sqrt{m} = A + B\sqrt{m} \quad (13)$$

where $\eta_r=\eta/\eta_o$, η and η_0 are the relative viscosities, the viscosities of the ternary solutions (amino acid + aq. FA) and binary aqueous FA mixture and m is the molarity of the ternary solutions. A and B are empirical constants known as viscosity A- and B-coefficients, which are specify to solute-solute and solute-solvent interactions, respectively. The values of A and B-coefficients are estimated by least-square method by plotting $(\eta_r - 1)/\sqrt{m}$ against $\sqrt{m}$, and reported in Table 4. The values of the A-coefficient are found to increases slightly with the increase in mass of FA in the solvent mixture. These results indicate the presence of very weak solute-solute interactions. These results are in excellent agreement with those obtained from S_V^* values.

The extent of solute-solvent interaction in the solution estimated from the viscosity B-coefficient [16] gives valuable information concerning the solvation of the solvated solutes and their effects on the structure of the solvent in the local vicinity of the solute molecules in the solutions. From Table 4 and Fig 2, it is evidence that the values of the B-coefficient are positive and much higher than A-coefficient, thereby suggesting the solute-solvent interactions are dominant over the solute-solute interactions. The higher B-coefficient values for higher viscosity values is due to the solvated solutes molecule associated by the solvent molecules all round to the formation of associated molecule by solute-solvent interaction, would present greater resistance, and this type of interactions are strengthen with increase of mass fraction (w_1) of FA in the solvent mixtures. These results are in good agreement with those obtained from ϕ_V^0 values discussed earlier in apparent molar volume section.

The Table 4 also shows that B-coefficients for all the amino acids are increase with the increase of the size of the side chains. The B-coefficients reflect the net structural effects of the charged groups and the hydrophobic CH_2- groups of the amino acids. As B-coefficients vary linearly with the number of carbon atoms of the alkyl chain (n_c), these two effects can be resolved as follows

$$B = B(NH_3^+, COO^-) + n_c B(CH_2) \quad (14)$$

The regression parameters, i.e., the zwitterionic group contribution B (NH_3^+, COO^-), and the methylene group contribution B (CH_2), to B-coefficients are listed in Table 7. It shows that both the $B(NH_3^+, COO^-)$ and $B(CH_2)$ values increases with increasing concentration (w_1) of FA in ternary solutions, indicated that the zwitterionic and CH_2-group enhances the structure to solute-solvent interaction in the aqueous salt solutions. The side chain contributions to B-coefficients, $B(R)$, has also been derived using the same scheme as that of ϕ_V^0(R)and are listed in Table 7, which shows that $B(R)$ values are positive and greater for L-valine than L-alanine in all of the concentrations of studied solutions. This order is due to the greater structure making tendency and these findings are in line with our volumetric results discuss earlier.

Moreover, it is interesting to note that the B-coefficients of the studied amino acids show a linear correlation with the limiting partial molar volumes ϕ_V^0 for the amino acids in aqueous FA solution. This means:

$$B = A_1 + A_2\phi_V^0 \qquad (15)$$

The coefficients A_1 and A_2 are included in Table 8. This correlation is not unexpected, as both the viscosity B-coefficient and the partial molar volume reflect the solute–solvent interactions in the solutions. The positive slope (or A_2) shows the linear variation of B-coefficient with limiting apparent molar volumes ϕ_V^0. A similar correlation was also used for amino acids in different solvents [27,39].

4.3.6 *Refractive index*

The refractive index measurement is also a convenient method for investigating the ion-solvent interaction of salts in solution. The values of n_D are reported in Table 2. The molar refraction, R_M can be evaluated from the Lorentz-Lorenz relation [40]

$$R_M = \left\{(n_D^2-1)/(n_D^2+2)\right\}(M/\rho) \qquad (16)$$

where R_M, n_D, M and ρ are the molar refraction, the refractive index, the molar mass and the density of solution respectively. The refractive index of a substance is defined as the ratio c_o/c, where c is the speed of light in the medium and c_o the speed of light in vacuum. Stated more simply, the refractive index of a compound describes

its ability to refract light as it moves from one medium to another and thus, the higher the refractive index of a compound, the more the light is refracted [41]. As stated by Deetlefs et al. [42] the refractive index of a substance is higher when its molecules are more tightly packed or in general when the compound is denser. The refractive index is directly proportional to molecular polarizability. Hence, a perusal of Table 2 and 3 we found that the refractive index (n_D) and the molar refraction (R_M) respectively are increases linearly with an increasing concentration of the solution and homologues series of amino acids.

The Limiting molar refraction (R_M^0) estimated from the following

$$R_M = R_M^0 + R_S \sqrt{m} \tag{17}$$

Accordingly, we found that the higher refractive index, and R_M^0 (Table 4) values indicating the fact that the salts are more tightly packed and more solvated in solution. This is also in good agreement with the results obtained from density and viscosity parameters discussed above.

4.3.7 Ultrasonic Speed

Apparent molar isentropic compressibility:

The adiabatic compressibility, defined by the thermodynamic relation:

$$\beta_s = -\frac{1}{V}\left(\frac{\partial V}{\partial P}\right)_S \tag{18}$$

where *V* is volume, *P* is pressure and *S* is entropy, is related to the solution density ρ, and the ultrasonic speed *(u)*, by the Newton-Laplace's equation:

$$\beta_s = 1 / u^2 \rho \tag{19}$$

providing the relation between thermodynamics and acoustics. The apparent molar adiabatic compressibility (ϕ_K), of the solutions was determined from the following relation,

$$\phi_K = M\beta_s / \rho + 1000\left(\beta_s \rho_o - \beta_o \rho\right) / m\rho\rho_o \tag{20}$$

where β_0, β_s are the adiabatic compressibility of the binary mixture and ternary solution respectively and *m* is the molarity of the ternary solution. The values of ϕ_K

are reported in Table 3. Limiting apparent molar adiabatic compressibility (ϕ_K^0) or apparent molar adiabatic compressibility at infinite dilution and experimental slopes (S_K^*), were obtained by fitting ϕ_K against the square root of concentration ($\sqrt{m}$) using the least squares method [43].

$$\phi_K = \phi_K^0 + S_K^* \cdot \sqrt{m} \tag{21}$$

The values of ϕ_K^0 and S_K^* are presented in Table 4. The values of ϕ_K^0 and S_K^* are important parameter providing information about the extent of solute-solvent and solute-solute interaction respectively. The behaviour is useful in characteristic of solvation and electrostriction (the contraction of the solvent around the solute) of salt in solutions.

From Table 4 and Fig. 1, it is observed that the value of limiting apparent molar isentropic compressibility ϕ_K^0 are positive and increases with the increase in concentration (w_1) of FA for all the studied solution, and shows the stronger solute-solvent interaction. The result is good agreement with the ϕ_V^0 value discussed earlier. It is also observed that the values of ϕ_K^0 for the studied amino acids follow the order:

Glycine < L-alanine < L-valine

Since the contribution of methylene group to the apparent compressibility is positive, it implies that the ions having the larger hydrophobic group may have more positive values for the partial molar expansibilities. Hence, L-valine may have largest hydrophobic group resulting higher values of ϕ_K^0.

Hydration number from apparent molar isentropic compressibility:

The limiting partial molar adiabatic compressibility of the amino acids also can be expressed by a simple model: [24]

$$\phi_K^0 = \phi_K^0(\text{int}) + \phi_K^0(\text{elect}) \tag{22}$$

where $\phi_K^0(\text{int})$ is the intrinsic partial molar adiabatic compressibility of the amino acid and $\phi_K^0(\text{elect})$ is the electrostriction partial molar adiabatic compressibility due to the hydration of the amino acid. As has been noted by Millero et. al. as a first approximation, one can assume that $\phi_K^0(\text{int}) \approx 0$, since one would expect $\phi_K^0(\text{int})$ to very small [24]. Thus ϕ_K^0 may be thought to represent $\phi_K^0(\text{elect})$. The ϕ_K^0 values of the

amino acids in water are all positive; this must come from the hydration of the charged centres of the amino acids, as the hydrated water molecules are already compressed and than that in the bulk. For the amino acids, the order of increasing ϕ_K^0 values as well as hydration number n_H in aqueous FA is:

glycine < L-alanine < L-valine

and reported in Table 6. As has been noted by Mathieson and Conway, ions which a slight hydrogen-bond with water have unusual compressibility [44]. This corresponds to the order of increasing absolute values of ϕ_K^0 in aqueous FA, which answers to the order of increasing hydration numbers. Thus, the less hydrated amino acids in water has the lower compressibility ratio in the mixed solvent and then loses hydrated water molecules more easily in the transfer from water to the mixed solvent.

4.3.8 Structural effect of the Cosolute Folic Acid

The interaction strength depends on the factors such as the size of the guest molecule, the van der Waals interactions, the release of water molecules, hydrogen bonding, charge transfer interactions, hydrophobic interactions, and the release of conformational strain, etc [45]. With considering the above factors, FA are proposed in such a way that the interaction with amino acids, the solute-solvent interaction is higher for L-valine than L-alanine which is also turn higher than glycine, this is also due to the +I effect. +I effect increases as alkyl chain group increases from glycine to L-valine, are more favourably interact, with retention of configuration of FA itself.

4.4 Conclusion

Physico-chemical and thermodynamic properties of simple amino acids in aqueous FA binary mixture were done. It is evident that the association of the investigated amino acids, the L-valine is greater than L-alanine which is, in turn, greater than that glycine. The reliable values of derivative obtained from the studies properties suggest that the solute-solvent interaction is dominant over the solute-solute interaction in solutions. The structural effect of folic acid gives the favourable support in the molecular interaction. Above all this study demands a novelty of some amino acids prevailing in the aqueous solutions of folic acid.

Tables:

Table 1. Values of density (ρ), viscosity (η), refractive index (n_D) and ultrasonic speed (u) in different mass fraction (w_1) of aqueous Folic Acid at 298.15K

Mass fraction of	$\rho \cdot 10^{-3}$/kg m^{-3}		η /mPa s		n_D		u /m s^{-1}	
aq. β-CD (w_1)	Expt	Lit	Expt	Lit	Expt	Lit	Expt	Lit
$w_1 = 0.0001$	0.99708	-	0.812	-	1.3331	-	1493.5	-
$w_1 = 0.0003$	0.99717	-	0.823	-	1.3332	-	1495.3	-
$w_1 = 0.0005$	0.99726	-	0.840	-	1.3333	-	1497.2	-

Table 2. Experimental values of density (ρ), viscosity (η), refractive index (n_D) and ultrasonic speed (u) of amino acids in different mass fraction (w_1) of aqueous Folic Acid (FA) at 298.15K

M/mol kg^{-1}	$\rho \cdot 10^{-3}$/kg m^{-3}	η/mPa s	n_D	u/m s^{-1}
$w_1 = 0.0001$				
Glycine + aq. FA				
0.0100	0.99742	0.82	1.3333	1493.8
0.0251	0.99797	0.83	1.3336	1496.9
0.0402	0.99855	0.84	1.3339	1502.0
0.0553	0.99915	0.85	1.3342	1508.7
0.0704	0.99978	0.86	1.3345	1517.0
0.0855	1.00042	0.87	1.3348	1526.6
Alanine + aq. FA				
0.0100	0.99741	0.82	1.3334	1494.2
0.0251	0.99797	0.84	1.3337	1498.6
0.0402	0.99858	0.85	1.3340	1505.7
0.0553	0.99924	0.86	1.3343	1514.8
0.0704	0.99992	0.87	1.3346	1526.2
0.0856	1.00064	0.89	1.3349	1539.3

Valine + aq. FA				
0.0100	0.99740	0.83	1.3333	1494.7
0.0251	0.99797	0.84	1.3337	1500.9
0.0402	0.99859	0.86	1.3341	1510.6
0.0554	0.99926	0.87	1.3344	1523.2
0.0706	0.99998	0.89	1.3348	1538.1
0.0858	1.00074	0.90	1.3352	1555.3
$w_1 = 0.0003$				
Glycine + aq. FA				
0.0100	0.99750	0.84	1.3335	1495.7
0.0251	0.99803	0.85	1.3338	1499.1
0.0402	0.99859	0.86	1.3341	1504.8
0.0553	0.99918	0.87	1.3344	1512.1
0.0704	0.99979	0.88	1.3347	1521.3
0.0855	1.00041	0.89	1.3350	1532.2
Alanine + aq. FA				
0.0100	0.99748	0.84	1.3336	1496.1
0.0251	0.99801	0.85	1.3339	1500.9
0.0402	0.99858	0.87	1.3342	1508.7
0.0553	0.99919	0.88	1.3345	1518.8
0.0705	0.99982	0.89	1.3348	1530.9
0.0856	1.00050	0.91	1.3351	1545.6
Valine + aq. FA				
0.0100	0.99747	0.84	1.3337	1496.6
0.0251	0.99800	0.86	1.3340	1503.1
0.0402	0.99859	0.88	1.3343	1513.2
0.0554	0.99921	0.89	1.3346	1526.4
0.0706	0.99987	0.91	1.3349	1542.8
0.0858	1.00058	0.93	1.3352	1561.3
$w_1 = 0.0005$				
Glycine + aq. FA				
0.0100	0.99757	0.85	1.3336	1497.7

0.0251	0.99807	0.86	1.3339	1501.6
0.0402	0.99860	0.87	1.3342	1507.7
0.0553	0.99915	0.89	1.3345	1516.0
0.0704	0.99972	0.90	1.3348	1526.3
0.0855	1.00031	0.91	1.3351	1538.3
Alanine + aq. FA				
0.0100	0.99755	0.85	1.3338	1498.2
0.0251	0.99805	0.87	1.3341	1503.6
0.0402	0.99859	0.88	1.3344	1512.5
0.0553	0.99917	0.90	1.3347	1524.0
0.0705	0.99977	0.91	1.3350	1537.6
0.0856	1.00040	0.93	1.3352	1554.2
Valine + aq. FA				
0.0100	0.99754	0.86	1.3339	1498.6
0.0251	0.99802	0.88	1.3342	1505.9
0.0402	0.99856	0.90	1.3345	1517.5
0.0554	0.99913	0.91	1.3348	1532.0
0.0706	0.99975	0.93	1.3351	1549.6
0.0858	1.00039	0.95	1.3353	1569.9

Table 3. Molarity (m), apparent molar volume (ϕ_V), $(\eta_r-1)/\sqrt{m}$, molar refraction (R_m) and apparent molar adiabatic compressibility (ϕ_K) of amino acids in different mass fraction of aqueous FA (w_1) at 298.15K

m /mol·kg^{-1}	$\phi_V \cdot 10^6$ /m^3·mol^{-1}	$(\eta_r-1)/\sqrt{m}$ /kg$^{1/2}$·mol$^{-1/2}$	R_m	$\phi_K \cdot 10^{10}$ /m^3·mol^{-1}·Pa^{-1}
$w_1 = 0.0001$				
Glycine + aq. FA				
0.0100	41.19	0.074	15.49	-0.149
0.0251	39.59	0.124	15.50	-0.798
0.0402	38.43	0.166	15.50	-1.260
0.0553	37.54	0.194	15.51	-1.636
0.0704	36.61	0.218	15.51	-1.978

0.0855	35.88	0.240	15.51	-2.276
		Alanine + aq. FA		
0.0100	56.25	0.123	18.39	-0.317
0.0251	53.65	0.179	18.40	-1.141
0.0402	51.74	0.215	18.40	-1.748
0.0553	49.96	0.251	18.40	-2.230
0.0704	48.66	0.283	18.41	-2.678
0.0856	47.35	0.311	18.41	-3.063
		Valine + aq. FA		
0.0100	85.40	0.172	24.18	-0.482
0.0251	81.79	0.233	24.19	-1.561
0.0402	79.63	0.276	24.20	-2.339
0.0554	77.74	0.314	24.21	-2.978
0.0706	75.94	0.347	24.22	-3.503
0.0858	74.31	0.378	24.22	-3.960
		$w_1 = 0.0003$		
		Glycine + aq. FA		
0.0100	42.19	0.084	15.50	-0.200
0.0251	40.79	0.137	15.51	-0.882
0.0402	39.68	0.175	15.51	-1.394
0.0553	38.63	0.206	15.51	-1.792
0.0704	37.75	0.232	15.52	-2.167
0.0855	37.06	0.260	15.52	-2.510
		Alanine + aq. FA		
0.0100	58.25	0.133	18.40	-0.359
0.0251	55.65	0.191	18.41	-1.239
0.0402	53.99	0.229	18.41	-1.900
0.0553	52.51	0.262	18.42	-2.432
0.0705	51.38	0.296	18.42	-2.880
0.0856	50.06	0.330	18.42	-3.321
		Valine + aq. FA		
0.0100	87.40	0.193	24.20	-0.524

0.0251	84.19	0.252	24.21	-1.631
0.0402	81.88	0.295	24.22	-2.429
0.0554	80.29	0.334	24.22	-3.092
0.0706	78.80	0.373	24.23	-3.696
0.0858	77.25	0.408	24.23	-4.186
		$w_1 = 0.0005$		
		Glycine + aq. FA		
0.0100	44.19	0.107	15.50	-0.242
0.0251	42.79	0.158	15.51	-1.004
0.0402	41.68	0.196	15.51	-1.519
0.0553	40.82	0.233	15.52	-1.978
0.0704	40.04	0.260	15.52	-2.392
0.0855	39.30	0.285	15.53	-2.757
		Alanine + aq. FA		
0.0100	60.26	0.155	18.41	-0.460
0.0251	57.65	0.211	18.42	-1.408
0.0402	55.99	0.255	18.42	-2.153
0.0553	54.51	0.294	18.43	-2.748
0.0705	53.38	0.323	18.43	-3.234
0.0856	52.29	0.354	18.43	-3.715
		Valine + aq. FA		
0.0100	89.39	0.214	24.22	-0.564
0.0251	86.99	0.278	24.22	-1.814
0.0402	84.88	0.327	24.23	-2.742
0.0554	83.38	0.364	24.24	-3.434
0.0706	81.80	0.403	24.24	-4.039
0.0858	80.55	0.435	24.24	-4.558

Table 4. Limiting apparent molar volumes (ϕ_V^0), experimental slopes (S_V^*), viscosity A, *B*-coefficients, limiting partial molar adiabatic compressibilities (ϕ_K^0), and experimental slopes (S_K^*) of amino acids in different mass fraction of aqueous FA (w_1) at 298.15K

Mass fraction of aq. FA (w_1)	$\phi_V^0 \cdot 10^6$ /$m^3 \cdot mol^{-1}$	$S_V^* \cdot 10^6$ /$m^3 \cdot mol^{-3/2} \cdot kg^{1/2}$	*B* /$kg^{1/2} \cdot mol^{-1/2}$	*A* /$kg \cdot mol^{-1}$	R_m^0	$\phi_K^0 \cdot 10^{10}$ /$m^3 \cdot mol^{-1} \cdot Pa^{-1}$	$S_K^* \cdot 10^{10}$ /$m^3 \cdot mol^{-3/2} \cdot Pa^{-1} \cdot kg^{1/2}$
Glycine + aq. FA							
w_1 = 0.0001	43.96	-27.60	0.869	-0.012	15.48	0.955	-11.04
w_1 = 0.0003	48.99	-27.07	0.905	-0.006	15.44	1.009	-11.99
w_1 = 0.0005	46.78	-25.45	0.935	0.011	15.49	1.070	-13.05
Alanine + FA							
w_1 = 0.0001	60.96	-46.48	0.975	0.023	18.38	1.115	-14.27
w_1 = 0.0003	65.40	-41.99	1.047	0.029	18.49	1.284	-15.36
w_1 = 0.0005	64.28	-41.20	1.038	0.048	18.40	1.248	-16.95
Valine + aq. FA							
w_1 = 0.0001	90.99	-56.77	1.065	0.064	24.15	1.324	-18.09
w_1 = 0.0003	92.50	-52.02	1.189	0.177	24.19	1.316	-19.06
w_1 = 0.0005	94.16	-46.25	1.145	0.097	24.20	1.498	-20.78

Table 5. Contributions of zwitter ionic group (NH_3^+, COO^-), CH_2 group, and the other alkyl chains to the limiting apparent molar volume, ϕ_V^0, for amino acids in different mass fraction of aqueous FA (w_1) at 298.15K

	$\phi_V^0 \cdot 10^6$ /m³·mol⁻¹				$\Delta\phi_V^0(R) \cdot 10^6$ /m³·mol⁻¹		
w_1 / groups	0.0000	0.0001	0.0003	0.0005	0.0001	0.0003	0.0005
NH_3^+, COO^-	27.98	27.79	28.77	30.67	-	-	-
(CH)	7.61	8.09	8.11	8.06	-	-	-
Gly (CH_2)	15.22	16.17	16.22	16.11	-	-	-
(CH_3)	22.83	24.26	24.33	24.17	-	-	-
Ala (CH_3CH-)	32.51	33.17	33.63	33.61	17.00	17.41	17.50
Val (CH_3CH_2CH-)	63.00	63.20	63.73	63.49	47.03	47.51	47.38

Table 6. Values of $\Delta\phi_V^0$, ϕ_V^0(elect), ϕ_K^0(elect), and hydration number (n_H) for amino acids in different mass fraction of aqueous FA (w_1) at 298.15 K

Mass fraction of aq. FA (w_1)	$\Delta\phi_V^0 \cdot 10^6$ /m³·mol⁻¹	$\phi_V^0 \cdot 10^6$(elect) /m³·mol⁻¹	$\phi_K^0 \cdot 10^{10}$(elect) /m³·mol⁻¹·Pa⁻¹	n_H	
				From volume	From compressibility
	Glycine				
0.0001	0.76	-7.89	0.96	2.63	3.18
0.0003	1.79	-6.86	1.01	2.29	3.36
0.0005	3.58	-5.07	1.07	1.69	3.57
	Alanine				
0.0001	0.47	-10.79	1.12	3.60	3.72
0.0003	1.91	-9.35	1.18	3.12	3.95
0.0005	3.79	-7.47	1.25	2.49	4.16
	Valine				
0.0001	0.01	-11.10	1.31	3.70	4.37
0.0003	1.52	-9.59	1.39	3.20	4.62
0.0005	3.18	-7.93	1.48	2.64	4.93

Table 7. Contributions of zwitter ionic group (NH_3^+, COO^-), CH_2 group, and the other alkyl chains to the *B*-coefficient in different mass fraction of aqueous FA (w_1) at 298.15 K

B / $kg^{1/2}·mol^{-1/2}$				B(R) / $kg^{1/2}·mol^{-1/2}$		
w_1 / groups	0.0001	0.0003	0.0005	0.0001	0.0003	0.0005
NH_3^+, COO^-	0.852	0.957	1.044	-	-	-
(CH)	0.009	0.009	0.011	-	-	-
Gly (CH_2)	0.017	0.018	0.021	-	-	-
(CH_3)	0.026	0.027	0.031	-	-	-
Ala (CH_3CH-)	0.053	0.050	0.065	0.036	0.032	0.044
Val (CH_3CH_2CH-)	0.083	0.081	0.101	0.066	0.063	0.080

Table 8. Values of A_1, and A_2 coefficient for the amino acids in different mass fraction of aqueous FA at 298.15 K

Solute	A_1	A_2
Glycine	-0.122	0.022
Alanine	-0.172	0.018
Valine	-1.223	0.025

Figures:

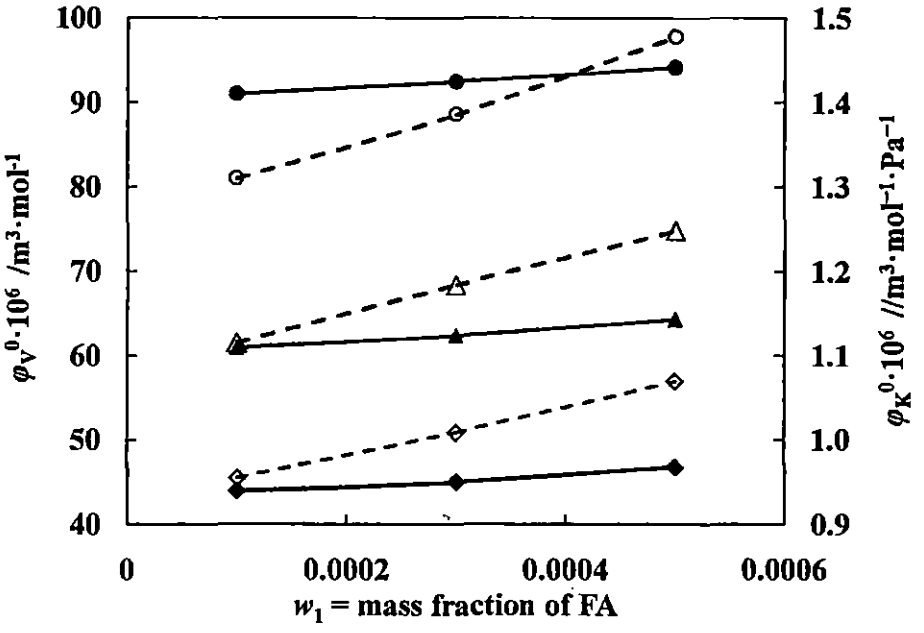

Figure 1. Plot of limiting apparent molar volume (ϕ_V^0) for glycine (♦), alanine (▲), valine (●), and limiting molar isentropic compressibility (ϕ_K^0) for glycine (◊), alanine (Δ), valine (○), against mass fraction of aq. FA (w_1) respectively

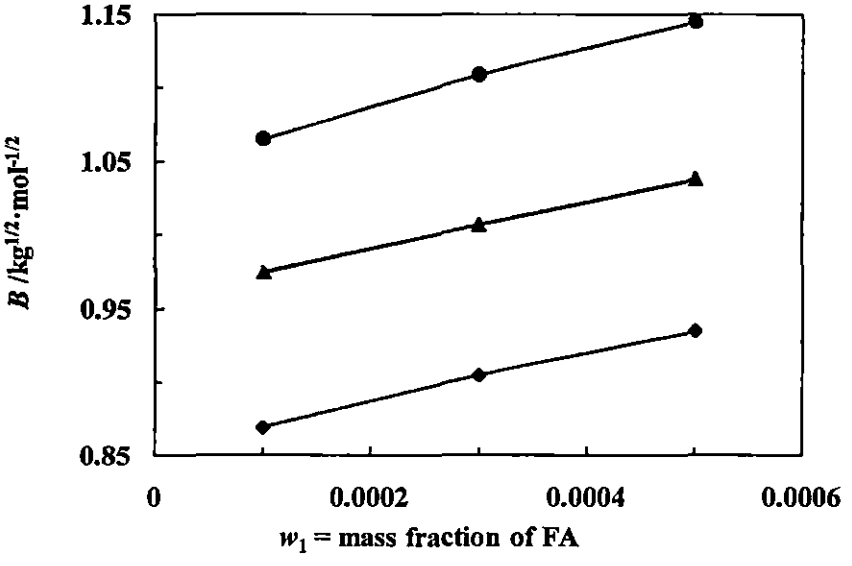

Figure 2. Plot of Viscosity *B*-coefficient for glycine (♦), alanine (▲) and valine (●) vs mass fraction of aq. FA (w_1)

Schemes:

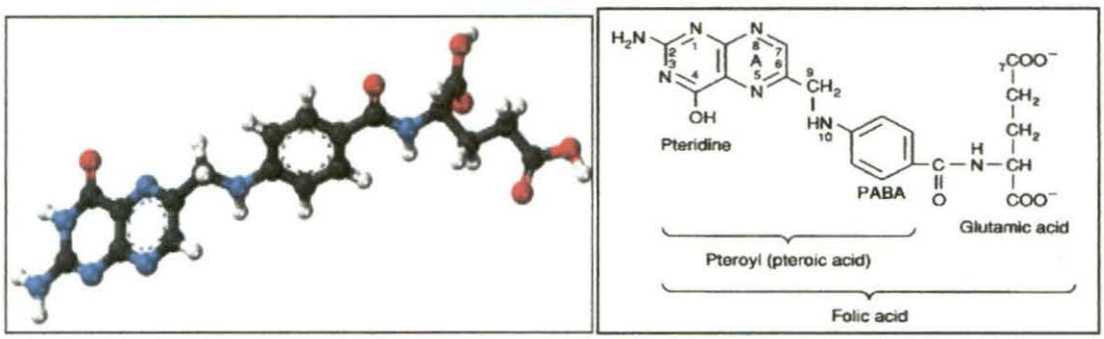

Scheme 1: The molecular structure of Folic Acid

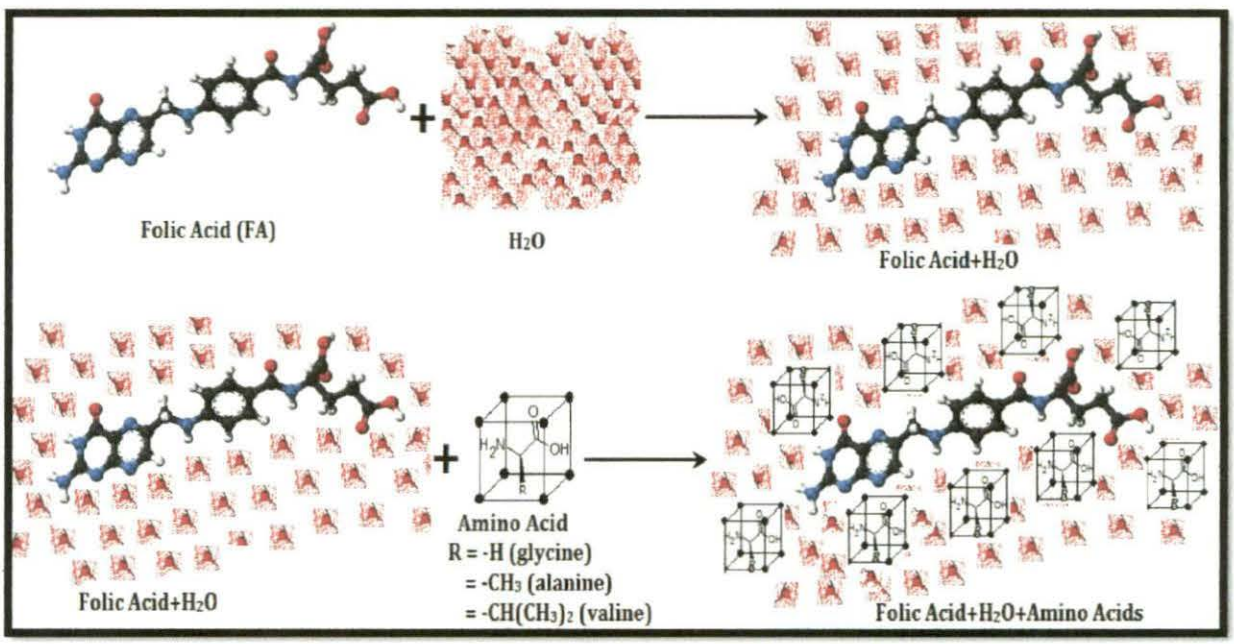

Scheme 2. The schematic representation of solute-solvent interaction, for the studied amino acids in aqueous folic acids binary mixtures

CHAPTER V

CONDUCTIVITY IS A CONTRIVANCE TO EXPLORE ION-PAIR AND TRIPLE ION STRUCTURE OF ETHANOATES IN TETRAHYDROFURAN, DIMETHYL SULPHOXIDE AND THEIR BINARIES

5.1 Introduction

Studies of the transport properties of electrolytes in different solvent media are of considerable importance for the information they provide on the behaviour of ions in solution.

Mixed solvents enable the variation of properties such as dielectric constant or viscosity and therefore the ion-ion and ion-solvent interactions can be better studied. Furthermore different quantities strongly influenced by solvent properties can be derived from concentration-dependence of the electrolyte conductivity. The conductometric method is well-suited to investigate the ion–solvent and ion–ion interactions in electrolyte solutions [1-6]. Ionic association of electrolytes in solution depends upon the mode of solvation of its ions, which in its turn depends on the nature of the solvent or solvent mixtures. Such solvent properties as viscosity and the relative permittivity have been taken into consideration as these properties help in determining the extent of ion association and the solvent-solvent interactions. Thus extensive studies on electrical conductances in various mixed organic solvents have been performed in recent years to examine the nature and magnitude of ion-ion and ion-solvent interactions.

Tetrahydrofuran (THF) is an important liquid which find a variety of applications in pharmaceuticals, cosmetics, etc. Dimethylsulphoxide (DMSO) is a powerful broad spectrum solvent for a wide variety of inorganic and organic reactants. Having low toxicity, DMSO can be used in biology and medicine, especially for low-temperature preservation. We have taken pure THF (ε = 7.58), DMSO (ε = 46.7) and their mixture for this study because we prefer non aqueous solvent which are nonprotic polar solvent and hydrogen bonding can be avoided. The experimental acetate salts are chosen as their charge densities are high and they form solvent-

Fluid Phase Equillibria 2012, 322, 159-166

separated ion pairs. Such studies have been assumed important because of their applications in modern technology [7]. This type of solvent mixture have applications in high energy batteries especially lithium batteries, in organic syntheses and cosmetics technology as manifested from the physicochemical studies in these media [8-10].

In this paper, an attempt has been made to reveal the nature of various types of interactions prevailing in solutions of some ethanoates in pure tetrahydrofuran (THF) and dimethylsulphoxide (DMSO) and their binary mixtures by using precise conductivity measurements at 298.15 K.

5.2 Experimental Section

Tetrahydrofuran, C_4H_8O (Merck, India) containing 0.1 % water and 0.005 % peroxide, was kept for several days over KOH, refluxed for 24 h , and distilled over $LiAlH_4$ [8, 11-13].

Dimethyl sulfoxide (SRL Extra pure) was kept for several days over anhydrous $CaSO_4$ and refluxed for 4 h over CaO. Finally, it was distilled according to the procedure described earlier [14]. Purity of the solvent checked by comparing their viscosity and density values with the literature values [15, 16].

The experimental ethanoates CH_3COOLi, CH_3COOK, CH_3COONH_4 and CH_3COONa are 99 % pure (Merck) and they were purified by recrystallization twice from conductivity water. The samples were dried in vacuum and stored over P_2O_5 under vacuum [17]. Tetrabutylammonium acetate (Bu_4NOAc) was purified by recrystallization from acetone, and the crystallized salt was dried in vacuum for 48 hrs. Sodium tetraphenylborate ($NaBPh_4$) was recrystallized three times from acetone and then dried under vacuum for 72 hrs[18]. Deionized water was used after further distillation having specific conductivity $1.99 \times 10^{-6}\ \Omega^{-1}cm^{-1}$ at 298.15 K. The materials finally obtained were found to be > 99.5 % pure

Binary solvent mixtures were prepared by mixing a required volume of THF and DMSO with earlier conversion of required mass of each liquid into volume at 298.15 K using experimental densities. A stock solution for each salt was prepared by mass, and the working solutions were obtained by mass dilution. The conversion

of molality into molarity was accomplished using density values. The uncertainty of molarity of different salt solutions is evaluated to ± 0.0001mol dm^{-3}.

The value of the relative permittivity (ε) of the solvent mixtures was assumed to be an average of those of the pure liquids and calculated using the procedure as described by Rohdewald and Moldner [19]. The density (ρ) was measured by means of vibrating-tube density-meter (Anton Paar, DMA 4500) which was calibrated with distilled water and air [18]. The uncertainty in the density measurement was ± 0.0002 g cm^{-3}.

Solvent viscosities were measured by means of a suspended Ubbelohde-type viscometer, calibrated at 298.15 K with doubly distilled water and purified methanol using density and viscosity values from the literature. A thoroughly cleaned and perfectly dried viscometer filled with experimental liquid was placed vertically in the glass-walled thermostat maintained to ± 0.01 K. After attainment of thermal equilibrium, efflux times of flow were recorded with a stopwatch correct to ± 0.1 s. The uncertainty of viscosity values is ± 0.003 cP. The details of the methods and measurement techniques had been described elsewhere [20, 21].

The conductance measurements were carried out in a systronic 308 conductivity bridge (accuracy ± 0.01 %) using a dip-type immersion conductivity cell, CD-10, having a cell constant of approximately (0.1 ± 10 %). Measurements were made in a water bath maintained within T = (298.15 ± 0.01) K and the cell were calibrated by the method proposed by Lind et al [22]. The entire conductance data were reported at 1 KHz and were found to be ± 0.3 % precise.

5.3 Results and Discussion

5.3.1 Electrical conductivity of ethanoates in pure DMSO and different binary mixtures of (THF + DMSO):

The physical properties of the binary solvent mixtures at 298.15 K are listed in Table1. The experimental values of the molar conductance, Λ against the respective concentration, c for different electrolytes in pure THF (w_1), DMSO (w_2) and their different binary mixtures at 298.15 K are recorded in Table 2.

The conductance data for different electrolytes in pure DMSO and different binary mixtures having higher to moderate relative permittivity values (ε = 46.70-

17.36), have been analyzed using the Fuoss conductance-concentration equation [23]. The conductance curves (Λ versus $\sqrt{c}$) were linear and extrapolation of $\sqrt{c} = 0$ evaluated the starting limiting molar conductances for the electrolytes. For a given set of conductivity values (c_j, Λ_j, j = 1, 2 . . , n), three adjustable parameters, i.e., Λ^0, K_A, and R are derived from the Fuoss equation. Here Λ_0 is the limiting molar conductance, K_A is the observed association constant, and R is the association distance, i.e., the maximum center to center distance between the ions in the solvent separated ion-pairs. There is no precise method [23] for determining the R value but in order to treat the data in our system, R value is assumed to be, R=a + d, where a is the sum of the crystallographic radii of the ions and d is the average distance corresponding to the side of a cell occupied by a solvent molecule. The distance, d is given by [24],

$$d = 1.183(M/\rho)^{1/3} \quad (1)$$

where M is the molecular weight and ρ is the density of the solvent. For mixed solvents, M is replaced by the mole fraction average molecular weight (M_{av}) which is given by,

$$M_{av} = M_1M_2/(W_1M_2 + W_2M_1) \quad (2)$$

where W_1 is the weight fraction of the first component of molecular weight M_1.

Thus the Fuoss conductance equation may be represented as follows:

$$\Lambda = p[\Lambda^o(1 + R_X) + E_L] \quad (3)$$

$$p = 1 - \alpha(1 - \gamma) \quad (4)$$

$$\gamma = 1 - K_A c\gamma^2 f^2 \quad (5)$$

$$-\ln f = \beta k/2(1 + k_R) \quad (6)$$

$$\beta = e^2/\varepsilon k_B T \quad (7)$$

$$K_A = K_R(1 + K_S) \quad (8)$$

where, R_X is the relaxation field effect, E_L is the electrophoretic countercurrent, k^{-1} is the radius of the ion atmosphere, ε is the relative permittivity of the solvent mixture, e is the electron charge, c is the molarity of the solution, k_B is the Boltzmann constant, K_S is the association constant of contact-pairs, K_R is the association constant of solvent-separated pairs, γ is the fraction of solute

present as unpaired ion, α is the fraction of contact pairs, f is the activity coefficient, T is the absolute temperature and β is twice the Bjerrum distance.

The computations are performed on a computer using the program suggested by Fuoss. The initial Λ^0 values for the iteration procedure are obtained from Shedlovsky extrapolation of the data [25, 26]. Now, we input for the program, the no. of data, n, followed by ε, η (viscosity of the solvent mixture), initial Λ^0 value, T, ρ (density of the solvent mixture), mole fraction of the first component, molecular weights, M_1 and M_2 along with c_j, Λ_j values where j = 1, 2.....n and an instruction to cover preselected range of R values.

In practice, calculations are performed by finding the values of Λ^0 and σ which minimize the standard deviation, σ, whereby

$$\sigma^2 = \Sigma[\Lambda_{j(calc)} - \Lambda^o{}_{j(obs)}]^2 / n-2 \quad (9)$$

for a sequence of R values and then plotting σ against R, the best- fit R corresponds to the minimum in σ versus R curve. So an approximate sum is made over a fairly wide range of R values using a 0.1 increment to locate the minimum, but no significant minima is found in the σ-R curves for the salt studied here, thus R values are assumed to be R= a + d, with terms having usual significance [27]. Finally, the corresponding Λ^0 and K_A values are obtained which are reported in Table 3, along with R and σ for the two binary mixtures of salts.

In order to investigate the specific behaviour of the individual ions comprising these electrolytes, it is necessary to split the limiting molar salt conductance into their ionic components. In the absence of accurate transference data for these systems, we have used the "reference electrolyte" method. Sodium tetraphenyleborate ($NaBPh_4$), tetrabutyleammonium acetate (Bu_4NOAc) and sodium acetate (NaOAc) were used to derive the Λ^0 of tetrabutylammonium tetraphenyl borate (Bu_4NBPh_4) as reference electrode following the Kohlrausch rule. The Λ^o (Bu_4NBPh_4) was obtained from the Λ^o values of tetrabutylammonium acetate (Bu_4NOAc), sodium tetraphenylborate ($NaBPh_4$), and sodium acetate (NaOAc) in the appropriate solvent mixture using the relation,

$$\Lambda^\circ(Bu_4NBPh_4) = \Lambda^\circ(Bu_4NOAc) + \Lambda^\circ(NaBPh_4) - \Lambda^\circ(NaOAc) \quad (10)$$

Ionic divisions were accomplished through the following relationships [28, 29]:

$$\Lambda^o(Bu_4NBPh_4) = \lambda^o(Bu_4N^+) + \lambda^o(BPh_4^-) \quad (11)$$

$$\lambda^0(Bu_4N^+) = 0.517\ \Lambda^o(Bu_4NBPh_4). \quad (12)$$

The limiting ionic conductances calculated from the above equation are recorded in Table 4.

The limiting ionic conductance $\lambda^0_{\pm}$ values were in turn utilized for the calculation of Stoke's hydrodynamic radii r_s according to the expression as modified by Gill [26] is given below.

$$r_S = \frac{F^2}{6\pi N_A \eta\ \lambda^o_{\pm}} \quad (13)$$

The Walden's product [30, 31], $\Lambda^0\eta$ of an ion is also calculated for the various solvent compositions and the results have has been given in Table 4.

The Gibbs' energy of ion-pair formation, ΔG^o for the electrolytes in different binary mixtures studied here calculated by the following relationship [32],

$$\Delta G^0 = -RT \ln K_A \quad (14)$$

Table 3 shows that the conductance of the electrolytes is observed to be lower when THF is present in lower proportion to the solvent mixtures of THF + DMSO considered. The increase in conductance with increase of concentration of THF in the mixture can probably be interpreted as a contraction of the solvent sheath (which envelops an ion and moves by ion-solvent interactions), whereas with increase of concentration of DMSO, the numbers of activated solvent molecules increase which forming the sheath. This trend also suggests predominance of the solvent viscosity (η_0) over relative permittivity (ε) in effecting the electrolytic conductance in these media as with the increase of concentration of THF, both viscosity and permittivity of solvent mixtures decreases.

It also shows that the limiting equivalent conductivity for acetate salts of common anion follow the sequence: $NH_4^+ > K^+ > Na^+ > Li^+$ in all the solvent mixtures studied here at the investigated temperature. The trend of variation of Λ^0 values also indicates the relative actual sizes of these ions as they exist in solution. Thus the sizes of these cations as they exist in solution, follow the order: $Li^+ > Na^+ > K^+ > NH_4^+$.

There is marked characteristic behaviour in the association constant *Ka* values. These electrolytes solutions, in general, show an increase in the *Ka* values

with an increase in mole fraction of THF in these solvent mixtures. This is expected as the relative permittivity (ε) decreases with the increase of THF.

The Walden products $\Lambda^o\eta$ of the ions are usually employed to discuss the interactions of the ions with the solvent medium. From the Table 4, we see that the Walden product of cations decrease in the order, $NH_4^+ > K^+ > Na^+ > Li^+$, and the Fig.1 also predicts that the electrolyte taken as a whole follows the same sequence. This is justified as the Walden product of an ion or solute is inversely proportional to the effective radius (r) of the ion or solute in a particular solvent [33],

$$\Lambda^o\eta = 1/6\Pi rT \qquad (15)$$

This points out that the electrostatic ion-solvent interaction is strong in these cases, apparently due to the very high surface charge density on small ions [34]. Fig.1. indicates the variation of the Walden product with solvent composition due to preferential solvation of cations by THF and DMSO molecules respectively [34, 35]. The decrease in the Walden product with increase of concentration of THF in indicates the preferential solvation of cations by THF in (THF + DMSO) mixture. However this decrease may also probably be due to the Zwanzig [8] solvent relaxation effect.

The starting point for most evaluations of ionic conductances is Stokes' law that states that the limiting Walden product for any singly charged, spherical ion is a function of only the ionic radius and thus, under normal conditions, is a constant. In Table 4, we have calculated the Stokes' radii r_s of these ions in these different solvent mixtures.

Fig. 2 shows that the trend in ionic Walden products ($\lambda^o_\pm\eta$) just mimics the trend in Walden product ($\Lambda^o\eta$) for all electrolytes in these solvent mixtures and hence Stokes' radii also follow the same trend $Li^+ > Na^+ > K^+ > NH_4^+$. For lithium, sodium, potassium and ammonium ions, the Stokes' radii are much higher than their crystallographic radii suggesting that these ions are significantly solvated in these solvent mixtures. The Stokes' radius of the acetate ion is, however, found to be either very close to or slightly higher than their corresponding crystallographic radii indicating their low degree of solvation. This also supports our earlier contention, derived from the Walden products of those ions.

Fig. 3 points out the nature of curve for the Gibbs energy for ion-pair formation, ΔG^o which clearly predicts that the tendency for ion-pair formation decreases significantly with an increase in the association factor for the ethanoates in different THF + DMSO mixtures. The ΔG^o curve in Fig. 3 along with the other parameters mentioned above are quite in accordance with the results observed by Barthel et al. [32] and Hazra et al [34, 35].

The schematic representation of solvation of ions, at a particular concentration, in the solvent mixtures studied here in view of various derived parameters can be depicted in scheme I. Here the blue and red circles refer to THF (w_1) and DMSO (w_2) respectively.

5.3.2. Electrical conductivity of ethanoates in pure THF:

The experimental values of the molar conductances, Λ against the respective concentration, c of different acetate salts in pure THF (ε = 7.58) at 298.15 K are presented in Table 2. Here the conductance curves (Λ versus $\sqrt{c}$) for all the electrolytes were follow the same trend, i.e., Λ decreases with increasing concentration, reaches a minimum and then increases.

The conductance data have been analyzed by the Fuoss-Kraus triple-ion theory [36] in the form as given below,

$$\Lambda g\sqrt{C} = \frac{\Lambda^o}{\sqrt{K_P}} + \frac{\Lambda_T^o K_T}{\sqrt{K_P}}\left(1-\frac{\Lambda}{\Lambda^o}\right) C \tag{16}$$

$$g(c) = \frac{\exp\left\{-\frac{\beta'}{\sqrt{\Lambda^o}}\sqrt{(c\Lambda)}\right\}}{\left\{1-\frac{S}{\Lambda^{o3/2}}\sqrt{(c\Lambda)}\right\}\sqrt{\left(1-\frac{\Lambda}{\Lambda^o}\right.}} \tag{17}$$

$$\beta' = \frac{1.8247\times 10^6}{(\varepsilon T)^{3/2}} \tag{18}$$

$$S = \alpha\,\Lambda^o + \beta = \frac{0.8206\times 10^6}{(\varepsilon T)^{3/2}}\Lambda^o + \frac{82.501}{\eta\,(\varepsilon T)^{1/2}} \tag{19}$$

In the above equations, Λ^o is the sum of the molar conductances of the simple ions at infinite dilution, Λ^o_T is the sum of the values for the two kinds

of triple-ions, Kp and K_T are the ion-pair and triple-ion formation constants respectively, S is the limiting Onsager coefficient, ε is the permitivitty of the solvent, T is the absolute temperature. The symmetrical approximation of the two possible formation constant of triple ions equal to each other has been considered [37]. g (c) is the factor which incorporates all interionic interaction terms [38].

Neglecting, Λ/Λ^o, $(S/\Lambda^{o3/2})(c\Lambda)^{1/2}$ and assuming $f_\pm = 1$, lead to $g(c) = 1$ in eq. 16, we get,

$$\Lambda\sqrt{C} = \frac{\Lambda^o}{\sqrt{K_P}} + \frac{\Lambda_T^o K_T}{\sqrt{K_P}} C \qquad (20)$$

Λ^o is obtained by applying the Walden's rule [39] as suggested by the work of Krumgalz [31]. Λ^o_T is calculated by setting the triple-ion conductance as equal to 2/3 Λ^o [40]. On running the Fuoss-Kraus equation, we get Kp, K_T from the slope and intercept. The results are listed in Table 5.

The limiting molar conductances of the simple ions, Λ^0 and limiting molar conductances of the triple ions, Λ^0_T of the acetate salts in pure THF at 298.15 K follow the trend,

$$CH_3COO\,NH_4 > CH_3COOK > CH_3COONa > CH_3COOLi$$

Increase in Λ^0 significantly increase the mobility of ions due to lower solvation of the ions by the solvent molecules. Thus, the tendency of the ion-pair and triple-ion formation of electrolytes depends on the size and the charge distribution of the ions. Similar type of results has been reported earlier by Roy et al [21].

K_P and K_T values predicts that major portion of the electrolyte exists as ion-pairs with a minor portion as triple-ions (neglecting quadruples). The values show that CH_3COOLi has the lowest K_P and highest K_T in pure THF as compared to the other salts. The tendency of triple-ion formation can be also judged from the K_T/K_P ratios, which is highest for CH_3COOLi. The large association between the ions may be due to the coulombic interactions as well as to covalent bonding forces, considering the ionic sizes of the species in the solution. The results are in good agreement with the works of Hazra and Muhuri [3].

At very low dielectric constant of the solvent, i.e. $\varepsilon < 10$, electrostatic ionic interactions are very large. So the ion-pairs attract the free present in

the solution medium as the distance of the closest approach of the ions becomes minimum. This results in the formation of symmetrical triple-ions in addition to ion-pairs which acquire the charge of the respective ions in the solution [13, 41].

$$M^+ + A^- \leftrightarrow M^+ \ldots\ldots A^- \leftrightarrow MA \quad (21)$$

$$MA + M^+ \leftrightarrow MA\,M^+ \quad (22)$$

$$MA + A^- \leftrightarrow MA\,A^- \quad (23)$$

The effect of ternary association [21] is to remove some non-conducting species MA from the solution and replace them by triple ions which contribute to the conductance.

Schematically the triple-ion formation for lithium acetate (for example) in pure THF can be depicted in scheme II.

Furthermore, the ion-pair and triple-ion concentrations, C_P and C_T respectively of the electrolyte are also calculated at the highest concentration, using the following relations [21, 42],

$$\alpha = 1/K_p^{1/2}.C^{1/2} \quad (24)$$

$$\alpha_T = (K_T/K_p^{1/2})C^{1/2} \quad (25)$$

$$C_p = c(1-\alpha-3\alpha_T) \quad (26)$$

$$C_T = (K_T/K_p^{1/2})C^{3/2} \quad (27)$$

Here, α and α_T are the fraction of ion-pairs and triple-ions and *Cp* and C_T are the concentration of ion-pair and triple-ion formation respectively. The *Cp* and C_T values show that, CH_3COOLi has the highest value of C_T in pure THF as compared to the other salts whereas CH_3COONH_4 has the highest value C_P. The results are in good agreement with the earlier conclusion and our results supports the general view that the tendency of ion-pair and triple-ion formation depends on the size and the charge distribution of the ions as well as on the solvent polarity. Similar type of work has been reported by Corti et al [43].

5.4 CONCLUSION

Through our work we have shown that the tendency of triple ion formation is proved in pure THF having low dielectric constant but that tendency has been diminished by the addition of DMSO. The electrolytes are remaining associated in solvent mixtures but the solvation of the ions weakened as soon as the ion pair is formed. The cations are found to be substantially solvated whereas the anions appear to have weak interactions with the solvent molecules. The coulombic force has a great effect on the association process.

List of symbols

ρ	solution density
ρ_o	solvent density
η	solution viscosity
η_o	solvent viscosity
ε	relative permittivity
c	molarity
m	molality
Λ	molar conductance
Λ^o	limiting molar conductance
K_A	association constant
K_S	association constant of contact-pairs
K_R	association constant of solvent-separated pairs
$f_\pm$	mean activity coefficient
R_X	relaxation field effect
E_L	electrophoretic counter current
Kp	ion-pair formation constants
K_T	triple-ion formation constants
C_P	ion-pair concentrations
C_T	triple-ion concentrations
γ	fraction of solute present as unpaired ion
β	twice the Bjerrum distance
κ	radius of ionic atmosphere

e electric charge

k_B Boltzmann constant

R association distance or co-sphere diameter

r_s Stoke's hydrodynamic radii

ΔG^o Gibbs energy of ion-association reaction

σ standard deviation

Tables:

Table 1. Physical properties of pure THF, DMSO and different binary mixtures of (THF + DMSO) at 298.15 K.

Mass % of THF (w_1)	ρ x 10^{-3} (kg m^{-3})		η (mPa s)		ε
	Observed	Literature	Observed	Literature	
0.00	1.0958	1.0951 [15]	1.9600	1.992 [15]	46.70 [16]
0.25	1.0367		1.5234		36.92 [19]
0.50	0.9847		1.1125		27.14 [19]
0.75	0.9340		0.7376		17.36 [19]
1.00	0.8811	0.8811 [16]	0.4630	0.463 [16]	7.58 [16]

Table 2. Molar conductivities and corresponding molarities of electrolytes in different binary mixtures of THF + DMSO at 298.15 K.

$c \times 10^4$ (mol dm^{-3})	$\Lambda \times 10^4$ (S m^2 mol^{-1})	$c \times 10^4$ (mol dm^{-3})	$\Lambda \times 10^4$ (S m^2 mol^{-1})	$c \times 10^4$ (mol dm^{-3})	$\Lambda \times 10^4$ (S m^2 mol^{-1})	$c \times 10^4$ (mol dm^{-3})	$\Lambda \times 10^4$ (S m^2 mol^{-1})
W_1=0.00							
CH_3COONH_4		CH_3COOLi		CH_3COONa		CH_3COOK	
29.226	24.85	39.312	21.72	29.636	24.26	45.187	23.41
37.344	24.14	47.174	21.23	37.868	23.65	54.224	22.78
44.813	23.39	54.432	20.91	45.442	23.06	62.566	22.39
51.707	22.57	61.152	20.42	52.433	22.67	70.290	21.74
58.091	21.94	67.392	20.20	58.907	22.11	77.463	21.21
64.018	21.67	73.201	19.90	64.917	21.64	84.141	20.89
69.537	21.12	78.624	19.34	70.514	21.32	90.373	20.52
74.688	20.68	83.696	19.17	75.737	20.89	96.204	20.11
79.507	20.22	88.452	18.86	80.623	20.48	101.670	19.70
84.024	19.75	92.919	18.69	85.204	20.13	106.805	19.32
W_1=0.25							
CH_3COONH_4		CH_3COOLi		CH_3COONa		CH_3COOK	
59.859	26.07	13.236	23.49	14.664	26.56	14.960	28.82
63.184	25.75	16.913	23.11	18.737	25.89	19.116	28.07
64.725	25.59	23.417	22.32	22.484	25.34	22.939	27.24

66.193	25.36	28.993	21.63	25.944	24.67	26.468	26.72
67.592	25.25	33.825	21.14	29.146	24.22	29.736	26.03
68.928	25.14	38.053	20.64	32.121	23.70	32.770	25.34
71.426	24.92	45.100	19.52	37.474	22.79	38.232	24.37
73.715	24.64	50.738	18.86	39.892	22.16	40.698	24.10
75.821	24.47	55.350	18.23	42.158	22.05	43.011	23.52
77.765	24.30	59.194	17.89	44.287	21.67	45.183	23.12
W_1=0.50							
CH_3COONH_4		CH_3COOLi		CH_3COONa		CH_3COOK	
25.195	29.23	16.467	23.89	17.028	26.55	9.605	30.55
26.595	28.87	19.211	23.45	19.866	26.13	10.790	30.13
27.861	28.57	23.731	22.61	22.349	25.53	11.891	29.72
28.450	28.41	27.300	22.23	24.541	25.12	13.873	28.96
29.012	28.26	30.189	21.78	26.488	24.62	14.768	28.63
29.550	28.12	33.620	21.45	28.231	24.34	15.608	28.29
30.064	28.01	36.288	20.83	29.799	23.93	16.396	28.04
30.556	27.87	39.042	20.55	31.218	23.71	17.138	27.79
31.027	27.76	41.167	20.27	32.508	23.54	18.498	27.28
31.914	27.55	43.225	19.93	33.686	23.32	19.715	26.87
W_1=0.75							

CH_3COONH_4		CH_3COOLi		CH_3COONa		CH_3COOK	
6.268	38.36	4.133	28.31	4.048	31.50	3.450	33.98
6.732	37.94	5.281	27.97	4.723	31.15	3.981	33.46
7.574	37.38	6.337	27.56	5.313	30.87	4.473	33.11
8.316	36.88	7.312	27.24	5.834	30.56	4.929	32.80
8.976	36.32	9.053	26.62	6.297	30.31	5.751	32.12
9.567	35.89	10.562	26.20	8.008	29.10	6.469	31.47
10.098	35.53	11.883	25.84	9.108	28.61	7.104	31.00
10.579	35.21	14.083	25.10	9.875	28.08	7.667	30.65
11.416	34.53	15.843	24.53	10.440	27.89	8.626	29.85
12.118	34.08	17.284	24.12	10.874	27.57	9.410	29.42
w_1=1							
CH_3COONH_4		CH_3COOLi		CH_3COONa		CH_3COOK	
0.820	10.89	0.559	12.76	0.405	22.71	0.254	40.40
0.946	10.24	0.645	10.65	0.517	16.43	0.352	29.30
1.171	9.67	0.798	8.75	0.716	10.28	0.435	21.50
1.366	9.56	1.048	8.35	0.887	7.55	0.480	18.40
1.537	9.74	1.323	12.41	1.164	8.48	0.677	10.60
1.821	10.32	1.464	16.50	1.278	11.73	0.762	10.00
2.049	11.13	1.579	20.35	1.471	19.71	0.831	11.73

2.235	11.71	1.676	24.37	1.626	30.46	0.889	13.70
2.459	13.05	1.759	28.86	1.755	39.78	0.938	16.21
2.634	14.34	1.831	32.39	1.863	49.62	0.998	20.72
w_1=0.25				w_1=0.50			
$NaBPh_4$		Bu_4NOAc		$NaBPh_4$		Bu_4NOAc	
13.75	24.11	14.74	24.77	18.58	24.21	17.25	24.81
17.56	23.76	18.83	24.21	22.30	23.75	18.04	24.65
21.08	23.41	22.60	23.55	25.73	23.34	18.77	24.47
24.32	23.17	26.07	23.10	28.91	22.85	19.47	24.35
27.32	22.89	29.29	22.64	31.86	22.53	20.12	24.26
30.11	22.64	32.28	22.23	34.61	22.12	20.75	24.14
32.704	22.46	35.06	21.73	37.17	21.78	21.34	24.05
35.127	22.22	37.66	21.42	41.82	21.41	21.90	23.92
37.393	22.03	40.09	21.07	43.93	21.15	22.43	23.80
39.517	21.84	42.37	20.71	45.92	21.00	22.94	23.71
w_1=0.75							
$NaBPh_4$		Bu_4NOAc					
2.786	28.34	2.419	29.90				
3.070	28.19	2.666	29.75				
3.582	27.87	3.110	29.44				

4.030	27.62	3.311	29.14
4.425	27.42	3.499	29.06
4.776	27.27	3.676	28.98
5.091	27.08	3.842	28.91
5.373	26.86	3.999	28.68
5.629	26.74	4.147	28.53
5.862	26.61	4.287	28.38

Table 3. Derived conductance and thermodynamic parameters for different electrolytes in different binary mixtures of THF + DMSO at 298.15 K.

Electrolytes	Λ^o x 10^4 (S m^2 mol^{-1})	K_A (dm^3 mol^{-1})	R (Å)	σ (%)	$\Lambda^o\eta$ x 10^4 (S m^2 mol^{-1} Pa s)	ΔG^o (kJ mol^{-1})
			w_1=0.00			
CH_3COONH_4	32.75 ± 0.71	148.08 ± 13	8.63	0.20	0.642	-12.38
CH_3COOLi	27.22 ± 0.47	84.11 ± 07	7.79	0.14	0.534	-10.98
CH_3COONa	29.80 ± 0.50	94.58 ± 08	8.15	0.18	0.584	-11.27
CH_3COOK	31.90 ± 0.80	118.01 ± 12	8.52	0.18	0.625	-11.82
$NaBPh_4$	24.15 ± 0.21	49.48 ± 03	10.67	0.10	0.473	-9.67
Bu_4NOAc	28.89 ± 0.56	108.52 ± 09	12.13	0.18	0.566	-11.61
			w_1=0.25			
CH_3COONH_4	44.86 ± 0.75	258.94 ± 14	8.68	0.03	0.683	-13.77

CH_3COOLi	28.70 ± 0.80	185.28 ± 25	7.84	0.40	0.437	-12.94
CH_3COONa	33.35 ± 0.69	216.53 ± 21	8.20	0.24	0.508	-13.32
CH_3COOK	36.94 ± 0.78	243.23 ± 23	8.57	0.25	0.563	-13.61
$NaBPh_4$	26.55 ± 0.09	71.28 ± 02	10.72	0.05	0.404	-10.57
Bu_4NOAc	30.11 ± 0.40	177.82 ± 12	12.18	0.15	0.459	-12.84
			w_1=0.50			
CH_3COONH_4	47.66 ± 0.49	511.36 ± 18	8.73	0.02	0.530	-15.45
CH_3COOLi	30.88 ± 0.50	250.05 ± 19	7.89	0.15	0.344	-13.68
CH_3COONa	35.99 ± 0.58	316.95 ± 23	8.25	0.11	0.400	-14.27
CH_3COOK	38.98 ± 0.37	391.27 ± 19	8.62	0.09	0.434	-14.79
$NaBPh_4$	30.19 ± 0.25	179.73 ± 07	10.77	0.08	0.336	-12.86
Bu_4NOAc	31.44 ± 0.21	223.68 ± 08	12.23	0.02	0.350	-13.40
			w_1=0.75			
CH_3COONH_4	50.64 ± 0.60	756.75 ± 46	8.79	0.12	0.374	-16.42
CH_3COOLi	32.50 ± 0.29	310.47 ± 24	7.95	0.18	0.240	-14.22
CH_3COONa	37.87 ± 0.37	556.71 ± 38	8.31	0.16	0.279	-15.66
CH_3COOK	40.85 ± 0.33	681.74 ± 36	8.68	0.13	0.301	-16.17
$NaBPh_4$	31.54 ± 0.11	364.73 ± 15	10.83	0.05	0.233	-14.62
Bu_4NOAc	33.56 ± 0.24	491.77 ± 38	12.29	0.07	0.248	-15.36

Table 4. Limiting ionic conductance, ionic Walden product, Stoke's radii (r_s) and crystallographic radii (r_c) in different binary mixtures of THF+DMSO at 298.15 K

Ions	$\lambda^0_{\pm} \times 10^4$ (S m^2 mol^{-1})	$\lambda^0_{\pm}\eta \times 10^4$ (S m^2 mol^{-1} Pa s)	r_s (Å)	r_c (Å)
w_1=0.00				
CH_3COO^-	16.87	0.331	2.48	2.28
NH_4^+	15.87	0.312	2.63	1.44
Li^+	10.35	0.203	4.04	0.60
Na^+	12.93	0.254	3.23	0.96
K^+	15.02	0.295	2.78	1.33
BPh_4^-	11.23	0.220	3.72	4.80
Bu_4N^+	12.02	0.236	3.48	4.94
w_1=0.25				
CH_3COO^-	18.06	0.275	2.98	2.28
NH_4^+	26.80	0.408	2.01	1.44
Li^+	10.64	0.162	5.06	0.60
Na^+	15.29	0.233	3.52	0.96
K^+	18.88	0.288	2.85	1.33
BPh_4^-	11.26	0.172	4.78	4.80
Bu_4N^+	12.05	0.184	4.47	4.94
w_1=0.50				
CH_3COO^-	18.18	0.202	4.05	2.28
NH_4^+	29.47	0.328	2.50	1.44
Li^+	12.70	0.141	5.80	0.60
Na^+	17.81	0.198	4.14	0.96
K^+	20.80	0.231	3.54	1.33
BPh_4^-	12.38	0.138	5.95	4.80
Bu_4N^+	13.25	0.147	5.56	4.94
w_1=0.75				
CH_3COO^-	19.48	0.144	5.71	2.28
NH_4^+	31.16	0.230	3.57	1.44
Li^+	13.01	0.096	8.54	0.60
Na^+	18.39	0.136	6.04	0.96
K^+	21.36	0.158	5.20	1.33
BPh_4^-	13.15	0.097	8.45	4.80
Bu_4N^+	14.08	0.104	7.90	4.94

Table 5. Calculated limiting molar conductance of ion pair and triple ions, slope and intercepts and ion pair and triple ion formation constant for different electrolytes in pure THF at 298.15 K.

lectrolytes	Λ^0 x 10^4 (Sm^2mol^{-1})	Λ^0_T x 10^4 ($S\ m^2\ mol^{-1}$)	Slope x 10^3	Intercept x 10^3	K_P x 10^{-9} $(mol\ dm^{-3})^{-1}$	K_T $(mol\ dm^{-3})^{-1}$	K_T / K_P x 10^9
H_3COONH_4	192.44	128.29	1.37	-2.83	4.611	0.725	0.157
H_3COOLi	145.26	96.84	3.29	-4.43	1.075	1.111	1.034
H_3COONa	156.38	104.25	2.58	-3.59	1.895	1.076	0.568
H_3COOK	174.27	116.18	2.17	-3.43	2.583	0.947	0.367

Table 6. Maximum concentration, the ion pair fraction (α), triple ion fraction (α_T), ion pair concentration (C_P) and triple ion concentration (C_T) for different electrolytes in pure THF at 298.15 K.

Electrolytes	C_{max} x 10^4 ($mol\ dm^{-3}$)	α x 10^5	α_T x 10^5	C_P x 10^4 ($mol\ dm^{-3}$)	C_T x 10^9 ($mol\ dm^{-3}$)
CH_3COONH_4	2.634	0.024	0.017	2.571	0.046
CH_3COOLi	1.831	0.041	0.046	1.755	0.084
CH_3COONa	1.863	0.031	0.034	1.804	0.063
CH_3COOK	0.998	0.020	0.019	0.979	0.019

Figures:

Figure 1: Plots of Walden product ($\Lambda^{o}\eta$) of CH_3COONH_4 (x), CH_3COOK (⍰), CH_3COONa (■) and CH_3COOLi (▲) in different THF + DMSO binary mixtures containing 0, 25, 50, and 75 mass % of THF at 298.15 K.

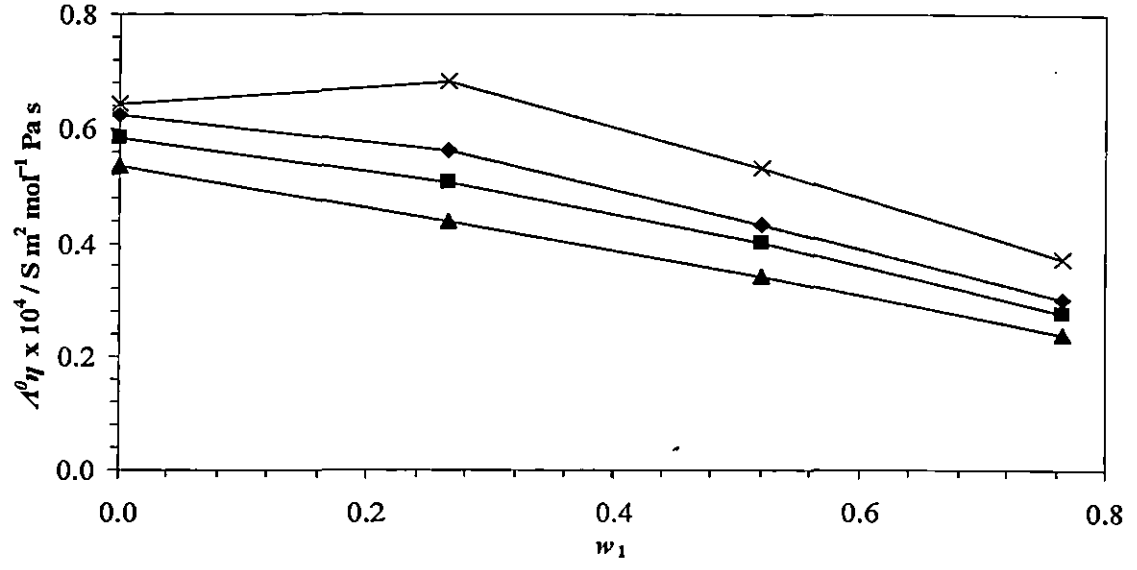

Figure 2: Plots of Ionic Walden product ($\lambda^{o}_{\pm}\eta$) of NH_4^+(x), K^+ (♦), Na^+(■) and Li^+(▲) in different THF + DMSO binary mixtures containing 0, 25, 50, and 75 mass % of THF at 298.15 K

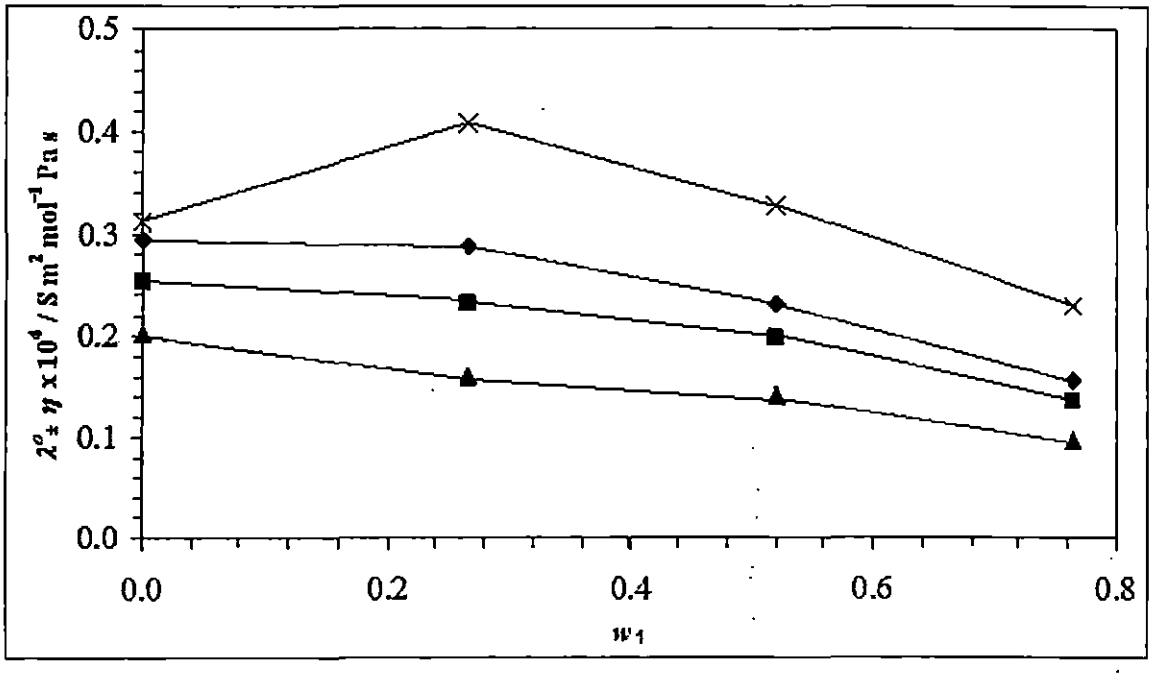

Figure 3: Plots of Gibbs energy of ion-pair formation (ΔG^o) of CH_3COONH_4 (x), CH_3COOK (♦), CH_3COONa (■) and CH_3COOLi (▲) in different THF + DMSO binary mixtures containing 0, 25, 50, and 75 mass % of THF at 298.15 K.

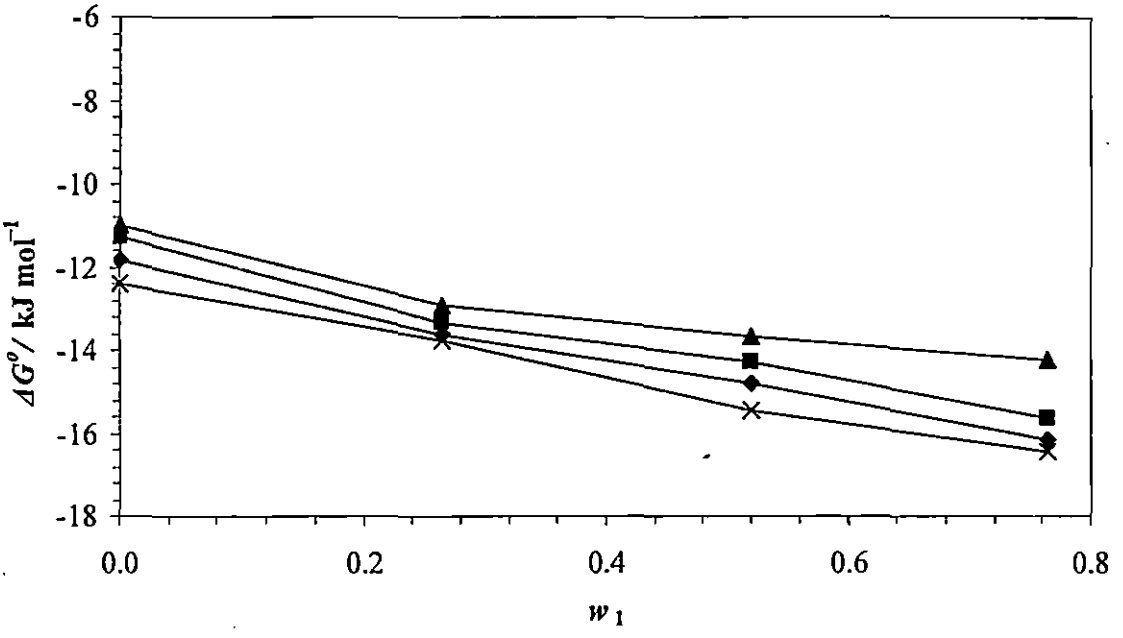

Schemes:

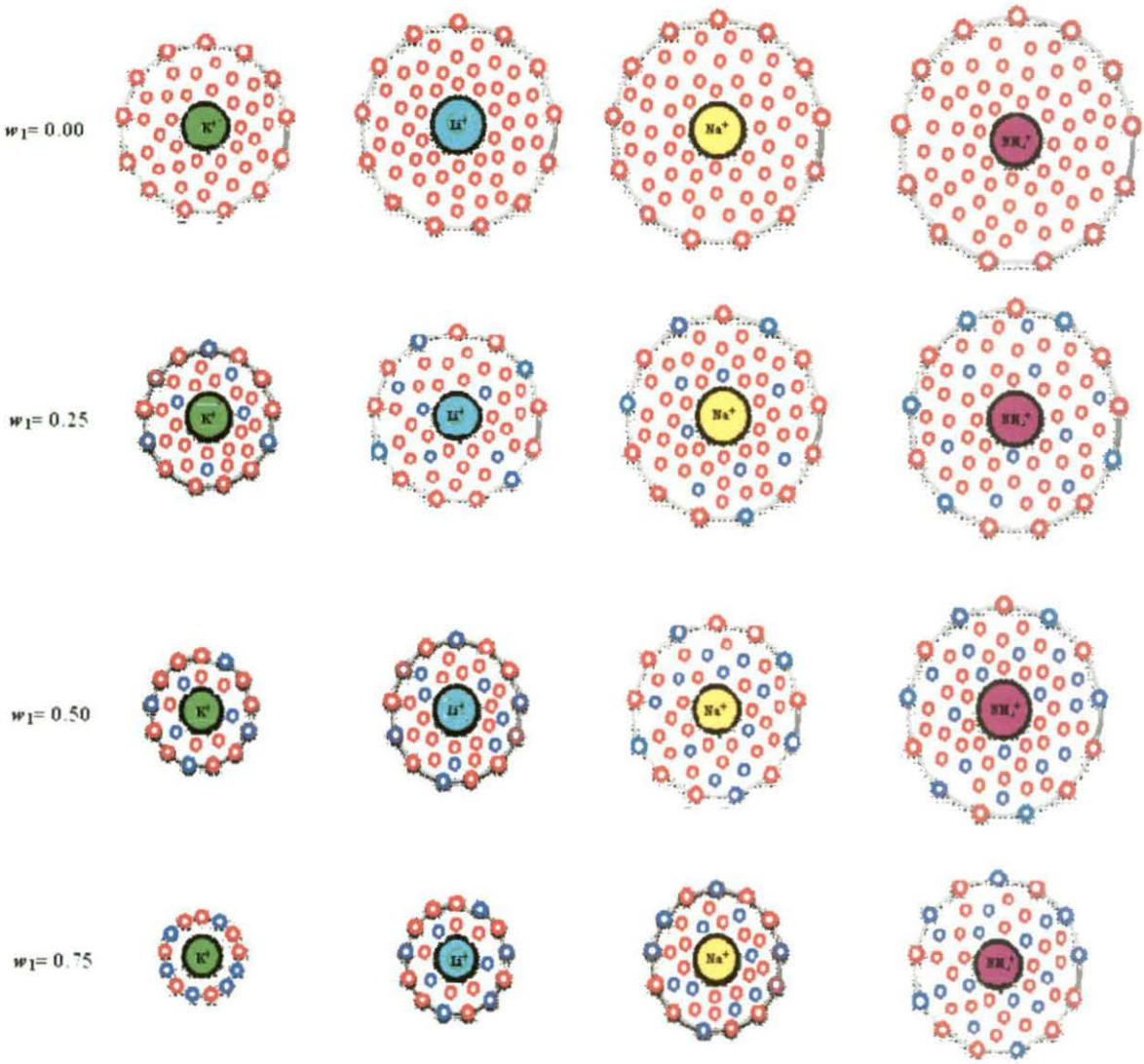

SCHEME I

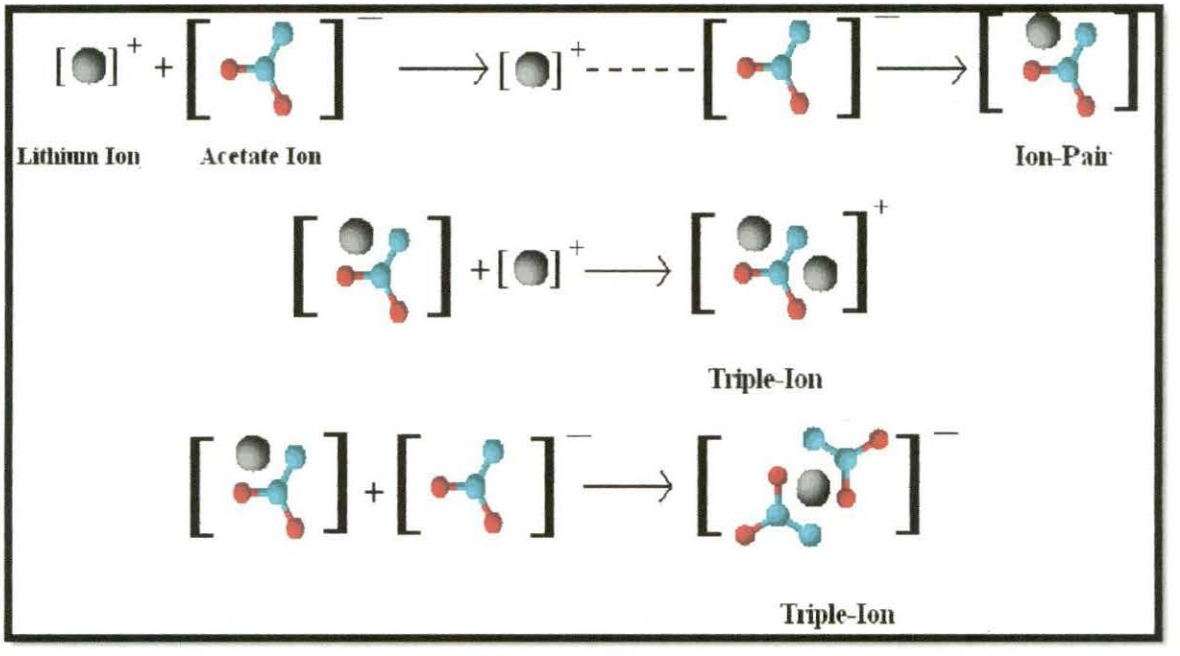

SCHEME II

CHAPTER VI

EXPLORATION OF MOLECULAR INTERACTIONS OF CARBOHYDRATES IN AQUEOUS VITAMIN-C ENVIRONMENTS WITH MANIFESTATION OF SOLVATION CONSEQUENCES

6.1 Introduction

Carbohydrates are sources of energy for vital metabolic processes. They are exceptionally important constituent of biological systems. Carbohydrates play an important role in animal and plant physiology. Water the most abundant molecule on earth is widely used in chemistry as a universal solvent. It is also the most important solvent for the simpler saccharides.

Ascorbic acid (vitamin C) is also very important constituent of our physiological system. Vitamin C is required for the synthesis of collagen, the intercellular "cement" which gives the structure of muscles, vascular tissues, bones, and tendon.. It also enhances the eye's ability and delay the progression of advanced age related muscular degeneration [1]. Hence understanding the molecular interaction of carbohydrates in ascorbic acid solutions may be helpful in formulation of many pharmaceutical products.

The thermodynamic properties are very useful in interpreting the molecular interaction occurring in solutions. The thermodynamic parameters have been extensively used to obtain information on solute-solute, solute-solvent, and solvent-solvent interactions [2-6]. Hence in order to study the thermodynamic properties in solution we have employed volumetric, viscometric and refractometric studies.

In this paper we have undertaken a systematic study on the density, viscosity and refractive index of some carbohydrates (D-Glucose, D-Sucrose, and D-Maltose monohydrate) in aqueous ascorbic acid solutions at 298.15 K and we have reported the limiting apparent molar volume (ϕ_V^0), experimental slopes (S_V^*), and viscosity *B*-coefficients and molar refraction (*R*) for the cited carbohydrates in ascorbic acid and the parameters are interpreted in terms of solute-solute and solute-solvent interaction.

6.2 Experimental Section

6.2.1 Source and purity of samples

Ascorbic acid, D-Glucose, D-Sucrose and D-Maltose monohydrate were procured form Sigma Aldrich, Germany and were used as purchased as the purity assay of the salts was ≥98%. Triply distilled water with a specific conductance $<10^{-6}$ S cm^{-1} was used for the preparation of different aqueous ascorbic acid solutions. The physical properties of different mass fraction of aqueous ascorbic acid mixture are listed in Table 1.

6.2.2 Apparatus and Procedure

Stock solutions were prepared by mass (Mettler Toledo AG285 with uncertainty 0.0003 g), and the working solutions were obtained by mass dilution at 298.15K. The uncertainty of molarity of different solutions was evaluated to ±0.0001 mol dm−3.

The density (ρ) was measured by means of vibrating-tube Anton Paar density-meter (DMA 4500M) with a precision of 0.00005 g·cm^{-3}. It was calibrated by double-distilled water and dry air [7].

The viscosity (η) was measured by means of suspended Ubbelohde type viscometer, calibrated at 298.15 K with doubly distilled water and purified methanol. A thoroughly cleaned and perfectly dried viscometer filled with experimental solution was placed vertically in a glass-walled thermostat (Bose Panda Instruments Pvt. Ltd.) maintained to 0.01 K. After attainment of thermal equilibrium, efflux times of flow were recorded with a stop watch. The flow times were accurate to ±0.1s. The mixtures were prepared by mixing known volume of solutions in airtight-stopper bottles and each solution thus prepared was distributed into three recipients to perform all the measurements in triplicate, with the aim of determining possible dispersion of the results obtained. Adequate precautions were taken to minimize evaporation loses during the actual measurements. Mass measurements were done on a Mettler AG-285 electronic balance with a precision of ±0.01 mg. Viscosity of the solution is evaluated using the following equation [8].

$$\eta = \left(Kt - \frac{L}{t} \right) \rho \qquad (1)$$

where K and L are the viscometer constants, t is the efflux time of flow in seconds and ρ is the density of the experimental liquid. The uncertainty in viscosity measurements is within ± 0.003 m Pa·s.

Refractive index was measured with the help of a Digital Refractometer (Mettler Toledo). The light source was LED, λ=589.3nm. The refractometer was calibrated twice using distilled water and calibration was checked after few measurements. The uncertainty of refractive index measurement was ± 0.0002 units.

The experimental values of densities (ρ), viscosities (η) and refractive indices (n_D) of solutions are reported in Table 2 and the derived parameters are reported in Table 3 and Table 4.

6.3. Result and Discussion

6.3.1. Density calculation

Apparent molar volume (ϕ_V) was determined from the solution density using the following equation [9].

$$\phi_V = M/\rho - 1000(\rho - \rho_o)/m\rho\rho_o \quad (2)$$

where M is the molar mass of the solute, m is the molality of the solution, ρ_0 and ρ are the densities of the solvent (ascorbic acid solution) and solution (carbohydrate in ascorbic acid solution) respectively. The limiting apparent molar volume ϕ_V^0 was calculated using a least-square treatment to the plots of ϕ_V versus $\sqrt{m}$ using the Masson equation [10].

$$\phi_V = \phi_V^0 + S_V^* \sqrt{m} \quad (3)$$

where ϕ_V^0 is the limiting apparent molar volume at infinite dilution and S_V^* is the experimental slope. The plots of ϕ_V against square root of molal concentration ($\sqrt{m}$) were found to be linear with slopes. Values of ϕ_V^0 and S_V^* are reported in Table 4.

A perusal of Table 4 and Figure 1 shows that ϕ_V^0 values for carbohydrates are positive and increases with the increase in concentrations of ascorbic acid solution indicating a presence of strong solute-solvent interactions. It can be seen that the ϕ_V^0 values of D-maltose monohydrate is higher than that of D-Sucrose which in turn higher than that of D-Glucose. This result in terms of solute-solvent interaction is enhanced by the following order: D-maltose monohydrate > D-Sucrose > D-Glucose.

The low solute-solvent interaction in D-Glucose may be due to the less —OH groups present in it as compared to D-Sucrose and D-Maltose Monohydrate. A comparison of solute-solvent interaction of D-Sucrose and D-Maltose Monohydrate in Ascorbic Acid solution shows slightly high interaction in D-Maltose Monohydrate which is probably due to the presence of water of crystallisation in it. The trend in the solute-solvent interaction is given below in the scheme I.

S_V^* values indicate the degree of solute-solute interaction in the solution. It can be seen from Table 4 that the S_V^* values are negative indicating very negligible amount of solute-solute interaction. The table shows that the solute-solute interaction is highest in case of D-Glucose and lowest in case of D-Maltose Monohydrate as shown in Scheme II. The magnitude of ϕ_V^0 values is much greater than those of S_V^* for all the studied carbohydrates as well as for the increasing concentration of ascorbic acid solution suggesting the fact that the solute-solvent interaction dominates over solute-solute interactions. The variation of solute-solute interaction of the various carbohydrates is due to the bulkiness of the molecules as mentioned in the scheme II.

6.3.2. Viscosity calculation

The viscosity data has been analysed using Jones-Dole equation [11]

$$(\eta / \eta_0 - 1) / \ m^{1/2} = A + Bm^{1/2} \qquad (4)$$

where η_0 and η are the viscosities of the solvent and the solution respectively. The viscosity A and B-coefficients are estimated by a least-squares method and are reported in Table 4. The values of the viscosity A-coefficient are found to be highest in case of glucose and it decreases with the concentration of the of ascorbic acid solution. The results obtained also indicate the presence of very weak solute-solute interactions. These results are in excellent agreement with those obtained from S_V^* values discuss earlier.

The effects of solute-solvent interactions on the solution viscosity can be inferred from the viscosity B-coefficient [12,13]. The viscosity B-coefficient is a valuable tool to provide information concerning the solvation of the solutes and their effects on the structure of the solvent. From Table 4 and Figure 2 it is evident

that the values of the *B*-coefficient are positive, thereby suggesting the presence of strong solute-solvent interactions, the greatest being in case of D-maltose monohydrate solution and it increases with the increase in the concentration of the ascorbic acid solution. The result is in excellent agreement the results obtained from ϕ_V^0 showing greater solute-solvent interaction in D-Maltose-ascorbic acid solution.

6.3.3. Refractive index calculation

The molar refraction, R can be evaluated from the Lorentz-Lorenz relation[14]

$$R = \left\{(n_D^2-1)/(n_D^2+2)\right\}(M/\rho) \quad (5)$$

where R, n_D, M and ρ are the molar refraction, the refractive index, the molar mass and the density of solution respectively. The refractive index of a substance is defined as the ratio c_0/c, where c is the speed of light in the medium and c_0 the speed of light in vacuum. Stated more simply, the refractive index of a compound describes its ability to refract light as it moves from one medium to another and thus, the higher the refractive index of a compound, the more the light is refracted [15]. As stated by Deetlefs et. al[16] the refractive index of a substance is higher when its molecules are more tightly packed or in general when the compound is denser and with the increase of mass fraction of ascorbic acid in solvent mixture refractive index value also increases. Hence a perusal of Table 2 & Table 3 we found that the refractive index and the molar refraction values respectively are higher for D-Maltose Monohydrate than D-Sucrose and D-Glucose, indicating the fact that the molecules are more tightly packed in the mixture. The interaction in the solution is basically solute-solvent interaction and a small amount of solute-solute interaction. This is also good agreement with the results obtained from density and viscosity parameters discussed above. The trend in the package of the studied carbohydrates in aqueous mixture of ascorbic acid is given below:

D-Glucose < D-Sucrose < D-Maltose Monohydrate

6.4 Conclusion

The values of the limiting apparent molar volume (ϕ_V^0) and viscosity *B*-coefficients indicate the presence of strong solute-solvent interactions. The interaction is highest in case of D-Maltose monohydrate solution and it increases

with the increase in the ascorbic acid solution. The refractive index and the molar refraction values suggest that D-Maltose Monohydrate and D-Sucrose molecules are more tightly packed in the solution leading to higher solute-solvent interaction than D-Glucose. The thorough study of carbohydrates in ascorbic acid solution indicates that the solute-solvent interaction dominants over the solute-solute interaction.

Tables:

Table 1. The values of Density (ρ), Viscosity (η) and Refractive index (n_D), in different mass fraction of Ascorbic acid in water at 298.15K

Mass-fraction Ascorbic acid	ρ x 10^{-3} (kg m^{-3})	η (mPa s)	n_D
w_1 = 0.01	0.99785	0.823	1.3323
w_1 = 0.03	0.99936	0.835	1.3330
w_1 = 0.05	1.00074	0.847	1.3338

Table 2. Experimental values of Densities (ρ), Viscosities (η) and Refractive Index (n_D) of D-Glucose, D-Sucrose and D-Maltose Monohydrate in different mass fraction of Ascorbic acid in water at 298.15K

molality (mol kg^{-1})	ρ x 10^{-3} (kg m^{-3})	η (mPas)	n_D	molality (mol kg^{-1})	ρ x 10^{-3} (kg m^{-3})	η (mPas)	n_D
w_1 = 0.01				w_1 = 0.03			
D-Glucose				D-Glucose			
0.1002	0.99849	0.838	1.3325	0.1001	0.99986	0.855	1.3335
0.1585	0.99948	0.850	1.3332	0.1584	1.00066	0.874	1.3344
0.2007	1.00050	0.859	1.3338	0.2006	1.00149	0.893	1.3351
0.2355	1.00154	0.868	1.3344	0.2354	1.00234	0.911	1.3358
0.2659	1.00260	0.876	1.3350	0.2658	1.00321	0.928	1.3364
0.2933	1.00368	0.884	1.3355	0.2932	1.00410	0.943	1.3370
D-Sucrose				D-Sucrose			
0.1002	0.99902	0.847	1.3328	0.1002	1.00029	0.862	1.3334
0.1587	1.00084	0.872	1.3341	0.1587	1.00181	0.895	1.3348
0.2011	1.00272	0.897	1.3352	0.2010	1.00343	0.926	1.3361
0.2362	1.00465	0.920	1.3363	0.2361	1.00512	0.957	1.3373
0.2669	1.00660	0.944	1.3373	0.2669	1.00689	0.989	1.3384

0.2946	1.00859	0.967	1.3383	0.2946	1.00872	1.019	1.3395
D-Maltose Monohydrate				D-Maltose Monohydrate			
0.1002	0.99902	0.847	1.3328	0.1002	1.00029	0.863	1.3334
0.1588	1.00085	0.874	1.3342	0.1587	1.00182	0.896	1.3350
0.2012	1.00275	0.899	1.3354	0.2011	1.00345	0.929	1.3363
0.2363	1.00469	0.923	1.3366	0.2363	1.00516	0.960	1.3376
0.2671	1.00669	0.948	1.3377	0.2670	1.00694	0.991	1.3388
0.2948	1.00870	0.971	1.3388	0.2948	1.00879	1.022	1.3400
$w_1 = 0.05$							
D-Glucose							
0.1000	1.00110	0.867	1.3346				
0.1583	1.00168	0.889	1.3355				
0.2005	1.00230	0.909	1.3363				
0.2353	1.00294	0.928	1.3370				
0.2658	1.00360	0.947	1.3376				
0.2932	1.00428	0.966	1.3382				
D-Sucrose							
0.1001	1.00149	0.874	1.3341				
0.1586	1.00277	0.909	1.3358				
0.2010	1.00415	0.942	1.3372				
0.2361	1.00565	0.974	1.3385				
0.2668	1.00719	1.007	1.3397				
0.2945	1.00886	1.038	1.3409				
D-Maltose Monohydrate							
0.1001	1.00149	0.875	1.3341				
0.1586	1.00278	0.910	1.3359				
0.2010	1.00417	0.944	1.3374				
0.2362	1.00568	0.976	1.3389				
0.2670	1.00723	1.011	1.3402				
0.2948	1.00890	1.042	1.3415				

Table 3. Molality, apparent molar volume (ϕ_V), $(\eta/\eta_0-1)/m^{1/2}$ and molar refraction (R), of D-Glucose, D-Sucrose and D-Maltose Monohydrate in different mass fraction of Ascorbic acid in water at 298.15K

Molality (mol kg^{-1})	ϕ_V x 10^6 (m^3 mol^{-1})	$(\eta/\eta_0-1)/m^{1/2}$ (kg$^{1/2}$ mol$^{-1/2}$)	R (cm^3 mol^{-1})
	w_1 = 0.01		
	D-Glucose		
0.1002	116.4103	0.185	37.0635
0.1585	115.2077	0.206	37.0976
0.2007	114.1554	0.220	37.1203
0.2355	113.3127	0.232	37.1422
0.2659	112.5448	0.243	37.1634
0.2933	111.8122	0.255	37.1736
	D-Sucrose		
0.1002	225.7854	0.287	70.4402
0.1587	223.1798	0.374	70.5613
0.2011	221.0252	0.447	70.6393
0.2362	219.1348	0.499	70.7134
0.2669	217.7682	0.551	70.7666
0.2946	216.4123	0.593	70.8166
	D-Maltose Monohydrate		
0.1002	243.8443	0.295	74.1485
0.1588	240.8378	0.389	74.2954
0.2012	238.3324	0.459	74.3961
0.2363	236.4648	0.512	74.4932
0.2671	234.5385	0.567	74.5654
0.2948	233.1743	0.612	74.6363
	w_1 = 0.03		
	D-Glucose		
0.1001	129.2440	0.238	37.1138
0.1584	127.8431	0.297	37.1749
0.2006	126.7424	0.346	37.2146
0.2354	125.8782	0.384	37.2535
0.2658	125.0985	0.416	37.2815
0.2932	124.3585	0.440	37.3086
	D-Sucrose		

0.1002	248.4615	0.326	70.4554
0.1587	244.0586	0.450	70.4659
0.2010	240.4563	0.542	70.6270
0.2361	237.5453	0.618	70.7612
0.2669	234.7383	0.690	70.8708
0.2946	232.2156	0.747	70.9552
	D-Maltose Monohydrate		
0.1002	266.4932	0.329	74.1755
0.1587	261.6901	0.462	74.3846
0.2011	257.9877	0.558	74.5250
0.2363	254.8493	0.633	74.6588
0.2670	252.0553	0.698	74.7668
0.2948	249.4233	0.760	74.8690
	$w_1 = 0.05$		
	D-Glucose		
0.1000	144.0534	0.233	37.1787
0.1583	142.4546	0.308	37.2478
0.2005	141.0556	0.361	37.3053
0.2353	140.0564	0.404	37.3518
0.2658	139.1998	0.443	37.3874
0.2932	138.4105	0.477	37.4223
	D-Sucrose		
0.1001	267.1023	0.319	70.5155
0.1586	260.9069	0.456	70.7505
0.2010	256.8599	0.557	70.9202
0.2361	252.8402	0.633	71.0617
0.2668	249.9722	0.708	71.1808
0.2945	246.5881	0.765	71.2901
	D-Maltose Monohydrate		
0.1001	285.1090	0.324	74.2277
0.1586	278.5139	0.463	74.4944
0.2010	274.3670	0.567	74.6923
0.2362	270.3018	0.645	74.8805
0.2670	267.4078	0.721	75.0249
0.2948	264.1245	0.779	75.1596

Table 4. Limiting apparent molar volumes (ϕ_V^0), experimental slopes (S_V^*) and *A*, *B* coefficients of D-Glucose, D-Sucrose and D-Maltose Monohydrate in different mass fraction of Ascorbic acid in water at 298.15

Solute	ϕ_V^0 x 10^6 (m^3 mol^{-1})	S_V^* x 10^6 (m^3 $mol^{-3/2}$ $kg^{1/2}$)	*A* (kg mol^{-1})	*B* ($kg^{1/2}$ $mol^{-1/2}$)
		$w_1 = 0.01$		
D-Glucose	118.9	-23.91	0.149	0.356
D-Sucrose	230.7	-48.73	0.127	1.582
D-Maltose Monohydrate	249.5	-55.50	0.130	1.627
		$w_1 = 0.03$		
D-Glucose	131.8	-25.29	0.130	1.068
D-Sucrose	257.1	-83.74	0.105	2.177
D-Maltose Monohydrate	275.4	-87.73	0.110	2.208
		$w_1 = 0.05$		
D-Glucose	147	-29.47	0.107	1.260
D-Sucrose	277.6	-104.4	0.090	2.303
D-Maltose Monohydrate	295.6	-106.7	0.091	2.346

Figures:

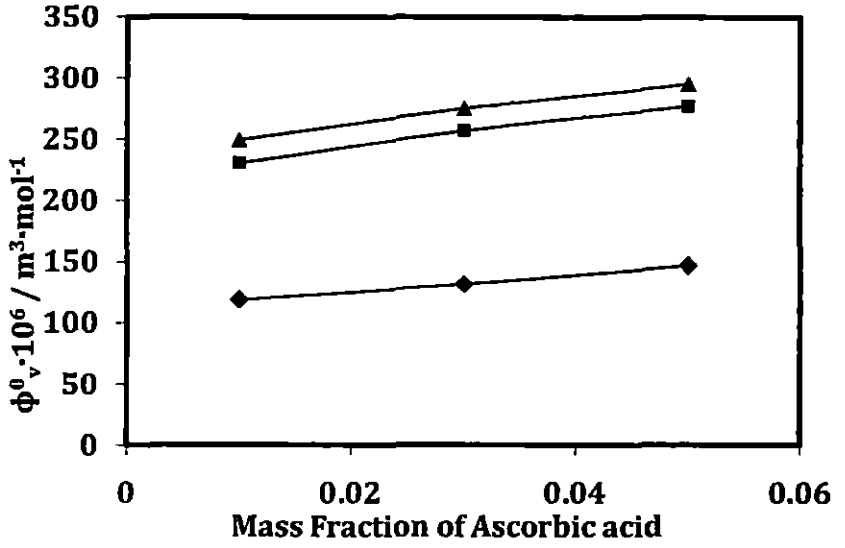

Figure 1. The plots of limiting apparent molar volumes (ϕ_V^0) for D-Glucose (—♦—), D-Sucrose (—■—), D-Maltose Monohydrate (—▲—) in different mass fractions (w_1) of ascorbic acid in aqueous mixture at 298.15K

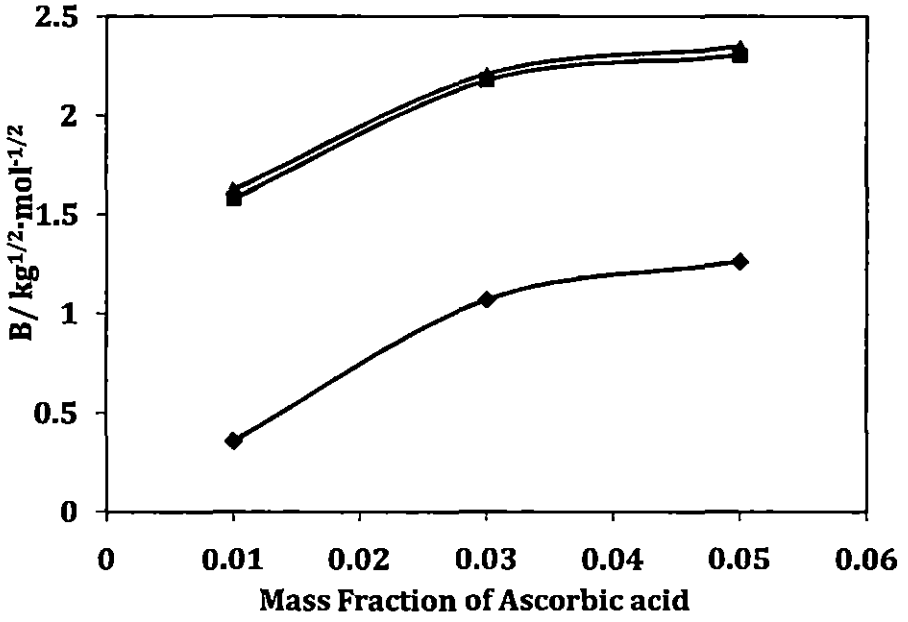

Figure 2. The plots of viscosity *B*-coefficient for D-Glucose (—♦—), D-Sucrose (—■—), D-Maltose Monohydrate (—▲—) in different mass fractions (w_1) of ascorbic acid in aqueous mixture at 298.15K.

Schemes:

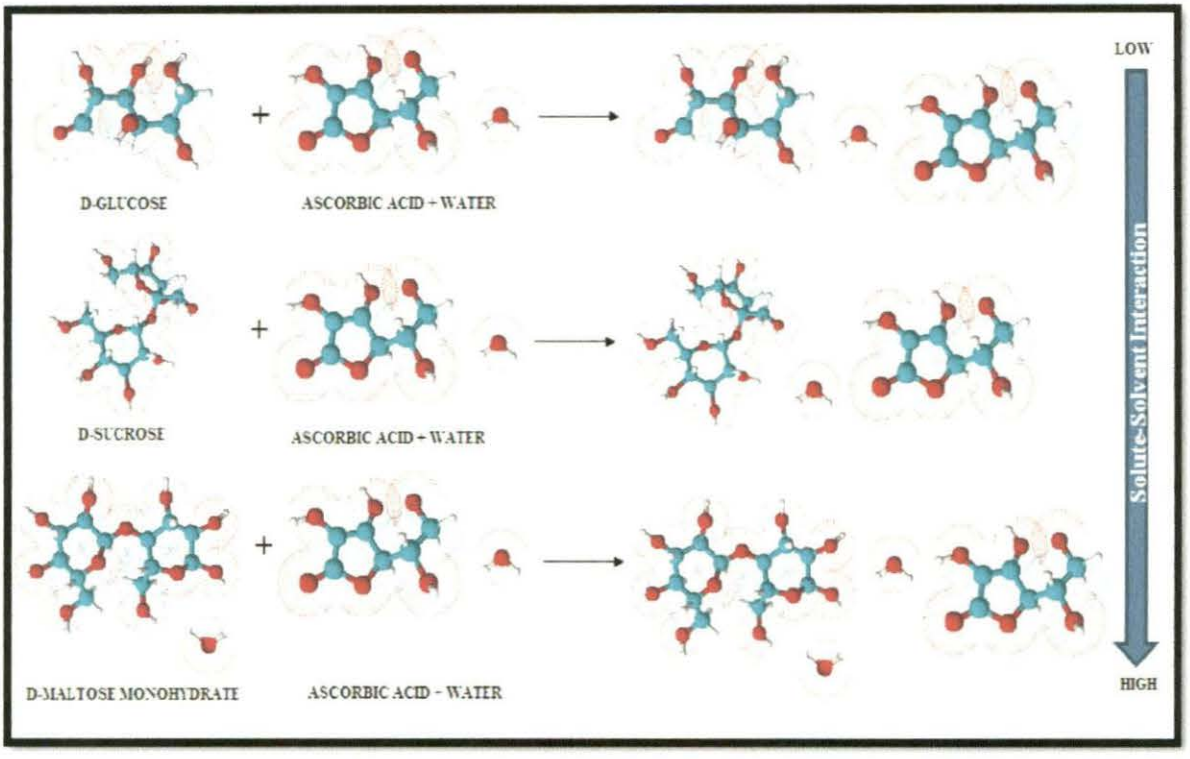

Scheme I

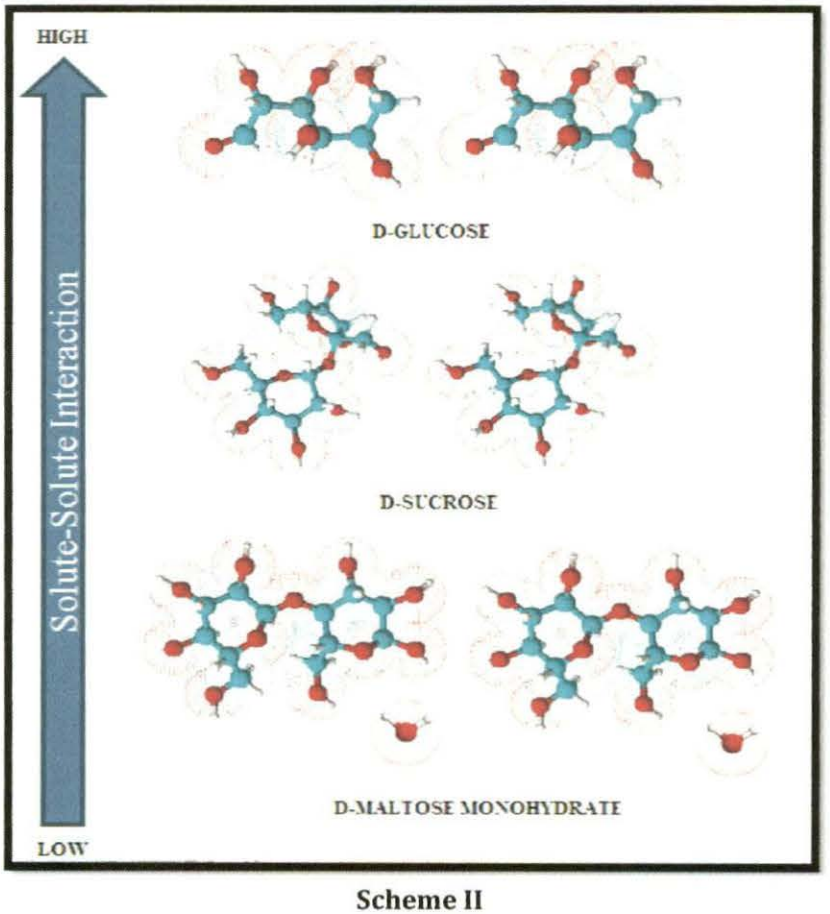

Scheme II

CHAPTER VII

INVESTIGATION ON MOLECULAR INTERACTIONS OF NICOTINAMIDE IN AQUEOUS CITRIC ACID SOLUTIONS WITH REFERENCE TO MANIFESTATION OF PARTIAL MOLAR VOLUME AND VISCOSITY *B*-COEFFICIENT MEASUREMENTS

7.1 Introduction:

Enzymes are the functional unit of cell metabolism as they catalyze different reactions to degrade nutrient molecules into simple ones. Many enzymes require a non-protein cofactor for their catalytic activities. Vitamins are essential precursors for various coenzymes. These coenzymes are therefore required in almost all metabolic pathways [1]. NA, commonly known as vitamin B3 [2], is a water-soluble vitamin, an essential micronutrient and a reactive moiety of the coenzyme nicotinamide adenine dinucleotide (NAD).

It is sometimes referred to as nothing more than vitamin PP (Pellagra Preventive) [3,4], since its deficiency in human diet causes pellagra. It is an essential part of the coenzyme – nicotinamide adenine dinucleotide phosphate (NADP), its reduced form NADPH, NAD and its reduced form NADH. It also serves to maintain normal function of the digestive systems and cholesterol levels in human body [1].The combination of nicotinic acid and nicotinamide is clinically referred as niacin [3-5], since nicotinic acid is converted in the body into the amide very fast and for nutritional purposes both of them have equal biological activities. NA is an interesting molecule because of its two nitrogen atoms – one in the heterocyclic ring and the other as the amide group.

Polybasic acids play an important role in biological and industrial processes and accurate knowledge of their properties is therefore required. Citric acid, $C_6H_8O_7.H_2O$ i.e., 2-hydroxypropane-1,2,3-tricarboxylic acid, is a tribasic, environmentally acceptable, and versatile chemical. As it occurs in metabolism of almost all living things, its interactions in an aqueous solution is of great value to the biological scientists. In pharmaceutical industry, citric acid is used as a stabilizer in

various formulations, as a drug component and as a anticoagulant in blood for transfusions and also used as an acidifier in many pharmaceuticals. In industry, it is used in the manufacture of the alkyl resins, as a sequestering agent to remove trace metals, in special inks, in electroplating, a chelate to form stable complexes with multivalent metal ions [6, 7]. It is used in personal care products [7, 8].

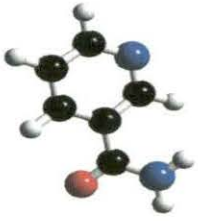

Nicotinamide

Citric acid

Water

Literature survey shows that there are few data on thermodynamic and transport properties for aqueous citric acid solutions. Marcia [9] reported the water activities and pH for aqueous solutions of citric acid at 298.15 K. The measurements were made from 5 to 50 mass % of citric acid. Apelblat [10, 11] and Parmer [12] studied partial molar volumes of citric acid in water at 298.15 and 298.15, 303.15, 308.15, 308.15, and 313.15 K respectively. Sijpkes [13] measured heat capacities and partial molar heat capacities at infinite dilution of citric acid in water at 298.15 K. Levien [14] carried the studies of apparent osmotic coefficients and molar conductivities. Although there have been extensive studies on various properties of NA [1,5,15-19], to the best of our knowledge, the properties of this ternary solution have not been reported earlier. As apparent molar volumes and viscosity *B*-coefficients of a solute gives cumulative effects [19,20] of solute-solute, solute-solvent and solvent-solvent interactions in solutions, in this paper we attempted to study these properties for NA in aqueous solutions of CA at 298.15, 308.15 and 318.15 K to explain the various interactions prevailing in the ternary systems under investigation.

7.2 Experimental Section:

7.2.1 Materials

NA was purchased from ACROS Organics Company and used as such. Its mass purity as supplied is 98%. Citric acid, monohydrate (Himedia) was used after drying over P_2O_5 in a desiccator for more than 48 h. The reagents were always placed in the

desiccator over P_2O_5 to keep them in dry atmosphere. Freshly distilled conductivity water (sp. cond. ≈ 10^{-6} ohm^{-1} cm^{-1}) was used as standard solvent and for making binary aqueous mixtures of CA. The physical properties of different aqueous CA solutions are listed in Table 1.

7.2.2 Apparatus and Procedure

Stock solutions of NA in different aqueous CA solutions were prepared by mass and the working solutions were prepared by mass dilution. The conversion of molality into molarity was accomplished using experimental density values. All solutions were prepared afresh before use. The uncertainty in molarity of the NA solutions is evaluated to ±0.0001 mol·dm^{-3}.

Density measurements of ternary mixtures were performed at atmospheric pressure at T = (298.15, 308.15, and 318.15) K by means of vibrating-tube densimeter (Anton Paar, DMA 4500) which was calibrated with distilled water and air. The uncertainty in the density measurement was ± 0.00002 g·cm^{-3}. The temperature was automatically kept constant within ±0.01 K. The mixtures were prepared by mass in 10 cm^3 bottles and precautions were taken to minimize evaporation losses. The apparatus was calibrated once a day with dry air and double-distilled freshly degassed water.

The viscosity was measured by means of a suspended Ubbelohde type viscometer thoroughly cleaned, dried and calibrated at T = (298.15, 308.15, and 318.15) K with triply distilled water and purified methanol. It was filled with experimental liquid and placed vertically in a glass sided thermostat maintained constant to ± 0.01 K. After attainment of thermal equilibrium, the efflux times of flow of liquids were recorded with a stopwatch correct to ± 0.1 s. Viscosity of the solution, η, is given by the following equation:

$$\eta = (Kt - L/t)\rho \quad (1)$$

where K and L are the viscometer constants and t and ρ are the efflux time of flow in seconds and the density of the experimental liquid, respectively. The uncertainty in viscosity measurements is within ±0.002 mPa·s. Details of the methods and techniques of density and viscosity measurements have been described elsewhere [21,22].

The nicotinamide solutions studied here were prepared by mass and the conversion of molality in molarity was accomplished [21,22] using experimental density values. The experimental values of concentrations c, densities ρ, viscosities η, and derived parameters at various temperatures are reported in Table 2.

7.3 Result and Discussion:

The densities, for the solutions of NA in aqueous CA measured at 298.15, 308.15, and 318.15K, have been used to calculate the apparent molar volumes (V_ϕ) of the solute using the following expression [21] and listed in Table 2

$$V_\phi = \frac{M_2}{\rho_0} - \frac{1000}{c}\left(\frac{\rho - \rho_0}{\rho_0}\right) \tag{2}$$

where c is the molar concentration of the solution; M_2 is the molecular weight of the solute; ρ and ρ_0 is the densities of the solution and solvent, respectively. The plots of V_ϕ against square root of molar concentration $c^{1/2}$, were non-linear and V_ϕ values were fitted to the following equation [14]:

$$V_\phi = V_\phi^0 + A_V c^{1/2} + B_V c \tag{3}$$

where V_ϕ^0 is the partial molar volume at infinite dilution, A_v and B_v are two adjustable parameters. The V_ϕ^0 values were calculated applying a least squares technique to the plots of V_ϕ vs. $c^{1/2}$ using equation (3). The values of V_ϕ^0, A_V and B_V at each temperature are listed in Table 3. The estimated uncertainties in V_ϕ^0 values are represented by standard deviation σ, which is equal to the root mean square of the deviations between the experimental and calculated V_ϕ for each data point. V_ϕ^0 values for the aqueous NA solutions at 298.15, 308.15 and 318.15 K were in good agreement with the V_ϕ^0 values reported earlier [23] . Table 3 shows that V_ϕ^0 values are generally positive and increase with a rise in both the temperature and molarity of CA in the solutions. This indicates the presence of strong solute–solvent interactions and these interactions are further strengthened at higher temperatures and higher concentration of CA in the solutions. The crystal structure of NA was reported by Wright and King [24]. In the crystal, NA is linked by two weak hydrogen bonds from the hydrogen atoms of amide N-atom to the O-atom of one neighbouring

molecule and to the ring N-atom of another molecules in such a fashion that a two-dimensional network parallel to (010) plane is formed with a inter-planer distance of 0.3579 nm at T = 295.15 K. Charman et al.[25] reported the structure of NA in aqueous solution. They studied the concentration-dependent self-association of NA in solution by ^{1}H and ^{13}C NMR spectroscopy and osmometric measurements. Their results revealed that NA associates in aqueous solution with the amide groups of each NA molecule creating large associated species at higher concentrations. This fact justifies the observed changes in the values of parameters A_v and B_v.

This can also be explained in view of molar volume of the solute and that of the solvent mixtures. Solute-solvent interactions depend on the fitness of solute molecules into the solvent molecules. Greater the difference of molar volumes between solute and solvent molecules, higher is the fitness of solute molecules into solvent molecules. In this paper, partial molar volume of NA, the values of which along with the values of (CA+water) are provided in Table 4, increases gradually with increasing temperature and higher molarity of (CA+water) mixtures. Hence, NA fits into (CA+water) mixture in the same order, resulting in more solute-solvent interactions i.e., they are more closely packed, with increasing temperature as well as concentration of (CA+water) mixtures. This is in excellent agreement with the conclusion drawn from the values of V_ϕ^0 as well as viscosity *B*-coefficient. Schematic representations of the relevant molecules, in connection with solute-solvent interactions, are shown below:

0.03(M):

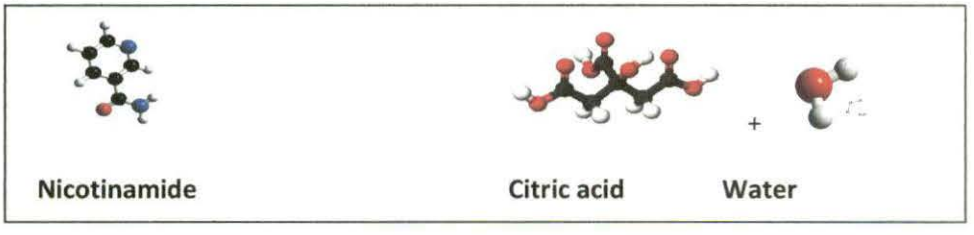

0.05(M):

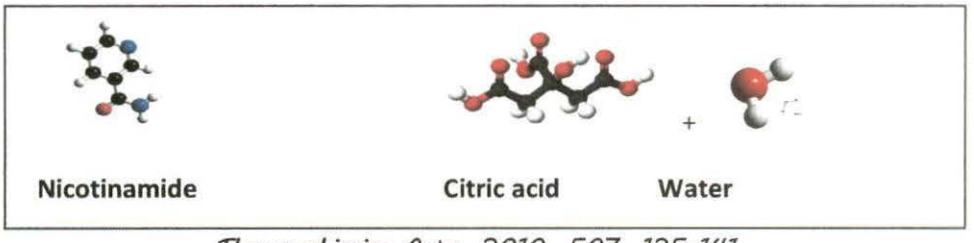

0.07(M):

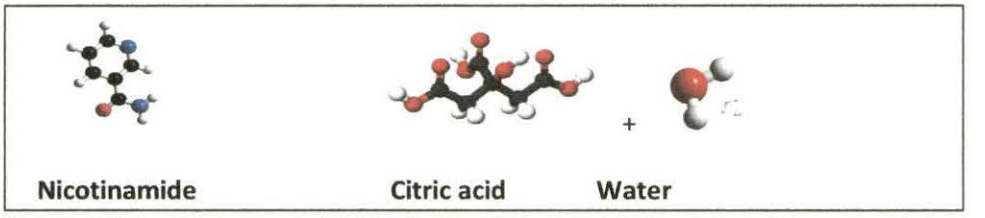

0.1(M):

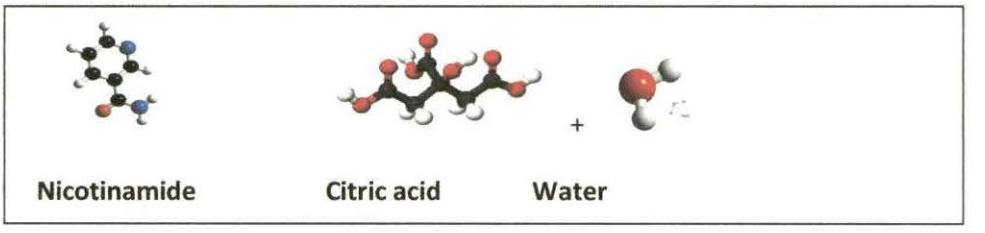

The partial molar volumes V_ϕ^0 were fitted to a polynomial of the following type in terms of absolute temperature T:

$$V_\phi^0 = a_0 + a_1 + a_2 T^2 \tag{4}$$

Values of the coefficients a_0, a_1, a_2 of the above equation for different NA solutions are reported in Table 5.

The partial molar expansibilities ϕ_E^0 can be obtained by the following equation [26]:

$$\phi_E^0 = \left(\frac{\delta V_\phi^0}{\delta T}\right)_P = a_1 + a_2 T \tag{5}$$

The values of ϕ_E^0 for different ternary solutions at T = (298.15, 308.15, and 318.15) K are given in Table 5 and it shows that ϕ_E^0 value increases as the temperature increases.

According to Hepler [27], the sign of $\left(\frac{\delta \phi_E^0}{\delta T}\right)_P$ or $\left(\frac{\delta^2 V_\phi^0}{\delta T^2}\right)_P$ is a better criterion in characterizing the long-range structure making and breaking ability of the solutes in solution. The general thermodynamic expression is as follows:

$$\left(\frac{\delta \phi_E^0}{\delta T}\right)_P = \left(\frac{\delta^2 \phi_V^0}{\delta T^2}\right)_P = 2a_2 \tag{6}$$

If the sign of $\left(\frac{\delta\phi_E^0}{\delta T}\right)_P$ is positive, the solute is a structure maker, otherwise it is a structure breaker. It is seen from Table 6, NA predominantly acts as a structure maker and its structure making ability increases with a rise in both the temperature and molarity of CA in the solutions. But its structure making ability decreases to some extent at higher concentration of resorcinol in the mixtures. This fact may be attributed to gradual disappearance of caging or packing effect [28,29] in the ternary solutions This observation is in line with the observation made by Kundu and Kishore [23]. They suggested that NA acts as a water-structure promoter due to hydrophobic hydration. The small negative values of $\left(\frac{\delta\phi_E^0}{\delta T}\right)_P$ at (0.10 and 0.15) mol·dm^{-3} aqueous CA solutions are probably due to higher structure promoting ability of CA than nicotinamide with comparatively higher V_ϕ^0 value in aqueous solution [7] originating from hydrophobic hydration with greater degree of hydrogen bonding than the bulk water [30].

Partial molar volumes ΔV_ϕ^0 of transfer from water to different aqueous CA solutions have been determined using the relations [31,32]:

$$\Delta V_\phi^0 = V_\phi^0 \text{ (aqueous CA solution)} - V_\phi^0 \text{ (water)} \quad (7)$$

The ΔV_ϕ^0 value is free from solute–solute interactions and therefore provides information regarding solute–cosolute interactions [31]. It can be seen from Table 8, the value of ΔV_ϕ^0 is positive at all the experimental temperatures and increases with the molarity of CA in the ternary solutions. The concentration dependence of the thermodynamic properties of the solutes in aqueous solutions can be explained in terms of overlap of hydration co-spheres. According to the co-sphere model, as developed by Friedman and Krishnan [33], the effect of overlap of the hydration co-spheres is destructive i.e., the overlap of hydration co-spheres of hydrophobic–hydrophobic groups results in a net volume decrease. However, in the present study the positive values of ΔV_ϕ^0 indicate that solute-solvent interactions are predominant and the overall effect of the overlap of the hydration co-spheres of NA and CA reduce the effect of electrostriction of water by NA molecules and this effect increases with the molarity of CA in the ternary mixtures as shown in Fig.1(a), Fig.1(b) and Fig.1(c)

(ΔV_ϕ^0 versus molarity of CA in solution). In addition, standard partial molar volumes of the solute have also been explained by a simple model [34,35]:

$$V_\phi^0 = V_{VW} + V_{Void} - V_S \quad (8)$$

where V_{VW} is the van der Waals volume, V_{Void} is the volume associated with voids or empty space, and V_S the shrinkage volume due to electrostriction. Assuming the V_{VW} and V_{Void} have the same magnitudes in water and in aqueous CA solutions for the same solute [36], the increase in V_ϕ^0 values and the positive ΔV_ϕ^0 values can be attributed to the decrease in the shrinkage volume of water by NA in presence of CA. This fact suggests that CA has a dehydration effect on the hydrated NA.

In the literature [23], pyridine has been stated as a structure-breaker in aqueous solution and the structure-promoting tendency of NA has been assigned to the $-CONH_2$ group. Thus the interactions between NA and CA in water can roughly be summarized as follows: (i) interaction of H-atom of –OH group of CA with the N-atom in the heterocyclic ring of NA, (ii) interaction of H-atom of –OH group of CA with the N-atom in the amide group of NA, (iii) interaction of H-atom of –OH group of CA with the O-atom in the amide group of NA. Therefore, the overall positive V_ϕ^0 values indicate that solute-solvent interactions predominate over solvent-solvent interactions and thus reduce the electrostriction of water molecules by NA imparting positive values of ΔV_ϕ^0.

The viscosity data of the aqueous and aqueous CA solutions of NA have been analyzed using the Jones–Dole [37] equation:

$$\frac{(\eta/\eta_0 - 1)}{\sqrt{c}} = \frac{(\eta_r - 1)}{\sqrt{c}} = A + B\sqrt{c} \quad (9)$$

where $\eta_r = \eta/\eta_0$, and η are the viscosities of solvent and solution respectively, c is the molar concentration of a solution . *A* and *B* are the Jones-Dole constants estimated by a least-squares method and reported in Table 7.

Table 7 shows that the values of the *A* coeffcient are generally negative. These results indicate the presence of weak solute–solute interactions, and these

interactions further decrease with an increase in both the temperature and molarity of CA in the mixtures.

The viscosity *B*-coefficient [38] reflects the effects of solute–solvent interactions on the solution viscosity.The viscosity *B*-coefficient is a valuable tool to provide information concerning the solvation of solutes and their effects on the structure of the solvent in the local vicinity of the solute molecules. Table 7 shows that the values of the viscosity *B*-coefficient for NA in the studied solvent systems are positive, thereby suggesting the presence of strong solute–solvent interaction and these types of interactions are strengthened with an increase in both the temperature and molarity of CA in the mixtures.

The ΔB values shown in Table 8 and depicted graphically in Fig.1(a), Fig.1(b) and Fig.1(c) (ΔB versus molarity of CA in solution) as a function of molarity of CA in solutions at the experimental temperatures support the results obtained from ΔV_ϕ^0 values discussed above.

The viscosity data have also been analyzed on the basis of transition state theory for relative viscosity of the solutions as suggested by Feakings et al.[39] using equation (11):

$$\Delta\mu_2^{0\neq} = \Delta\mu_1^{0\neq} + \frac{RT}{\bar{V}_1^0}(1000B + \bar{V}_2^0 - \bar{V}_1^0) \qquad (10)$$

where the $\bar{V}_1^0$ and the $\bar{V}_2^0$ are the partial molar volumes of the solvent and solute respectively. $\Delta\mu^o{}_2{}^{\neq}$ is the contribution per mole of the solute to the free energy of activation for the viscous flow of solutions have been determined from the above relation and $\Delta\mu^o{}_1{}^{\neq}$ is the free energy of activation per mole of solvent mixture is calculated by the following relation [39]:

$$\Delta\mu_1^{0\neq} = \Delta G_1^{0\neq} = RT\ln(\frac{\eta_0 \bar{V}_1^0}{hN_A}) \qquad (11)$$

where h is Planck's constant, N_A is Avogadro's number and $\Delta G^0{}_1{}^{\neq}$ is the free-energy of activation per-mole of solvent mixture. From Table 9, it is seen that $\Delta\mu^0{}_1{}^{\neq}$ is almost constant at all temperatures and solvent compositions. It implies that $\Delta\mu^0{}_2{}^{\neq}$ is dependent mainly on the values of viscosity *B*-coefficients and $(\bar{V}_2^0 - \bar{V}_1^0)$ terms. $\Delta\mu^0{}_2{}^{\neq}$ values were positive at all experimental temperatures and this and this suggests that the process of viscous flow becomes difficult as the temperature and molarity of CA

in solution increases. So the formation of the transition state becomes less favorable. According to Feakins et al. [39], $\Delta\mu^0{}_2{}^{\neq} > \Delta\mu^0{}_1{}^{\neq}$ for solutes having positive viscosity *B*-coefficients indicates stronger ion-solvent interactions, suggesting the formation of a transition state which is accompanied by the rupture and distortion of the intermolecular forces in the solvent structure [40]. The entropy of activation for electrolytic solutions has been calculated using the following relation [39]:

$$\Delta S_2^{0\neq} = -\frac{d(\Delta\mu_2^{0\neq})}{dT} \tag{12}$$

$\Delta S^o{}_2{}^{\neq}$ has been calculated from the slope of the plots of $\Delta\mu^o{}_2{}^{\neq}$ versus T by using a least -square treatment. The enthalpy of activation has been determined by using the following relation [39]:

$$\Delta H_2^{0\neq} = \Delta\mu_2^{0\neq} + T\Delta S_2^{0\neq} \tag{13}$$

The values of $\Delta S^o{}_2{}^{\neq}$ and $\Delta H^o{}_2{}^{\neq}$ are reported in Table 9. They are negative for all experimental solutions at all temperatures which suggest that the transition state is associated with bond formation and an increase in order.

7.4 Conclusion:

In summary, V_ϕ^0 and viscosity *B*-coefficient values for NA indicate the presence of strong solute–solvent interactions and these interactions are further strengthened at higher temperatures and higher concentration of CA in the ternary solutions. This study also reveals that NA acts as a water-structure promoter due to hydrophobic hydration in the presence of CA and CA has a dehydration effect on the hydrated NA.

Tables:

Table1: Density ρ and viscosity η, of different aqueous CA solution at different temperatures

Aqueous CA solution /(mol·dm^{-3})	T/K	$\rho \times 10^{-3}$/(kg·m^{-3})	η/(mPa·s)
0.03	298.15	0.9995	0.8766
	308.15	0.9963	0.7136
	318.15	0.9925	0.6253
0.05	298.15	1.0009	0.8921
	308.15	0.9977	0.7253
	318.15	0.9938	0.6261
0.07	298.15	1.0026	0.9048
	308.15	0.9993	0.7595
	318.15	0.9954	0.6527
0.10	298.15	1.0048	0.9254
	308.15	1.0018	0.7855
	318.15	0.9979	0.6766

Table 2: Molarity c, density ρ, viscosity η, apparent molar volumes V_ϕ^0, and $(\eta_r - 1)/c^{1/2}$ for NA in different aqueous CA solutions at different temperatures

c/(mol· dm^{-3})	$\rho \times 10^{-3}$/(kg·m^{-3})	η/(mPa·s)	$V_\phi^0 \times 10^6$/(m^3·mol^{-1})	$(\eta_r - 1)/c^{1/2}$
		0.03[a]		
		T=298.15 K		
0.01200	0.9998	0.8836	97.65	0.0723
0.02401	1.0001	0.8878	97.20	0.0822
0.04001	1.0005	0.8940	96.86	0.0988
0.05601	1.0009	0.8992	96.63	0.1085
0.07201	1.0013	0.9048	96.51	0.1198
0.08402	1.0016	0.9085	96.43	0.1255

		T=308.15 K		
0.01197	0.9966	0.7189	101.02	0.0678
0.02392	0.9968	0.7233	100.37	0.0879
0.03989	0.9972	0.7285	99.93	0.1041
0.05584	0.9976	0.7340	99.59	0.1211
0.07179	0.9980	0.7397	99.31	0.1363
0.08376	0.9983	0.7440	99.14	0.1469
		T=318.15 K		
0.01192	0.9927	0.6292	103.85	0.0571
0.02384	0.9929	0.6335	102.58	0.0858
0.03973	0.9933	0.6394	101.52	0.1132
0.05562	0.9937	0.6451	100.66	0.1343
0.07151	0.9941	0.6501	100.10	0.1487
0.08343	0.9944	0.6546	99.88	0.1624
		0.05[a]		
		298.15 K		
0.01202	1.0012	0.8974	98.69	0.0542
0.02405	1.0015	0.9016	98.05	0.0689
0.04008	1.0019	0.9075	97.56	0.0863
0.05611	1.0023	0.9144	97.31	0.1056
0.07214	1.0027	0.9198	97.16	0.1158
0.08417	1.0030	0.9234	97.07	0.1211
		308.15 K		
0.01199	0.9979	0.7287	102.94	0.0422
0.02397	0.9982	0.7320	102.00	0.0594
0.03996	0.9985	0.7373	101.05	0.0828
0.05594	0.9989	0.7423	100.33	0.0989
0.07192	0.9993	0.7482	99.78	0.1178
0.08390	0.9996	0.7518	99.50	0.1261
		318.15 K		
0.01194	0.9940	0.6274	106.83	0.0191
0.02388	0.9942	0.6308	105.28	0.0494

0.03980	0.9945	0.6358	104.23	0.0778
0.05572	0.9949	0.6410	103.55	0.1009
0.07164	0.9952	0.6462	103.13	0.1204
0.08357	0.9955	0.6493	102.87	0.1283
		0.07[a]		
		T=298.15 K		
0.01201	1.0028	0.9055	101.54	0.0072
0.02402	1.0031	0.9082	100.77	0.0244
0.04003	1.0034	0.9132	100.21	0.0467
0.05604	1.0038	0.9187	99.75	0.0649
0.07206	1.0042	0.9255	99.45	0.0853
0.08407	1.0045	0.9298	99.31	0.0954
		T=308.15 K		
0.01197	0.9995	0.7605	105.52	0.0116
0.02394	0.9998	0.7639	104.23	0.0372
0.03991	1.0001	0.7695	103.38	0.0657
0.05587	1.0004	0.7763	102.87	0.0933
0.07183	1.0007	0.7828	102.45	0.1144
0.08380	1.0010	0.7883	102.19	0.1309
		T=318.15 K		
0.01193	0.9956	0.6532	109.91	0.0076
0.02385	0.9958	0.6570	108.52	0.0429
0.03975	0.9960	0.6634	107.31	0.0823
0.05565	0.9963	0.6698	106.77	0.1115
0.07154	0.9966	0.6778	106.30	0.1440
0.08347	0.9968	0.6845	106.09	0.1688
		0.10[a]		
		T=298.15 K		
0.01215	1.0051	0.9258	102.67	0.0043
0.02430	1.0053	0.9292	101.92	0.0262
0.04049	1.0057	0.9357	101.30	0.0556
0.05669	1.0060	0.9423	100.81	0.0766

0.07289	1.0064	0.9502	100.55	0.0992
0.08504	1.0066	0.9563	100.39	0.1146
		T=308.15 K		
0.01211	1.0020	0.7863	108.47	0.0087
0.02422	1.0022	0.7903	107.38	0.0392
0.04037	1.0025	0.7972	106.28	0.0744
0.05651	1.0027	0.8049	105.54	0.1036
0.07265	1.0031	0.8133	105.08	0.1312
0.08477	1.0033	0.8198	104.84	0.1498
		T=318.15 K		
0.01206	0.9980	0.6771	113.84	0.0061
0.02413	0.9981	0.6824	112.56	0.0547
0.04021	0.9983	0.6898	111.57	0.0972
0.05629	0.9985	0.6981	110.98	0.1337
0.07237	0.9987	0.7059	110.44	0.1609
0.08443	0.9989	0.7119	110.18	0.1793

[a] Molarity of CA in water in mol·dm^{-3}

Table 3. Limiting Partial molar volume V_ϕ^0, and adjustable parameters A_v and B_v for NA in different aqueous CA acid solutions with standard deviations σ at different temperatures

T/K	$V_\phi^0 \times 10^6$ ($m^3 \cdot mol^{-1}$)	A_v /($m^3 \cdot mol^{-1.5}$)	B_v /($m^3 \cdot mol^{-2}$)	σ (%)
		0.03[a]		
298.15	99.11	-15.92	-23.05	0.004
308.15	102.74	-18.04	-19.54	0.007
318.15	107.78	-40.87	-46.23	0.016
		0.05[a]		
298.15	100.85	-23.88	-37.50	0.006
308.15	105.74	-27.62	-20.52	0.013
318.15	111.64	-52.84	-78.23	0.015
		0.07[a]		
298.15	103.80	-23.81	-28.52	0.008
308.15	109.28	-40.99	-57.59	0.012
318.15	114.65	-51.72	-76.65	0.014
		0.10[a]		
298.15	105.04	-24.79	-30.19	0.009
308.15	112.17	-38.18	-44.21	0.014
318.15	117.64	-40.23	-50.50	0.013

[a] Molarity of CA in water in $mol \cdot dm^{-3}$

Table 4. Partial molar volume of NA and (CA + Water) mixtures at different temperatures

T/K	Partial molar volume of NA × 10^6/(m^3·mol^{-1})	Partial molar volume of (CA + Water) × 10^6/(m^3·mol^{-1})
	0.03[a]	
298.15	99.11	18.13
308.15	102.74	18.19
318.15	107.78	18.26
	0.05[a]	
298.15	100.85	18.17
308.15	105.74	18.23
318.15	111.64	18.30
	0.07[a]	
298.15	103.80	18.21
308.15	109.28	18.27
318.15	114.65	18.34
	0.10[a]	
298.15	105.04	18.27
308.15	112.17	18.33
318.15	117.64	18.40

[a] Molarity of CA in water in mol·dm^{-3}

Table 5. Values of various coefficients of Eq. 4 for NA in different aqueous CA solutions.

Aqueous CA solution/(mol·dm^{-3})	a_0/(m^3·mol^{-1})	a_1/(m^3·mol^{-1}·K^{-1})	a_2/(m^3·mol^{-1}·K^{-2})
0.03	638.60	-3.911	0.007
0.05	419.02	-2.573	0.005
0.07	-110.12	0.882	-0.001
0.10	-870.10	5.747	-0.008

Table 6. Partial molar expansibility ϕ_E^0 for NA in different aqueous CA solutions at different temperatures

Aqueous CA solution/(mol·dm^{-3})	$\phi_E^0 \times 10^6$ /(m^3·mol^{-1}·K^{-1})			$\left(\frac{\delta\phi_E^0}{\delta T}\right)_P \times 10^6$ /(m^3·mol^{-1}·K^{-2})
	298.15K	308.15K	318.15K	
0.03	0.322	0.464	0.606	0.014
0.05	0.409	0.509	0.609	0.010
0.07	0.583	0.573	0.563	-0.001
0.10	0.798	0.632	0.466	-0.016

Table 7. Values of *A* and *B* coefficients with standard errors for NA in different aqueous CA solutions at different temperatures.

Aqueous CA solution /(mol·dm^{-3})	$A \times 10^{-3}$/(m$^{3/2}$·mol$^{-1/2}$)			$B \times 10^6$/(m^3·mol^{-1})		
	298.15 K	308.15 K	318.15 K	298.15 K	308.15 K	318.15 K
0.03	0.0375 (±0.002)	0.0196 (±0.002)	-0.0046 (±0.002)	0.3036 (±0.009)	0.4347 (±0.010)	0.5814 (±0.012)
0.05	0.0105 (±0.003)	-0.0121 (±0.003)	-0.0466 (±0.004)	0.3877 (±0.015)	0.4768 (±0.013)	0.6172 (±0.016)
0.07	-0.0507 (±0.004)	-0.0643 (±0.003)	-0.0927 (±0.006)	0.4986 (±0.019)	0.6669 (±0.017)	0.8870 (±0.027)
0.10	-0.0664 (±0.004)	-0.0807 (±0.004)	-0.0960 (±0.004)	0.6116 (±0.019)	0.7833 (±0.018)	0.9567 (±0.018)

Table 8. Partial molar volumes V_ϕ^0, Partial molar volumes of transfer, ΔV_ϕ^0, viscosity *B*-coefficients, and Viscosity *B*-coefficients of transfer, ΔB, from water to different aqueous CA solutions for NA at three different temperatures.

Aqueous CA solutions /(mol·dm^{-3})	$V_\phi^0 \times 10^6$ /(m^3·mol^{-1})	$\Delta V_\phi^0 \times 10^6$ /(m^3·mol^{-1})	$B \times 10^6$ /(m^3·mol^{-1})	$\Delta B \times 10^6$ /(m^3·mol^{-1})
		T= 298.15 K		
0.03	96.87[41]	0	0.221[41]	0
0.05	99.11	2.24	0.334	0.113
0.07	100.85	3.98	0.388	0.187
0.10	103.80	6.93	0.499	0.298
		T= 308.15 K		
0.03	97.71[41]	0	0.424[41]	0
0.05	102.74	5.03	0.435	0.011
0.07	105.74	8.03	0.477	0.053
0.10	109.28	11.57	0.667	0.243
		T= 318.15 K		
0.03	100.86[41]	0	0.538[41]	0
0.05	107.78	6.92	0.581	0.043
0.07	111.64	10.78	0.617	0.079
0.10	114.65	13.79	0.887	0.349

Table 9. Values of $\overline{V}_1^0$, $\Delta\mu_1^{0\neq}$, $\overline{V}_2^0$ - $\overline{V}_1^0$, $\Delta\mu_2^{0\neq}$, $T\Delta S_2^{0\neq}$, and $\Delta H_2^{0\neq}$ for NA in different aqueous CA solutions at different temperatures

Parameters	298.15 K	308.15 K	318.15 K
	0.03 mol·dm^{-3}		
$\overline{V}_1^0 \times 10^6$/(m^3·mol^{-1})	18.08	18.14	18.21
$\Delta\mu_1^{0\neq}$ / (kJ·mol^{-1})	9.13	8.62	8.31
$(\overline{V}_2^0 - \overline{V}_1^0) \times 10^6$/(m^3·mol^{-1})	81.03	84.60	89.57
$\Delta\mu_2^{0\neq}$ / (kJ·mol^{-1})	45.90	61.49	84.55

$T\Delta S_2^{0\neq}$ / (kJ·mol^{-1})	-576.09	-595.41	-614.73
$\Delta H_2^{0\neq}$ / (kJ·mol^{-1})	-530.18	-533.92	-530.18
0.05 mol·dm^{-3}			
$\overline{V}_1^0 \times 10^6$/(m^3·mol^{-1})	18.09	18.15	18.22
$\Delta\mu_1^{0\neq}$ / (kJ·mol^{-1})	9.17	8.67	8.31
$(\overline{V}_2^0 - \overline{V}_1^0) \times 10^6$/(m^3·mol^{-1})	82.76	87.59	93.42
$\Delta\mu_2^{0\neq}$ / (kJ·mol^{-1})	53.21	67.39	89.69
$T\Delta S_2^{0\neq}$ / (kJ·mol^{-1})	-543.80	-562.03	-580.27
$\Delta H_2^{0\neq}$ / (kJ·mol^{-1})	-490.59	-494.65	-490.59
0.07 mol·dm^{-3}			
$\overline{V}_1^0 \times 10^6$/(m^3·mol^{-1})	18.10	18.16	18.23
$\Delta\mu_1^{0\neq}$ / (kJ·mol^{-1})	9.21	8.78	8.42
$(\overline{V}_2^0 - \overline{V}_1^0) \times 10^6$/(m^3·mol^{-1})	85.70	91.12	96.42
$\Delta\mu_2^{0\neq}$ / (kJ·mol^{-1})	68.37	94.18	128.79
$T\Delta S_2^{0\neq}$ / (kJ·mol^{-1})	-900.65	-930.86	-961.07
$\Delta H_2^{0\neq}$ / (kJ·mol^{-1})	-832.28	-836.68	-832.28
0.10 mol·dm^{-3}			
$\overline{V}_1^0 \times 10^6$/(m^3·mol^{-1})	18.12	18.17	18.24
$\Delta\mu_1^{0\neq}$ / (kJ·mol^{-1})	9.27	8.87	8.51
$(\overline{V}_2^0 - \overline{V}_1^0) \times 10^6$/(m^3·mol^{-1})	86.92	94.00	99.40
$\Delta\mu_2^{0\neq}$ / (kJ·mol^{-1})	83.78	110.54	138.82
$T\Delta S_2^{0\neq}$ / (kJ·mol^{-1})	-820.42	-847.94	-875.45
$\Delta H_2^{0\neq}$ / (kJ·mol^{-1})	-736.64	-737.40	-736.64

Figures:

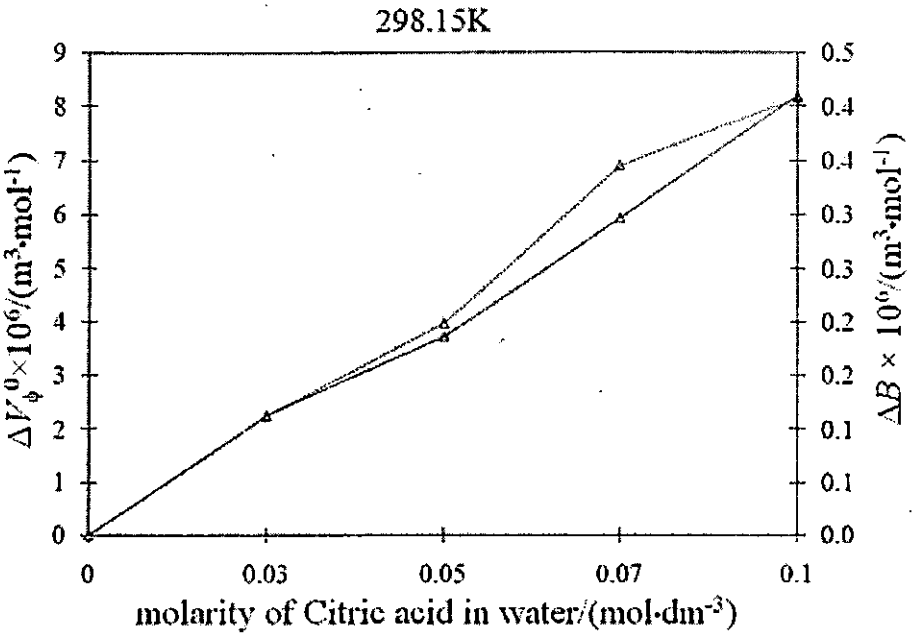

Fig. 1(a) Plots of partial molar volume (ΔV_ϕ^0) and viscosity *B*-coefficients (ΔB) against molarity for the transfer from water to different aqueous CA solutions for NA at T = 298.15 K. Dotted lines for ΔV_ϕ^0 and solid lines for ΔB.

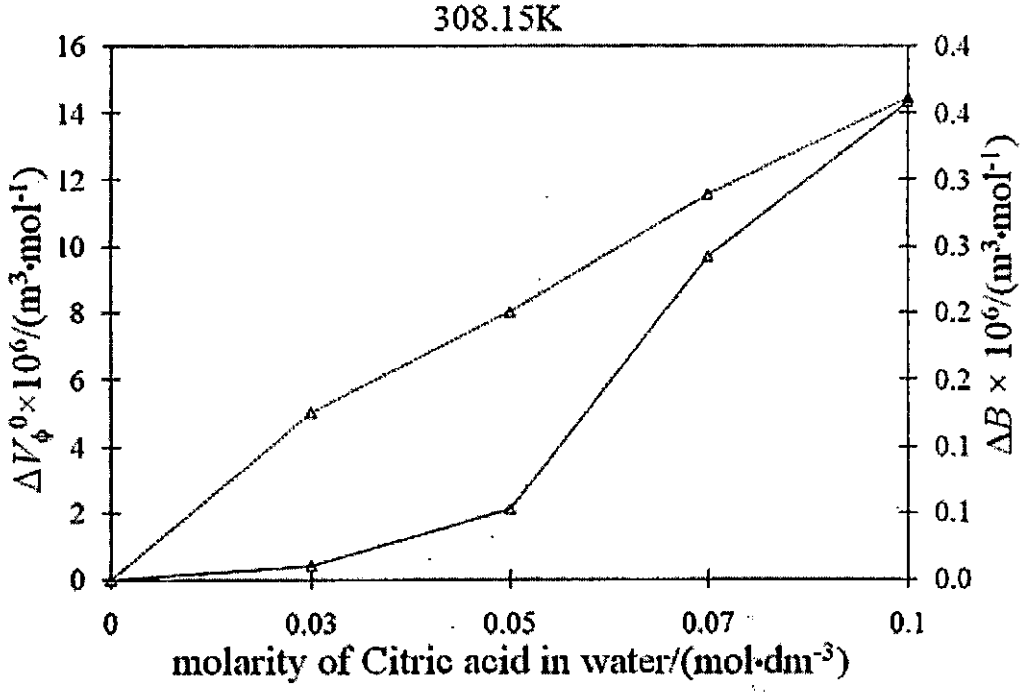

Fig. 1(b) Plots of partial molar volume (ΔV_ϕ^0) and viscosity *B*-coefficients (ΔB) against molarity for the transfer from water to different aqueous CA solutions for NA at T = 308.15 K. Dotted lines for ΔV_ϕ^0 and solid lines for ΔB.

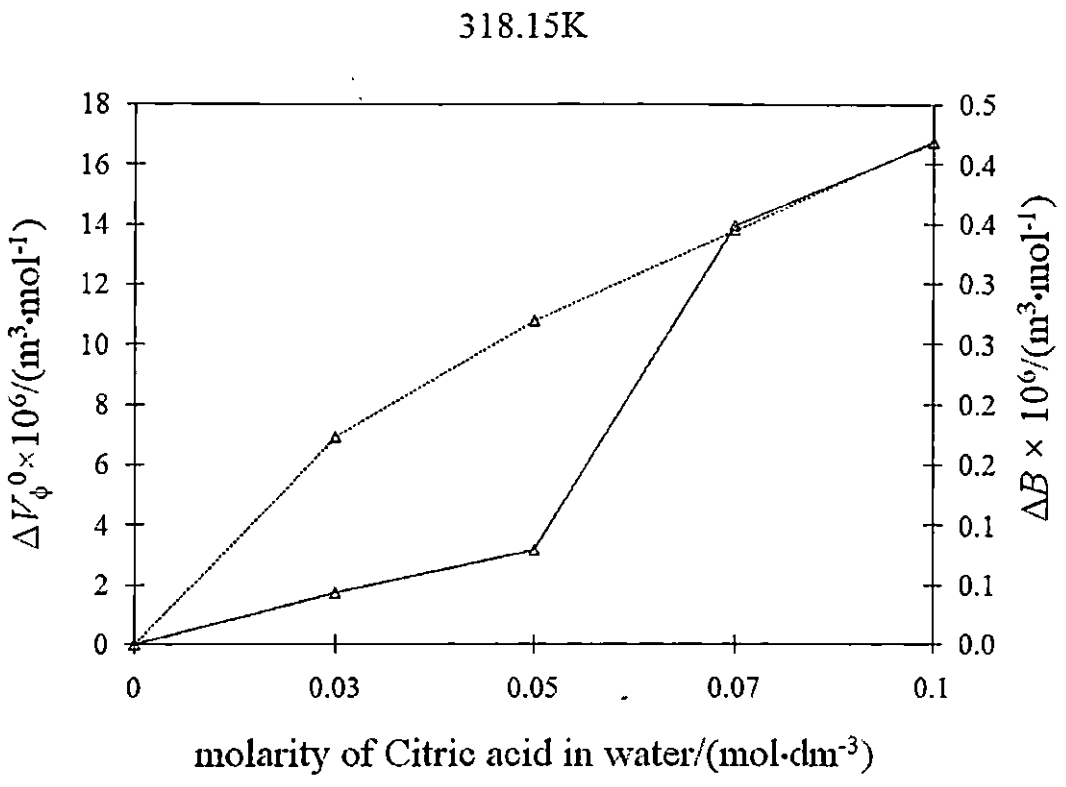

Fig. 1(c) Plots of partial molar volume (ΔV_ϕ^0) and viscosity *B*-coefficients (ΔB) against molarity for the transfer from water to different aqueous CA solutions for NA at T = 318.15 K. Dotted lines for ΔV_ϕ^0 and solid lines for ΔB.

CHAPTER VIII

EXPLORATION OF DIVERSE INTERACTIONS OF SOME VITAMINS IN AQUEOUS MIXTURES OF CYSTEINE

8.1 Introduction:

A vitamin is an organic compound required by an organism as a vital nutrient in limited amounts. Vitamins are essential precursors for various coenzymes. These coenzymes are therefore required in almost all metabolic pathways [1]. Nicotinic Acid, commonly known as vitamin B3 [2], is a water-soluble vitamin, an essential micronutrient and a reactive moiety of the coenzyme nicotinamide adenine dinucleotide (NAD). Ascorbic acid, known as vitamin C is water soluble vitamin, required for the synthesis of collagen, the intercellular "cement" which gives the structure of muscles, vascular tissues, bones, and tendon. Vitamin C plays an important role for the synthesis of several important peptide hormones neurotransmitters and creatinine. It also enhances the eye's ability and delay the progression of advanced age related muscular degeneration [3]. Folic acid is water-soluble vitamin, known as vitamin B9 (folate). It is an essential vitamin that is yellow-orange in color, is reported to be present in photosensitive organs, various mammalian metabolic pathways, and possibly involved in photosynthesis [4]. Humans cannot synthesize folate inside body; therefore, folate has to be supplied through the diet to meet their daily requirements. Children and adults both require folic acid to produce healthy red blood cells and prevent anemia [5].

Cysteine is a semi-essential amino acid, which means that it can be bio-synthesized in human body [6] under normal physiological conditions if a sufficient quantity of methionine is available. Although classified as a non-essential amino acid, in rare cases, cysteine may be essential for infants, the elderly, and individuals with certain metabolic disease.

To interpret various interactions occurring in solutions, the volumetric, viscometric and interferometric behavior of solutes has been proved to be very useful. To obtain information on solute-solute, solute-solvent, and solvent-solvent interactions, studies on the effect of concentration (molality), the apparent molar volumes of solutes have been extensively used.

Journal Of Mexican Chemical Society, 2014, 58(2), 106-112

In view of the above and in continuation of our studies, we have undertaken a systematic study on the density, viscosity, refractive index and ultrasonic speed of some vitamins in aqueous cysteine solutions at 298.15 K and we have attempted to report the limiting apparent molar volume (ϕ_V^0), experimental slopes (S_V^*), viscosity *B*-coefficients, molar refraction (*R*) and limiting apparent molar adiabatic compressibility (ϕ_K^0) for the cited vitamins in aqueous cysteine solution. The nature and mode of the cysteine, interacting with the additionally input vitamins has also been discussed.

8.2 Experimental section:

8.2.1 Source and purity of samples

The studied salts (Nicotinic acid, Ascorbic acid and Folic acid) and cysteine, puriss grade was purchased from Sigma-Aldrich, Germany and was used as purchased. The mass purity of salts were ≥ 0.99. The salts were dried from moisture at 353K for 24 h, and then they were cooled and store in a desiccator prior to use. Triply distilled water with a specific conductance $<10^{-6}$ S cm^{-1} was used for the preparation of different aqueous cysteine solutions. The physical properties of different mass fraction of aqueous cysteine mixture are listed in Table 1.

8.2.2 Apparatus and Procedure

Aqueous binary solution of cysteine was prepared by mass (Mettler Toledo AG-285 with uncertainty ±0.0003g), which are used as solvent. Stock solutions of the salts (vitamins) were also prepared by mass and the working solutions were obtained by mass dilution. The conversion of molarity into molality was accomplished using experimental density values. All solutions were prepared afresh before use. The experimental values of densities (ρ), viscosities (η), refractive indices (n_D) and ultrasonic speeds (u) of solutions are reported in Table 2 and the derived parameters are reported in Table 3 and Table 4 .

The densities of the solutions (ρ) were measured by means of vibrating-u-tube Anton Paar digital density meter (DMA 4500M) with a precision of ±0.00005g cm^{-3} maintained at ±0.01K of the desired temperature. It was calibrated by triply-distilled water and passing dry air.

The viscosities were measured using a Brookfield DV-III Ultra Programmable Rheometer with fitted spindle size-42. The viscosities were obtained using the following equation

$$\eta = (100 / \text{RPM}) \times \text{TK} \times \text{torque} \times \text{SMC} \quad (1)$$

where RPM, TK (0.09373) and SMC (0.327) are the speed, viscometer torque constant and spindle multiplier constant, respectively. The instrument was calibrated against the standard viscosity samples supplied with the instrument, water and aqueous $CaCl_2$ solutions [7]. Temperature of the solution was maintained within ± 0.01°C using Brookfield Digital TC-500 temperature thermostat bath. The viscosities were measured with an accuracy of ± 1.0 % [viscosity of 0.01 molar aqueous $CaCl_2$ solution is 0.896 mPa s (at 25°c), water is 0.890 mPa s (at 25°c)]. Each measurement reported herein is an average of triplicate reading with a precision of 0.3 %.

Refractive index was measured with the help of a Digital Refractometer Mettler Toledo (Refracto 30GS). The light source was LED, λ=589.3nm. The refractometer was calibrated twice using tripply distilled water, benzene and dry air and calibration was checked after every few measurements. The uncertainty of refractive index measurement was ±0.0002 units.

The ultrasonic speed (u) was measured by multi frequency ultrasonic interferometer (Model M-81) from Mittal Enterprises, India. The interferometer working at 5 MHz is based on the same principle as was used by Freyer et al. [8] and Kiyoharo et al. [9]. The obtained speeds were corrected for diffraction errors as given by Subrahmayan et al. [10]. The uncertainty in the speed is ±0.2 m s^{-1}. The temperature was controlled within ±0.01 K using a Lauda thermostat during the measurement.

8.3 Results and Discussions:

8.3.1 Density measurement

Apparent molar volumes (ϕ_V) were determined from the solution densities using the equation 2 [11].

$$\phi_V = M / \rho - 1000(\rho - \rho_o) / m\rho\rho_o \quad (2)$$

where M(g mol^{-1}) is the molar mass of the solute, m(mol kg^{-1}) is the molality of the solution, ρ_0 (kg m^{-3}) and ρ (kg m^{-3}) are the densities of the mixture and the solution respectively. The plots of ϕ_V against square root of molal concentration ($\sqrt{m}$) were found to be linear. Using a least-square treatment to the plots of ϕ_V versus $\sqrt{m}$ using the Masson equation, equation 3 [12], the limiting apparent molar volume ϕ_V^0 was calculated.

$$\phi_V = \phi_V^0 + S_V^* \sqrt{m} \quad (3)$$

where ϕ_V^0 is the limiting apparent molar volume at infinite dilution and S_V^* is the experimental slope. Values of ϕ_V^0 and S_V^* are reported in Table 4.

A glance of Table 4 shows that ϕ_V^0 values for vitamins are positive and increase with increasing concentrations in aqueous cysteine mixture, indicating the presence of strong solute-solvent interactions and these interactions are further strengthened as increases the mass fraction of cysteine in the mixture. A probable interaction pattern is shown in SCHEME I.

Interaction of vitamins with cysteine increases with increasing interacting centre of vitamins. The trend in the solute-solvent interaction is

Nicotinic Acid (NA) < Ascorbic Acid (AA) < Folic Acid (FA)

The S_V^* values of the vitamin solution given in Table 4 decreases with increase in the interactive centres of the studied vitamins and with increase in the mass fraction of cysteine in the solvent mixture rendering minimum solute-solute interaction.

The magnitude of ϕ_V^0 (Fig.1) valuesis much greater than those of S_V^* for all studies vitamins as well as mass fraction of cysteine in the mixture suggests that solute-solvent interactions dominate over solute-solute interactions.

8.3.2 Viscosity measurement

The viscosity data has been analyzed using Jones-Dole equation, equation 4 [13].

$$(\eta/\eta_0 - 1)/\ m^{1/2} = A + Bm^{1/2} \quad (4)$$

where η_0(mPa s) and η (mPa s) are the viscosities of the solvent and solution respectively, m(mol kg^{-1}) is the molality of the solution. A(kg mol^{-1}) and B(kg$^{1/2}$

$mol^{-1/2}$) are the viscosity co-efficient estimated by a least-squares method and are reported in Table 4. The values of the *A* co-efficient are found to decrease with the increase in the mass fraction of cysteine in solvent mixture. The results indicate the presence of very weak solute-solute interactions. These results are in excellent agreement with those obtained from S_V^* values discussed earlier.

The effects of solute-solvent interactions on the solution viscosity can be inferred from the *B*-coefficient [14,15]. The viscosity *B*-coefficient is a valuable tool to provide information concerning the solvation of the solutes and their effects on the structure of the solvent. From Table 4 and Figure 2 it is evident that the values of the *B*-coefficient are positive, thereby suggesting the presence of strong solute-solvent interactions, and strengthened with increase of mass fraction of cysteine in the solvent mixture, are in agreement with the results obtained from ϕ_V^0 values discussed.

8.3.3. Refractive index measurement

The molar refraction, *R* can be evaluated from the Lorentz-Lorenz relation, equation 5 [16].

$$R = \left\{(n_D^2-1)/(n_D^2+2)\right\}(M/\rho) \quad (5)$$

where *R* ($cm^3\ mol^{-1}$), n_D, *M* ($gm.mol^{-1}$) and ρ ($kg\ m^{-3}$) are the molar refraction, the refractive index, the molar mass and the density of solution respectively. The refractive index of a substance is defined as the ratio c_0/c, where c is the speed of light in the medium and c_0 the speed of light in vacuum. Stated more simply, the refractive index of a compound describes its ability to refract light as it moves from one medium to another and thus, the higher the refractive index of a compound, the more the light is refracted [17], as stated by Deetlefs et al. [18]

The refractive index of a substance is higher when its molecules are more tightly packed or in general when the compound is denser and with the increase of mass fraction of cysteine in solvent mixture refractive index value also increases. Hence a perusal of Table 2 & Table 3 we found that the refractive index and the molar refraction values respectively are higher for Folic Acid than Ascorbic Acid and Nicotinic Acid, indicating the fact that the molecules are more tightly packed in the mixture. The interaction in the solution is basically solute-solvent interaction and a

small amount of solute-solute interaction. This is also good agreement with the results obtained from density and viscosity parameters discussed above. The trend in the package of the studied vitamins in aqueous mixture of cysteine is

Nicotinic Acid < Ascorbic Acid < Folic Acid.

8.3.4. Ultrasonic speed measurement

The adiabatic compressibility (β) was evaluated from the following equation:

$$\beta = 1 / u^2 \rho \quad (6)$$

where ρ (kg m^{-3}) is the density of solution and u(ms^{-1})is the speed of sound in the solution. The apparent molal adiabatic compressibility (ϕ_K) of the solutions was determined from the relation [19].

$$\phi_K = M\beta / \rho + 1000(\beta \rho_o - \beta_o \rho) / m \rho \rho_o \quad (7)$$

where β_0 , β are the adiabatic compressibility of the solvent and solution respectively and m (mol kg^{-1}) is the molality of the solution. Limiting partial molal adiabatic compressibilities (ϕ_K^0) and experimental slopes (S_K^*) were obtained by fitting ϕ_K against the square root of molality of the electrolyte ($\sqrt{m}$) using the method of least squares.

$$\phi_K = \phi_K^0 + S_K^* . \sqrt{m} \quad (8)$$

The values of β and ϕ_K are reported in Table 3. The values of ϕ_K^0 (m^3 mol^{-1} Pa^{-1}) and S_K^* (m^3 $mol^{-3/2}$ Pa^{-1} $kg^{1/2}$) are presented in Table 4. Since the values of ϕ_K^0 and S_K^* are measures of solute-solvent and solute-solute interactions respectively, a perusal of Table 4 and Figure 3 shows that the ϕ_K^0 values are in good agreement with those drawn from the values of ϕ_V^0 discussed earlier.

8.4 Conclusion:

The positive effects of the derived parameters, as limiting apparent molar volume (ϕ_V^0), viscosity *B*-coefficients and limiting partial isentropic compressibility (ϕ_K^0) suggested the presence of strong solute(vitamins)-solvent(aq. mix. of Cystine) interactions; which increases with the increase in the interacting centres (groups) of

vitamins and with increase of mass fraction of cysteine in the aqueous mixture. The refractive index and the molar refraction values imply that Folic Acid molecules are more tightly packed in the solution leading to higher solute-solvent interaction than the other vitamins. The conclusions from experimental and derived parameters also provides important working function of the cysteine with vitamins in biological systems; which demands the uniqueness of the work.

Tables:

Table 1. The values of Density (ρ), Viscosity (η), Refractive index (n_D), and Speed of sound (u) in different mass fraction of Cysteine at 298.15K

Mass-fraction Cysteine	ρ x 10^{-3} (kg m^{-3})	η (mPa s)	n_D	u (ms^{-1})
$w_1 = 0.01$	0.99752	0.81	1.3319	1499.8
$w_1 = 0.03$	0.99854	0.83	1.3326	1503.2
$w_1 = 0.05$	0.99951	0.86	1.3334	1506.7

Uncertainty of density measurement: ±0.00005g cm^{-3}

Uncertainty of viscosity measurement: ±0.02 mPa s

Uncertainty of refractive index measurement: ±0.0002

Uncertainty of ultrasonic speed measurement: ±0.2 m s^{-1}

Table 2. Experimental values of Densities (ρ), Viscosities (η), Refractive Index (n_D) and Ultrasonic Speed (u) of Nicotinic Acid, Ascorbic Acid and Folic Acid in different mass fraction of Cysteine at 298.15K

m (mol kg^{-1})	ρ x 10^{-3} (kg m^{-3})	η (mPas)	n_D	u (m s^{-1})	m (mol kg^{-1})	ρ x 10^{-3} (kg m^{-3})	η (mPas)	n_D	u (m s^{-1})
w_1 = 0.01					w_1 = 0.03				
Nicotinic Acid					Nicotinic Acid				
0.0100	0.99761	0.83	1.3322	1502.2	0.0100	0.99861	0.85	1.3329	1506.1
0.0251	0.99776	0.85	1.3327	1508.5	0.0251	0.99873	0.88	1.3334	1514.0
0.0403	0.99792	0.87	1.3331	1516.8	0.0402	0.99887	0.91	1.3338	1524.9
0.0555	0.99809	0.89	1.3335	1526.9	0.0554	0.99902	0.94	1.3342	1538.3
0.0707	0.99827	0.91	1.3338	1538.7	0.0707	0.99918	0.97	1.3345	1554.3
0.0860	0.99845	0.93	1.3341	1552.3	0.0860	0.99935	1.00	1.3348	1572.4
Ascorbic Acid					Ascorbic Acid				
0.0100	0.99767	0.84	1.3322	1503.2	0.0100	0.99867	0.86	1.3331	1507.0
0.0252	0.99792	0.88	1.3328	1512.7	0.0251	0.9989	0.91	1.3338	1518.2
0.0404	0.99819	0.92	1.3333	1525.5	0.0403	0.99915	0.96	1.3344	1533.4
0.0556	0.99847	0.96	1.3337	1541.2	0.0556	0.99943	1.01	1.3349	1551.6
0.0710	0.99876	1.00	1.3341	1559.2	0.0709	0.99972	1.06	1.3354	1573.1
0.0864	0.99907	1.03	1.3344	1579.4	0.0863	1.00002	1.11	1.3358	1598.8
Folic Acid					Folic Acid				
0.0101	0.99773	0.86	1.3325	1504.2	0.0101	0.99873	0.87	1.3331	1507.7
0.0253	0.99808	0.92	1.3332	1516.5	0.0253	0.99906	0.93	1.3338	1520.6
0.0408	0.99846	0.98	1.3338	1533.4	0.0407	0.99942	0.99	1.3344	1539.2
0.0564	0.99887	1.04	1.3343	1554.4	0.0564	0.99981	1.05	1.3349	1561.9
0.0723	0.99929	1.10	1.3348	1578.8	0.0722	1.00022	1.12	1.3354	1590.7
0.0883	0.99973	1.16	1.3352	1607.3	0.0883	1.00066	1.18	1.3359	1622.4
w_1 = 0.05									
Nicotinic Acid									
0.0100	0.99956	0.88	1.3337	1509.8					
0.0251	0.99966	0.92	1.3343	1518.9					
0.0402	0.99979	0.96	1.3347	1532.0					
0.0554	0.99994	1.00	1.3351	1547.8					
0.0706	1.0001	1.04	1.3355	1566.4					
0.0859	1.00028	1.08	1.3358	1588.5					

		Ascorbic Acid		
0.0100	0.99962	0.88	1.3338	1510.6
0.0251	0.99983	0.93	1.3346	1522.3
0.0403	1.00007	0.98	1.3352	1539.4
0.0555	1.00033	1.03	1.3358	1561.0
0.0708	1.00062	1.09	1.3363	1586.4
0.0862	1.00093	1.14	1.3368	1614.7
		Folic Acid		
0.0100	0.99966	0.89	1.334	1511.4
0.0253	0.99994	0.95	1.3349	1526.5
0.0407	1.00027	1.02	1.3357	1547.8
0.0563	1.00063	1.08	1.3363	1574.5
0.0722	1.00103	1.15	1.3369	1605.3
0.0882	1.00143	1.21	1.3375	1642.9

Uncertainty of density measurement: ±0.00005g cm^{-3}

Uncertainty of viscosity measurement: ±0.02 mPa s

Uncertainty of refractive index measurement: ±0.0002

Uncertainty of ultrasonic speed measurement: ±0.2 m s^{-1}

Table 3. Molality, apparent molar volume (ϕ_V),$(\eta/\eta_0-1)/m^{1/2}$, molar refraction (R), adiabatic compressibility (β) and apparent molal adiabatic compressibility (ϕ_K) of Nicotinic Acid, Ascorbic Acid and Folic Acid in Cysteine at 298.15 K

molality (mol kg^{-1})	ϕ_V x 10^6 (m^3 mol^{-1})	$(\eta/\eta_0-1)/m^{1/2}$ ($kg^{1/2}$ $mol^{-1/2}$)	R (cm^3 mol^{-1})	β x 10^{10} (Pa^{-1})	ϕ_K x 10^{10} (m^3 mol^{-1} Pa^{-1})
		w_1 = 0.01			
		Nicotinic Acid			
0.0100	114.39	0.25	25.33	4.44	-0.95
0.0251	113.79	0.31	25.36	4.40	-1.59
0.0403	113.39	0.37	25.38	4.35	-2.03
0.0555	113.02	0.42	25.41	4.30	-2.40
0.0707	112.67	0.46	25.42	4.23	-2.74
0.0860	112.45	0.51	25.44	4.16	-3.05

			Ascorbic Acid		
0.0100	161.52	0.37	36.23	4.43	-1.36
0.0252	160.52	0.54	36.28	4.38	-2.39
0.0404	159.77	0.68	36.32	4.30	-3.10
0.0556	159.24	0.79	36.35	4.21	-3.68
0.0710	158.80	0.88	36.38	4.12	-4.16
0.0864	158.28	0.93	36.40	4.01	-4.56
			Folic Acid		
0.0101	421.44	0.62	90.88	4.43	-0.83
0.0253	420.04	0.86	91.02	4.36	-2.16
0.0408	418.94	1.05	91.13	4.26	-3.13
0.0564	417.89	1.21	91.22	4.14	-3.94
0.0723	417.15	1.35	91.30	4.01	-4.60
0.0883	416.43	1.47	91.36	3.87	-5.22
			$w_1 = 0.03$		
			Nicotinic Acid		
0.0100	116.28	0.19	25.35	4.41	-1.22
0.0251	115.68	0.34	25.38	4.37	-2.05
0.0402	115.03	0.45	25.41	4.30	-2.67
0.0554	114.55	0.54	25.43	4.23	-3.18
0.0707	114.13	0.61	25.45	4.14	-3.65
0.0860	113.75	0.68	25.46	4.05	-4.05
			Ascorbic Acid		
0.0100	163.36	0.32	36.28	4.41	-1.57
0.0251	161.96	0.57	36.35	4.34	-2.84
0.0403	161.10	0.75	36.40	4.26	-3.69
0.0556	160.17	0.89	36.43	4.16	-4.33
0.0709	159.49	1.02	36.47	4.04	-4.90
0.0863	158.94	1.13	36.50	3.91	-5.46
			Folic Acid		
0.0101	423.02	0.42	90.93	4.40	-0.86

0.0253	421.21	0.72	91.08	4.33	-2.29
0.0407	420.01	0.93	91.19	4.22	-3.42
0.0564	418.92	1.10	91.28	4.10	-4.29
0.0722	418.01	1.29	91.37	3.95	-5.18
0.0883	417.07	1.41	91.45	3.80	-5.84
			$w_1 = 0.05$		
			Nicotinic Acid		
0.0100	118.17	0.23	25.38	4.39	-1.31
0.0251	117.17	0.44	25.42	4.34	-2.34
0.0402	116.17	0.58	25.44	4.26	-3.14
0.0554	115.35	0.69	25.47	4.17	-3.74
0.0706	114.74	0.79	25.49	4.07	-4.26
0.0859	114.11	0.87	25.51	3.96	-4.77
			Ascorbic Acid		
0.0100	165.20	0.23	36.32	4.38	-1.60
0.0251	163.40	0.51	36.39	4.32	-2.94
0.0403	162.20	0.70	36.44	4.22	-4.00
0.0555	161.29	0.84	36.49	4.10	-4.86
0.0708	160.34	1.01	36.53	3.97	-5.57
0.0862	159.49	1.11	36.57	3.83	-6.12
			Folic Acid		
0.0100	426.61	0.35	91.07	4.38	-0.93
0.0253	424.41	0.66	91.27	4.29	-2.79
0.0407	422.61	0.93	91.44	4.17	-4.07
0.0563	421.24	1.09	91.55	4.03	-5.10
0.0722	419.89	1.27	91.66	3.88	-5.91
0.0882	419.02	1.39	91.77	3.70	-6.71

Uncertainty in molality:±0.0002 mol kg^{-1}

Table 4. Limiting apparent molar volumes (ϕ_V^0), experimental slopes (S_V^*), *A*, *B* coefficients, limiting partial adiabatic compressibility (ϕ_K^0), and experimental slope (S_K^*) of Nicotinic Acid, Ascorbic Acid, and Folic Acid in aqueous Cysteine at 298.15 K

Solute	ϕ_V^0 x 10^6 (m^3 mol^{-1})	S_V^* x 10^6 (m^3 $mol^{-3/2}$ $kg^{1/2}$)	*A* (kg mol^{-1})	*B* ($kg^{1/2}$ $mol^{-1/2}$)	ϕ_K^0 x 10^{10} (m^3 mol^{-1} Pa^{-1})	S_K^* x 10^4 (m^3 $mol^{-3/2}$ Pa^{-1} $kg^{1/2}$)
			$w_1 = 0.01$			
Nicotinic Acid	115.40±0.02	-10.16±0.01	0.102±0.02	1.363±0.02	0.135±0.01	-10.84±0.02
Ascorbic Acid	163.1±0.01	-16.54±0.02	0.075±0.03	2.984±0.01	0.270±0.01	-16.67±0.02
Folic Acid	424±0.03	-25.74±0.02	0.158±0.02	4.465±0.02	1.444±0.02	-22.77±0.02
			$w_1 = 0.03$			
Nicotinic Acid	117.6±0.03	-13.35±0.02	-0.063±0.02	2.552±0.01	0.272±0.02	-14.75±0.02
Ascorbic Acid	165.6±0.02	-22.95±0.03	-0.098±0.03	4.210±0.02	0.379±0.02	-20.04±0.01
Folic Acid	426±0.02	-29.97±0.02	-0.093±0.02	5.137±0.02	1.778±0.03	-25.99±0.02
			$w_1 = 0.05$			
Nicotinic Acid	120.4±0.01	-21.37±0.02	-0.093±0.02	3.331±0.02	0.487±0.01	-17.98±0.02
Ascorbic Acid	168±0.01	-29.15±0.02	-0.220±0.02	4.574±0.03	0.789±0.02	-23.83±0.03
Folic Acid	430.5±0.02	-39.25±0.02	-0.192±0.01	5.458±0.02	1.980±0.02	-29.87±0.02

Figures:

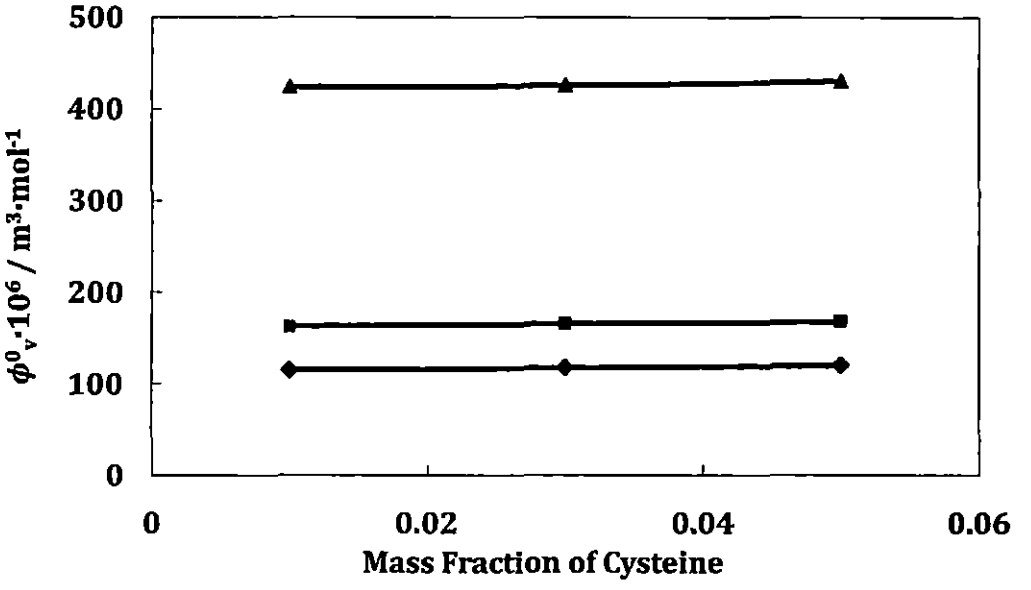

Fig. 1. The plots of limiting apparent molar volumes (ϕ_V^0) for Nicotinic Acid (—♦—), Ascorbic Acid (—■—), Folic Acid (—▲—) in different mass fractions (w_1) of Cysteine in aqueous mixture at 298.15K

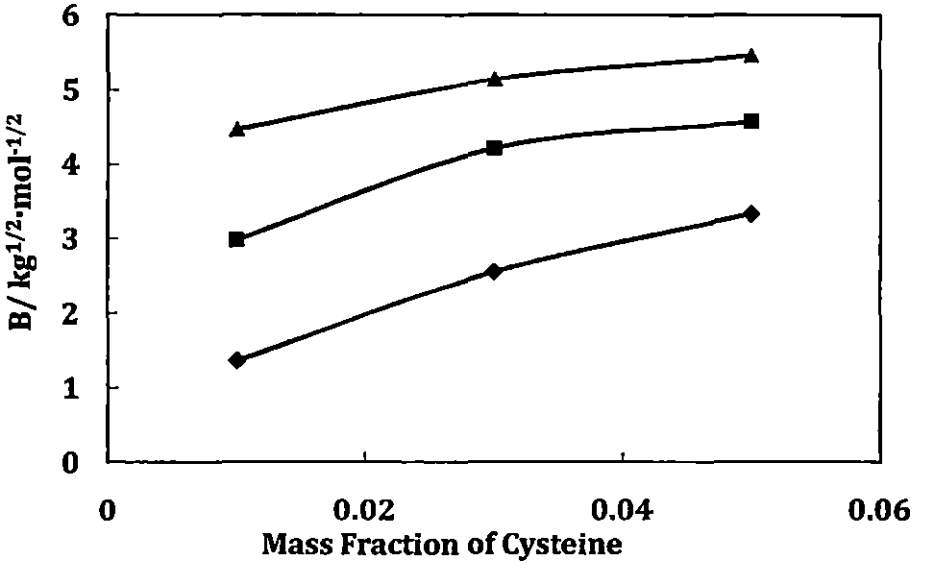

Fig. 2. The plots of viscosity *B*-coefficient for Nicotinic Acid (—♦—),Ascorbic Acid (—■—), Folic Acid (—▲—) in different mass fractions (w_1) of Cysteine in aqueous mixture at 298.15K

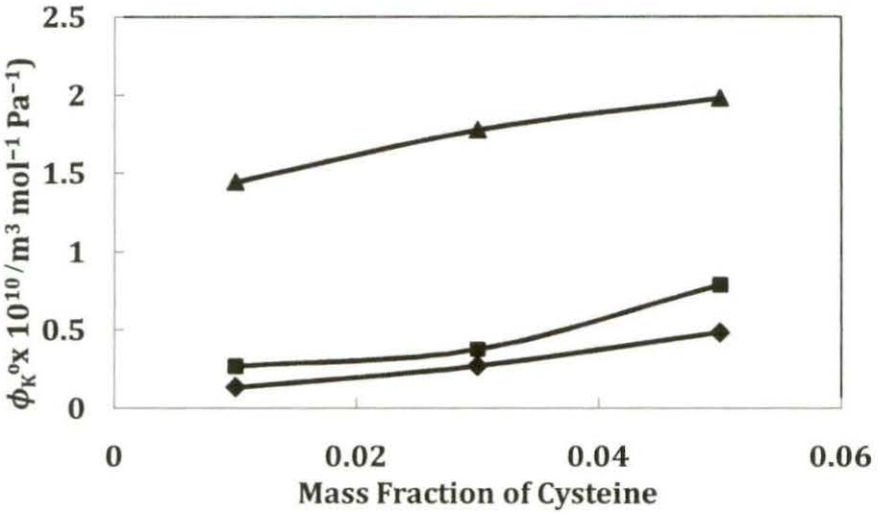

Fig. 3. The plots of limiting partial adiabatic compressibility (ϕ_K^0) for Nicotinic Acid (—♦—), Ascorbic Acid (—■—), Folic Acid (—▲—) in different mass fractions (w_1) of Cysteine in aqueous mixture at 298.15K

Scheme:

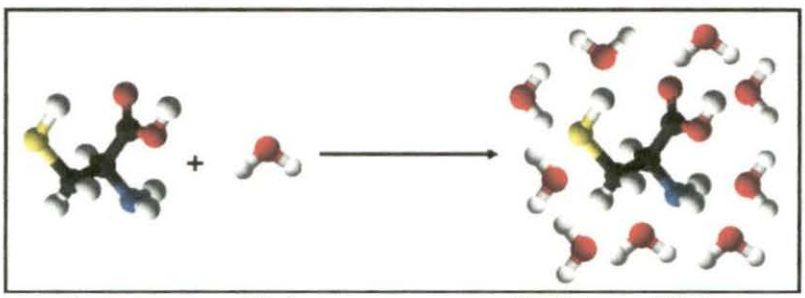

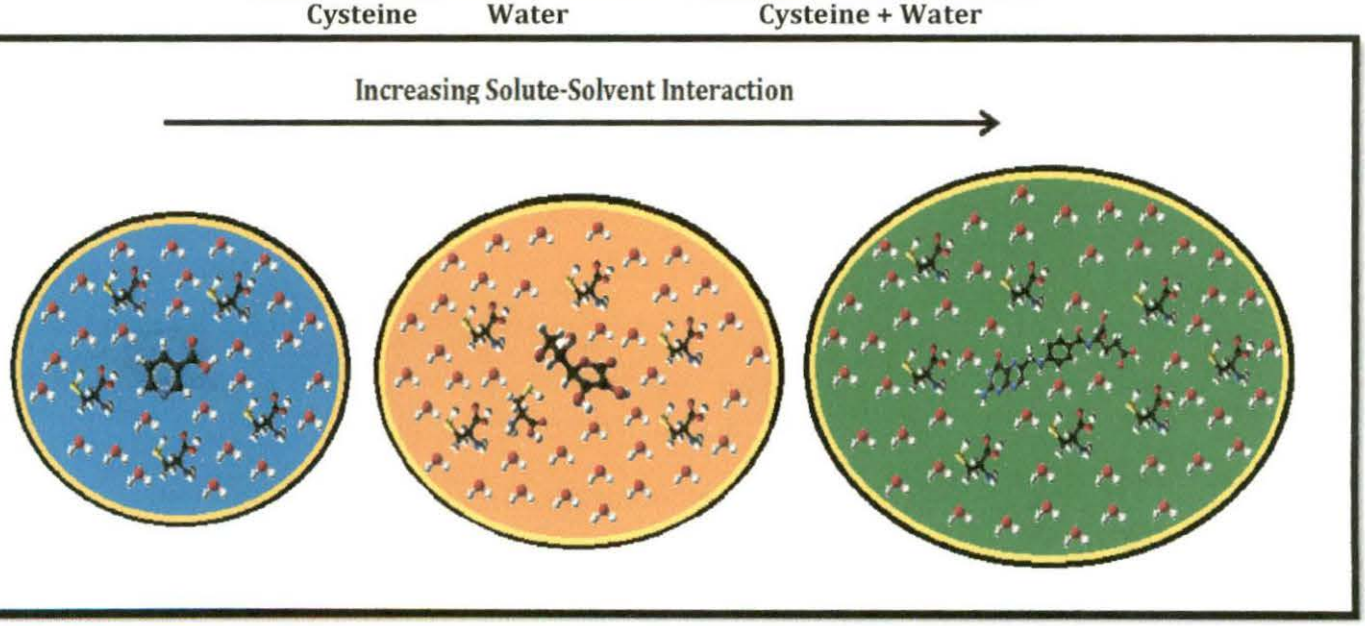

(Cysteine + Water)+ NA (Cysteine + Water) + AA (Cysteine + Water) + FA

SCHEME I

CHAPTER IX

EXPLORATION OF MOLECULAR INTERACTIONS OF SOME STANDARD AMINO ACIDS IN H_2O + VITAMIN-B_3 MIXTURES

9.1 Introduction:

Amino acids are important in biochemistry, not only in biochemistry it also takes part a central role to life, and have many functions in metabolism. One particularly important function is to serve as the building blocks of proteins. Due to their central role in biochemistry; amino acids are important in nutrition and are commonly used in food technology and industry. Amino acids exist as zwitterions in aqueous solution. Thus, the study of low molecular model compounds such as amino acids, peptides and their derivatives which represents the building block of proteins in a variety of media is of immense importance.

On the other hand vitamins are essential precursors for various coenzymes. These coenzymes are therefore required in almost all metabolic pathways [1]. Nicotinic acid also known as Vitamin B3 is a water-soluble vitamin and an essential in micronutrient [2,3].

Studying the behavior of amino acids in aqueous nicotinic acid solutions will be useful in pharmaceutical industries and food technology as well as in every process of the reaction occurring in protein and peptides chain. Keeping in mind the great applicability of the studied systems, here, we have attempted to ascertain the molecular interaction of the cited amino acids in 0.01, 0.03, 0.05 mass fraction of aqueous nicotinic acid solutions at 298.15 K in terms of limiting apparent molar volume (ϕ_V^0), viscosity *B*-coefficients, limiting apparent molar adiabatic compressibility (ϕ_K^0) and molar refraction (*R*).

9.2 Experimental Section:

9.2.1 Materials

Glycine, L-Alanine, L-Valine and Nicotinic acid were procured from (Sigma Aldrich, purity > 99 %) and were used as such without further purification. Triply distilled water was used for the preparation of different aqueous nicotinic solutions, where the aqueous nicotinic solutions are treated as solvent in the present study. The experimentally observed physical properties of different aqueous nicotinic acid solutions are listed in Table 1.

9.2.2 Apparatus and Procedure

We have precisely checked the solubility of the chosen amino acids in aq. niconitic acid mixtures, and seen that the amino acids were freely soluble in all proportions of the nicotinic acid-water mixtures. 0.1 (M) stock solutions of amino acids in different mass fraction of aqueous nicotinic acid mixture were prepared by mass (Mettler Toledo AG-285 with uncertainty 0.0003g) and the working solutions were prepared by mass dilution. The uncertainties of concentration of different solutions were evaluated to ±0.0001 mol kg^{-1}.

The density, ρ, was measured with an Anton Paar density-meter (DMA 4500M). The uncertainty in the density measurements were within ± $5 \cdot 10^{-5} g \cdot cm^{-3}$. It was calibrated by double-distilled water and dry air [4].

The viscosity, η, was measured by means of a suspended Ubbelohde type viscometer, calibrated at the experimental temperatures with doubly distilled water and purified methanol. A thoroughly cleaned and perfectly dried viscometer filled with experimental solution was placed vertically in a glass-walled thermostat maintained to ± 0.01 K. After attainment of thermal equilibrium, efflux times of flow were recorded with a stop watch correct to ± 0.1 s. At least three repetition of each data reproducible to ± 0.1 s were taken to average the flow time. Viscosity of solution, η, was obtained using the following equation:

$$\eta = (Kt - L/t)\rho \qquad (1)$$

where K and L are the viscometer constants and t and ρ are the efflux time of flow in seconds and the density of the experimental liquid, respectively. The uncertainty in viscosity measurements is within ± 0.003 mPa·s [4].

Refractive index was measured with the help of a Digital Refractometer Mettler Toledo. The light source was LED, λ=589.3nm. The refractometer was calibrated twice using distilled water, and calibration was checked after every few measurements. The uncertainty of refractive index measurement was ±0.0002 units.

The ultrasonic velocities, u (m s^{-1}), were measured using an ultrasonic interferometer (Model M-83) from Mittal enterprises, India. The interferometer working at 2 MHz is based on the same principle as was used by Freyer et al. [5] and Kiyoharo et al.[6, 7] The obtained velocities were corrected for diffraction errors as given by Subrahmayan et al.[8] The maximum uncertainty in the velocity is ±0.5 m s^{-1}. The temperature was controlled within ±0.01 K using a Lauda thermostat for velocity measurements.

9.3 Results and Discussion:

The apparent molar volume (ϕ_V) was determined from the solution densities using the following equation: [9]

$$\phi_V = \frac{M}{\rho} - \frac{1000(\rho - \rho_0)}{m\rho\rho_0} \qquad (2)$$

where the symbols are usual meaning. The plots of ϕ_V values against square root of molality ($\sqrt{m}$), the trends is approximate linear; thus the ϕ_V values were fitted to the Masson equation: [10]

$$\phi_V = \phi_V^0 + S_V^* \sqrt{m} \qquad (3)$$

From where, ϕ_V^0, the limiting apparent molar volume at infinite dilution and S_V^* is the experimental slope have been determined and listed in Table 2. Graphical representation (in Figure 1) of limiting apparent molar volume, ϕ_V^0, of the Glycine, L-alanine, and L-valine in different concentrations of aqueous nicotinic acid solutions at 298.15K, shows that the ϕ_V^0 values are positive, which indicates the presence of strong solute-solvent interaction. The increasing ϕ_V^0 values with increase in the

concentration of the nicotinic acid in solution, also shows the positive trend of solute-solvent interaction with increasing amount of nicotinic acid in solution.

In solid state the nicotinic acid exists as neutral molecule instead of zwitterion; on the other hand in aqueous solution it exists as zwitterionic form according to the equilibrium of neutral aqueous solutions is shown in bellow;

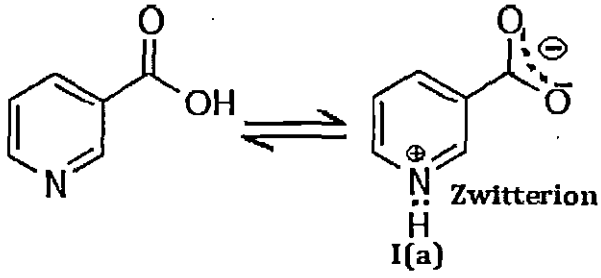

I(a)

and as acidic and basic form in acidic and basic medium shown in I(a) and I(b), i.e.:

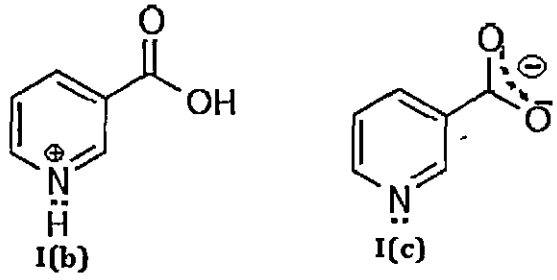

I(b) I(c)

The zwitterionic I(a), acidic I(b), and basic I(c) form of the nicotinic acid exists in aqueous, are open the phase of interacting centre to interact with the incoming solute or studies α-amino acids molecules in the present chosen solution systems; as a result, strong interactions are present between amino acids and nicotinic acid in solution media.

As evident from the ϕ_V^0 values, the solute-solvent interaction is high in case of L-valine as compared to the other two amino acids. The trend in the solute-solvent interaction of the amino acid is given below:

glycine < L-alanine < L-valine

The trend also supports the same shape, i.e., the interaction arises positively with growing number of -CH_2 groups in the chain length of the chosen amino acids. The positive strength of solute-solvent interactions taking placed in solutions have been explained by plausible interaction between

(i) The positive centre of N atom of the ring of nicotinic acid I(a) and nucleophile (-COO^-) of the zwiterionic form of the amino acid

(ii) The nucleophile (-COO^-) of the nicotinic acid and -CH_2 groups of the hydrophobic part of the chain of amino acids.

(iii) When nicotinic acid exists as zwiterionic form, than both the electrophile (positive centre of N atom of the ring) and nucleophile (-COO^-) group is interacting with the incoming -NH_2 and –COO^- group of the zwiterionic form of the amino acid.

(iv) Hydrophobic- hydrophobic interaction of the amino acids itself.

Since the hydrophobic-hydrophobic interaction (iv) is gives the negative change in ϕ_V^0, so it is neglected. The assumptions of type the interactions (i) to (iii) are give the positive change in ϕ_V^0. Therefore, we may say that the interaction must be occurred through the nucleophilic groups, ion-ion or ion-dipole interactions. A schematic representation of the plausible interaction is represented in **Scheme I**.

The parameter, S_V^*, is the volumetric virial coefficient that characterizes the pair-wise interaction of solvated species in solution [11-14]. The sign of S_V^* is determined by the interaction between the solute species. In the present study S_V^* values were found to be negative and decrease with the increase in the concentration of the nicotinic acid solution. This trend in S_V^* values indicates weak solute-solute interactions in the mixtures. A quantitative comparison of the magnitude of values shows that ϕ_V^0 values are much greater in magnitude than those of S_V^* for all the solutions. These suggest that solute-solvent interactions dominate over solute-solute interactions in all the solutions. Again, the S_V^* values decrease with the increase in the concentration of the nicotinic acid solution which may be attributed due to the increase in the solute-solvent interaction.

The viscosity data of the experimental solutions have been analyzed using the Jones–Dole equation [15]

$$(\eta/\eta_0 - 1)/\sqrt{m} = (\eta_r - 1)/\sqrt{m} = A + B\sqrt{m} \qquad (4)$$

where $\eta_r = \eta/\eta_0$, and η are the viscosities of the solvent and solution respectively, and m is the molality of a solution. A and B are the Jones-Dole [15] constants indicating the solute-solute and solute-solvent interaction respectively, estimated by

a least-squares method and reported in Table 3. The values of the *A*-coefficient are found to decrease with the increase in the concentration of the nicotinic acid solution for each amino acid and with increase in alkyl chain in amino acids. These results are in excellent agreement with those obtained from S_v^* values which indicate that the solute-solute interaction decreases with the increase in the concentration of the nicotinic acid solutions. Also the solute-solute interaction is more in case of glycine compared to the other two amino acids in all the concentration of nicotine acid solutions. The viscosity *B*-coefficient [16, 17] is a valuable tool to provide information concerning the solvation of solutes and their effects on the structure of the solvent in the local vicinity of the solute molecules. The viscosity *B*-coefficient reflects the solute-solvent interactions on the solutions. From the Figure 2 it is evident that the *B*-coefficients of amino acids in the aqueous nicotinic acid solution suggests the presence of strong solute-solvent interactions, and these type of interactions are strengthened with the increase in the concentration of the nicotinic acid solution and with increase in alkyl chain in amino acids. Thus the trend in viscosity *B*-coefficient is

L-valine > L-alanine > glycine

The solute-solvent interaction is more in case of L-valine compared to the other two amino acids in all the concentration of nicotine acid solutions. These conclusions are in excellent agreement with the results drawn from the limiting apparent molar volume, ϕ_v^0, discussed earlier.

The molar refraction *R* can be evaluated from the Lorentz-Lorenz relation [18]

$$R = \{(n_D^2-1)/(n_D^2+2)\}\ (M/\rho) \qquad (5)$$

where *R*, n_D, M and ρ are the molar refraction, refractive index, molar mass and density of solution respectively. The refractive index of a substance is defined as the ratio c_0/c, where c is the speed of light in the medium and c_0 the speed of light in vacuum. Stated more simply, the refractive index of a compound describes its ability to refract light as it moves from one medium to another and thus, the higher the refractive index of a compound, the more the light is refracted [18]. As stated by Deetlefs et al. [19] the refractive index of a substance is higher when its molecules are more tightly packed or in general when the compound is denser. Hence a perusal of Table 4 we found that the refractive index and molar refraction are higher for L-

Valine in nicotinic acid solution indicating the fact that the valine are more interact with the nicotinic acid in solution or tightly packed in the solution. As R is directly proportional to molecular polarisability, it is evident from the Table 4 that the overall polarisability of the studied amino acids increases with the increase in the concentration of the nicotinic acid in solution, leading to more solute-solvent interaction. The molecular polarisability is higher for L-Valine compared to the other two amino acids in all the concentration of nicotine acid solutions. This shows that L-Valine is more solvated by the aqueous solution of nicotinic acid rendering to high solute-solvent interaction.

The Limiting apparent molar adiabatic compressibility (ϕ_K^0) is another tool, which also deals the ion-solvent interaction in solution. For this reason, the adiabatic compressibility (β_S) was evaluated from the following equation:

$$\beta_S = 1/u^2\rho \tag{6}$$

where ρ is the density of solution and u is the speed of sound in the solution. Using β_S values, the apparent molar adiabatic compressibility (ϕ_K) of the solutions was determined from the relation,

$$\phi_K = M\beta_S/\rho + 1000(\beta_S\rho_o - \beta_o\rho)\ /m\rho\rho_o \tag{7}$$

where β_0, β_S are the adiabatic compressibility of the solvent and solution respectively and m is the molality of the solution. After that the limiting apparent molar adiabatic compressibilities (ϕ_K^0) and experimental slopes (S_K^*) were obtained by fitting ϕ_K against the square root of molarity ($\sqrt{m}$) of the amino acids using the method of least squares.

$$\phi_K = \phi_K^0 + S_K^* \cdot \sqrt{m} \tag{8}$$

The values of β_S and ϕ_K are reported in Table 5. Since the values of ϕ_K^0 and S_K^* are measures of solute-solvent and solute-solute interactions respectively, a perusal of Table 5 and Figure 3 the values of ϕ_K^0 increases from glycine to L-valine; which shows that the solute-solvent interaction is highest in case of L-valine in comparison to glycine and L-alanine in all the concentration of nicotine acid solutions and the solute-solvent interaction increases with the increase in the concentration of the

nicotinic acid solutions. From the S_K^* values it was seen that the solute-solute interaction is highest in case of glycine and the values decrease with the increase in the nicotinic acid solution. The values are in agreement with results drawn from the values of ϕ_V^0 and S_V^* discussed earlier.

9.4 Conclusion:

In summary, ϕ_V^0 and viscosity *B*-coefficient values for amino acids indicate the presence of strong solute-solvent interactions and these interactions are further strengthened at higher concentration of aqueous nicotinic acid solution. The solute-solvent interaction is dominant over the solute-solute interaction for all the amino acids in all the aqueous solution of nicotinic acid. The molecular polarisability is higher for L-valine leading to more solute-solvent interaction compared to the other two amino acids. ϕ_K^0 and *R* also supports the same fact.

Tables:

Table 1. The values of density (ρ), viscosity (η), refractive index (n_D), and speed of sound (u) in different mass fractions (m_1) of aqueous nicotinic acid (NA) solutions at 298.15K.

Mass fraction of NA	ρ x 10^{-3} (kg m^{-3})	η (mPa s)	n_D	u (ms^{-1})
$m_1 = 0.01$	0.99757	0.817	1.3320	1492.8
$m_1 = 0.03$	0.99841	0.823	1.3326	1495.7
$m_1 = 0.05$	0.99922	0.828	1.3332	1498.4

Table 2. Values of concentration, density (ρ), apparent molar volume, limiting apparent molar volume and experimental slope (obtained from eq. 3) of glycine, L-alanine and L-valine in different mass fractions (m_1) of aqueous nicotinic acid solutions at 298.15K.

molality (mol kg^{-1})	ρx 10^{-3} (kg m^{-3})	ϕ_V x 10^6 (m^3 mol^{-1})	$^a\phi_V^0$ x 10^6 (m^3 mol^{-1})	S_V^* x 10^6 (m^3 mol$^{-3/2}$ kg$^{1/2}$)
		m_1 = 0.01		
		Glycine		
0.0100	0.99782	50.19		
0.0251	0.99823	48.79		
0.0402	0.99866	47.94	52.38	−22.22
0.0553	0.99911	47.18		
0.0704	0.99958	46.47		
0.0855	1.00006	45.89		
		L-Alanine		
0.0100	0.99778	68.26		
0.0251	0.99814	66.45		
0.0402	0.99853	65.25	71.10	−28.97
0.0553	0.99894	64.33		
0.0705	0.99938	63.38		
0.0857	0.99983	62.65		
		L-Valine		
0.0100	0.99771	103.40		
0.0251	0.99798	100.99		
0.0403	0.99829	99.39	107.10	−38.05
0.0554	0.99863	98.11		
0.0707	0.99899	97.10		
0.0859	0.99939	95.97		
		m_1 = 0.03		
		Glycine		
0.0100	0.99860	56.15		
0.0251	0.99892	54.75		
0.0401	0.99927	53.65	58.68	−25.03
0.0552	0.99964	52.79		
0.0704	1.00003	52.00		
0.0855	1.00043	51.38		

Communicated

		L-Alanine		
0.0100	0.99855	75.20		
0.0251	0.99881	73.20		
0.0402	0.99911	71.70	78.87	−35.97
0.0553	0.99944	70.47		
0.0705	0.9998	69.34		
0.0856	1.00019	68.25		
		L-Valine		
0.0100	0.99847	111.32		
0.0251	0.99864	108.12		
0.0402	0.99887	105.81	116.70	−54.74
0.0554	0.99915	103.86		
0.0706	0.99947	102.16		
0.0859	0.99981	100.83		
		$m_1 = 0.05$		
		Glycine		
0.0100	0.99936	61.11	64.21	−31.67
0.0251	0.99962	59.11		
0.0401	0.99991	57.86		
0.0552	1.00023	56.75		
0.0703	1.00057	55.82		
0.0855	1.00093	54.99		
		L-Alanine		
0.0100	0.99926	85.15		
0.0251	0.99939	82.35		
0.0402	0.99957	80.40	89.85	−47.14
0.0553	0.99979	78.78		
0.0704	1.00005	77.29		
0.0856	1.00033	76.09		
		L-Valine		
0.0100	0.99920	119.24		
0.0251	0.99928	114.83		
0.0402	0.99944	111.73	126.3	−72.13
0.0554	0.99965	109.41		
0.0706	0.99993	107.09		
0.0858	1.00023	105.34		

[a] The values have been tally with the Ref. [20].

Table 3. Values of concentration, viscosity (η), $(\eta/\eta_0-1)/m^{1/2}$, Viscosity *A*, *B* coefficients of L -glycine, L-alanine, and L-valine in different mass fractions (m_1) of aqueous nicotinic acid solutions at 298.15K.

molality (mol kg^{-1})	η (mPas)	$(\eta/\eta_0-1)/m^{1/2}$ (kg$^{1/2}$ mol$^{-1/2}$)	*A* (kg mol^{-1})	^{a}B (kg$^{1/2}$ mol$^{-1/2}$)
		m_1 = 0.01		
		Glycine		
0.0100	0.825	0.098		
0.0251	0.832	0.116		
0.0402	0.838	0.128	0.068	0.299
0.0553	0.844	0.141		
0.0704	0.849	0.148		
0.0855	0.854	0.155		
		L-Alanine		
0.0100	0.825	0.098		
0.0251	0.833	0.124		
0.0402	0.840	0.140	0.054	0.430
0.0553	0.847	0.156		
0.0705	0.854	0.171		
0.0857	0.860	0.180		
		L-Valine		
0.0100	0.827	0.1222		
0.0251	0.839	0.1699		
0.0403	0.850	0.2013	0.049	0.752
0.0554	0.861	0.2287		
0.0707	0.871	0.2487		
0.0859	0.881	0.2673		
		m_1 = 0.03		
		Glycine		
0.0100	0.830	0.085		
0.0251	0.837	0.107		
0.0401	0.843	0.121	0.052	0.337
0.0552	0.849	0.134		
0.0704	0.854	0.142		
0.0855	0.859	0.150		

		L-Alanine		
0.0100	0.832	0.109		
0.0251	0.842	0.146		
0.0402	0.852	0.176	0.043	0.657
0.0553	0.862	0.202		
0.0705	0.871	0.220		
0.0856	0.879	0.233		
		L-Valine		
0.0100	0.832	0.109		
0.0251	0.844	0.161		
0.0402	0.855	0.194	0.030	0.810
0.0554	0.866	0.222		
0.0706	0.877	0.247		
0.0859	0.887	0.265		
		$m_1 = 0.05$		
		Glycine		
0.0100	0.831	0.036		
0.0251	0.836	0.061		
0.0401	0.841	0.078	−0.004	0.412
0.0552	0.846	0.093		
0.0703	0.851	0.105		
0.0855	0.856	0.116		
		L-Alanine		
0.0100	0.831	0.036		
0.0251	0.838	0.076		
0.0402	0.846	0.108	−0.039	0.741
0.0553	0.854	0.134		
0.0704	0.863	0.159		
0.0856	0.871	0.177		
		L-Valine		
0.0100	0.832	0.048		
0.0251	0.843	0.114		
0.0402	0.854	0.157	−0.062	1.099
0.0554	0.866	0.195		
0.0706	0.878	0.227		
0.0858	0.892	0.264		

[a] The values have been tally with the Ref. [20].

Table 4. Values of concentration, refractive indices (n_D) and molar refraction (R) of of Glycine, L-alanine and L-valine in different mass fractions (m_1) of aqueous nicotinic acid solutions at 298.15K

molality (mol kg^{-1})	n_D	R (cm^3 mol^{-1})	molality (mol kg^{-1})	n_D	R (cm^3 mol^{-1})	molality (mol kg^{-1})	n_D	R (cm^3 mol^{-1})
				m_1 = 0.01				
	Glycine			L-Alanine			L-Valine	
0.0100	1.3323	15.45	0.0100	1.3323	18.33	0.0100	1.3324	24.11
0.0251	1.3327	15.46	0.0251	1.3328	18.35	0.0251	1.3328	24.13
0.0402	1.333	15.46	0.0402	1.3332	18.36	0.0403	1.3332	24.15
0.0553	1.3333	15.47	0.0553	1.3336	18.37	0.0554	1.3335	24.16
0.0704	1.3336	15.47	0.0705	1.334	18.39	0.0707	1.3338	24.17
0.0855	1.3339	15.48	0.0857	1.3343	18.39	0.0859	1.3341	24.18
				m_1 = 0.03				
	Glycine			L-Alanine			L-Valine	
0.0100	1.3332	15.47	0.0100	1.333	18.35	0.0100	1.3331	24.14
0.0251	1.3338	15.49	0.0251	1.3337	18.38	0.0251	1.3337	24.18
0.0401	1.3343	15.51	0.0402	1.3343	18.41	0.0402	1.3341	24.20
0.0552	1.3348	15.52	0.0553	1.3348	18.43	0.0554	1.3345	24.22
0.0704	1.3352	15.53	0.0705	1.3352	18.44	0.0706	1.3349	24.23
0.0855	1.3356	15.54	0.0856	1.3356	18.45	0.0859	1.3353	24.25
				m_1 = 0.05				
	Glycine			L-Alanine			L-Valine	
0.0100	1.3338	15.49	0.0100	1.3338	18.38	0.0100	1.3342	24.20
0.0251	1.3345	15.51	0.0251	1.3346	18.42	0.0251	1.3351	24.25
0.0401	1.3351	15.53	0.0402	1.3352	18.44	0.0402	1.3359	24.30
0.0552	1.3355	15.54	0.0553	1.3358	18.47	0.0554	1.3365	24.34
0.0703	1.336	15.56	0.0704	1.3363	18.49	0.0706	1.3371	24.37
0.0855	1.3364	15.57	0.0856	1.3368	18.51	0.0858	1.3376	24.39

Table 5. Values of concentration, ultrasonic speed (u), adiabatic compressibility (β), apparent molar adiabatic compressibility (ϕ_K), limiting apparent molar adiabatic compressibility (ϕ_K^0), and experimental slope (S_K^*) (obtained from eq. 8) of Glycine, L-alanine, and L-valine in different mass fractions (m_1) of aqueous nicotinic acid solutions at 298.15K

molality (mol kg^{-1})	u (m s^{-1})	β x 10^{10} (Pa^{-1})	ϕ_K x 10^{10} (m^3 mol^{-1} Pa^{-1})	ϕ_K^0 x 10^{10} (m^3 mol^{-1} Pa^{-1})	S_K^* x 10^4 (m^3 mol$^{-3/2}$ Pa^{-1} kg$^{1/2}$)
			m_1 = 0.01		
			Glycine		
0.0100	1495.8	4.4792	-2.3674		
0.0251	1504.4	4.4263	-3.7936		
0.0402	1516.7	4.3529	-4.7626	0.107	−17.65
0.0553	1531.8	4.2656	-5.6308		
0.0704	1550.4	4.1619	-6.3018		
0.0855	1571.3	4.0500	-6.9824		
			L-Alanine		
0.0100	1494.6	4.4865	-1.7987		
0.0251	1502.3	4.4391	-3.2169		
0.0402	1514.2	4.3678	-4.2272	1.145	−20.32
0.0553	1529.1	4.2818	-5.0864		
0.0705	1546.6	4.1832	-5.9037		
0.0857	1568.2	4.0669	-6.6275		
			L-Valine		
0.0100	1493.7	4.4923	-1.0809		
0.0251	1500.8	4.4486	-2.5738		
0.0403	1512.1	4.3810	-3.6863	2.062	−22.48
0.0554	1527.1	4.2939	-4.5725		
0.0707	1544.7	4.1951	-5.3977		
0.0859	1565.9	4.0807	-6.1489		
			m_1 = 0.03		
			Glycine		
0.0100	1499.3	4.4548	-2.5846		
0.0251	1510.4	4.3881	-4.1839		
0.0401	1526.2	4.2962	-5.2589	0.194	−22.15
0.0552	1546.0	4.1854	-6.1701		
0.0704	1568.3	4.0656	-7.0559		

0.0855	1595.2	3.9281	-7.7790		
			L-Alanine		
0.0100	1498.4	4.4604	-2.0036		
0.0251	1508.1	4.4020	-3.6683		
0.0402	1522.5	4.3178	-4.8442	1.631	−25.83
0.0553	1541.2	4.2123	-5.8090		
0.0705	1565.1	4.0832	-6.6564		
0.0856	1591.5	3.9473	-7.4649		
			L-Valine		
0.0100	1497.5	4.4661	-1.2925		
0.0251	1506.3	4.4133	-3.0819		
0.0402	1520.5	4.3303	-4.3159	2.538	−27.82
0.0554	1539.2	4.2245	-5.3670		
0.0706	1562.1	4.1002	-6.2677		
0.0859	1588.1	3.9657	-7.0826		
			$m_1 = 0.05$		
			Glycine		
0.0100	1503.7	4.4254	-2.8085		
0.0251	1516.8	4.3481	-4.5722		
0.0401	1535.6	4.2411	-5.8505	0.390	−26.72
0.0552	1559.2	4.1124	-6.9133		
0.0703	1588.0	3.9632	-7.7756		
0.0855	1620.3	3.8054	-8.6352		
			L-Alanine		
0.0100	1501.8	4.4370	-2.1905		
0.0251	1513.5	4.3681	-4.0256		
0.0402	1532.1	4.2619	-5.2728	2.168	−32.21
0.0553	1556.2	4.1300	-6.3868		
0.0704	1585.1	3.9798	-7.3201		
0.0856	1618.4	3.8166	-8.2226		
			L-Valine		
0.0100	1500.9	4.4426	-1.4384		
0.0251	1511.4	4.3808	-3.3035		
0.0402	1529.1	4.2792	-4.6369	3.136	−34.33
0.0554	1552.5	4.1503	-5.7678		
0.0706	1581.4	3.9989	-6.7293		
0.0858	1615.9	3.8288	-7.6119		

Figures:

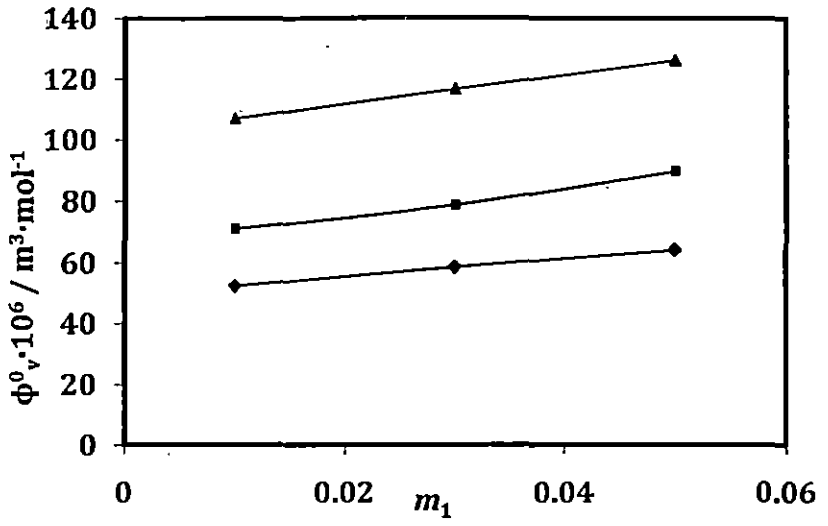

Figure 1: Plot of $\phi_v^\circ \cdot 10^6/m^3 \cdot mol^{-1}$ of Glycine (—▯—), L-Alanine (—■—) and L-Valine (—▲—) in different mass fractions (m_1)of aqueous nicotinic acid solutions at 298.15K.

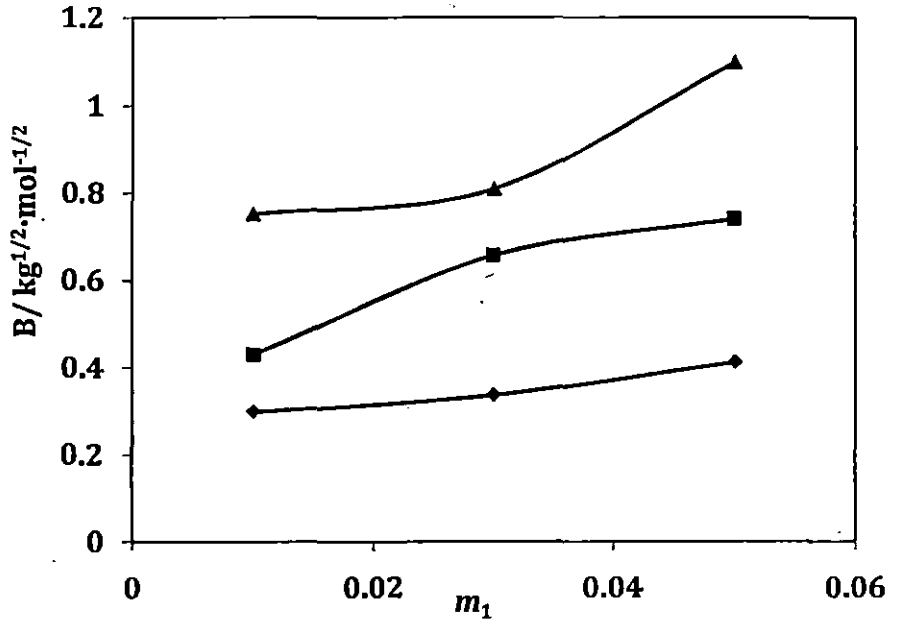

Figure 2: Plot of $B/kg^{1/2}$ $mol^{-1/2}$ of Glycine (—♦—), L-Alanine (—■—) and L-Valine (—▲—) in different mass fractions (m_1)of aqueous nicotinic acid solutions at 298.15K.

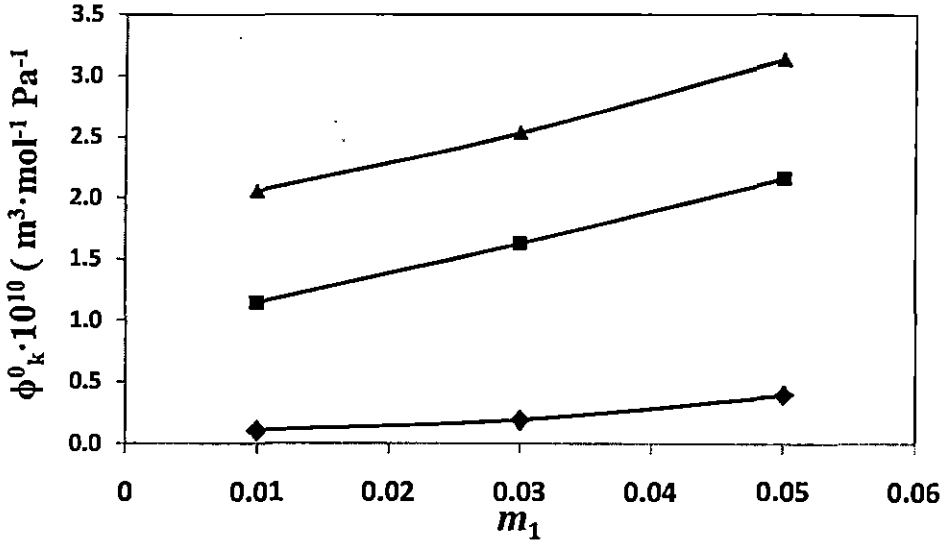

Figure 3: Plot of ϕ_K x 10^{10} (m^3 mol^{-1} Pa^{-1}) of Glycine (—▫—), L-Alanine (—■—) and L- Valine (—▲—) in different mass fractions (m_1) of aqueous nicotinic acid solutions at 298.15K

Scheme:

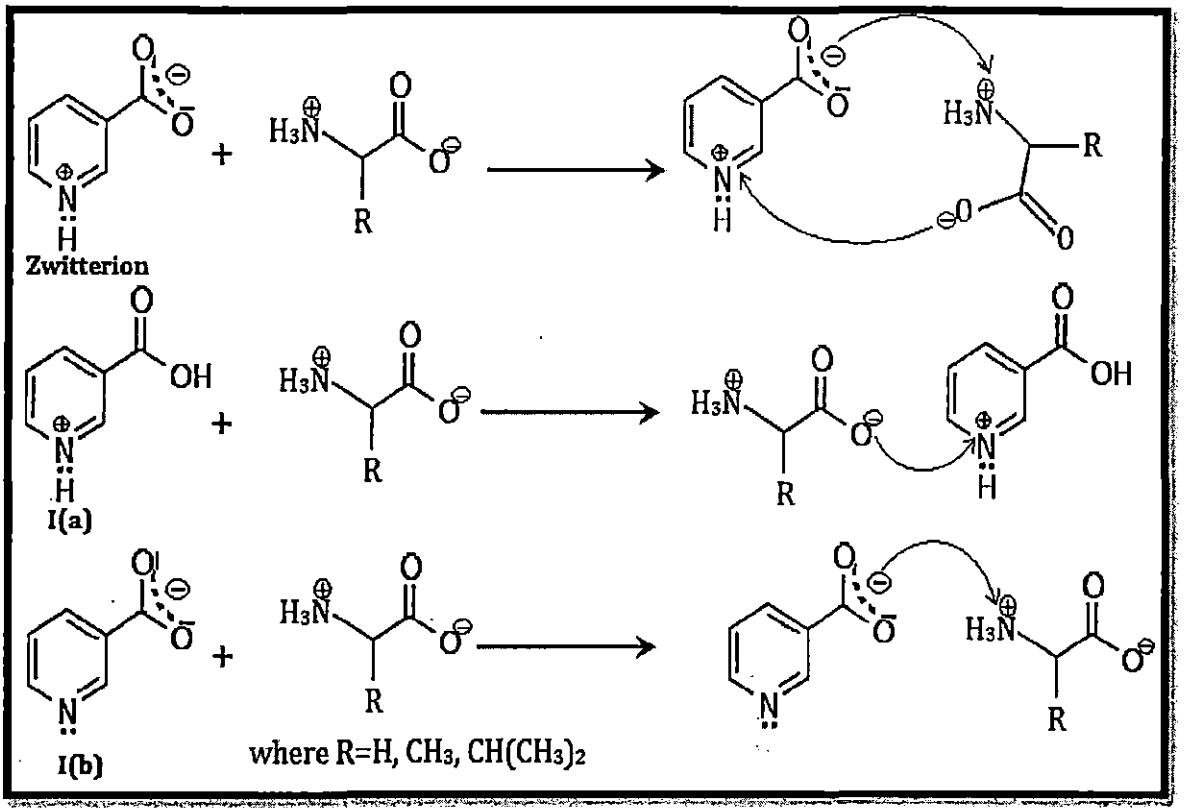

Scheme I: A schematic representation of the plausible interaction amino acids with nicotinic acids in aqueous solution

CHAPTER X

CONCLUDING REMARKS

In this research work, I have tried to investigate the interaction of some vitamins with some solution systems. Molecular interactions have been studied with the help of thermodynamic and transport properties of solutions. Various types of interactions exist in solution ,of these, solute-solute and solute-solvent interactions are of much interest in all branches of chemistry. Such a study will find importance in chemical engineering areas and pharmaceutical industry.

In this **chapter IV**, we have analyzed molecular interaction prevailing in α-amino acids (glycine, L-alanine, L-valine) and aqueous solution of Folic acid (FA) physico-chemical properties as density (ρ), viscosity (η), refractive index (n_D) and ultrasonic speed (u) at 298.15 K. The role of the cosolute (FA), and the contribution of solute-solute and solute-solvent interactions to the solution complexes, has also been analyzed through the derived properties. We have tried to find out the trends in transfer volumes, $\Delta\phi_V^\circ$, which have been interpreted in terms of solute-cosolute interactions on the basis of a cosphere overlap model. Our analysis revealed that strong solute-solvent interaction predominates.

In **chapter V**, precise electrical conductance measurements are reported for some ethanoates, viz. ammonium, lithium, sodium and potassium in pure tetrahydrofuran (THF) and dimethyl sulphoxide (DMSO) and their binary mixtures at 298.15 K. The conductance data have been analyzed by the Fuoss conductance-concentration equation in terms of the limiting molar conductance (Λ_0), the thermodynamic association constant (K_A) and the association diameter (R). The limiting ionic conductances have been estimated from the appropriate division of the limiting molar conductivity value of the "reference electrolyte" Bu_4NBPh_4. It was concluded that the ion-pair and triple-ion formation of salt depends on the size, the charge distribution of the ions and also the relative permittivity of the solvent mixtures. Here too the classical Fuoss-Kraus theory of triple-ion formation which occurs in low dielectric solvent was found to be valid in the study.

The apparent molar volume (ϕ_V), viscosity *B*-coefficient and molal refraction (R) of some carbohydrates (D-Glucose, D-Sucrose, and D-Maltose monohydrate) have been determined in 0.01, 0.03, 0.05 mol·dm^{-3} aqueous ascorbic acid solutions at 298.15 K from the experimental density (ρ), viscosity (η) and refractive index (n_D) values respectively in **chapter VI.** Solute-solvent and solute-solute interaction pattern, we have tried to interpret using Massion equation. From different measurements we have concluded that solute-solvent interaction dominates.

In **chapter VII** apparent molar volumes (V_ϕ), viscosity *B*-coefficients for Nicotinamide (NA) in (0.03, 0.05, 0.07 and 0.10) mol·dm^{-3} aqueous Citric Acid monohydrate (CA) solutions have been determined from solution density and viscosity measurements at (298.15, 308.15 and 318.15) K as function of concentration of NA. The structure making or breaking ability of NA has been discussed. V_ϕ^0 and viscosity *B*-coefficient values for NA indicate the presence of strong solute–solvent interactions and these interactions are further strengthened at higher temperatures and higher concentration of CA in the ternary solutions. This study also reveals that NA acts as a water-structure promoter due to hydrophobic hydration in the presence of CA and CA has a dehydration effeect on the hydrated NA.

Here, In **chapterVIII** apparent molar volume (ϕ_V), viscosity *B*-coefficient, molal refraction (R) and adiabatic compressibility (ϕ_K) of Nicotinic Acid, Ascorbic Acid, and Folic Acid have been determined in 0.01, 0.03, 0.05 mol·dm^{-3} aqueous Cysteine solutions at 298.15 K from density (ρ), viscosity (η), refractive index (n_D) and speed of sound (u) respectively. We have investigated presence of strong solute-solvent interactions which increases with the increase in the interactive centres of vitamins and with increase of mass fraction of cysteine in the aqueous mixture. The refractive index and the molar refraction values imply that Folic Acid molecules are more tightly packed in the solution leading to higher solute-solvent interaction than the other vitamins.

In this **chapter IX** we have tried to find molecular interaction in terms of apparent molar volume (ϕ_V), viscosity *B*-coefficient, apparent molar adiabatic compressibility (ϕ_K) and molar refraction (R) of Glycine, L-Alanine, L-Valine in 0.01, 0.03, 0.05 mass fraction of aqueous nicotinic acid solutions at 298.15 K.

Analysing experimental results we have found that solute-solvent interaction is dominant over the solute-solute interaction for all the amino acids in all the aqueous solution of nicotinic acid. The molecular polarisability is higher for L-valine leading to more solute-solvent interaction compared to the other two amino acids. ϕ_K^0 and R also supports the same fact.

It is necessary to remember that molecular interactions are very complex in nature. There are strong forces existing in the molecule and it is not really possible to separate them all. Nevertheless, if careful judgement is used, valid conclusions can be drawn in many cases relating to degree of structure and order of the system. More extensive studies of the different thermodynamic properties will be of sufficient help in understanding the nature of the solute-solvent interactions and the role of solvents in different chemical processes.

In the near future we endeavour to extend our research work which I hope will certainly compliment our present findings.

BIBLIOGRAPHY

References of Chapter I

1. A.S. Fauci, E. Braunwald, K.J. Isselbacher, J.D. Wilson, J.B. Martin, D.L. Kasper, S.L. Hauser, D.L. Long, Harrison's Principles of Internal Medicine, 14th ed., (McGraw-Hill, New York,(**1998**).
2. A.K. Covington, T. Dickinson, *Physical Chemistry of Organic Solvent Systems,* Plenum, New York, (**1973**).
3. P. Pradhan, R.S. Sah, M.N. Roy, *Journal of Molecular Liquids,* 144 (**2009**) 149.
4. A. Ali, A.K. Nain, *J. Pure. Appl. Ultrasonics.,* 22 (**2000**) 121.
5. J.H. Dymond, *Chem. Soc. Rev.,* 14 (**1985**) 417.
6. B. Giner, S. Martin, H. Artigas, M.C. Lopez, C.J. Lafuente, *Phys. Chem. B.,* 110 (**2006**) 17683.
7. B. Garcia, R. Alcalde, S. Aparicio, J.M. Leal, *Phys. Chem. Chem. Phys.,* 4 (**2002**) 5833.
8. M.I. Aralaguppi, T.M. Aminabhavi, S.B. Harogoppad, R.H. Balundgi, *J. Chem Eng. Data,* 37 (**1992**) 298.
9. A.F. Fucaloro, *J. Chem. Educ.,* 79 (**2002**) 865.
10. B.Giner, C. Lafuente, A. Villares, M. Haro, M.C. Lopez, *J. Chem. Thermodyn.,* 3 (**2007**) 148.
11. A. Pineiro, P. Brocos, A. Amigo, M. Pintos, R. Bravo, *Phys. Chem. Liq., 38* (**2000**) 251.
12. G.S. Kell, C. M. Daries, J. Jarynski, *Water and Aqueous Solution, Structure, Thermodynamics and Transport Process,* Ed. R. A. Horne, Wiley, (**1972**), Chapters 9 and 10.
13. Faraday, *Discussion of the Chemical Society,* No.67 (**1977**).
14. E.L. Herric, J.G. Brewer, *J. Chem. Eng. Data.,* 14 (**1969**) 55.
15. P.K. Gessner, M.P. Shakarjian, *J. Pharm. Exptal. Therap.,* 235 (**1988**) 32.

References of Chapter II

1. F. A. Robinson, *"The Vitamin B-Complexes"*, 4th ed., Chapman & Hall, London, (**1951**).
2. S. Cakir, I. Bulut, E. Bicer, O. Cakir, *J. Coord. Chem.* 56 (**2003**) 511.
3. A.N. Nesmeyanov, N.A. Nesmeyanov, *Fundamentals of Organic Chemistry*, vol.3, p. 393, Mir, Moscow,(**1981**)
4. A.S. Fauci, E. Braunwald, K.J. Isselbacher, J.D. Wilson, J.B. Martin, D.L. Kasper, S.L. Hauser, D.L. Long, *Harrison's Principles of Internal Medicine*, 14th ed., McGraw-Hill, New York, (**1998**).
5. C.R.W. Edwards, I.A.D. Bouchier, C. Haslett, E.R. Chilvers, *Davidson's Principles and Practice of Medicine*, 17th ed., BPC Paulton Books Limited, Great Britain, (**1996**).
6. C. Chahidi, M. Aubailly, A. Momzikoff, and M. Bazin, *Photochem. Photobiol.* 33 (**1981**) 641.
7. S.W. Bailey and J.E. Ayling, *Proceedings of the National Academy of Sciences of the United States of America* 106 (36) (**2009**) 15424.
8. S.J. Weinstein, T.J. Hartman and R. Stolzenberg-Solomon, *Cancer Epidemiol. Biomarkers Prev.* 12 (**2003**) 1271.
9. "Dietary Supplement Fact Sheet: Folate", Office of Dietary Supplements, National Institutes of Health, http://ods.od.nih.gov/factsheets/folate.asp
10. B. Kamen, *Semin. Oncol.* 24 (**1997**) 18.
11. *"The primary structure of proteins is the amino acid sequence". The Microbial World.* University of Wisconsin-Madison Bacteriology Department. Retrieved 16 September (2012)
12. J. J. Lagowski, *The Chemistry of Non-Aqueous Solvents, Academic*, New York (**1966**).
13. B.E. Conway, R.G. Barradas, *Chemical Physics of Ionic Solutions*, Wiley, New York (**1966**).
14. D.T. Richens, *The Chemistry of Aqua Ions*; Wiley, New York (**1997**).
15. K. Ibuki, M. Nakahara, *J. Phys. Chem.*, 94 (**1990**) 8370.
16. A. Henni, J.H. Jonathan, T. Paitoon, C. Amit, *J. Chem. Eng. Data*, 48 (**2003**) 1062.
17. J. Burgess, *Metal Ions in Solutions*; Ellis Horwood, New York (**1978**).

18. H.S. Harned, B.B. Owen, *The Physical Chemistry of Electrolytic Solutions*, Reinhold Publishing Corporation, New York (**1958**).
19. J. J. Lagowski, *The Chemistry of Non-Aqueous Solvents, Academic*, New York (**1966**).
20. B.E. Conway, R.G. Barradas, *Chemical Physics of Ionic Solutions*, Wiley, New York (**1966**).
21. J.S. Muishead-Gould, K.J. Laidler, *Chemical Physics of Ionic Solutions*, Wiley, New York (**1966**).
22. J.F. Coetzee, C.D. Ritchie, *Solute-Solvent Interactions*, Marcel Dekker, New York (**1969**).
23. R.G. Bates, *J. Electroanal. Chem.*, 29 (**1972**) 1.
24. G.S. Kell, C.M. Daries, J. Jarynski, *Water and Aqueous Solutions, Structure, Thermodynamics and Transport process*, Wiley, New York (**1972**).
25. E.S. Amis, J.F. Hinton, *Solvent effects on Chemical Phenomena*, Academic, New York (**1973**).
26. A.K. Covington, T. Dickinson, *Physical Chemistry of Organic Solvent Systems*, Plenum Press, New York (**1973**).
27. J.E. Gordon, *The Organic Chemistry of Electrolyte Solutions*, Wiley-Interscience, New York (**1975**).
28. F. Franks, *Physico-Chemical processes in Mixed Aqueous Solvents*, Heinemann, London (**1967**).
29. F. Franks, *Water–A Comprehensive Treatise*, Plenum Press, New York (**1973**).
30. V. Gutmann, *Electrochim. Acta.*, 21 (**1967**) 661.
31. U. Mayer, V. Gutmann, *Adv. Inorg.Chem. Radiochem.*, 17 (**1975**) 189.
32. R.G. Pearson, *Hard and Soft Acids and Bases*, Strondsburgh (**1973**).
33. G.R. Behbehani, M. Dillon, J. Symth, W.E. Waghorne, *J. Solution Chem.*, 31 (**2002**) 811.
34. C. Guha, J.M. Chakraborty, S. Karanjai, B. Das, *J. Phys. Chem. B*, 107 (**2003**) 12814.
35. L. Jones, J.F. Devonshire, *A. F. Proc. Royal Soc.*, (**1937**).
36. I. Prigogine, S. Garikian, *Physica*, 16 (**1950**) 239.
37. I. Prigogine, A. Belleman, *J. Phys. Chem.*, 21 (**1953**) 561.
38. A.J. Treszczanowicz, G.C. Benson, *Fluid Phase Equilib.*, 23 (**1985**) 117.

39. Wen-Lu Weng, *J. Chem. Eng. Data*, 45 (**2002**) 606.
40. P.S. Nikam, S.J. Kharat, *J. Chem. Eng. Data*, 50 (**2005**) 455.
41. R.P. Rastogi, J. Nath, J. Mishra, *J. Phys. Chem.*, 71 (**1966**) 1277.
42. K.S. Pitzer, G. Mayora, *J. Phys. Chem.*, 77 (**1973**) 2300.
43. D. Cook, L-Higgins, *H. C. Proc. Royal. Soc.*, A209 (**1951**) 28.
44. J.S. Rowlinson, *Liquid and Liquid Mixtures*, Scientific Publications, London (**1959**).
45. J.S. Rowlinson, *Proc. Royal. Soc.*, A214 (**1952**) 192.
46. J.L. Lebowitz, J. S. Rowlinson, *J. Chem. Phys.*, 41 (**1964**) 133.
47. J.A. Barker, D.J. Henderson, *J. Phys. Chem.*, 47 (**1967**) 4714.
48. P.J. Flory, R.A. Orwoll, A. Vrij, *J. Am. Chem. Soc.*, 86 (**1964**) 3507.
49. P.J. Flory, A. Abe, *J. Am. Chem. Soc.*, 86 (**1964**) 3563.
50. P.J. Flory, *J. Am. Chem. Soc.*, 87 (**1965**) 1833.
51. D. Patterson, G. Delmas, *Discuss. Faraday Soc.*, 49 (**1970**) 98.
52. A. Heintz, *Ber. Bunsenges. J. Phys.*, 89 (**1985**) 172.
53. H. Funke, M. Wetzel, A. Heintz, *J. Pure. Appl. Chem.*, 61 (**1989**) 1429.
54. A. Heintz, D. Papaioannou, *Thermochimica Acta.*, 310 (**1998**) 69.
55. A. Heintz, P.K. Naicker, S.P. Verevkin, R. Pfestrof, B. Bunsenges, *Phys. Chem.*, 102 (**1998**) 953.
56. S. Villa, N. Riesco, I. Garcia de la Fuente, J.A. Gonzalz, J.C. Cobos, *Fluid Phase Equilib.*, 216 (**2004**) 123.
57. S.L. Oswal, J.*Thermochim. Acta.*, 425 (**2005**) 59.
58. A. Pineiro, A. Amigo, R. Bravo, P. Brocos, *Fluid Phase Equilib.*, 173 (**2000**) 211.
59. A.Pineiro, *Fluid Phase Equilib.*, 216 (**2004**) 245.
60. M. Gepert, B. Stachowska, *J. Sol. Chem.*, 35 (**2006**) 425.
61. H.S. Harned, B.B. Owen, *The Physical Chemistry of Electrolyte Solutions*, Reinhold Publishing Corporation, New York (**1943**).
62. C. Tanford, *Hydrophobic Effect: Formation of Micelles and Biological Membranes*, Wiley-Interscience, New York (**1980**).
63. E. Vikingstad, *Aggregation Process in Solutions*, Elsevier, Amsterdam (**1983**).
64. J.E. Desnoyers, M. Arel, H. Perron, C. Jolicoenn, *J. Phys. Chem.*, 73 (**1969**) 3347.
65. A.K. Covington, T. Dickinson, *Physical Chemistry of Organic Solvent Systems*, Plenum Press, New York (**1973**).

66. D.K. Hazra, B. Das, *J. Chem. Eng. Data*, 36 (**1991**) 403.
67. D.O. Masson, *Phil. Mag.*, 8 (**1929**) 218.
68. O. Redlich, D.M. Meyer, *Chem. Rev.*, 64 (**1964**) 221.
69. B.B. Owen, S.R. Brinkley, *J. Ann. N. Y. Acad. Sci.*, 51 (**1949**) 753.
70. F.J. Millero, *Water and Aqueous Solutions: Structure, Thermodynamics and Transport Processes*, Wiley- Interscience, New York (**1972**).
71. R. Gopal, M.A. Siddiqi, *J. Phys. Chem.*, 73 (**1969**) 3390.
72. J. Padova, I. Abrahmen, *J. Phys. Chem.*, 71 (**1967**) 2112.
73. R. Gopal, D.K. Agarwal, R. Kumar, *Bull. Chem. Soc. Jpn.*, 46 (**1973**) 1973.
74. R. Gopal, P.P. Rastogi, *Z. Phys. Chem. (N.F.)*., 69 (**1970**) 1.
75. B. Das, D.K. Hazra, *J. Chem. Eng. Data*, 36 (**1991**) 403.
76. L. G. Hepler, *Can. J. Chem.*, 47 (**1969**) 4617.
77. R. Pogue, G. Atkinson, *J. Chem. Eng. Data*, 33 (**1988**) 370.
78. B.E. Conway, R.E. Verral, J.E. Desnoyers, *Trans. Faraday Soc.*, 62 (**1966**) 2738.
79. K. Uosaki, Y. Koudo, N. Tokura, *Bull. Chem. Soc. Jpn.*, 45 (**1972**) 871.
80. B.S. Krumgalz, *J. Chem. Soc. Faraday Trans. I*, 76 (**1980**) 1887.
81. A.W. Quin, D.F. Hoffmann, P. Munk, *J. Chem. Eng. Data*, 37 (**1992**) 55.
82. Z. Atik, *J. Sol. Chem.*, 33 (**2004**) 1447.
83. R.H. Stokes, R. Mills, *Viscosity of Electrolytes and Related Properties*, Pergamon, Great Britain (**1965**).
84. F. Vaslow, *Water and Aqueous Solutions*, Wiley- Interscience, New York (**1972**).
85. E.N.da C. Andrade, *Phil. Mag.*, 17 (**1934**) 698.
86. J. Frankel, *Kinetic Theory of Liquids*, Dover Publications, New York (**1955**).
87. R. Furth, *Proc. Camb. Phil. Soc.*, 37 (**1941**) 281
88. R. Furth, *Proc. Camb. Phil. Soc.*, 37 (**1941**) 252.
89. R.H. Ewell, H. Eyring, *J. Chem. Phys.*, 5 (**1937**) 726.
90. F.C. Auluck, S.C. De, D.S. Kothari, *Proc. Natl. Inst. Sci.*, 10(4) (**1944**) 397.
91. R. Eisenschitz, *Proc. Roy. Soc.*, 215A (**1952**) 29.
92. J.E. Lennard-Jones, A.F. Devonshire, *Proc. Roy. Soc.*, 163A (**1937**) 53.
93. J.E. Lennard-Jones, A.F. Devonshire, *Proc. Roy. Soc.*, 165A (**1938**) 1.
94. J.A. Pople, *Proc. Roy. Soc.*, 215A (**1952**) 67.
95. R. Eisenchitz, *Proc. Phys. Soc.*, 62A (**1949**) 41.

96. J.G. Kirkwood, *J. Chem. Phys.*, 14 (**1946**) 180.
97. J.G. Kirkwood, *Theory of Liquids*, Science Publishers, New York (**1968**).
98. J.E. Mayer, E. Montroll, *J. Chem. Phys.*, 9 (**1941**) 2.
99. J.E. Mayer, *J. Chem. Phys.*, 15 (**1947**) 187.
100. M. Born, H.S. Green, *Proc. Roy. Soc.*, 188A (**1946**) 10.
101. M. Born, H.S. Green, *Proc. Roy. Soc.*, 190A (**1947**) 455.
102. J.G. Kirkwood, F.P. Buff, M.S. Green, *J. Chem. Phys.*, 17 (**1949**) 988.
103. J.G. Kirkwood, *J. Chem. Phys.*, 3 (**1935**) 300.
104. J.G. Kirkwood, *J. Chem. Phys.*, 7 (**1939**) 919.
105. J.G. Kirkwood, Z.W. Salsburg, *Faraday Soc. Discuss.*, 15 (**1953**) 25.
106. J.G. Kirkwood, E.M. Boggs, *J. Chem. Phys.*, 10 (**1942**) 394.
107. J.G. Kirkwood, E.K. Maun, B.J. Alder, *J. Chem. Phys.*, 18 (**1950**) 1040.
108. J.G. Kirkwood, V.A. Lewinson, B.J. Alder, *J. Chem. Phys.*, 20 (**1952**) 929.
109. R.W. Zwanzig, J.G. Kirkwood, K.F. Stripp, I. Oppenheim, *J. Chem. Phys.*, 21 (**1953**) 2050.
110. S.A. Rice, P. Gray, *The Statistical Mechanics of Simple Liquids. An introduction to the theory of equilibrium and Non-equilibrium Phenomena*, Interscience Publishers, New York (**1965**).
111. S.A. Rice, *The Kinetic Theory of Dense Fluids, Colloquium Lecturers in Pure and Applied Science*, No. 9 Mobil Oil Corp. Research Lab., Dallas, Texas (**1964**).
112. S.A. Rice, A.R. Allnatt, *J. Chem. Phys.*, 34 (**1961**) 2144.
113. A.R. Allnatt, S.A. Rice, *J. Chem. Phys.*, 34 (**1961**) 2156.
114. H.C. Longuet-Higgins, J.P. Valleau, *Mol. Phys.*, 1 (**1958**) 284.
115. H.T. Davis, S.A. Rice, J.V. Sengers, *J. Chem. Phys.*, 35 (**1961**) 2210.
116. H.T. Davis, K.D. Luks, *J. Phys. Chem.*, 69 (**1965**) 869.
117. J.O. Hirschfelder, C.F. Curtis, R.B. Bird, *Molecular Theory of Gases and Liquids*, John Wiley and Sons, New York, (**1954**), reprinted with notes added (**1964**).
118. J.D. Rogers, F.G. Brickwedde, *Physica*, 32 (**1966**) 100.
119. J.P. Boon, G. Thomaes, *Physica*, 29 (**1963**) 208.
120. J.P. Boon, G. Thomaes, *Physica*, 28 (**1962**) 1074.
121. J.P. Boon, J. C. Legros, G. Thomaes, *Physica*, 33 (**1967**) 547.
122. T.H. Holleman, J. Hijmans, *Physica*, 28 (**1962**) 604.
123. H. Eyring, *J. Chem. Phys.*, 4 (**1936**) 283.

124. J.F. Kincaid, H. Eyring, A.E. Stearn, *Chem. Rev.*, 28 (**1941**) 301.
125. H. Eyring, T. Ree, N. Hirai, *Proc. Natl. Acad. Sci.*, 44 (**1958**) 683.
126. E.J. Fuller, T. Ree, H. Eyring, *Proc. Natl. Acad. Sci.*, 45 (**1959**) 1594.
127. C.M. Carlson, H. Eyring, *Proc. Natl. Acad. Sci.*, 46 (**1960**) 333.
128. T.R. Thomson, H. Eyring, T. Ree, *Proc. Natl. Acad. Sci.*, 46 (**1960**) 336.
129. J. Walter, H. Eyring, *J. Chem. Phys.*, 9 (**1941**) 393
130. T. Ree, H. Eyring, *Ind. Eng. Chem.*, 50 (**1958**) 1036.
131. C.M. Carlson, H. Eyring, T. Ree, *Proc. Natl. Acad. Sci.*, 46 (**1960**) 649.
132. H. Eyring, T. Ree, *Proc. Natl. Acad. Sci.*, 47 (**1961**) 526.
133. H. Eyring, M.S. John, *Significant Liquid Structures*, John Willey & Sons, New York (**1969**).
134. Gruneisen, Wiss, Abhaudl, *Physik-tech. Reich-austatt.*, 4 (**1905**) 239.
135. G. Jones, M. Dole, *J. Am. Chem. Soc.*, 51 (**1929**) 2950.
136. P. Debye, E. Hückel, *Z. Phys. Chem.*, 24 (**1923**) 185.
137. H. Falkenhagen, M. Dole, *Phys. Z.*, 30 (**1929**) 611.
138. H. Falkenhagen, E.L. Vernon, *Phys. Z.*, 33 (**1932**) 140.
139. H. Falkenhagen, E.L. Vernon, *Phil. Mag.*, 14 (**1983**) 537.
140. M. Kaminsky, *Discuss Faraday Soc.*, 24 (**1957**) 171.
141. D. Feakins, D.J. Freemantle, K.G. Lawrence, *J. Chem. Soc. Faraday Trans. I*, 70 (**1974**) 795.
142. J. Crudden, G.M. Delancy, D. Feakins, P.J. O'Relly, W. E. Waghorne, K. G. Lawrence, *J. Chem. Soc. Faraday Trans I.*, 82 (**1986**) 2195.
143. A.K. Covington, T. Dickinson, *Physical Chemistry of Organic Solvent Systems*, Plenum Press, New York (**1973**).
144. H.S. Harned, B.B. Owen, *The Physical Chemistry of Electrolytic Solutions*, Reinhold Publishing Corporation, New York (**1958**).
145. M. Kaminsky, *Z. Phys. Chem.*, 12 (**1957**) 206.
146. J. Desnoyers, G. Perron, *J. Solution Chem.*, 1 (**1972**) 199.
147. R.J.M. Bicknell, K.G. Lawrence, D. Feakins, *J. Chem. Soc. Faraday I*, 76 (**1980**) 637.
148. R.L. Kay, T. Vituccio, C. Zawoyski, D.F. Evans, *J. Phys. Chem.*, 70 (**1966**) 2336.
149. N.P. Yao, D.N. Bennion, *J. Phys. Chem.*, 75 (**1971**) 1727.
150. M. Kaminsky, *Discussions Faraday Soc.*, 24 (**1957**) 171.

151. D. Feakins, K.G. Lawrence, *J. Chem. Soc.*, A (**1966**) 212.
152. V. Vand, *J. Phys. Chem.*, 52 (**1948**) 277.
153. D.G. Thomas, *J. Colloid Sci.*, 20 (**1965**) 267.
154. S.P. Moulik, *J. Ind. Chem. Soc.*, 49 (**1972**) 483.
155. D. England, G. Pilling, *J. Phys. Chem.*, 76 (**1972**) 1902.
156. D.E. Goldsack, R.C. Franchetto, *Can. J. Chem.*, 55 (**1977**) 1062.
157. D.E. Goldsack, R.C. Franchetto, *Can. J. Chem.*, 56 (**1978**) 1442.
158. C.A. Angell, *J. Phys. Chem.*, 70 (**1966**) 2793.
159. C.A. Angell, *J. Chem. Phys.*, 46 (**1967**) 4673.
160. K.R. Chowdhury, D.K. Majumdar, *Electrochim. Acta.*, 28 (**1983**) 23.
161. K.R. Chowdhury, D.K. Majumdar, *Electrochim. Acta.*, 28 (**1983**) 597.
162. K.R. Chowdhury, D.K. Majumdar, *Electrochim. Acta.*,29 (**1984**) 1371.
163. P.P. Rastogi, *Bull. Chem. Soc. Japan*, 43 (**1970**) 2442.
164. R. Gopal, P.P. Rostogi, *Z. Phys. Chem. (N.F.)*, 69 (**1970**) 1.
165. C.M. Criss, M.J. Mostroianni, *J. Phys. Chem.*, 75 (**1971**) 2532.
166. K. Tamaski, Y. Ohara, Y. Isomura, *Bull. Chem. Soc. Japan*, 46 (**1973**) 951.
167. P.P. Deluca, T.V. Rabagay, *J. Phys. Chem.*, 79 (**1975**) 2493.
168. B.N. Prasad, N.P. Singh, M.M. Singh, *Ind. J. Chem.*, 14A (**1976**) 322.
169. B.N. Prasad, M.M. Agarwal, *Ind. J. Chem.*, 14A (**1976**) 343.
170. R.T.M. Bicknell, K.G. Lawrence, M.A. Scelay, D. Feakins, L. Werblan, *J. Chem. Soc. Faraday I.*, 72 (**1976**) 307.
171. J.M. Mcdowall, N. Martinus, C.A. Vincent, *J. Chem. Soc. Faraday I*, 72 (**1976**) 654.
172. A. Sacco, G. Petrella, M. Castagnola, *J. Phys. Chem.*, 80 (**1976**) 749.
173. R.L. Blokhra, Y.P. Segal, *Ind. J. Chem.*, 15A (**1977**) 36.
174. N.C. Das, P.B. Das, *Ind. J. Chem.*, 15A (**1977**) 826.
175. A. Sacco, G. Petrella, M. Della Monica, M. Castagnola, *J. Chem. Soc. Faraday I.*, 73 (**1977**) 1936.
176. P.K. Mandal, B.K. Seal, A.S. Basu, *Z. Phys. Chem.*, 258 (**1977**) 809.
177. J.I. Kim, *J. Phys. Chem.*, 82 (**1978**) 191.
178. S.K. Vijaylakshamna, *Indian J. Chem.*, 17A (**1979**) 511.
179. A. Sacco, G. Petrella, M.D. Monica, *J. Chem. Soc. Faraday I*, 75 (**1979**) 2325.
180. P.T. Thomson, M. Durbana, J.L. Turner, R.H. Wood, *J. Sol. Chem.*, 9 (**1980**) 955.

181. K. Kurotaki, S. Kawamura, *J. Chem. Soc. Faraday I*, 77 (**1981**) 217.
182. N. Martinus, C.A. Vincent, *J. Chem. Soc. Faraday Trans I*, 77 (**1981**) 141.
183. A. Sacco, A. D. Giglio, A. D. Atti, *J. Chem. Soc. Faraday I*, 77 (**1981**) 2693.
184. D.S. Gill, A.N. Sharma, *J. Chem. Soc. Faraday I*, 78 (**1982**) 78475.
185. A. Sacco, G. Petrella, A.D. Atti, M. Castagnolo, *J. Chem. Soc. Faraday I*, 78 (**1980**) 955.
186. A. Sacco, A.D. Giglio, A.D. Atti, M. Castagnolo, *J. Chem. Soc. Faraday I*, 79 (**1983**) 431.
187. K.G. Lawrence, A. Sacco, *J. Chem. Soc. Faraday I*, 79 (**1983**) 615.
188. K. Miyajima, M. Sawada, M. Nakagaki, *Bull. Chem. Soc. Jpn.*, 56 (**1983**) 827.
189. J. Doenech, S. Rivera, *J. Chem. Soc. Faraday I*, 80 (**1984**) 1249.
190. D. Dasgupta, S. Das, D.K. Hazra, *Bull. Chem. Soc. Jpn.*, 62 (**1989**) 1246.
191. S. Taniewska-Osinska, M. Jozwaik, *J. Chem. Soc. Faraday Trans I*, 85 (**1989**) 2147.
192. D. Nandi, D.K. Hazra, *J. Chem. Soc. Faraday Trans I*, 85 (**1989**) 4227.
193. I. Ibulci, M. Nakahara, *J. Phys. Chem.*, 94 (**1990**) 8370.
194. W.M. Cox, J. H. Wolfenden, *Proc. Roy. Soc. London*, 145A (**1934**) 475.
195. R.W. Gurney, *Ionic Processes in Solution*, Mc Graw Hill, New York (**1953**).
196. E.R. Nightingale, *J. Phys. Chem.*, 63 (**1959**) 1381.
197. A. Einstein, *Ann. Phys.*, 19 (**1906**) 289.
198. G.S. Benson, A.R. Gordon, *J. Chem. Phys.*, 13 (**1945**) 473.
199. [D.F.T. Tuan, R.M. Fuoss, *J. Phys. Chem.*, 67 (**1963**) 1343.
200. G. Petrella, A. Sacco, *J. Chem. Soc. Faraday I*, 74 (**1978**) 2070.
201. B.S. Krumgalz, J. Chem. Soc. Faraday I, 76 (**1980**) 1275.
202. B.S. Krumgalz, *Russ. J. Phys. Chem.*, 46 (**1972**) 858.
203. B.S. Krumgalz, *Russ. J. Phys. Chem.*, 47 (**1973**) 956.
204. B.S. Krumgalz, *Russ. J. Phys. Chem.*, 48 (**1974**) 1163.
205. B.S. Krumgalz, *Russ. J. Phys. Chem.*, 45 (**1971**) 1448.
206. H.D.B. Jenkins, M.S.F. Pritcheit, *J. Chem. Soc. Faraday I*, **80** (**1984**) 721.
207. K. Fajan, *Naturwissenschaften*, 9 (**1921**) 729.
208. D.F.C. Morris, *Struct. Bonding*, 6 (**1969**) 157.
209. R.W. Gurney, *Ionic Processes in Solutions*, Doves, New York (**1962**).
210. H.S. Frank, W.Y. Wen, *Disc. Farad. Soc.*, 24 (**1957**) 133.

211. Z. Asmus, *Naturforsch.*, 4A (**1949**) 589.

212. M.H. Abraham, J. Liszi, E. Papp, *J. Chem. Soc. Faraday I*, 78 (**1982**) 197.

213. M.H. Abraham, J. Liszi, L. Meszaros, *J. Chem. Phys.*, 70 (**1979**) 249.

214. M.H. Abraham, J. Liszi, *J. Chem. Soc. Faraday I*, 76 (**1980**) 1219.

215. S. Glasstone, K.J. Laidler, H. Eyring, *The Theory of Rate Process*, McGraw Hill, New York (**1941**).

216. E.R. Nightingale, R.F. Benck, *J. Phys. Chem.*, 63 (**1959**) 1777.

217. D. Feakins, D.J. Freemantle, K.G. Lawrence, *J. Chem. Soc. Faraday I*, 70 (**1974**) 795.

218. R. Sinha, *J. Phys. Chem.*, 44 (**1940**) 25.

219. V. Vand, *J. Phys. Chem.*, 52 (**1948**) 277.

220. D.G. Thomas, *J. Colloid Sci.*, 20 (**1965**) 267.

221. S.P. Moulik, *J. Phys. Chem.*, 72 (**1968**) 4688.

222. S.P. Moulik, *Electrochim. Acta.*, 17 (**1972**) 1491.

223. S.P. Moulik, *J. Indian Chem. Soc.*, 49 (**1972**) 483.

224. R.J. Fort, W.R. Moore, *Trans. Faraday Soc.*, 62 (**1966**) 1112.

225. G.R. Naidu, P.R. Naidu, *Ind. J. Chem.*, 22A (**1983**) 324.

226. O. Redlich, A.T. Kister, *Ind. Eng. Chem.*, 40 (**1948**) 345.

227. L. Pikkarainen, *J. Chem. Eng. Data*, 28 (**1983**) 344.

228. L. Pikkarainen, *J. Chem. Eng. Data.*, 28 (**1983**) 381.

229. L.S. Manjeshwar, T. Aminabhavi, *J. Chem. Eng. Data*, 33 (**1988**) 184.

230. K.P. Rao, K.S. Reddy, *J. Chem. Eng. Data*, 33 (**1988**) 130.

231. S. Glasstone, K.J. Laidler, H. Eyring, *The Theory of Rate Process*, McGraw Hill, New York (**1941**).

232. D.S. Gill, T.S. Kaur, H. Kaur, I.M. Joshi, J. Singh, *J. Chem. Soc. Faraday Trans.*, 89 (**1993**) 1737.

233. J.V. Herraez, R. Belda, *J. Soln. Chem.*, 33 (**2004**) 117.

234. J. Ferguson, Z. Kemblonski, *Applied Fluid Rheology*, Elsevier, Cambridge (**1991**).

235. H.A. Barnes, J.F. Hutton, K. Walters, *An Introduction to Rheology*, Elsevier, Amsterdam (**1993**).

236. C.W. Macosk, *Rheology. Principles, Measurements and Applications* (VCH), New York (**1994**).

237. M. Garcıa-Velarde, *Revista Esp. Fisica.*, 9 (**1995**) 12.
238. R. Shukla, M. Cheryan, *J. Membrane Sci.*, 198 (**2002**) 104.
239. J.M. Resa, C. Gonzalez, J. Lanz, *J. Food Eng.*, 51 (**2002**) 113.
240. M.J. Assael, N.K. Dalaouti, I. Metaxa, *Fluid Phase Equilibria.*, 199 (**2002**) 237.
241. A. Darr, *Technologia Farmaceútica.*, S.A. Acribia, Zaragoza (**1979**).
242. R. Voight, S.A. Acribia, *Tratado de Tecnolog´ıa Farmaceutica.*, Zaragoza (**1982**).
243. C.K. Z´eberg-Mikkelsen, S.E. Quiˆnones-Cisneros, S.H. Stenby, *Fluid Phase Equilibria.*, 1191 (**2002**) 194.
244. C. Fauli-Trillo, *Tratado de Farmacia Galénica*, S.A. Lujan, Madrid (**1993**).
245. J. Swarbrik, J.C. Boyland, *Encyclopedia of Pharmaceutical Technology*, Marcel Dekker, NewYork (**1993**).
246. J. Pellicer, *Sinergia Viscosa*, Valencia, Spain (**1997**).
247. G. Copetti, R. Lapasin, E.R. Morris, *Proceedings of the Fourth European Rheology Conference*, Seville, Spain (**1994**).
248. G. Kalentunc-Gencer, M. Peleg, *J. Texture Studies.*, 17 (**1986**) 61.
249. D.D. Christianson, *Hydrocolloidal Interactions with Starches*, Wesport. Conn. (**1982**).
250. N.K. Howell, *Proceedings of the Seventh International Conference*, Wales (**1993**)
251. J.G. Mathieson, B.E. Conway, *J. Sol. Chem.*, 3 (**1974**) 455.
252. S. Bhowmik, R.K. Mohanty, *Ind. J. Chem.*, 25A (**1986**) 416.
253. M.V. Kaulgud, K.S. Mohan Rao, *Ind. J. Chem.*, 27A (**1988**) 12.
254. K.J. Patil, A.B. Wazalwar, G.R. Mehta, *Ind. J. Chem.*, 27A (**1988**) 799.
255. M. Iqbal, R.E. Verral, *Can. J. Chem.*, 67 (**1989**) 727.
256. M. Kikuchi, M. Sakurai, K. Nitta, *J. Chem. Eng. Data*, 41 (**1996**) 1439.
257. B.E. Conway, R.E. Verral, *J. Phys. Chem.*, 70 (**1966**) 3952.
258. K. Gekko, H. Noguchi, *J. Phys. Chem.*, 83 (**1979**) 2706.
259. W.L. Masterson, *J. Chem. Phys.*, 22 (**1954**) 1830.
260. L.G. Hepler, *Can. J. Chem.*, 47 (**1969**) 4613.
261. M.V. Kaulgud, K.J. Patil, *J. Phys. Chem.*, 80 (**1976**) 138.
262. K.J. Patil, G.R. Mehta, R.K. Chandewar, *Ind. J. Chem.*, 25A (**1986**) 1147.

263. C. Lafuente, B. Ginar, A. Villares, I. Gascon, P. Cea, *Int. J. Thermophys.*, 25 (**2004**)1735.

264. G. Douheret, A. Pal, M.I. Davis, *J. Chem. Thermodyn.*, 22 (**1990**) 99.

265. I. Gascon, S. Martin, P. Cea, M.C. Lopez, F.M. Royo, *J. Sol. Chem.*, 31 (**2002**) 905.

266. R. Mehra, M. Pancholi, *J. Ind. Chem. Soc.* 82 (**2005**) 791.

267. S.L Oswal, K.D. Prajapati, J. *Chem. Eng. Data.*, 43 (**1998**) 367.

268. K. Hsu-Chen, T. Chein-Hsium, *J. Chem. Eng. Data*, 50 (**2005**) 608.

269. D.W. Marquardt, *J. Soc. Ind. Appl. Math.*, 11 (**1963**) 431.

270. L. Onsager, *Z. Phys. Chem.*, 28 (**1927**) 277.

271. R.M. Fuoss, *Rev. Pure Appl. Chem.*, 18 (**1968**) 125.

272. E. Pitts, *Proc. Roy. Soc.*, 217A (**1953**) 43.

273. R.M. Fuoss, L. Onsager, *J. Phys. Chem.*, 61 (**1957**) 668.

274. R.M. Fuoss, *Chemical Physics of Ionic Solutions*, Wiley, New York (**1966**).

275. E. Pitts, R.E. Tabor, J. Daly, *Trans. Faraday Soc.*, 65 (**1969**) 849.

276. (a) R.M. Fuoss, K.L. Hsia, *Proc. Natl. Acad. Sci.*, 57 (**1967**) 1550.
(b) R.M. Fuoss, K.L. Hsia, *J. Am. Chem. Soc.*, 90 (**1968**) 3055.

277. R. Fernandez-Prini, *J.E. Prue. Z. Phys. Chem.*, 228 (**1965**) 373.

278. R. Fernandez-Prini, *J.E. Prue. Z. Phys. Chem.*, 228 (**1965**) 473.

279. D.F. Evans, R.L. Kay, *J. Phys. Chem.*, 70 (**1966**) 366.

280. D. F. Arrington, E. Griswold, *J. Phys. Chem.*, 74 (**1970**) 123.

281. R.M. Fuoss, C.A. Kraus. *J. Am. Chem. Soc.*, 55 (**1933**) 476.

282. T. Shedlovsky, J. Franklin, *Instt.*, 225 (**1938**) 739.

283. (a) J.C. Justice, *J. Chem. Phys.*, 65 (**1968**) 353.
(b) J.C. Justice, R. Bury, C. Treiner, *J. Chem. Phys.*, 65 (**1968**) 1708.

284. R.M. Fuoss, F. Accascina, *Electrolytic Conductance*, Wiley, New York (**1959**

285. N.K. Bjerrum, Dan. Vidensk. Selek. *Mat.Fys.Medd*, 7 (**1926**) 9.

286. M. Tissier, G. Douheret, *J. Soln. Chem.*, 7 (**1978**) 87.

287. R. Fernandez-Prini, *J. Prue, Trans. Faraday Soc.*, 62 (**1966**) 1257.

288. (a) R.M. Fuoss, L. Onsager, *J. Phys. Chem.*, 66 (**1962**) 1722.
(b) R.M. Fuoss, L. Onsager, *J. Phys. Chem.*, 67 (**1963**) 621.

289. R.M. Fuoss, *J. Phys. Chem.*, 49 (**1975**) 525.

290. (a) B.S. Krumgalz, *J. Chem. Soc. Faraday I*, 79 (**1983**) 571.
(b) B.S. Krumgalz, *J. Chem. Soc. Faraday I.* 81 (**1985**) 241.

291. P. Walden, H. Ulich, D. Bush, *Z. Phys. Chem.*, 123 (**1926**) 429.
292. R.H. Stokes, R.A. Robinson, *Trans. Faraday Soc.*, 53 (**1957**) 301.
293. M. Born, *Z. Phys. Chem.*, 1 (**1920**) 221.
294. R.H. Boyd, *J. Chem. Phys.*, 35 (**1961**) 1281.
295. R. Zwanzig, *J. Chem. Phys.*, 38 (**1963**) 1603.
296. E.J. Passeron, *J. Phys. Chem.*, 68 (**1964**) 2728.
297. (a)P. Walden, *Z. Phys. Chem.*, 55 (**1906**) 207.
(b) P. Walden, *Z. Phys. Chem.*, 78 (**1912**) 257.
298. R.A. Robinson, R.H. Stokes, *Electrolyte Solutions*, Butterworths, London (**1959**)
299. R. Gopal, M.M. Hussain, *J. Ind. Chem. Soc.*, 40 (**1963**) 981.
300. L.G. Longsworth, *J. Phys. Chem.*, 67 (**1963**) 689.
301. M. Della Monica, U. Lamauna, L. Seutatore, *J. Phys. Chem.*, 72 (**1968**) 2124.
302. S. Brocus, *J. Chem. Phys.*, 28 (**1958**) 1158.
303. D.G. Miller, *J. Phys. Chem.*, 64 (**1960**) 1598.
304. G.J. Hills, *Chemical Physics of Ionic Solutions*, Wiley, New York (**1966**).
305. R.H. Stokes, I.A. Weeks, *Aust. J. Chem.*, 17 (**1964**) 304.
306. R.H. Stokes, *The Structure of Electrolytic Solutions*, Wiley, New York (**1959**).
307. D.S. Gill, *J. Chem. Soc. Faraday Trans .I*, 77 (**1981**) 751.
308. R. Zwanzig, *J. Chem. Phys.*, 52 (**1970**) 3625.
309. G. Atkinson, S.K. Koz, *J. Phys. Chem.*, 69 (**1965**) 128.
310. R.L. Kay, G.P. Cunningham, D.F. Evans, *Hydrogen bonded Solvent Systems*, Taylor and Francis, London (**1968**).
311. R.L. Kay, B.J. Hales, G.P. Cunningham, *J. Phys. Chem.*, 71 (**1967**) 3925.
312. R.L. Kay, C. Zawoyski, D.F. Evans, *J. Phys. Chem.*, 69 (**1965**) 4208.
313. D. F. Evans, J. L. Broadwater, *J. Phys. Chem.*, 72 (**1968**) 1037.
314. M. Spiro, *Physical Chemistry of Organic Solvent Systems*, Plenum Press, New York (**1973**).
315. R. Fernandez-Prini, G. Atkinson, *J. Phys. Chem.*, 75 (**1971**) 239.
316. L. Bahadur, M.V. Ramanamurti, *J. Chem. Soc. Faraday I*, 76 (**1980**) 1409.
317. L. Bahadur, M.V. Ramanamurti, *J. Electrochem. Soc.*, 128 (**1981**) 339.
318. L. Bahadur, M.V. Ramanamurti, *Can. J. Chem.*, 62 (**1984**) 1051.
319. J.L. Broadwater, R.L. Kay, *J. Phys. Chem.*, 74 (**1970**) 3803.

320. S. Das, D.K. Hazra, *Indian J. Chem.*, 274 (**1988**) 1073.

321. S. Das, D.K. Hazra, *J. Ind. Chem. Soc.*, LXV (**1988**) 100.

322. (a) R.L. Kay, J.L. Broadwater, *Electrochim. Acta.*, 16 (**1971**) 667.
(b) R.L. Kay, J.L. Broadwater, *J. Sol. Chem.*, 5 (**1976**) 57.

323. A.D. Aprano, R.M. Fuoss, *J. Phys. Chem.*, 67 (**1963**) 1704.

324. P. Hemmes, *J. Phys. Chem.*, 78 (**1974**) 907.

325. J. Hubbard, L. Onsager, *J. Chem. Phys.*, 53 (**1977**) 4850.

326. N. Islam, M.R. Islam, M. Ahmed, *Z. Phys. Chem.*, 262 (**1981**) 129.

327. D.S. Gill, A.N. Sharma, H. Schneider, *J. Chem. Soc. Faraday I*, 78 (**1982**) 465.

328. C.J. Cramer, D.G. Truhlar, *J. Am. Chem. Soc.*, 113 (**1991**) 8305.

329. D.J. Giesen, J.W. Stores, C.J. Cramer, D.G. Truhlar, *J. Am. Chem. Soc.*, 117 (**1995**) 1057.

330. (a) C.J. Cramer, D.G. Truhlar, *J. Org. Chem.*, 61 (**1996**) 8720.
(b) C.J. Cramer, D.G. Truhlar, *Erratum.*, 101 (**1999**) 309.

331. G.D. Hawkins, CJ. Cramer, D.G. Truhlar, *J. Phys. Chem. B*, 101 (**1997**) 7147.

332. G.D. Hawkins, C.J. Cramer, D.G. Truhlar, *J. Phys. Chem. B*, 102 (**1998**) 3257.

333. A. Gil-Villegas, A. Galindo, P.J. Whitehead, S.J. Mills, G. Jackson, A.N. Burgess, *J. Chem. Phys.*, 106 (**1997**) 4168.

334. A. Galindo, L.A. Davies, A. Gil-Villegas, *G. Jackson, Mol. Phys.*, 93 (**1998**) 241.

335. M. Roses, C. Rafols, J. Ortega, E. Bosch, *J. Chem. Soc. Perkin Trans.*, 2 (**1995**) 1607.

336. W. Heller, *J. Phys. Chem.* 69 (**1965**) 1123.

337. O. Redlich, A. Kister, *Ind. Eng. Chem.* 40 (**1948**) 345.

References of Chapter III

1. "Dietary Supplement Fact Sheet: Folate", Office of Dietary Supplements, National Institutes of Health, http://ods.od.nih.gov/factsheets/folate.asp.
2. E. M. Goncaives, T. S. Rego and M. E. Minas da Piedade, *J. Chem. Thermodynamics.* 43 (**2011**) 974.
3. S. H. Talkowsky and Y. He, P. Jain, Handbook of aqueous solubility data, 2nd Ed., (**2010**), CRC Press, Boca Raton,
4. M. N. Roy, R. K. Das, and A. Bhattacharjee, *Russian J. Phys. Chem A.* 84 (**2010**) 2201.

5. D.D. Perrin, W.L.F. Armarego, *Purification of Laboratory Chemicals*, 3rd Ed., (**1988**), Pergamon Press, Oxford, England.
6. Oscillating U-tube. Electronic document, http://en.wikipedia.org/wiki/Oscillating U-tube, accessed January 21(**2013**).
7. J.E. Lind Jr., J.J. Zwolenik, R.M. Fuoss, *J. Chem. Soc. Faraday Trans I.* 81(**1959**) 1557.
8. B. Das, N. Saha, *J. Chem. Eng. Data* 45 (**2000**) 2.

References of Chapter IV

1. C. Chahidi, M. Aubailly, A. Momzikoff, and M. Bazin, *Photochem. Photobiol.* 33 (**1981**) 641.
2. Spina Bifida and Hydrocephalus Association of Nova Scotia, "Folic Acid information," http://www3.ns.sympatico.ca/spina.bifida/folicacid.htm.
3. S.W. Bailey and J.E. Ayling, *Proceedings of the National Academy of Sciences of the United States of America* 106 (36) (**2009**) 15424.
4. S.J. Weinstein, T.J. Hartman and R. Stolzenberg-Solomon, *Cancer Epidemiol. Biomarkers Prev.* 12 (**2003**) 1271.
5. "Dietary Supplement Fact Sheet: Folate", Office of Dietary Supplements, National Institutes of Health, http://ods.od.nih.gov/factsheets/folate.asp
6. B. Kamen, *Semin. Oncol.* 24 (**1997**) 18.
7. R.L. Vanetten, G.A. Clowee, J.F. Sebastian and M. L. Bender, *J. Am. Chem. Soc.* 89 (**1967**) 3253.
8. O. Enea and C. Jolicoeur, *J. Phys. Chem.* 86 (**1982**) 3870.
9. A. Kumar and P. Venkatesu, *Chem. Rev.* 112 (**2012**) 4283.
10. W. Kauzmann, *Adv. Protein Chem.* 14 (**1979**) 1.
11. I.M. Abdulagatov and N.D. Azizov, Fluid Phase Equilibria, 240 (**2006**) 204.
12. E.B. Freyer, J.D. Hubbard and D.H. Andrews, *J. Am. Chem. Soc.* 51 (**1929**) 759.
13. O. Kiyohara, J.P.E. Grolier and G. C. Benson, *Can. J. Chem.* 52 (**1974**) 2287.
14. N.M. Murthy and S.V. Subrahmanyam, *Bull. Chem. Soc. Jpn.* 50 (**1977**) 2589.
15. D. O. Masson, *Phil. Mag.* 8 (**1929**) 218.
16. F. Millero, *J. Chem. Rev.* 71 (**1971**) 332.

17. Y. Marcus and G. Hefter, *Chem. Rev.* 104 (**2004**) 3405.
18. Y. Marcus, *J. Chem. Soc., Faraday Trans.* 89 (**1993**) 713.
19. F.J. Millero, *The partial molar volumes of electrolytes in aqueous solutions*, in: R.A. Horne (Ed.), *Water and Aqueous Solutions: Structure, Thermodynamics, and Transport Processes* (Wiley Interscience, New York, (**1972**) pp. 519.
20. K. Belibagli and E. Agranci, *J. Solution Chem.* 19 (**1990**) 867.
21. T.S. Banipal, G. Singh and B.S. Lark, *J. Solution Chem.* 30 (**2001**) 657.
22. H.L. Friedman and C.V. Krishnan, *Water: A comprehensive Treatise*; F. Franks, Ed., Plenum, New York, (**1973**) Vol. 3, Chapter 1.
23. A.K. Mishra, K.P. Prasad and J.C. Ahluwalia, *Biopolymers*, 22 (**1983**) 2397.
24. F.J. Millero, A.L. Surdo and C. Shin, *J. Phys. Chem.* 82 (**1978**) 784.
25. Li. Xu, C. Ding and R. Lin, *J. Solution Chem.* 35 (**2006**) 19.
26. R.K. Wadi and P. Ramasami, *J. Chem. Soc. Faraday Trans.* 93 (**1997**) 243.
27. T.S. Banipal, D. Kaur and P.K. Banipal, *J. Chem. Eng. Data.* 49 (**2004**)1236.
28. T. Banerjee and N. Kishore, *J. Solution Chem.* 35 (**2005**) 13.
29. J. Wang, Z. Yan, Y. Zhao and F. Cui, *J. Chem. Eng. Data.* 49 (**2002**) 135.
30. M. Natarajan and R.K. Wadi, *J. Chem. Eng. Data.* 35 (**1990**) 87.
31. R. Bhat and J.C Ahluwalia, *J. Phys. Chem.* 89 (**1985**) 1099.
32. K. Mishra and J.C. Ahluwalia, *J. Chem. Soc. Faraday Trans. 1*, 77 (**1981**) 1469.
33. S. Li, X. Hu, R. Lin, W. Sang and W. Fang, *J. Solution Chem.* 30 (**2001**) 365.
34. E. Berlin and M. J. Pallansch, *J. Phys. Chem.* 72 (**1968**) 188.
35. F.T. Gucker, W.L. Ford and C.E. Moser, *J. Phys. Chem.* 43 (**1939**) 153.
36. F. Franks, M.A. Quickenden, D.S. Reid and B. Watson, *Trans. Faraday Soc.* 66 (**1970**) 582.
37. T .Owaga, K. Mizutami and M. Yasuda, *Bull. Chem. Soc. Jpn.* 57 (**1984**) 2064.
38. G. Jones and D. Dole, *J. Am. Chem. Soc.* 51 (**1929**) 2950.
39. Z. Yan, J. Wang, and J. Lu, *Biophys. Chem.* 99 (**2002**) 199.
40. V. Minkin, O. Osipov, Y. Zhdanov, *Dipole Moments in Organic Chemistry*, Plenum Press, New York, London, (**1970**).
41. M. Born and E. Wolf, *Principles of Optics: Electromagnetic Theory of Propagation, Interference and Diffraction of Light*, Cambridge University Press, London, 7th Ed., (**1999**).
42. M. Deetlefs, K. Seddon, M. Shara, *Phys. Chem. Chem. Phys.* 8 (**2006**) 642.

43. M.N Roy, D. Ekka and R. Dewan, *Acta Chim. Slov.* 58 (**2011**) 792.
44. J.G. Mathieson and B.E. Conway, *J. Sol. Chem.* 3 (**1974**) 781.
45. T. Loftsson, *Expert Opinion Drug Delivery*, 2(2) (**2005**) 33.

References of Chapter V

1. R.L.Kay, D.F. Evans, *J. Phys. Chem.* 70 (**1966**) 2325.
2. B.Das, D.K. Hazra, *J. Phys. Chem.* 99 (**1995**) 269.
3. P.K.Muhuri, B.Das, D.K. Hazra, *J. Phys. Chem.* B 101 (**1997**) 3329.
4. P.J.Victor, P.K. Muhuri, B. Das, D.K. Hazra, *J. Phys. Chem.B* 103 (**1999**) 11227.
5. C. Guha, J.M. Chakraborty, S. Karanjai, B.Das, *J.Phys.Chem.B* 107 (**2003**) 12814.
6. R.M. Fuoss, Proc. Nat. *Acad. Sci.* 71 (**1974**) 4491.
7. J. Barthel, H.G. Gores, *Top. Curr. Chem.* 70 (**1983**) 495.
8. N. Inove, M. Xu, S. Petrucci, *J. Phys. Chem.* 91 (**1987**) 4628.
9. C.G. Janz, R.P.T. Tomkins, *Non Aqueous Electrolytes Handbook, Academi*, New York, (**1973**).
10. R. Jasinki, *High Energy Battery*, Plenum, New York, (**1967**).
11. M.N. Roy, A. Jha, R. Dey, *J. Chem. Eng. Data.* 46 (**2001**) 1327.
12. D. Nandi, M.N. Roy, D.K.Hazra, *J. Indian Chem. Soc.* 70 (**1993**) 305.
13. R.M. Fuoss, C.A. Kraus, *J. Am.Chem.Soc.* 55 (**1933**) 2387.
14. D.D.Perrin, W.L.F. Armarego, *Purification of Laboratory Chemicals*, Pergamon, Great Britain, (**1988**).
15. M.N. Roy, M. Das, *Russian J. Phys. Chem.* 80 (**2006**) S163.
16. A.K. Covington, T. Dickinson, *Physical Chemistry of Organic Solvent Systems*, Plenum, New York,(**1973**).
17. R. De, C. Guha, B.Das, *J. Sol. Chem.* 35 (**2006**) 1505.
18. A. Bhattacharjee, M.N. Roy, *Phys. Chem. Chem. Phys.* 12 (**2010**) 1.
19. P. Rohdewald, M. Moldner, *J. Phys. Chem.* 77 (**1973**) 373.
20. R. Chanda, M.N. Roy, *Fluid Phase Equilib.* 269 (**2008**) 134.
21. M.N. Roy, B. Sinha, V.K. Dakua, *J. Chem. Eng. Data.* 51 (**2006**) 590.
22. J.E. Lind, J.J. Zwolenik, R.M. Fuoss, *J. Am. Chem. Soc.* 81 (**1959**) 1557.
23. R.M. Fuoss, *J. Phys. Chem.* 82 (**1978**) 2427.
24. R.M. Fuoss, Paired ions: Dipolar pairs as subset of diffusion pairs. Proc. Natl. Acad. Sci. U.S.A. 75 (**1978**) 16.

25. R.M. Fuoss, T. Shedlovsky, *J. Am. Chem.* Soc. 71 (**1949**) 1496.
26. D.S.Gill, M.S. Chauhan, *Z. Phys. Chem. NF*, 140 (**1984**) 139.
27. B. Per, *Acta Chem. Scand. Ser. A* 31 (**1977**) 869.
28. B.Das, D.K. Hazra, *J. Solution Chem.* 27 (**1998**) 1021.
29. P.K. Muhuri, D.K. Hazra, *Z. Phys. Chem.* 190 (**1995**) 111.
30. D.Dasgupta, S. Das, D.K. Hazra, *J.Chem. Soc. Faraday Trans.* I 84 (**1988**) 1057.
31. B.S. Krumgalz, *J.Chem. Soc. Faraday Trans.I* 79 (**1983**) 571.
32. J. Barthel, M.B.Rogac, R. Neueder, *J. Solut. Chem.* 28 (**1999**) 1071.
33. A. Sinha, M.N. Roy, *Phys. Chem. Liqs.* 45 (**2007**) 67.
34. D. Das, B. Das, D.K. Hazra, *J. Sol. Chem.* 32 (**2003**) 77.
35. D.K. Hazra, D. Das, B. Das, *Z. Phys.Chem.* 218 (**2004**) 341.
36. R.M. Fuoss, F. Accascina, *Electrolytic Conductance, Interscience*, New York, (**1959**).
37. H. Maser, M. Delsignore, M. Newstein, S. Petrucci, *J. Phys. Chem.* 88 (**1984**) 5100.
38. A.A. Ansari, M.R. Islam, *Can. J. Chem.* 66 (**1988**) 1223.
39. P. Walden, H. Ulich, G. Busch, *Z. Phys. Chem.* 123 (**1926**) 429.
40. S. Boileau, P. Hemery, *Electrochim. Acta* 21 (**1976**) 647.
41. E. Hirsch, R.M. Fuoss, *J. Am. Chem. Soc.* 82 (**1960**) 1018.
42. D. Nandi, S. Das, D.K. Hazra, *Ind. J. Chem. A* 27 (**1988**) 574.
43. H.R. Corti, D.L. Goldfarb, M.P. Longinotti, *J. Sol. Chem.* 30 (**2001**) 307.

References of Chapter VI

1. M. N. Roy, R. K. Das, and A. Bhattacharjee, *Russian J. Phys. Chem A.* 84 (**2010**) 2201.
2. J. M. McDowall, and C.A. Vincent, *J. Chem. Soc. Faraday Trans.* 1. 70 (**1974**) 1862.
3. M.R.J. Deck, K.J Bird, and A.J. Parker, *Aust. J. Chem.* 28 (**1975**) 955.
4. M.N.Roy, B. Sinha, R. Dey, and A. Sinha, *Int. J. Thermophy.* 26 (**2005**) 1549.
5. M.N. Roy, R. Dewan, P. K. Roy, and D. Biswas, *J. Chem. Eng. Data.* 55 (**2010**) 3617.
6. M.N. Roy, A. Bhattacharjee, and P.Chakraborti, *Thermochim. Acta.* 507 (**2010**) 135.
7. A. Bhattacharjee and M.N.Roy, *Phys. Chem. Chem. Phys.* 12 (**2010**) 14534.
8. M.N. Roy, A Jha and A. Choudhury, *J. Chem. Eng. Data.* 49 (**2004**) 291.
9. E.Ayranci, *J. Chem. Eng. Data.* 42 (**1997**) 934.
10. D.O.Masson, *Phil. Mag.* 8 (**1929**) 218.
11. G. Jones and M. Dole, *J. Am. Chem. Soc.* 51(**1929**) 2950.

12. F. J. Millero, *Chem. Rev.* 71 (1971)147.
13. F. J. Millero , A. Losurdo and C. Shin, *J. Phys. Chem.* 82 (**1978**) 784.
14. V. Minkin, O. Osipov and Y. Zhdanov, "Dipole Moments in Organic Chemistry", Plenum Press, New York, London, (**1970**).
15. M. Born and E. Wolf, "Principles of Optics: Electromagnetic Theory of Propagation, Interference and Diffraction of Light", 7th ed, Cambridge University Press, London, (**1999**).
16. M. Deetlefs, K. Seddon and M. Shara, *Phys. Chem. Chem. Phys.* 8 (**2006**) 642.

References of Chapter VII

1. F.A. Robinson, The Vitamin B-Complexes, Chapter 4 ,Chapman & Hall,London, (**1951**)
2. S. Cakir, I. Bulut, E. Bicer, O. Cakir, J. Coord. *Chem.* 56 (**2003**) 511.
3. A.N. Nesmeyanov, N.A. Nesmeyanov, Fundamentals of Organic Chemistry, vol. 3, p. 393 ,Mir, Moscow,(**1981**)
4. A.S. Fauci, E. Braunwald, K.J. Isselbacher, J.D. Wilson, J.B. Martin,D.L. Kasper, S.L. Hauser, D.L. Long, Harrison's Principles ofInternal Medicine, 14th ed., McGraw-Hill, New York,(**1998**)
5. C.R.W. Edwards, I.A.D. Bouchier, C. Haslett, E.R. Chilvers, Davidson's Principles and Practice of Medicine, 17th ed., BPC Paulton Books Limited, Great Britain, (**1996**).
6. The Merck index- An Encyclopedia of Chemicals, Drugs, Biologicals, 13th ed; Merck and Co., Inc: (**2001**), 405.
7. Kirk-Othmer Encyclopedia of Chemical Technology, 4th ed.: John Willey and Sons: New York (**1993**), 354.
8. J. Kent, A. Kent and Riegels, Handbook of Industrial Chemistry and Biotechnology; Spingerlink:(**2008**), XIV, 1386.
9. M .C. Maffia, J. A. Meirelles, *J. Chem. Eng. Data* 46 (**2001**) 582.
10. A.Apelblat, E.Manzurola, *Fluid Phase Equilibria,* 60 (**1990**) 157.
11. A.Apelblat, E.Manzurola, *J. Chem. Thermodyn.* 6 (**1985**) 579.
12. M.L. Parmar, R.K Awasthi, M.K. Guleria, *J. Chem. Sci.* 116(**2004**) 33.
13. A.H.Sijpkes, P.A. Rossum, J. S. Raad, G. Somsen, *Chem. Thermodyn.* 9(**1989**) 1061.

14. B.J. Levien, *J. Phys. Chem.* 59 (**1955**) 640.
15. M.N. Roy, B. Sinha, V.K. Dakua, *Pakistan J. Sci. Ind. Res.* 49 (**2006**) 153.
16. L.H. Blanco, E.F. Vargas, *J. Solution Chem.* 35 (**2006**) 21.
17. 17. H.G. Windmuller, C.J. Ackerman, H. Bakerman, O. Mickelsen, *J. Biol. Chem.* 234 (**1959**) 889.
18. 18. M. Iwaki, N.P.J. Cotton, P.G. Quirk, P.R. Rich, J.B. Jackson, *J.Am. Chem. Soc.* 128 (**2006**) 2621.
19. J.M. McDowali, C.A. Vincent, *J. Chem. Soc., Faraday Trans.* 1 (**1974**) 1862.
20. M.R.J. Deck, K.J. Bird, A.J. Parker, *Aust. J. Chem.* 28 (**1975**) 955.
21. M.N. Roy, B. Sinha, V.K. Dakua, *J. Chem. Eng. Data* 51,(**2006**) 590.
22. M.N. Roy, B. Sinha, *J. Mol. Liq.* 133 (**2007**) 89.
23. A. Kundu, N. Kishore, *J. Solution Chem.* 32 (**2003**) 703.
24. W.B. Wright, G.S.D. King, *Acta Crystallogr.* 7 (**1954**) 283.
25. W.N. Charman, C.S.C. Lai, D.J. Craik, *Aust. J. Chem.* 46 (**1993**) 377.
26. M.N. Roy, B. Sinha, R. Dey, A.Sinha, *Int. J. Thermophys.* 26, (**2005**) 1549.
27. L.G. Hepler, *Can. J. Chem.* 47 (**1969**) 4617.
28. F.J. Millero, Structure and Transport Process in Water and AqueousSolutions,R.A. Horne, New York,(**1972**)
29. M.L. Parmar, D.S. Banyal, *Indian J. Chem.* 44 A (**2005**) 1582.
30. W.Y. Wen, in: R.A. Horne (Ed.), Water and Aqueous Solution, Willey–Interscience, New York, (**1972**), p. 613.
31. K. Belibagli, E. Agranci, *J. Solution Chem.* 19 (**1990**) 867.
32. C. Zhao, P. Ma, J. Li, *J. Chem. Thermodyn.* 37 (**2005**) 37.
33. H.L. Friedman, C.V. Krishnan, in: F. Franks (Ed.), Water: A Comprehensive Treatise, vol. 3, Chapter 1 ,Plenum Press, New York, (**1973**).
34. R.K. Wadi, P. Ramasami, *J. Chem. Soc. Faraday Trans.* 93 (**1997**) 243.
35. R. Bhat, J.C. Ahluwalia, *J. Phys. Chem.* 89 (**1985**) 1099.
36. A.K. Mishra, J.C. Ahluwalia, *J. Chem. Soc. Faraday Trans.* 1 77 (**1981**) 1469.
37. G. Jones, M. Dole, *J. Am. Chem. Soc.* 51 (**1929**) 2950.
38. F.J. Millero, A. Losurdo, C. Shin, *J. Phys. Chem.* 82, (**1978**) 784.
39. D. Feakins, D.J. Freemantle, K.G. Lawrence, *J. Chem. Soc. Faraday Trans.* 70 (**1974**) 795.
40. B. Samantaray, S. Mishra, U.N. Dash, *J. Teach. Res. Chem.* 11 (**2005**) 87.

41. B,Sinha, B.K.Das, M.N.Roy, *J. Chem. Thermodyn.* 40 (**2008**) 394.

References of Chapter VIII

1. F.A. Robinson, *The Vitamin B-Complexes*, Chapter 4, Chapman&Hall, London, (**1951**).
2. S. Cakir,; I. Bulut,; Bicer,.; E. Cakir, O.; J. Coord.; *Chem.* 56 (**2003**) 511.
3. M. N. Roy,; R. K Das,.; A. Bhattacharjee, *Russian J. Phys. Chem. A.* 84 (**2010**) 2201.
4. C. Chahidi ; M. Aubailly; A. Momzikoff.; M. Bazin, *Photochem. Photobiol.* 33(**1981**) 641.
5. "Dietary Supplement Fact Sheet: Folate", Office of Dietary Supplements, National Institutes of Health, http://ods.od.nih.gov/factsheets/folate.asp.
6. "The primary structure of proteins is the amino acid sequence". *The Microbial World.* University of Wisconsin-Madison Bacteriology Department. Retrieved 16 September (**2012**).
7. I.M. Abdulagatov; N.D. Azizov, *Fluid Phase Equilibria*, 240 (**2006**) 204.
8. E.B. Freyer; J.D.Hubbard; D.H. Andrews *J. Am. Chem. Soc.* 51 (**1929**) 759.
9. O. Kiyohara; J.P.E. Grolier; G. C. Benson, *Can. J. Chem.* 52(**1974**) 2287 .
10. N.M .Murth.; S.V. Subrahmanyam, *Bull. Chem. Soc. Jpn.* 50 (**1977**) 2589.
11. E. Ayranci, *J. Chem. Eng. Data.* 42 (**1997**) 934.
12. D.O. Masson, *Phil. Mag.* 8 (**1929**) 218.
13. G. Jones; M. Dole, *J. Am. Chem. Soc.* 51(**1929**) 2950.
14. 14 F. Millero; J. *Chem. Rev.* 71 (**1971**) 147.
15. F.J Millero; A. Losurdo; C. Shin, *J. Phys. Chem.* 82 (**1978**) 784.
16. 16. V. Minkin; O. Osipov; Y. Zhdanov; *Dipole Moments in Organic Chemistry*, Plenum Press, New York, London, (**1970**).
17. M. Born; E. Wolf; *Principles of Optics: Electromagnetic Theory of Propagation, Interference and Diffraction of Light*, 7th ed., Cambridge University Press, London, (**1999**).
18. M. Deetlefs;K. Seddon, M. Shara; *Phys. Chem. Chem. Phys.* 8 (**2006**) 642.
19. M. N. Roy; D. Ekka ; R. Dewan; *Acta Chim. Slov.* 58 (**2011**) 792.

References of Chapter IX

1. F. A. Robinson, "The Vitamin B-Complexes", 4th ed., Chapman & Hall, London, (**1951**).
2. E. M. Goncaives, T. S. Rego and M. E. Minas da Piedade, *J. Chem. Thermodynamics.* 43 (**2011**) 974.
3. S. H. Talkowsky and Y. He, P. Jain, Handbook of aqueous solubility data, 2nd Ed., CRC Press, Boca Raton, (**2010**).
4. D. Ekka and M.N. Roy, *J. Phys. Chem. B*, 116 (**2012**)11687.
5. E. B Freyer, J. D Hubbard, and D. Andrews, *J. Am. Chem. Soc.*, 51 (**1929**) 759.
6. O. Kiyohara, and K. Arakawa, *Bull. Chem. Soc. Japan.*, 43 (**1970**) 3037.
7. O. Kiyohara, J. P. E. Grolier and G. C Benson, *Can. J. Chem.*, 52 (**1974**) 2287.
8. N. M. Murthy and S. V. Subrahmanyam, *Bull. Chem. Soc. Japan.*, 50 (**1977**) 2589.
9. E. Ayranci, *J. Chem. Eng. Data*, 42 (**1997**) 934.
10. D. O. Masson, *Philos. Mag.*, , 8 (**1929**) 218.
11. R. K. Wadi, P. Ramasami, *J. Chem. Soc. Faraday Trans.*, 93 (**1997**) 243.
12. T. S. Banipal, D. Kaur and P. K. Banipal, *J. Chem. Eng. Data*, 49 (**2004**) 1236.
13. M. Natarajan, R. K. Wadi and H. C. Gaur, *J. Chem. Eng. Data*, 35 (**1990**) 87.
14. K. Belibagli and E. Agranci, *J. Solution Chem.*, 19 (**1990**) 867.
15. G. Jones and M. Dole, *J. Am Chem. Soc.*, 51 (**1929**) 2950.
16. F. J. Millero, *Chem. Rev.*, 71 (**1971**) 147.
17. F. J. Millero, A. Lo Surdo and C. Shin, *J. Phys. Chem.*, 82 (**1978**) 784.
18. M. Born and E. Wolf, "Principles of Optics: Electromagnetic Theory of Propagation, Interference and Diffraction of Light", Cambridge University Press, London, (**1999**).
19. M. Deetlefs, K. Seddon and M. Shara, *Phys. Chem. Chem. Phys.* 8 (**2006**) 642.
20. H. Zhao, *Biophys. Chem.* 122 (**2006**) 157.

INDEX

Subject	Page No.
A	
L-Alanine	15, 79, 102, 105,114,198,215
Ammonium acetate	15,86,126,129
Apparent molal isentropic compressibility	56,57
Ascorbic acid	15,17,78,149,154,183,188,216
B	
Bio-active solutes	13,19
C	
Citric acid	15, 83, 216,
Conductance	25, 42, 58, 65, 125, 128, 215
Cosolute	102, 114, 215
Covalent bonding	22, 133
D	
Densitometry	16
Dimethyl sulphoxide	43, 125, 215
Dipole-dipole forces	13, 20
E	
Ethanoates	125, 132, 215
F	
Folate	18, 77, 101, 183
Folic acid	15, 18, 77, 183, 189, 216
Fuoss-Kraus equation	60, 133
G	
D-Glucose	81, 149, 216
Glycine	15, 79, 102, 199, 216
Gibbs energy	16, 29, 71, 130
H	
Hydrogen bond	13, 21, 38, 66, 88, 114, 125, 167
I	
Ion-pair formation	71, 130

L
Limiting equivalent conductance 65
Lithium acetate 15, 84, 134
London dispersion forces 20

M
D-Maltose 15, 82, 149, 216
Masson equation 30, 104, 151, 186, 199
Metallic bonding 22

N
Nicotinamide 15, 84, 161, 183, 216
Niacin 18, 84, 161

P
Partial molar volumes 26, 29, 32, 50, 102, 162
Potassium acetate 15, 85

R
Refractometry 16

S
Sodium acetate 15, 85, 129
Solution chemistry 17, 23, 72
Solvation 13, 20, 28, 40, 67, 72, 125, 149, 202
Solvent – solvent interactions 19
Stokes' law 34, 67, 131

T
Tetrabutylammonium tetraphenylborate 129
Tetrahydrofuran 15, 89, 125, 215

V
L-Valine 15, 80, 102, 198
Viscometry 16

W
Walden's rule 59, 68, 133

Z
Zwitter ion 121